BIOLOGICAL CARBON MONOXIDE CONVERSION FOR HYDROGEN PRODUCTION AND ENVIRONMENTAL APPLICATIONS

A Thesis

Submitted in partial fulfilment of the requirements for the award of the degree of

DOCTOR OF PHILOSOPHY

by

ARINDAM SINHAROY

DEPARTMENT OF BIOSCIENCES AND BIOENGINEERING

INDIAN INSTITUTE OF TECHNOLOGY GUWAHATI

GUWAHATI - 781039, ASSAM, INDIA

December 2018

श्री कृष्ण अर्पणमस्तु

Dedicated to my parents

INDIAN INSTITUTE OF TECHNOLOGY GUWAHATI

DEPARTMENT OF BIOSCIENCES & BIOENGINEERING

DECLARATION

I, hereby declare that the content embodied in this thesis entitled "**Biological carbon monoxide conversion for hydrogen production and environmental applications**" is the result of investigations carried out by me at the Department of Biosciences and Bioengineering, Indian Institute of Technology Guwahati, Guwahati, India, under the supervision of **Prof. Kannan Pakshirajan.**

In keeping with the general practice of reporting scientific observations, due acknowledgements have been made wherever the work described is based on the findings of other investigators.

Date: **Arindam Sinharoy**

Place: IIT Guwahati

INDIAN INSTITUTE OF TECHNOLOGY GUWAHATI

DEPARTMENT OF BIOSCIENCES & BIOENGINEERING

CERTIFICATE

It is certified that the work described in this thesis entitled **"Biological carbon monoxide conversion for hydrogen production and environmental applications"** by **Arindam Sinharoy** for the award of degree of Doctor of Philosophy is an authentic record of the results obtained from the research work carried out under my supervision in the Department of Biosciences and Bioengineering, Indian Institute of Technology Guwahati, India, and this work has not been submitted either in whole or in part elsewhere for a degree.

Date:

Place: IIT Guwahati

_____

(Signature of Thesis Supervisor)

Prof. Kannan Pakshirajan

Professor and Head

Department of Biosciences & Bioengineering

Indian Institute of Technology Guwahati

Guwahati-781039, Assam, India

ACKNOWLEDGEMENTS

"मूकं करोति वाचालं पङ्गुं लङ्घयते गिरिं । यत्कृपा तमहं वन्दे परमानन्द माधवम् ॥"

First and foremost, I would like to thank God Almighty for giving me the strength, knowledge, ability and opportunity to undertake this work and to persevere and complete it satisfactorily. Without his blessings, this achievement would not have been possible.

In my journey towards this degree, I have found a teacher, an inspiration, a role model and a pillar of support in my Supervisor, Prof. Kannan Pakshirajan, Professor and Head, Department of Biosciences and Bioengineering, IIT Guwahati. Without his able guidance, this thesis would not have been possible and I shall eternally be grateful to him for his assistance.

I take this opportunity to express my gratitude to my Doctoral committee members, Prof. Debasish Das, Dr. Senthilkumar Sivaprakasam and Dr. Vairakannu Prabu for their constructive criticism and precious suggestions throughout this work. I also express my gratitude to Prof. V.V. Dasu former head of the department and former chairman of my doctoral committee for his support and help.

I extend my gratitude to the Department of Biosciences and Bioengineering, Centre for the Environment, Department of Chemical Engineering, Centre for Energy and Central Instruments Facility, IIT Guwahati for providing technical and instrumental support to this work. I also take this opportunity to thank all the non teaching staff and teaching assistants who helped in different instrumentations. I would gratefully acknowledge the fellowship provided to me by Institute during all these years and Department of Biotechnology, Government of India for funding this work.

I am grateful to all my former and current lab mates Dr. Vibha Sinha, Dr. Madhavi Singh, Dr. M. Gopi Kiran, Jayeeta Hazarika, Lalit Goswami, Dr. Akoijam Chingkheihunba, Dr. Arvind Kumar Shakya, Sanjay Kumar, M.M

Tejas Namboodiri, Nikhil Gupta, Surjith Ramasamy, Arul Manikandan, Arun Sakthivel, Tanushree Paul, Manoj Kumar, Dipak Kumar Kanaujiya, Sudeshna Saikia, V. Divyabaskaran and Bharat Bhushan Negi for their help and support during my research work.

At last but not the least, I am thankful to my family and friends for their patience, understanding and encouragement. This would not have been possible without their unwavering and unconditional love and support given to me at all times for which I shall ever remain indebted.

December 2018 *Arindam Sinharoy*

IIT Guwahati

Contents

List of Figures

List of Tables

Abbreviations

AGS: anaerobic granular sludge

ANOVA: analysis of variance

APHA: American public health association

ATP: adenosine triphosphate

BOD: biological oxygen demand

BES: 2-bromoethano sulfonate

CH_4: methane

CO: carbon monoxide

CO_2: carbon dioxide

CoA: acetyl-coenzyme A

COD: chemical oxygen demand

CSTR: continuously stirred tank reactor

Df: Degree of freedom

F: Test static

F crit: Critical value

FBR: fluidized bed reactor

FETEM: field emission transmission electron microscopy energy dispersive X-ray spectroscopy

FESEM-EDX: field emission scanning electron microscopy

FTIR: Fourier transforms infrared spectrometer

GT-INP: green tea- iron nanoparticle

GTE: green tea extract

HRT: hydraulic retention time

H_2: hydrogen

H_2S: hydrogen sulfide

MS: Mean square

MW: Molecular weight

MBR: membrane bio-reactor

MSM: mineral salt media

P: probability 'P' value

PBS: Phosphate buffer saline

PBR: packed med reactor

PRESS: predicted residual error sum of squares

RTD: residence time distribution

R^2 Adj: adjusted R^2

SS: Sum of square

SRB: sulfate reducing bacteria

STP: sewage treatment plant

UV-vis: ultra violet-visible spectrophotometer

UASB: upflow anaerobic sludge blanket reactor

VFA: volatile fatty acid

XRD: X-ray diffraction

Notations

°C: degree centigrade

ΔG°: Gibbs free energy change

mmol/L: Mini mol per liter

µl: Micro liter

g: gram

h: hour

k_d: decay constant

K_i: inhibition constant

$k_L a$: volumetric mass transfer coefficient

KPa: Kilo Pascal

d: day

g/L: gram per liter

min: minute

ml/min: milliliter per minute

mg/L: milligram per liter

µM: Micro mol

µ: specific growth rate

μ_{max}: maximum specific growth rate

P_{CO}: partial pressure of CO

R^2: regression coefficient

rpm: rotational per minute

s: second

S/N: signal-to-noise ratio

v/v: volume/volume

w/v: weight/volume

Chapter 1

Introduction

1.1 Introduction

Energy crisis and environmental pollution are highlighted to be one of the major global problems in the 21st century. Over past centuries, massive increase in human population and industrial revolution has resulted in energy crisis, global climate change, environmental degradation and health problems (Kumari and Das, 2017). Therefore, greatest challenge for the researchers is to find alternative sources of energy and means to prevent and reduce environmental degradation. Due to which biotechnological products and processes using renewable resources have gained attraction during recent time. This study, therefore, focused on biological CO conversion for biohydrogen production and environmental applications.

Although CO is harmful, it is an excellent industrial feedstock for producing a wide range of useful products such as ethanol, methanol, diesel, hydrogen, acetic acid etc. The conventional process for CO conversion is catalytic or thermochemical, either utilize direct route such as Fischer-Tropsch process or indirect route like methanol carbonylation (methanol/CO/H_2) reaction water gas shift (WGS) reaction (Mahmoudi et al., 2018; LeValley et al., 2014). The WGS reaction is the basis for most of the industrial H_2 produced in the world from methane (CH_4) in natural gas through steam-methane reforming (Zhu and Wachs, 2015; Petrus and Noordermeer, 2006). Although catalytic process serves as a rapid route with high product yield, the process has its own disadvantages such as very high operating cost, restricted choice of metallic catalyst, perishable nature of the catalyst, high energy requirement, etc. (Venvik and Yang, 2017; Ail and Dasappa, 2016; Hahn-Hägerdal et. al., 2006).

Due to these limitations, cost-effective and novel technologies for CO conversion are the need of the hour. Also from an environmental and economical point of view, biological methods of CO conversion are of great interest. Over the past two decades various carboxydotrophic bacteria/archia capable of effective CO conversion have been reported

(Henstra et al., 2007). These bacteria are not only able to grow chemolithotrophically on CO but can also convert CO into commercially important compounds, such as hydrogen, ethanol, butanol, acetic acid, etc., under both thermophilic and mesophilic temperature conditions (Bender, 2011; Munasinghe and Khanal, 2010a). Among those products H_2 is attractive as it potentially provides an abundant, clean, secure and flexible energy carrier (Kalamaras and Efstathiou, 2013). H_2 is high in energy and yet engine using pure H_2 does produce any pollution. Use of H_2 in fuel cell where H_2 and O_2 combines to produce electricity makes its application more futuristic (Hallenbeck and Benemann, 2002). However, as fuel it is not yet competitive with fossil fuel economically and storage, performance, and reliability is still questionable (Kumar et al., 2017).

Another lesser explored application of biological CO conversion is the biodesulfurization, where H_2 rich gas produced from the process can directly be utilized as carbon source and electron donor by sulfate reducing bacteria (SRB). Sulfate rich wastewater generated by different industries, such as metal processing industry, mining industry, galvanic processes, flue gas desulfurization processes etc. are generally low in organic content (Hao et al., 2014; Sun et al., 2018). Hence, an efficient electron donor is necessary to enable the activity of SRB. Over the past decade, a lot of research has been undertaken to find cheap and efficient electron donors for biological treatment of inorganic sulfate rich wastewater (Liu et al., 2015). Many types of organic waste materials have been investigated as potential substrate for the SRB which includes molasses, whey, tannery effluents, dried algal biomass, solid waste materials, and sheep and poultry manures (Liamleam and Annachhatre, 2007; Sipma et. al., 2006). Despite the fact that all these organic substrates have been shown to stimulate sulfate reduction, their use in high-rate bioreactors is rather complicated due to their largely undefined composition and structure. Hence, organic waste materials seems to be less

suitable as electron donors; besides, they as their use would result in an additional pollution of the wastewater and this would require a supplementary treatment (Lens et al., 1998).

On the other hand, any H_2 produced through hydrogenogenic CO conversion may be consumed during the process start, particularly when using mixed microbial populations as the inoculum. Successful application of biohydrogen production implies the need to minimize undesired H_2 consumption (Sipma et. al., 2006). For practical applications, therefore, H_2 production combined with a desired H_2 consumption process, such as for biological sulfate reduction, might result in maximal utilization of H_2, provided the sulfate reducers can out-compete the other H_2 consuming microorganisms (Kumar et al., 2018). Only problem with this technology seems to be from CO toxicity towards SRB. However, several strains of SRB have been recently reported to be able to use CO as the sole carbon and energy source for biological sulfate reduction without much difficulty (Parshina et al., 2010).

Most of these carboxydotrophic sulfate reducers are extremophilies (Parshina et al., 2010) and therefore have high energy requirements to maintain suitable environmental condition, which makes the process scaleup and its commercialization rather difficult. Moreover, it is reported that mixed microbial consortium compared to pure culture are better in terms of CO utilization and resistance to CO toxicity. The poor aqueous solubility of CO is also a major concern as it limits its utilization by carboxydotrophic microorganisms.

Hence, there is a need to explore hydrogenogenic CO utilizing mesophilic organisms capable of sulfate reduction, which can convert CO as well as reduce sulfate present in wastewater utilizing the *in situ* produced H_2. Also, the effect of different process parameters, such as initial CO concentration, sulfate concentration, temperature, etc. on sulfate reduction using CO as the sole carbon and energy source should be evaluated in detail. The CO solubility improvement strategies also need to be looked into for achieving high process efficiency.

Moreover, to examine the scale up potential of this process suitable bioreactor system with gas liquid mass transfer of CO needs to be evaluated.

1.2 Aim and objectives

This study was aimed at biological carbon monoxide conversion for hydrogen production and environmental applications.

To accomplish this aim, the following investigations were carried out:

i. Screening, pathway elucidation, metagenomic analysis of anaerobic biomass and batch process parameter optimization for CO bioconversion and sulfate reduction

ii. Kinetics of biomass growth, substrate utilization and biohydrogen production from CO by anaerobic biomass

iii. Simultaneous removal of heavy metal and sulfate using CO as the sole carbon and energy source

iv. Evaluation of biologically synthesized nanoparticles for enhanced CO bioavailability for improving CO bioconversion and sulfate reduction

v. Performance evaluation of gas lift and moving bed biofilm bioreactor systems for hydrogenogenic CO conversion and sulfate reduction under continuous operation mode

1.3 Organization of thesis

The present work has been divided into seven chapters. The first chapter gives a general introduction, aim and objectives of this work. The Chapter 2 presents the available literatures on sources and properties of CO, conventional methods of CO conversion, biological CO conversion methods, different applications of CO bioconversion, bioreactors for CO

conversion, effect of various process conditions, methods to enhance CO solubility, etc. In Chapter 3, details on screening of anaerobic biomass capable of CO conversion, CO conversion pathway elucidation, effect of process parameters on CO conversion and sulfate reduction in batch system, microbial community analysis of the biomass are reported. In Chapter 4, the kinetics of biohydrogen production from CO, substrate utilization and biomass growth using anaerobic biomass is described. Chapter 5 describes the simultaneous removal of heavy metals and sulfate using CO as the sole carbon and energy source. Synthesis and characterization of GT-INP using green tea extract, and its effect on CO solubility, hydrogenogenic CO conversion and sulfate reduction are described in detail in Chapter 6. Chapter 7 reports the performance evaluation of gas lift reactor and moving bed biofilm reactor for hydrogenogenic CO conversion and sulfate reduction under continuous operation mode. The effect of different process parameters on reactor performance are also discussed in this chapter. Chapter 8 draws summary and appropriate conclusions based on the previous chapters. This chapter also provides some useful recommendations for future research in the relevant area.

Chapter 1

Literature review

2.1 Carbon monoxide

2.1.1 Properties and uses of CO

Carbon monoxide has properties that are similar to H_2, i.e. high reactivity, low solubility, high flammability and strong reducing potential (Bender et al., 2011). CO is highly combustible when mixed with air and, to a certain extent, it is even referred to as an explosive. Flammability of CO in the air ranges from 12.5 - 74 % by volume. Like any other gas the solubility of CO greatly depends on the surrounding temperature and partial pressure exerted on the headspace of the system. For instance, 22.66 ml kg^{-1} (1 mM) of CO is soluble in water at 20 ℃ and 1 atm. Carbon monoxide is simply CO_2 short of two moles of electron. In most cases, incomplete combustion of any organic material leads to the formation of carbon monoxide. CO is often considered as an electron donor and a strong reducing agent in heavy metal processing industry (O'Leary, 2000; Haynes, 2012). CO can cause harmful health effects by reducing oxygen delivery to the body's vital organs and tissues. Upon inhalation, CO displaces oxygen from the blood stream, thereby leaving the vital organs to oxygen deficit condition, a state often referred to as hypoxia (Ernst and Zibrak, 1998). Exposure to lower levels of CO is most serious for those who suffer from heart disease, and can cause chest pain, reduce the ability to exercise, or with repeated exposures, may contribute to other cardiovascular effects (Ndisang et al., 2004). Even healthy people can get affected by high levels of CO. People who breathe high levels of CO can develop vision problems, reduced ability to work or learn, reduced manual dexterity, and difficulty performing complex tasks. At very high levels, CO is poisonous and can cause death. The environmental protection agency (EPA) guidelines restrict the maximum allowed concentration of CO as 9 ppm for an eight hour exposure period and 35 ppm for one hour exposure period (OSHA, 2002). Although CO is toxic to most organisms, anaerobic bacteria,

particularly carboxydotrophs, are well known for their ability to utilize CO as the sole source of carbon and energy.

2.1.2 Natural sources

In nature, methane oxidation due to the hydroxyl radicals present in the atmosphere is one of the main source of CO, which mostly occurs on the surface of the soil. Oxidation of organic compounds such as phenolics and humic acids in the absence of light can also lead to the formation of CO. CO formation is affected due to temperature fluctuations in the atmosphere. For example, the process of organics conversion to CO is higher at 60ºC than at 20ºC (Tranvik, 1996). Another important natural source of CO is volcanic eruption, during which eruption gases may contain 1-2% of CO. Other natural sources of CO emission include numerous reactions occuring in the world's oceans and forest fires. Further, it is speculated that unless a major CO degradation could take place in the atmosphere the ambient concentration of CO present in the atmosphere will multiply after every half a decade (Conrad, 1988; Conrad and Seiler, 1985).

There are varieties of biotic factors in the environment which are responsible for carbon monoxide emission to the biosphere. Predominantly, heme oxygenase and heme oxygenase-like activity in mammals, plants and lower animals are evident for CO emission. Further, through developmental genetics, it is understood that these enzymes are found to be ubiquitous in nature and conserved across millions of organisms during its evolution from their direct ancestors (O'Leary, 2000). Some other few biotic factors include biological oxidation and auto-oxidation of organic compounds, such as phenols, halomethanes and flavenoids along with the lipid peroxidation of membrane lipids. It is observed that each molecule of heme degrades to give one molecule of bilirubin and one mole of CO. The evolved CO is then transported to the blood and excreted in the lungs. Hence, measuring the

exhaled CO is an indirect measure of end-tidal CO concentration and blood COHb levels (Rodgers, 1994).

Few thermophilic acetogenic species under the bacterial kingdom and some methanogenic species under the archaea kingdom are known to produce fewer amounts of carbon monoxide. Lupton *et* al. (1984) in their study found that a small quantity of CO is produced by *Desulfovibrio vulgaris* and *Desulfovibrio desulfuricans* when grown under heterotrophic conditions. The CO production was observed during the analysis of vent gas from an anaerobic digester fed with waste activated sludge. Further, the produced CO was found to be consumed by the organisms when the substrate in the digester was almost depleted. The CO produced during the anaerobic digestion process was solely due to the action of CO dehydrogenase enzyme found in few methanogens. However, a considerable amount of CO production cannot be observed in anaerobic digestion as most of the methanogens are found to be devoid of CO dehydrogenase activity (Bander, 2011; Conrad, 1988).

2.1.3 Anthropogenic sources

In addition to a few production processes and laboratory activities, the major intervention of humans in carbon monoxide emission is through combustion of solid, liquid and gaseous fuels (Sipma et al., 2010). An excess amount of air/oxygen in the combustion process completes the burning of fuels, which results in the formation of carbon dioxide, water and other oxides. Whereas, incomplete combustion of fuels due to inadequate air/oxygen supply results in the emission of CO. Major anthropogenic sources of CO include exhaust from vehicles, portable generators, natural gas space heaters, gasoline-powered tools (for example, chop saws), kilns, furnaces, and boilers, fires and explosions, welding and even by smoking of cigarettes (Fig. 2.1) (Webster et al., 1999).

Several industrial processes also produce CO as a waste. But there are few industries, which use CO as the main stream feedstock: fuel gas mixtures - water gas (44% CO), producer gas (34% CO), blast furnace gas (30% CO), coal gas or illuminating gas (7.4% CO); hydrocarbon synthesis; ethylene, esters, alcohols and aldehydes, acids, recovery of metals from ores, reducing oxides, metals of high purity and hydrogenation of fats and oils, etc (IAPA, 2008). Among these different anthropogenic sources of CO, synthesis gas is important as it is cheaply available, renewable and can be produced onsite from any type of carbonaceous materials. Fig. 2.1 shows the typical CO emission at different natural and anthropogenic sources.

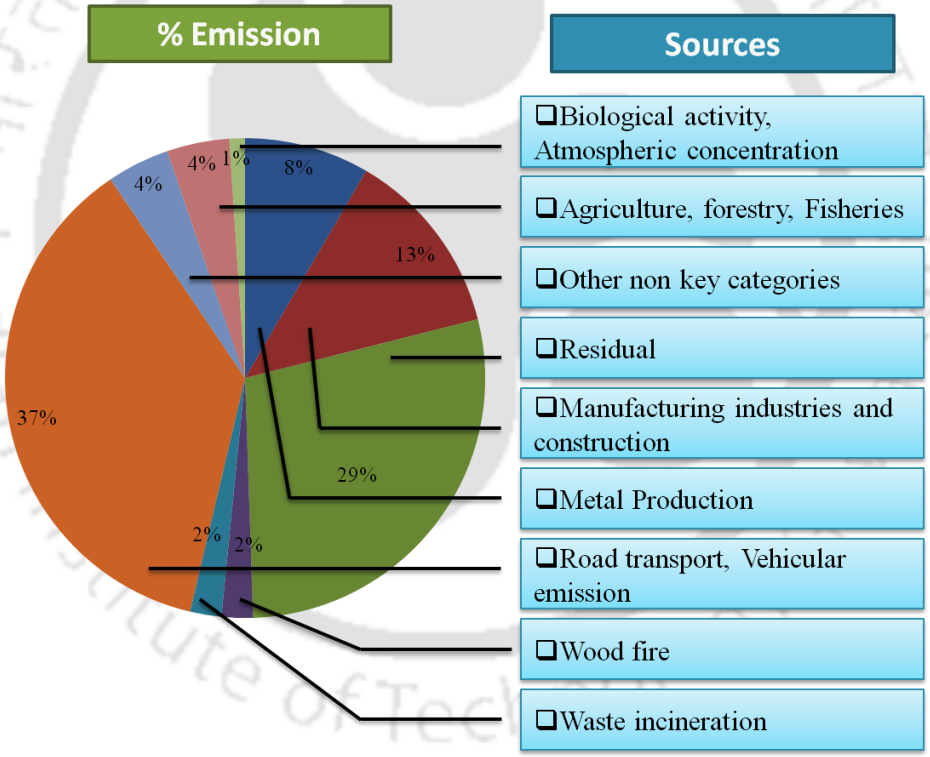

Fig. 2.1 Typical CO emission from different sources (US EPA, 2015).

2.1.4 Synthesis gas

Synthesis gas is mainly composed of carbon monoxide (CO), methane (CH_4), hydrogen (H_2), carbon dioxide (CO_2), nitrogen (N_2) and some higher hydrocarbons. Among these gases, CO

is the major component, due to which syngas is often referred to as a strong source of CO. Usually the CO concentration in the syngas mixture ranges from 5-60%, which can be further steam reformed to get H_2 upto some extent (Datar et al., 2004). Since, the biomass gasification is an endothermic process and requires heat energy as an input, gasification of organic compounds is often carried out at an elevated temperature of 750 - 800 °C (Alauddin et al., 2010). Coal, petroleum, coke, lignocellulosic biomass and even municipal waste are considered as the feedstock for biomass gasification process (Mohammadi et al., 2011). For an efficient gasifier operation, a certain amount of feedstock homogeneity should be maintained. If the feedstock is heterogeneous in nature, then the product composition may change widely. In order to overcome this drawbacks a few pre-treatment and post-treatment steps need to be included in the gasification process, which make the process more uneconomical (Ganigue et al., 2016). For this reason, fossil fuels, waste plastics and homogeneous lignocellulosic materials, such as timber industry waste, paper mill waste and agricultural residues, etc., were used as the potent feedstock for biomass gasification. Usage of municipal waste is still under consideration as it comes with a variety of materials mixed with it (Alauddin et al., 2010).

2.2 Thermocatalytic CO conversion

A number of thermo-chemical catalytic processes such as water gas shift reaction, Fischer–Tropsch (FT) synthesis, etc. can be applied for converting CO to valuable products, as shown in Fig. 2.2. Most of these methods operate at high temperature and pressure conditions and need catalysts. Some of these important methods are discussed further.

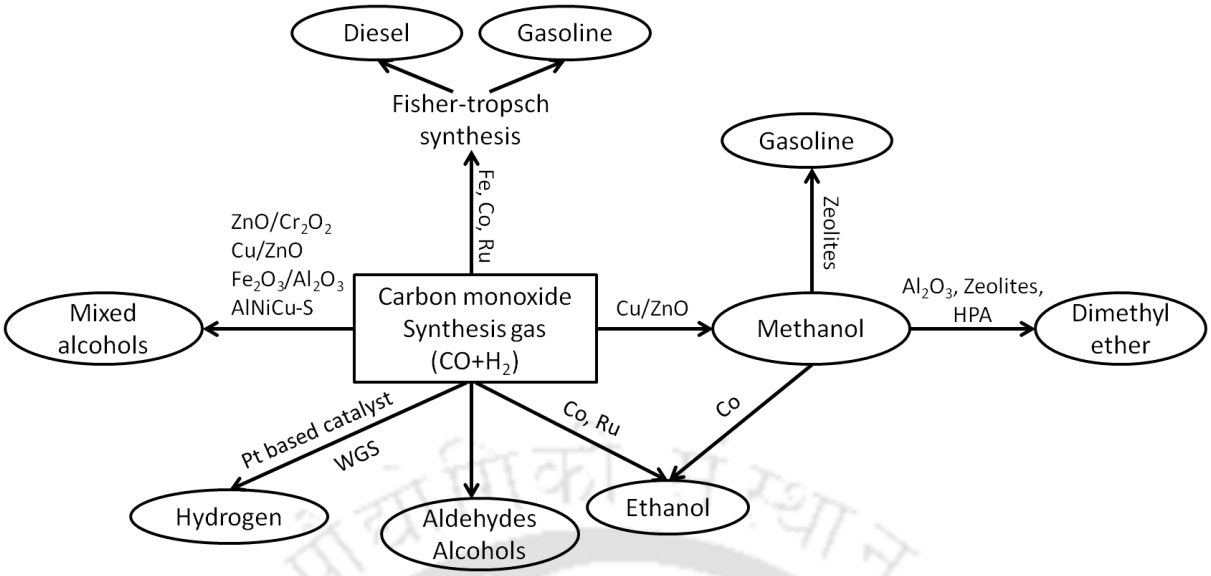

Fig. 2.2 Thermo-chemical catalytic CO conversion to different products (Subramani and Gangwal, 2008).

2.2.1 Water-gas shift reaction

CO is most often used as the feed source for hydrogen production and this process of converting CO to H_2 is called water-gas shift (WGS) reaction (RJ et al., 2010). In this reaction, the carbon monoxide (CO) upon reacting with water (H_2O) in presence of a metallic catalyst gives hydrogen (H_2) and carbon dioxide (CO_2) as the main product (Mendes et al., 2010). The water-gas shift reaction is represented as follows (Eq. 2.1).

$$CO + H_2O \rightarrow CO_2 + H_2 \quad \text{……..(2.1)}$$

The aforementioned reaction is mostly preferred when removal of CO from the gas stream is required along with the H_2 production. The reaction is found to be exothermic, which means that the reaction can spontaneously move towards the forward direction even at lower temperatures (Lin et al., 2013). This reaction is also widely known for H_2 production using methane, wherein the methane is first reformed to CO, H_2 and CO_2 in presence of a catalyst (Pakhare and Spivey, 2014). Later, a conventional water-gas shift reaction is carried out in

presence of a metallic catalyst as per eq. 2.1. which enriches the H_2 concentration and removes CO from the inlet. Though the process is referred as exothermic and tangible at lower temperatures, the reaction is carried out at an elevated temperature to increase the rate of CO conversion and H_2 production. The reactor in which these reactions are carried out is called as high-temperature shift (HTS) reactor and the temperature in this reactor often ranges from 350-370°C. Almost 90% of CO is converted to H_2 in this process, whereas a small amount of unreacted CO left out from the HTS process is converted in a low-temperature shift (LTS) reactor operated at 200-220°C (Mendes et al., 2010). The exhaust coming out of the entire process is composed of mainly H_2 leaving only traces of CO (Kirk-Othmer, 1995; Ulllman's, 1989).

These traces of CO are removed and purified H_2 is produced by passing the gas through a CO_2 scrubbing tower, which removes all the CO_2, and the residual CO upon reaction with H_2 forms methane. This reaction is called as methanation reaction and it is shown in Eq. 2.2:

$$CO + 3H_2 \longrightarrow CH_4 + H_2O \quad \text{……..(2.2)}$$

Usually most of the CO left out in the HTS will be converted in the LTS. Otherwise, in the metahanation process, each mole of remaining CO will consume 3 moles of H_2, thereby leaving the product less concentrated with H_2. Instead of methanation, pressure-swing adsorption (PSA) process could be carried out in which both the remaining CO and CO_2 are cleaned without the necessity for a methanation reaction, as it enhances the product purity and reduces the overall system cost.

2.2.2 Fischer-Tropsch (FT) reaction

A wide range of useful hydrocarbons can be produced from a gas mixture of CO and H_2 by Fischer–Tropsch (FT) reaction as shown in Eq. 2.3. (Tsakoumis et al., 2010)

$$CO + 2H_2 \longrightarrow -CH_2- + H_2O \quad \text{……(2.3)}$$

This $–CH_2–$ acts as a precursor for producing other long-chain hydrocarbons such as diesel, kerosene, gasoline, etc. A number of industries in different countries employing this technology for commercial production of liquid fuel from coal or natural gas derived syngas (Yang et al., 2014). But this reaction takes place at high pressure (20 to 40 bar) and high temperature (180 and 250 °C) conditions and in the presence of cobalt catalyst. Besides, the process requires a very specific H_2 to CO ratio of 2:1, which is quite difficult to achieve as syngas contains H_2 and CO in the ratio in the range 0.45 - 2 depending upon gasification method and substrate used (Jahangiri et al., 2014). In case of this ratio being too low, an additional step of water-gas shift reaction may be necessary to improve H_2 concentration in syngas (Ail and Dasappa, 2016).

2.2.3 Hydrogenation reaction

Methanol can be produced by hydrogenation reaction of CO or CO_2 as shown in the following reactions (Bonura et. al., 2014; Breen et al., 1999) (Eqs. 2.4 & 2.5)

$$CO + 2H_2 \longrightarrow CH_3OH \quad \text{……..(2.4)}$$

$$CO_2 + 3H_2 \longrightarrow CH_3OH + H_2O \quad \text{……..(2.5)}$$

Apart from being a clean fuel methanol can used for producing biodiesel by reacting it with triacylglycerols. Dimethyl ether **(**DME) is synthesized by further dehydration of methanol as per the following reaction (Eq. 2.6) (Ogawa et. al., 2004)

$$2CH_3OH \longrightarrow CH_3OCH_3 + H_2O \quad \text{……..(2.6)}$$

The molar ratios of H_2/CO and CO_2/CO also play a critical role in these reactions and hence need to be optimized. Various researchers have reported use of different Cu, Zn, Al, Cr based catalyst to improve methanol or DME yield from syngas (Iwasa et al., 1998).

2.2.4 Ethanol production

The chemical reaction for producing ethanol form syngas is similar to that for methanol production and it occurs at a high pressure and high temperature condition. But it requires different catalyst than that for methanol; conventional sulfide-type mixed alcohol catalyst and Rh-based catalyst give optimum results (Kharas and Durand, 2011). Extensive gas cleaning is required before using any feed gas as some of these catalysts are extremely sensitive to CO_2 (>7% *v/v*). The reactor effluent consists of mixed alcohols (including higher alcohols such as propanol and butanol), gaseous byproducts such as CH_4 and CO_2, and unconverted syngas (Gong et. al., 2012). This hot stream is cooled to condense out the alcohols for separation and the unreacted syngas can be used either as a fuel, or recycled back to any gas reformers, or recycled back to the alcohol synthesis reactor (after any required cleaning or compression) (Fernando et. al., 2006).

Though the thermo-catalytic process has been commercialized and works successfully in all installed plants, it has several disadvantages such as high operating cost, limited choice of metallic catalysts, perishable nature of the catalyst, huge requirement of heat energy, environmental concern, etc. (Clark, 2007). Furthermore, these catalyst based processes are often prone to catalyst poisoning due to generation of unwanted gases such as hydrogen sulfide and other inhibitory substances (Huang et. al., 2008). All these disadvantages have resulted in the need for better alternative technologies. Biological methods using different carboxydotrophic bacteria seems to be a good alternative as it offer certain advantages such as high tolerance to trace contaminants, high product specificity and environmental friendly.

2.3 Biological CO conversion methods

Carboxydotrophic microorganisms are a special kind of microorganisms with an inherent capability to utilize CO as both carbon and energy source. These bacteria are known to

produce a variety of products from CO, which include hydrogen, methane, carbon dioxide, butanol, ethanol, acetic acid, etc. In addition, these biocatalysts are not prone to poisoning effect as in the case of chemical catalyst. Unlike chemical catalyst, these biocatalyst can resist the poisoning effect posed by trace contaminants as they are metabolized further for product formation. For instance, sulphur compounds present in the gas stream can be used as a nutrient source to lower the redox potential of the culture medium, enhance the biomass growth and finally resulting in acetic acid production (Vega et al., 1990). Irreversibility and very high specificity of biological CO conversion make this process more attractive than the chemical processes (Klasson et al., 1992).

CO conversion can be carried out by a wide variety of microorganisms, which can be broadly classified as aerobic and anaerobic species; this classification is based on the enzyme system used for CO biotransformation. The aerobic CO utilizing microorganisms can further be classified into metabolic and co-metabolic groups. The metabolic group of CO utilizing organism uses CO as an energy source for its growth. Whereas in the case of co-metabolic group of CO utilizing organism the CO is used as a pseudo-substrate for its enzyme system (Hanstra et al., 2010).

Incase of an energy yielding CO metabolism, the aerobic CO converting organisms oxidize CO and results in the formation of CO_2 and biomass. Whereas, anaerobic CO converting organisms convert CO through a complex pathway resulting in a variety of valuable compounds (Morsdorf et al., 1992; Meyer et al., 1990). The key enzyme involved in the process of CO conversion is commonly referred as carbon monoxide dehydrogenase (CODH). The reversible reaction catalysed by the CODH is as follows (Eq. 2.7):

$$CO + H_2O \rightarrow 2H^+ + CO_2 + 2e^- \quad \text{..... (2.7)}$$

Different carboxydotrophic bacteria, which can utilize CO as the sole source of carbon and energy are presented along with their products and biochemical reactions in Table 2.1.

There are several other classes of anaerobic bacteria known to metabolize CO using a distinct pathway, which include hydrogenogens, homoacetogens, sulfate reducers and methanogens. The homoacetogens follow the reductive acetyl-CoA pathway to convert CO into acetate involving CO_2 as an electron acceptor, as shown in Fig. 2.3 (Wood et al., 1991). In this pathway, two moles of CO_2 combine to form an acetyl portion of the acetyl-CoA and the main product is acetate. But homoacetogens are also known to produce a wide range of compounds, including butanol, ethanol and butyrate from CO conversion.

Similar to homoacetogens, methanogens are also reported to fix CO via the reductive acetyl-CoA pathway. This pathway has an assimilatory role in autotrophic methanogens, in which a part of the CO_2 reduction steps is employed for methanogenesis. Unlike the other classes of organisms, a very less number of methanogenic species are studied to grow on CO as the sole source of energy. In methanogens, CO conversion takes place with the production of H_2 and CO_2 as the intermediates (Sipma et al., 2006; Davidova et al., 1994).

Sulfate reducing bacteria are well known for H_2 production from CO, which is indirectly used for sulfate reduction. This type of sulfate reduction through hydrogen production is advantageous as in the absence of sulfate the process of CO to CO_2 and H_2 probably acts as a CO detoxification pathway. This is because the process of H_2 generation does not result in ATP synthesis, due to which there is no growth on utilizing CO as the carbon source (Parshina et al., 2010).

Table 2.1 Various classes of CO utilizing bacteria, their products and biochemical reactions

Type of organism	Example	Biochemical reaction	Product	Reference
Homoacetogen	*Clostridium ljungdahlii*, *Clostridium carboxidivorans*, *Clostridium autoethanogenum*, *Clostridium ragsdalei*, *Alkalibaculum bacchii*, *Clostridium thermoaceticum*	$6CO + 3H_2O \rightarrow CH_3CH_2OH + 4CO_2$ $2CO_2 + 6H_2 \rightarrow CH_3CH_2OH + 3H_2O$ $4CO + 2H_2O \rightarrow CH_3COOH + 2CO_2$ $2CO_2 + 4H_2 \rightarrow CH_3COOH + 2H_2O$ $6CO + 6H_2 \rightarrow 2CH_3CH_2OH + 2CO_2$	Ethanol, butanol, acetic acid, butyric acid	Younesi et al., 2005; Hurst and Lewis, 2010; Abubackar et al., 2016; Kundiyana et al., 2011a
Hydrogenogen	*Rhodospirillum rubrum* , *Rubrivivax gelatinosus*, *Citrobacter* sp. Y19, *Rhodopseudomonas palustris* P4, *Carboxydothermus hydrogenoformans*, *Carboxydocella thermautotrophica*	$CO + H_2O \rightarrow CO_2 + H_2$	Hydrogen	Najafpour et al., 2004; Pakpour et al., 2014; Haddad et al., 2014; Weghoff et al., 2016
Methanogen	*Methanobacterium formicicum*, *Methanobrevibacter smithu*, *Methanosarcina barkeri*, *Methanobacterium thermoautotrophicum*	$4H_2 + CO_2 \rightarrow CH_4 + H_2O$ $4CO + 2H_2O \rightarrow CH_4 + 3CO_2$	Methane	Daniels et al., 1977; Ferry, 1999
Sulfate reducers	*Desulfovibrio africanus*, *Desulfovibrio baculatus*, *Desulfosporosinus orientis*, *Desulfovibrio desulfuricans*	$4CO + SO_4^{2-} + 4H_2O \rightarrow 4HCO_3^- + HS^- + 3H^+$ $4H_2 + SO_4^{2-} + H^+ \rightarrow HS^- + H_2O$	Sulfide, hydrogen	Parshina et al., 2010; Sipma et al., 2006

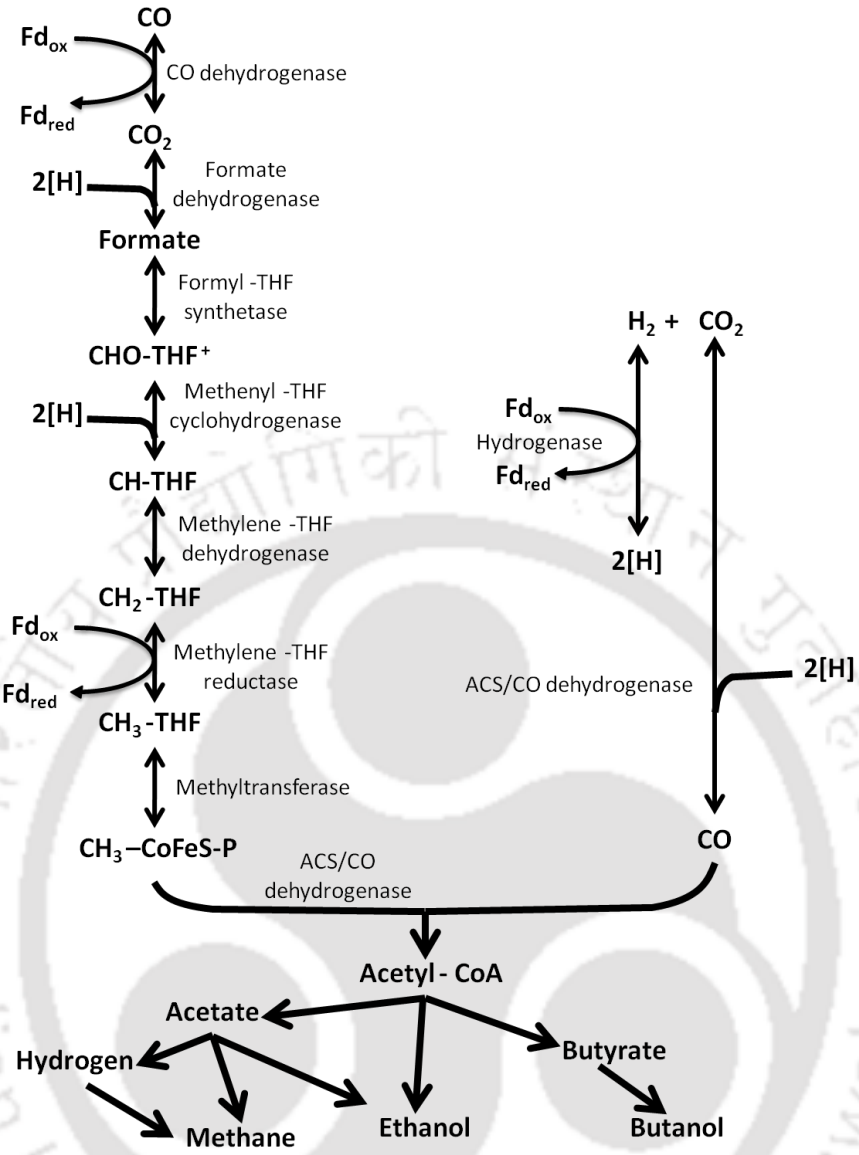

Fig. 2.3 Biochemical pathway for CO bioconversion to different products (CH-THF: methylenetetrahydrofolate, CH_2-THF: methenyltetrahydrofolate, CH_3-THF: methyltetrahydrofolate).

2.4 Potential applications of CO bioconversion

2.4.1 Bioenergy applications

Most of the research work on fermentation of CO or CO rich syngas has focused on ethanol production, but other products such as butanol, hydrogen, methane, etc. can also be obtained by using suitable CO converting microorganisms. Integration of these biofuels and other

value added products with waste resources as feedstock would improve the commercial viability of the CO conversion process. Fig. 2.4 provides a general schematic of CO bioconversion for biofuel production.

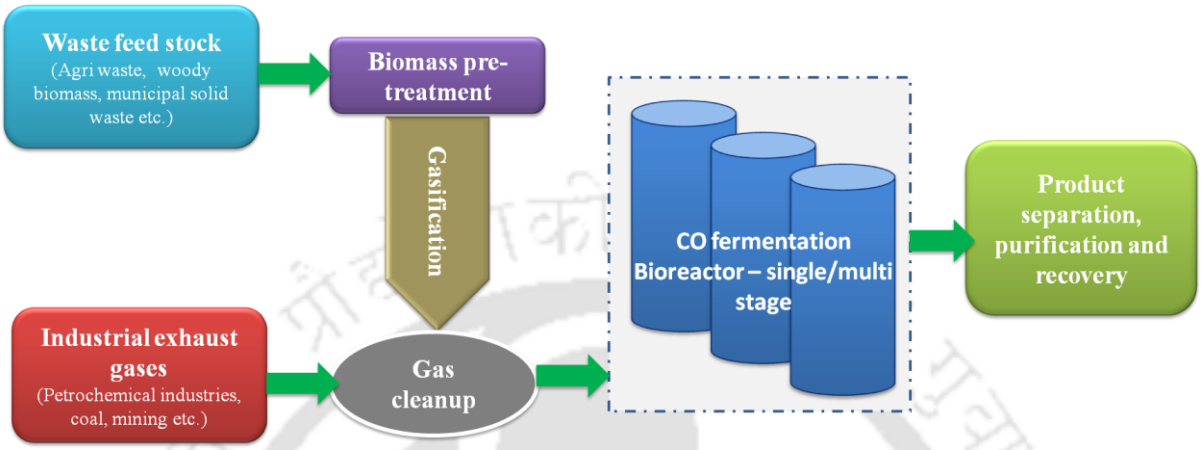

Fig. 2.4 Process outline of biofuel production from CO.

2.4.1.1 Hydrogen production from CO

Hydrogenogenic microorganisms use CO as the sole source of carbon and energy to form equimolar amounts of CO_2 and H_2, similar to the catalytic water gas-shift reaction described earlier. However, the H_2/CO_2 does not support growth of the organisms (Sipma et al., 2006). Over the past decade, a number of hydrogenogens have been reported (Table 2.2), which are mainly classified into three different groups: mesophilic Gram-negative bacteria, thermophilic Gram-positive bacteria and thermophilic archaea.

Gram negative mesophilic bacteria are facultative in nature, but produce H_2 from CO strictly under anaerobic environment. These are mostly non-sulfur purple photosynthetic bacteria, including *Rhodopseudomonas gelatinosa*, *Rhodocyclus gelatinosa*, *Rubrivivax gelatinosus*, *Rhodospirillum rubrum*, etc.

Among these bacteria, *R. rubrum* is well studied including its genetic makeup, enzyme system and even employing suitable reactor systems. The optimum temperature and pH for

growth of this organism are in the range of 34-40 ^{o}C and 6.5-7.5, respectively. In general, high levels of CO are inhibitory to this class of bacteria. Another problem is the additional cost due to light requirement. Other than these phototrophic organisms, certain nonphototrophic gram negative anaerobes capable of converting CO to H_2 have been reported. These are *Citrobacter* strain Y19, isolated from an activated sludge plant (Jung et al., 1999), anaerobic microbial consortia predominantly *Petrobacter* sp. (Pakshirajan and Mal, 2014).

A large number of carboxydotrophic hydrogenogenic bacteria are extremophilies, isolated from extreme environmental conditions such as hot spring, submarine hot vent, etc. This group of bacteria is mainly anaerobic prokaryotes of *Bacillus/Clostridium* subclass. Some examples of these bacteria are *Carboxydothermus hydrogenoformans, Carboxydobrachium pacificum, Thermincola carboxydophila, Thermosinus carboxydivorans*, etc. The optimum temperature and pH for the bacteria are in the range of 50-90 ^{o}C and 6.8-8.0, respectively. The use of thermophilic organism is more advantageous for using syngas as substrate, as the temperature of syngas exiting a gasifier is around 700 to 800 ^{o}C.

The cost of bringing down the temperature of syngas to moderate range can be avoided in this case, though the high energy requirement of maintaining large scale reactor at elevated temperature is still not economically feasible. Though a large number of archaea have been isolated from extreme temperature environments, only a few of these are capable of chemolithotrophic growth on CO and can produce H_2, which includes *Thermococcus* AM4, *Thermofilum carboxyditrophus* (Sokolova et al., 2009).

Table 2.2 Hydrogen production by different organisms from CO

Organisms	Experimental conditions				Substrate		Products		References
	Experimental setup	Temp °C	pH	Agitation (rpm)	Initial CO conc.	Extra carbon source	H_2 production rate /yield	Other products	
Rhodospirillum rubrum	Batch serum bottle	30	6.9	200	55 % (v/v) CO	Acetate	85.7 % mol/mol of CO	NR	Najafpour et al., 2004
Rhodospirillum rubrum	Continuous stirred tank reactor	30	6.5	NR	P_{CO} = 0.55 atm	Acetate	16 mmol H_2/h	NR	Najafpour et al., 2003
Rhodospirillum rubrum	Continuous stirred tank reactor	30	6.9	350-800	55 % (v/v) CO	Malic acid/ sodium acetate	9.6 mmol H_2/h	NR	Ismail et al., 2008
Rhodospirillum rubrum	Continuous stirred tank reactor	30	6.9	150-500	55 % (v/v) CO	Malic acid/ sodium acetate	80 % mol/mol of CO	NR	Younesi et al., 2008
Rhodospirillum rubrum	Continuous stirred tank reactor	30	7.0	400-750	17.2% CO	Acetate	0.75 mol H_2/day	Poly-β-hydroxyalkanoate	Do et al., 2007
Thermoanaerobacter kivui	Batch serum bottle	60	7.5	NR	100 % (v/v) CO	NR	45 mmol/L	Acetic acid	Weghoff and Müller, 2016
Rubrivivax gelatinosus	Batch serum bottle	30	7.0	250	20 % (v/v) CO	Sodium malate	0.9 mmol/ min/ g cell	NR	Vanzin et al., 2002
Rubrivivax gelatinosus	Batch serum bottle	30	7.0	250	20 % (v/v) CO	Sodium malate	1.0 mmol/ min/ g cell	NR	Maness et al., 2005
Rubrivivax gelatinosus	Batch serum bottle	30	7.0	NR	17% (v/v) CO	NR	263 mmol of H_2 /min / mg of cells DW	NR	Maness et al., 2002
Rhodopseudomonas palustris P4	Batch serum bottle	30	7.0	NR	60 % (v/v) CO	Sodium acetate	7 mmol/L	NR	Pakpour et al., 2014
Rhodopseudomonas	Batch serum	30	NR	NR	20 % (v/v)	NR	25 mmol/g cell/h	NR	Jung et al.,

palustris P4	bottle				CO				1999a
Rhodopseudomonas palustris P4	Continuous stirred tank reactor	30	7.0	500-700	20 % (v/v) CO	NR	41 mmol/g cell/h	NR	Oh et al., 2005
Citrobacter sp. Y19	Batch serum bottle	25-40	5-9	250	NR	Glucose	32.3 mmol H_2/g cell/ h	ethanol, acetic acid	Oh et al., 2003
Citrobacter sp. Y19	Batch serum bottle	30-40	5-8	250	20 % (v/v) CO	Sucrose	27.1 mmol H_2/g cell/ h	NR	Jung et al., 2002
Citrobacter sp. Y19	Batch stirred tank reactor (two stage)	30	7	300-700	2.5 -10 % (v/v) CO	Sucrose	20 mmol/g cell/h	NR	Jung et al., 2002
Carboxydocella thermautotrophica	Batch serum bottle	50-70	6.8	NR	100 % (v/v) CO	NR	0.2 mmol/ml	NR	Sokolova et al., 2002
Carboxydothermus hydrogenoformans	Continuous gas-lift reactor	70	6.8-7.2	NR	0.05 to 0.46 mol/L reactor /day	bacto-peptone	95 % mol/mol of CO	NR	Haddad et al., 2014
Carboxydothermus hydrogenoformans	hollow fiber membrane bioreactor	60-70	6.8-7.0	Nil	100 % (v/v) CO	NR	92% mol/mol of CO	Acetic acid	Zhao et al., 2013
Carboxydothermus hydrogenoformans	Batch serum bottle	65	7.0	100	100% (v/v) CO	NR	NR	Acetic acid	Henstra and Stams, 2011
Carboxydothermus hydrogenoformans	Batch serum bottle	70	6.8-7.0	100	100% (v/v) CO	NR	90.9% mol/mol of CO	NR	Zhao et al., 2011a
Carboxydothermus hydrogenoformans	Batch serum bottle	70	6.8-7.0	100	100% (v/v) CO	NR	98% mol/mol of CO	NR	Zhao et al., 2011b
Carboxydothermus pertinax	Batch serum bottle	50-70	6.0-6.5	NR	100% (v/v) CO	Ferric citrate	NR	NR	Yoneda et al., 2012
Moorella stamsii	Batch serum bottle	65	7.5	NR	100% (v/v) CO	NR	NR	NR	Alves et al., 2013
Anaerobic granular sludge biomass	Batch serum bottle	55	7.5	300	P_{CO} = 0.2 atm	NR	0.25 ± 0.05 mmol/L	Acetate and methane	Liu et al., 2016

NR: Not reported

2.4.1.2 Alcohol production from CO

Some of the carboxydotrophic acetogens are capable of producing alcohols along with volatile fatty acids from CO. These classes of bacteria are obligate anaerobes and can utilize CO or CO_2 as the sole carbon and energy source. Some of such solventogenic carboxydotrophic bacteria are *Clostridium ljungdahlii, Clostridium carboxidivorans, Clostridium autoethanogenum, Clostridium ragsdalei, Alkalibaculum bacchi, Eubacterium limosum, Butyribacterium methylotrophicum, Clostridium thermoaceticum and Clostridium formicoaceticum*, etc. Table 2.3 provides a list of various alcohol producing homoacetogens along with their characteristics and culture conditions. Most of these microorganisms can grow on multiple carbon sources, but their potential to utilize gaseous substrates, such as CO, CO_2 and H_2 and produce useful products make them commercially important. All of these strains are capable of producing ethanol, butanol and acetic acid, utilizing CO as the sole carbon substrate.

Some strains such as *Clostridium ragsdalei* and *Clostridium propionicum* are reported to produce propanol from syngas. The biochemical pathway used by these bacteria for the production of ethanol is reductive acetyl-CoA pathway or Wood-Ljungdahl pathway (Fig. 2.3). The Wood-Ljungdahl pathway is followed by several organisms including homoacetogenic bacteria and methanogenic archea. It consists of two branches, eastern branch and western branch. The eastern branch has a number of reductive steps where CO_2 is reduced to produce the methyl group of acetyl-CoA. Whereas, in the western branch, CO is obtained from CO_2 or directly from carbonyl group for the acetyl-CoA synthesis.

Table 2.3 Ethanol production by different organisms using CO

Organisms	Experimental conditions				Substrate		Products		References
	Exp. setup	Temp ºC	pH	Agitation (rpm)	Initial CO conc.	Any other carbon substrate	Ethanol concentration /yield	Other products	
Clostridium ljungdahlii	Batch serum bottle	37	NR	180	55%	Fructose	0.41 g/g of CO	Acetic acid	Younesi et al., 2005
Clostridium ljungdahlii	CSTR	37	NR	450	55%	Fructose	NR	Acetic acid	Aghbashlo et al., 2016
Clostridium ljungdahlii	Batch serum bottle	37	NR	200	20%	NR	0.5 g/L	Acetic acid	
Clostridium carboxidivorans P7									
Clostridium carboxidivorans	Batch stirred reactor	37	6.15	120	80%	NR	2.6 g/g of cells	Acetic acid	Hurst and Lewis, 2010
Clostridium carboxidivorans	Monolithic biofilm reactor	37	6.0	NR	20%	Fructose	0.17 mole/ mole of CO	Acetic acid	Shen et al. 2014
Clostridium carboxidivorans	Horizontal rotating packed bed biofilm reactor	37	6.0	NR	20%	Fructose	7 g/L and 6.7 g/L/d	Acetic acid	Shen et al., 2017
Clostridium carboxidivorans	Batch serum bottle	37	6.0	150	70%	NR	3.0 g/L	Butanol and hexanol	Phillips et al., 2015
Clostridium carboxidivorans	Batch serum bottle	37	6.0	100	70%	acetic acid, butyric acid, hexanoic acid, ethanol or butanol	NR	Acetic acid, butanol	Zhang et al., 2016
Clostridium carboxidivorans	Batch serum bottle	37	6.0	100	56%	NR	4.07 g/L	Butanol and hexanol	Shen et al., 2017

Clostridium autoethanogenum	CSTR	30	6.0	250	100%	Xylose (under mixotrophic condition)	7.143 g/L	Acetic acid	Abubackar et al., 2016
Clostridium autoethanogenum	CSTR	30	6.0	250	30%	NR	2.22 g/l	Acetic acid and 2,3-butanediol	Lagoa-Costa et al., 2017
Clostridium autoethanogenum	CSTR	30	6.0	250	100%	NR	907.72 mg/L	Acetic acid	Abubackar et al., 2015
Clostridium autoethanogenum	Batch serum bottle	30	6.0	150	100%	NR	0.65 g/L	Acetic acid	Abubackar et al., 2012
Clostridium ragsdalei	Batch serum bottle	32	6.0	150	20%	NR	1.89 g/L	Acetic acid	Kundiyana et al., 2011a
Clostridium ragsdalei	Two stage CSTR	32	6.0	NR	40%	NR	14.74 g/g of cells	Acetic acid	Kundiyana et al., 2011b
Clostridium ragsdalei	Batch serum bottle	37	5.5	150	20%	NR	11 g/g of cells	Acetic acid	Gao et al., 2013
Clostridium ragsdalei	CSTR	37	6.1	150	20%	NR	9.6 g/L	Acetic acid	Maddipati et al., 2011
Clostridium ragsdalei	trickle bed reactor	37	5.8	NR	38%	NR	5.7 g/L	Acetic acid	Devarapalli et al., 2016
Clostridium ragsdalei	CSTR (pilot scale 100L)	37	6.0	150	20%	NR	25.26 g/L	2-propanol, Acetic acid, 1-butanol	Kundiyana et al., 2010
Alkalibaculum bacchi	Serum bottle – fed batch mode	37	8.0-8.5	150	20% and 40%	NR	1.75 g/L	Acetic acid	Liu et al., 2012
Alkalibaculum bacchi	Batch serum bottle	37	8.0	150	20 %	Corn steep liquor	6 g/L	Acetic acid	Liu et al., 2014a
Alkalibaculum bacchi	CSTR	37	8.0	NR	20-40%	Corn steep liquor	8 g/L	Acetic acid, n-propanol and n-butanol	Liu et al., 2014b
Anaerobic mixed consortium	Batch serum bottle	37	6.0	100	P_{CO} = 2 kg/cm^2	NR	2.2 g/L	Acetic acid	Singla et al., 2014

NR: Not reported

There are two ways to generate reducing equivalent for the pathway. Most commonly, hydrogenase enzyme supplies the reducing equivalent from H_2 using the following reaction (Eq. 2.8).

$$H_2 \longrightarrow 2H^+ + 2e^- \quad \text{……..(2.8)}$$

However, when there is inadequate amount of H_2 gas available or inhibition of hydrogenase enzyme occurs, CODH enzyme generates reducing equivalent by oxidation of CO to CO_2 as per the following reaction (Eq. 2.9).

$$CO + H_2O \longrightarrow CO_2 + 2H^+ + 2e^- \quad \text{……..(2.9)}$$

Almost all these organisms are mesophilic in nature, but media pH is found to have a great impact on the product formation. In most cases, low pH range tends to favour solventogensis over acetogenesis. Hence, recent research work is focused on examining different ways to increase the alcohol production over acids and on the culture stability throughout its growth on syngas.

2.4.1.3 Methane production from CO

Methane can be produced under anaerobic condition from any carbonaceous material, including acetate, lactate, formate, lignocellulosic matter, gaseous substrate such as H_2/CO_2, etc. But a few methanogenic organisms capable of utilizing CO as the sole carbon and energy source have been reported. From the literature, it is evident that CO is not a very efficient substrate for methane production, as only three pure strains namely *Methanobacterium Thermoautotrophicus, Methanosarcina acetivorans* and *Methanosarcina barkeri* are capable of methane production from CO. Methanogenic metabolism can be of two type, i.e., hydrogenotrophic and aceticlastic methanogenesis. In both the types of metabolic pathway CO is an intermediate and hence, CODH enzyme is commonly present in these methanogenic

organisms. In some of the organisms, such as *Methanococcu jannaschii* the gene coding CODH is located on the same operon as that of hydrogenase, signifying its potential for hydrogenogenic carboxydotrophic metabolism. However, many such organisms have not been tested for CO utilization, and therefore, their growth potential on CO or product formation capabilities is mostly unknown. Some researchers have studied undefined mixed consortium for their capability of CO utilization and methane production. For example, Sipma et al. (2003) studied CO conversion using seven different anaerobic sludges isolated from wastewater treatment plants. Results showed that all the sludges were capable of converting CO to methane and acetate at 30 °C, and the methane production is via acetate not H_2. Whereas, at a high temperature, CO was converted rapidly into hydrogen or methane, and for the second case it is via H_2 as the intermediate.

2.4.2 Biological sulfate reduction using CO

Another lesser explored application of biological CO conversion is the biodesulfurization, in which CO, either directly or via H_2 produced from hydrogenogenic CO conversion, can be utilized as electron donor for sulfate reduction process. A number of sulfate reducing bacteria (SRB) are capable of utilizing CO as the sole source of carbon and energy. Although SRB can utilize CO, for most of them it is toxic at a certain concentration. Both thermophilic and mesophilic carboxydotrophic sulfate reducers are reported in the literature. For example, *Desulfotomaculum thermoacetoxidans* strain CAMZ, *Thermodesulfovibrio yellowstonii*, *Desulfotomaculum kuznetsovii* and *Desulfotomaculum thermobenzoicum* sub sp. *Thermosyntrophicum* are moderately thermophilic with an optimum temperature in the range 55-60 ^{o}C, whereas, for extremophilies such as *Archaeoglobus fulgidus* VC 16 strain it is 75-80 ^{o}C. Some of the mesophilic strains with optimum temperature in the range 30-37 ^{o}C are *Desulfovibrio vulgaris* str. *Madison, Desulfovibrio baarsii* 2st14, *Desulfovibrio desulfuricans, Desulfovibrio baculatus, Desulfovibrio africanus, Desulfosporosinus orientis*.

Majority of these strains do not grow in the absence of sulfate. The major products from CO metabolism by sulfate reducers are H_2, acetate, formate and other volatile fatty acids. Both pure culture and co-culture strategies for effective sulfate reduction using CO have been reported (Table 2.4). But co-culture systems seem to be superior in terms of avoiding CO toxicity and high CO utilization efficiency. For instance, Svetlichny et al. (1991) found that *Desulfotomaculum kuznetsovii* and *Desulfotomaculum thermobenzoicum* sub sp. *Thermosyntrophicum* can grow with 100 % CO when cultivated with the hydrogenogenic carboxydotrophic bacterium *C. hydrogenoformans* compared to pure culture, which can tolerate only upto 50-70% of CO. Sipma et al. (2003) reported that the CO toxicity to SRB can be reduced by growing these organisms together with other CO utilizing bacteria, for example homo-acetogenic bacteria that are capable of performing biological water-gas shift reaction. Therefore, in such a mixed culture system, sulfate is reduced to sulfide along with an effective utilization of CO.

Table 2.4 Sulfate reduction by different organisms using CO or syngas

Organisms	Experimental conditions				Substrate		Sulfate conc. used	Sulfate reduction efficiency	References
	Exp. setup	Temp °C	pH	Agitation (rpm)	CO conc. used	Extra carbon source			
PVA and sodium alginate immobilized anaerobic sludge biomass	Packed bed reactor	30	7	NA	100%	NR	250-1000 mg/L sulfate	61-94%	Kumar et al., 2018
Anaerobic granular sludge	Batch serum bottle	55	7	NR	160 kPa	NR	NR	NR	Sipma et al., 2004
Anaerobic granular sludge	Gas lift reactor	55	7	NA	100-250 mmol/L/d	Ethanol (initial 7 d)	30-37 mmol/L/d	NR	Sipma et al., 2006
Anaerobic aggregated biomass	Gas lift reactor	30	7	NA	1 %	NR	4.97 g/L sodium sulfate	12-14 & 6-8 g SO_4^{2-}/L/d	van Houten et al, 1996
Archaeoglobus fulgidus	Batch serum bottle	80	6.8	NR	80 %	NR	2.2 g/L sodium sulfate	NR	Hocking et al., 2015
Anaerobic sludge biomass	500 m^3 full scale gas lift reactor	30-35	7-7.5	NA	NR	Acetate	5-30 g/L sulfate	295 kg sulfate/h	Van Houten et al., 2009
Anaerobic granular sludge	Gas lift reactor	55	6.9	NA	18-110 mmol/L/d	NR	20-60 mmol/ L/d	17 mmol/ L/d	Sipma et al., 2007
Carboxydothermus pertinax	Batch serum bottle	65	6-6.5	NR	100%	NR	NR	NR	Yoneda et al., 2012
Desulfotomaculum carboxydivorans	Batch serum bottle	55	6.8-7.2	NR	100%	NR	NR	NR	Parshina et al., 2005

Co-culture of *Desulfotomaculum thermoacetoxidans, Thermodesulfovibrio yellowstonii, Desulfotomaculum kuznetsovii, Desulfotomaculumthermobenzoicum* subsp. *Thermosyntrophicum, Carboxydothermus hydrogenoformans*	Batch serum bottle	60	7	150	50–70%	NR	20 mM	NR	Parshina et al., 2005

NR: Not reported

2.5 Factors influencing CO bioconversion

A number of important factors such as media constituents, pH, temperature, CO concentration, presence of inhibitory compounds, product concentration, agitation, etc. influence both CO bioconversion and formation of useful products. Table 2.5 compares all the afore-mentioned important process parameters and their effects.

2.5.1 Microbial growth media

Macro and micro nutrients, such as minerals, trace elements and vitamins added in the form of growth media, are not only responsible for bacterial growth but are also essential for enzymatic bioconversion of CO by microorganism. However, the type and concentration of media component depend upon the type of organism. For example, American Type Culture Collection media (ATCC Medium 112 and ATCC Medium 18) is used for *R. rubrum*, the most common bacteria for biological CO conversion to H_2. But, in case of new isolates optimization of media components plays an important role. Pakshirajan and Mal (2014) reported that compared with temperature, pH, inocculum size, nitrogen to phosphorus ratio, Fe^{2+} and Ni^{2+} in the media played a significant role in biohydrogen production from CO. The authors suggested that iron and nickel can improve the hydrogen production by influencing the activity of the two key enzymes carbon monoxide dehydrogenase and hydrogenases involved in CO bioconversion. In another study, it was reported that among the media components, calcium, magnesium, phosphate and bicarbonate were important for microbial activity and H_2 production from CO using *Carboxydothermus hydrogenoformans* (Zhao et al., 2011). Similarly, for ethanol production by *Clostridium autoethanogenum*, $MgSO_4$, NH_4Cl showed significant positive impact among all the nutrients studied (Guo et al., 2010). Abubackar et al. (2015) found that addition of a small amount of tungsten (0.75µM) increased ethanol production from CO by 128%.

Kundiyana et al. (2011) found that under limiting condition of three nutrients namely, calcium pantothenate, vitamin B_{12} and $CoCl_2$, *Clostridium ragsdalei* showed enhanced product yield in a two-stage fermentation system. Shen et al. (2017) optimized trace metal concentration present in ATCC medium 1754 for enhanced alcohol fermentation by *Clostridium carboxidivorans* P7 strain and reported the optimum levels were higher than that provided in the defined medium.

Addition of extra organic carbon source such as sodium acetate to the media has significant positive impact on bacterial growth, CO uptake and hydrogen production by *Rhodopseudomonas palustris* PT strain in batch system (Pakpour et al., 2014). Similar findings were reported by Najafpour et al. (2004) that suggest addition of 1-2 g/L of acetate significantly enhanced the H_2 production from CO by *Rhodospirillum rubrum*.

Economics of alcohol fermentation from CO can also be kept low by replacing or removing some of the media components, as reported in the literature. For instance, Gao et al., (2013) reduced the cost of ethanol fermentation from syngas by eliminating morpholinoethane sulfonic acid (MES) buffer and KCl, and reducing the levels of yeast extract by 50%, NH_4Cl by 98%, KH_2PO_4 by 88%, $MgSO_4$ by 95% and $CaCl_2$ by 87.5% in the medium. All these changes resulted in 29% higher ethanol yield from CO at only 3% of the original cost for *C. ragsdalei* bacteria. Liu et al. (2014) found that replacing yeast extract with corn steep liquor reduced the medium cost by 27% and produced 78% more ethanol using *Alkalibaculum bacchi* strain CP15 in batch fermentations. Similarly, Saxena and Tanner (2012) reported that by replacing yeast extract, vitamins and minerals with corn steep liquor in the medium and thus could improve the overall cost of ethanol production from syngas by *C. ragsdalei.* Maddipati et al. (2011) reported that ethanol production by *Clostridium* strain P11 increased by 32% by replacing yeast extract with cheaply available corn steep liquor. Phillips et al. (2015) optimized the concentration of nitrogen, phosphate and trace metals and omitted other

media components, such as yeast extract, MES buffer and minimal complex chemicals to reduce ethanol production cost by a native strain of *Clostridium carboxidivorans*.

Table 2.5 Important parameters influencing CO bioconversion and strategies to improve the process efficiency

Parameter	Effect
Growth media	• Essential for biomass growth and enzyme activity
Temperature	• Influences the biomass growth and metabolic pathway • Affects CO solubility in aqueous medium
pH	• Influences the biomass growth and metabolic pathway • Low pH favours solventogenesis over acetogenesis
CO concentration	• Low concentration limits the conversion efficiency • Toxic at high concentration
Product concentration	• Inhibition at high concentration
Inhibitory compounds	• Toxic to biomass • Enzyme inhibition
Agitation	• Influences gas liquid mass transfer • High agitation speed causes shear stress on bacteria

2.5.2 Temperature

The temperature has two main effects on biological CO conversion and product formation. First, it influences the biomass growth and metabolic pathway; second, it alters the CO solubility in aqueous medium. Based on optimum temperature condition, carboxydotrophic bacteria are classified into mesophilic and thermophilic organisms with optimum temperature in the range 30 - 40 °C and 50 - 80 °C, respectively. Kundiyana et al. (2011) reported that the solubility of CO decreases with an increase in the temperature, and therefore reduce the

bioavailability of CO to bacteria. Moreover, an increase in the temperature resulted in *Clostridium ragsdalei* to switch from acetogenesis to solventogenesis. Shen et al. (2017) reported that alcohol production increased from 4.40 g/L to 6.97 g/L by *C. carboxidivorans* with temperature control in a time bound manner, i.e. maintaining temperature of 37 °C for first 24 h followed by 25 °C for rest of the fermentation period.

2.5.3 pH

pH is one of the most important factor, slightest variation of which can significantly influence biomass and product yield (Table 2.5). Optimum pH for most of the hydrogenogenic carboxydotrophic bacteria is reported to be in a neutral range (pH ~7.0); however, for organisms like *Citrobacter* sp Y19, *Rubrivivax gelatinosus*, etc. the optimum pH is slightly acidic. But in case of homoacetogenic bacteria producing ethanol, butanol or acetic acid, pH modulation can often change the primary product. According to Fernández-Naveira et al. (2016a) a high pH is favourable for CO conversion to fatty acids rather than alcohol, whereas, low pH value enhances the alcohol production but significantly inhibits biomass growth. A 110 % increase in the ethanol concentration in media at pH 6.8 than that at pH 5.5 was reported by Cotter et al. (2009) using *Clostridium ljungdahlii* and *Clostridium autoethanogenum* strains. Abubackar et al. (2016a) reported that pH change from 5.75 to 4.75 provides reducing equivalents to cells which helps in increased CO consumption for ethanol fermentation by *Clostridium autoethanogenum*. It also enabled the consumption of acetic acid produced in the reactor for ethanol production. These results indicate that for *C. autoethanogenum* media pH need to be initially kept at an optimum for biomass growth, and following which when the pH lowered, ethanol production in enhanced without acetic acid accumulation. Mohammadi et al. (2012) also reported a drop in the cell dry weight and CO consumption rate with a decrease in the media pH during continuous ethanol production from syngas using *Clostridium ljungdahlii*. In case of *Clostridium ragsdalei* low pH (<5.0) and

morpholinoethanesulfonic acid addition as media buffer increased the lag time for ethanol production (Kundiyana et al., 2011).

2.5.4 Initial CO concentration

Carboxydotrophic bacteria are capable of utilizing CO as the sole substrate, but a high CO concentration is inhibitory to both CO utilization and product formation by the bacteria. However, different microorganisms have different optimum CO concentrations for its utilization (Tables 2.2 & 2.3). Most of the thermophilic extremophiles such as *Carboxydothermus hydrogenoformans* (Haddad et al., 2014), *Carboxydocella thermautotrophica* (Sokolova et al., 2002), *Carboxydothermus pertinax* (Yoneda et al., 2012), *Thermoanaerobacter Kivui* (Weghoff et al., 2016), *Clostridium thermoaceticum* (Martin et al., 1983) are capable of withstanding high P_{CO} (100% *v/v*) in the medium. But there are other moderately tolerant bacteria that cannot grow beyond even 20 % (*v/v*) CO concentration. Sinharoy et al. (2015) reported the highest μ_{max} value at 90 KPa of P_{CO}, above which the specific growth rate reduces according to Halden's model. Product yield from CO as well depends on intial CO concentration. For example, Younesi et al. (2005) studied ethanol production from synthesis gas using the autotrophic bacterium *Clostridium ljungdahlii*, and reported a maximum ethanol titer of 0.6 g/L for an initial total syngas partial pressure of 1.8 atm. The cell and ethanol yields were 0.3 and 0.41 g/g of CO, respectively. The CO partial pressure did not significantly affect acetate production, but ethanol production increased with an increase in H_2 and CO concentration in the culture medium. The inhibitory concentration of CO for this study was estimated to be 2 mmol/L from Andrew's model. In another study, cell concentration of *C. ljungdahlii* increased with an increase in CO percentage in the gas phase reaching 2 g/L cell concentration with 70% CO containing syngas at 14 ml/min of gas flow rate in a CSTR bioreactor (Younesi et al., 2006). In a similar study, the effect of partial pressure of CO on ethanol production by *Clostridium carboxidivorans* P7 was assessed, and a

440% increase in the cell concentration with an increase in P_{CO} from 0.35 to 2.0 atm was reported (Hursta and Lewis, 2010). Also, the ethanol production significantly increased to a maximum value of 2 g/L at 2 atm P_{CO}. On the other hand, the acetic acid production decreased with an increase in CO partial pressure. The authors found that P_{CO} and P_{CO}/P_{CO2} ratio largely affected the metabolic pathway of the organism, particularly on electron and ATP production, which in turn affected the ethanol and acetic acid production. In another study, ethanol yield *Alkalibaculum bacchi* increased by 11 % by changing CO concentration from 20 to 40 % (Liu et al., 2012). Weghoff et al. (2016) found that H_2 production by *Thermoanaerobacter kivui* improved from 6.8 to 44.9 mmol/L when CO was increased from 30 to 70 %.

2.5.5 Product concentration

Inhibition of CO conversion due to product accumulation is a key factor and needs significant consideration for proper design of the process. In case of continuous H_2 production from CO it is well known that hydrogenase, the key enzyme in H_2 production pathway, is highly sensitive to H_2 concentrations and shows typical end product inhibition. The inhibition due to H_2 is mainly dependent on the type of microorganism and the metabolic pathway followed. A thorough study of the enzymatic system and metabolomics involved will help in understanding the inhibition problem for increasing the H_2 yield. An effective alternative is the quick recovery of product as soon it is produced in the reactor, which avoids shift in metabolic pathway and production of more reduced products such as acetate, lactate, etc. (Kumar et al., 2018). Skidmore et al. (2013) studied the effect of H_2 partial pressure on *Clostridium* P11 hydrogenase enzyme activity, which revealed that H_2 utilization rate is maximum for a H_2 partial pressure of 30 kPa. In order to study the effect of various end products on CO conversion by *Clostridium carboxidivorans* P7, Zhang et al. (2016) added acetic acid, butyric acid, hexanoic acid, ethanol and butanol in fermentation medium. The

results showed that addition of fatty acids at slightly high temperature (37 °C) resulted in production of corresponding alcohol, whereas, at low temperature (25 °C) only fatty acids accumulated in the medium. Alcohol addition in the medium resulted in increased fatty acid production at both low and high temperature. Fernández-Naveira et al. (2016b) studied the effect of butanol, ethanol and their mixtures on CO conversion by *C. carboxidivorans*. Butanol showed higher inhibitory effect than ethanol on cell growth and CO utilization. Butanol concentration in the range 14 - 14.50 g/L reduced cell growth by 50 % and at a concentration more than 20% it completely inhibited the bacterial growth. In case of ethanol, 35 g/L concentration decreased the final biomass concentration by 50 %. Similar results an inhibition of biomass growth were obtained for a mixture containing both ethanol and butanol with a least growth rate of 0.014 h^{-1} obtained at a maximum total alcohol concentration of 25 g/L.

2.5.6 Inhibitory compounds in feed gas

Obtaining CO in the pure form is difficult, and therefore, syngas derived from biomass gasification is used as the feed gas for the production of different value added products. The concentration of CO in syngas ranges between 5 and 60 %. In addition to CH_4, CO_2 and a small amount of H_2, other gases such as SOx, NOx, ethylene (C_2H_4), ethane (C_2H_6), acetylene (C_2H_2) are present in different concentration depending upon the feedstock used. These gases along with tar, char, ash particles can inhibit biological CO conversion to useful products. The exact mechanism by which these compounds inhibit CO conversion and product formation is largely unknown, but inhibition due to reduced enzyme activity has been reported in the literature (Ahmed et al., 2006). Xu and Lewis (2012) found that ammonia (NH_3) inhibits hydrogenase activity that plays an important role in the syngas fermentation. Ahmed and Lewis (2007) studied the effect of nitric oxide (NO) on hydrogenase inhibition in *C. carboxidivorans* and found that at a NO concentration above 40 ppm inhibited

hydrogenase activity, cell growth and product formation. Hence, it is suggested to remove these compounds or reduce their concentrations for a successful CO bioconversion.

2.5.7 Agitation

Agitation is another important factor for CO utilization and product formation as it influences the CO-water volumetric mass transfer and it, therefore, indirectly enhances the bioavailability of CO to microorganisms (Table 2.5). In bioreactor systems, sufficient agitation is achieved with the help of impellers. But at a high agitation speed, microorganisms may experience cell damage, further inhibiting microbial growth and product formation. Hence, agitation speed needs to be optimized for achieving a maximum CO conversion and product formation. Other important parameters such as gas liquid mass transfer and bioreactor system and are discussed further in detail in sections 2.6 and 2.7.

2.6 Strategies to overcome gas liquid mass transfer problems for CO bioconversion

In a system involving gas phase substrate such as CO, a high product yield directly depends upon its high mass transfer rate (Liu et al., 2014). The high cell concentration necessary for the high yield is also dependent on the mass transfer rate of gaseous substrates, as low mass transfer rates lead to reduced cell concentrations in the fermentation media (Yasin et al., 2015). Experimental studies have shown that the most rate limiting factor in fermentations of gaseous substrate is typically gas-to-liquid mass transfer, similar to aerobic fermentations where oxygen mass transfer is the rate limiting step (Worden et al., 1997). The limitation of gas liquid mass transfer are more problematic for CO or synthesis gas fermentations compared to that of aerobic fermentations, because the solubility of CO is only 60% of O_2 solubility (on a mass basis). Hence, in order to get an equivalent product yield on substrate, sufficiently large amount of CO needs to be transferred per carbon equivalent consumed in

this case than in aerobic fermentations that utilizes easily substrates like glucose (Zhu et al., 2009; Abubackar et al., 2011; Munasinghe and Khanal, 2010b).

Hence, for this technology to be economically viable and commercially successful, the CO-water mass transfer rate must be improved. The different strategies suggested to improve CO solubility and CO-water mass transfer are discussed further.

2.6.1 Agitation speed and impeller configuration

The easiest way to improve the gas liquid mass transfer is by enhancing the agitation speed (rpm). Bredwell et al. (1999) reported a high K_La value of 101 h^{-1} for CO at 450 rpm agitation speed. In another study, an increase in the agitation speed upto 700 rpm is reported to enhance the CO liquid mass transfer (Klasson et al., 1993). For achieving a high mechanical agitation speed, a high power input is required, and, therefore, a high ratio of power required to reactor volume makes this strategy economically weak for large scale industrial reactors, merely because of the excessive power costs (Yasin et al., 2014). A different strategy to improve the mass transfer employing different impeller design was studied by Ungerman and Heindel (2007). The effect of six different impeller configurations, namely Rushton-type, Philadelphia Mixing concave (hollow blade) turbine, Philadelphia Mixing pitched blade turbine (PBT), Philadelphia Mixing LS hydrofoil, Lightnin A315 fluidfoil and Lightnin A310, on gas liquid mass transfer rate was analyzed. The Rushton-type impeller performed better compared with the other five impeller types; also, the dual Rushton type showed a 27% higher gas liquid mass transfer compared with the conventional single Rushton type impeller. However, its performance in terms of the ratio of volumetric mass transfer coefficient to power input was poor. Hence, it could be concluded that improved gas liquid mass transfer in a stirred system requires a high power consumption and cost associated with it. Also, increase in the agitation speed to enhance gas liquid mass transfer

may be damaging to shear sensitive microorganisms, thereby hampering microbial growth in the bioreactor (Munasinghe and Khanal, 2012).

2.6.2 Additives

The use of additives such as electrolytes, surfactants, alcohols, nano particles, with or without surface modification, has been reported to enhance the gas liquid mass transfer. The effect of various electrolytes, such as sulfate, nitrate and chloride on CO water mass transfer was studied, and the results show an enhancement of 1.5 to 4.7 times due to these electrolytes compared to that without any added electrolytes (Zhu et al., 2009). It is also reported that among the different metal ions, viz. copper, cobalt, nickel, iron, manganese and magnesium, copper containing electrolyte is the best for enhancing the volumetric gas liquid mass transfer. This is attributed to an increase in the gas-liquid interfacial area and a reduction in the gas bubble coalescence in the liquid phase. These findings on enhancement in gas liquid mass transfer due to the addition of electrolyte or metallic salts are also valid for aerobic systems. For example, Zuidervaart et al. (2000) reported a 250% enhancement in the oxygen water mass transfer rate when metal sulfate based electrolytes (e.g., $CuSO_4$, $FeSO_4$, $ZnSO_4$, and $Al_2(SO_4)_3$) were added to the liquid media. Use of surfactants, e.g. Tween (polyoxyethylene sorbitans) and Brij (polyoxyethylene alcohols), for enhancing the CO water mass transfer is also reported (Bredwell et al., 1997).

The increase in CO water mass transfer due to addition of nano or micro particles was reported by Zhu et al. (2008). Nano particles made of mesoporous silica materials and coated with different hydroxyl groups, mercaptopropyl groups and organic groups enhanced the gas liquid mass transfer, and the mercaptopropyl groups grafted nano particles yielded the maximum CO water mass transfer (upto 1.9 times increase). The presence of functional groups on nano particles and their hydrophobicity is reported to significantly enhance the CO

water mass transfer (Zhu et al., 2008). Similarly, in aerobic systems, a 600% increase in oxygen water mass transfer rate upon addition of magnetite (Fe_3O_4) nanoparticles coated with oleic acid is reported (Olle et al., 2006). Beenackers and Swaaij (1993) reviewed five different mechanisms of gas liquid mass transfer enhancement due to small particle addition, which included physical adsorption, homogeneous reactions in a slurry, dissolved reactive particles, reactive particles in heterogeneous reactive systems, etc. According to these authors, small sized particles in the system transport an additional amount of gas to the bulk liquid through adsorption from the gas liquid diffusion layer to desorption in the liquid, which is referred to as the shuttle or grazing effect. This method of enhancement is influenced greatly by particle size and surface characteristics.

2.6.3 Use of microbubble dispersion system

Microbubbles differ from regular bubbles in having a multilayered "shell" entrapping water and gas in the different layers. Microbubbles are created by high shear zone at the gas liquid interface with a spinning-disk microbubble generator (Bredwell et al., 1999). This equipment is essentially a modification of an electrical motor driven stirred reactor system, with a high-speed spinning disk rotated at several thousand rpm for creating a high shear force. Small-sized bubbles are created from the bigger ones in the high-shear zone of the equipment. A surfactant is added in the liquid, which stabilizes the microbubbles against coalescence by creating ionic and/ or steric repulsion between adjacent bubbles at the gas liquid interface (Bredwell et al., 1999). Other similar equipment, such as emulsion phase contactor, shear mixing apparatus, etc. are also reported to produce microbubbles (Shirtum et al., 1998; Scott et al., 1994). Instead of introducing gas directly into the reactor in microbubble dispersion systems, microbubbles of gases are generated separately prior to its sparging into the reactor.

Bredwell et al. (1998) reported six fold increase in the CO mass transfer in such microbubble disparaging systems compared to that in a conventional gas sparging system. A similar study, involving an aerobic system, achieved four fold high volumetric mass transfer value for oxygen using microbubble sparging mechanism (Kaster et al., 1990). The exact mechanism of mass transfer enhancement in microbubble disparging system is two way; first, a decrease in the bubble size increases the driving force due to increased internal pressure in gas bubbles. Second, the liquid phase concentration gradient for the gas is inversely proportional to the bubble diameter. Therefore, as the bubble size decreases the flux increases, enhancing the overall gas liquid mass transfer (Munasinghe and Khanal, 2010; Bredwell et al., 1999). However, special care must be taken to avoid coalescence of microbubbles. This problem occurs following the transfer of consumable gases into the liquid phase and if the inert and waste gases (CO_2) containing spent microbubbles are not removed from the reactor. Larger sized bubbles rise to the surface of the liquid and get released due to coalescence, reducing the overall $K_L a$ values and gas conversion (Bredwell et al., 1999; Tsouris et al., 1994).

2.7 Reactor consideration

Proper design of bioreactor and its mode of operation is one of the main concerns for successful scale up of CO bioconversion to useful products (Yasin et al., 2015). The key parameters necessary while considering a suitable bioreactor are mainly related to CO gas-liquid mass transfer, which includes agitation speed, impeller design, power consumption, temperature, pressure conditions, bioreaction kinetics, etc. Both batch and continuously operated bioreactors have been employed for CO conversion to useful products. Under batch operation mode, bioreactor is operated as a closed system with the introduction of gaseous CO at the start of the batch; whereas, in continuous operation mode the gaseous substrate is supplied continuously. Both liquid and gaseous samples are withdrawn periodically at a set time interval during the operation and analyzed for CO conversion, product formation, cell

concentration, etc. Continuous stirred-tank reactor (CSTR) is the most commonly used bioreactor system for CO bioconversion, but other types of reactor such as bubble column reactor (BCR), trickling bed reactor (TBR), packed bed bioreactor (PBR), gas lift reactor (GLR) and membrane bioreactor (MBR), etc., have also been examined under both batch and continuous operation modes. Fig. 2.5 shows schematic of the different bioreactors used for CO bioconversion. Table 2.6 compares the commonly used bioreactors for CO conversion along with their volumetric gas liquid mass transfer coefficient (K_La) values. The volumetric mass-transfer rate is defined as the product of volumetric mass-transfer coefficient (KLa) and mass-transfer driving force (C^* - C), where C is the liquid-phase concentration of the transferred gas and C^* is the liquid-phase concentration that is in equilibrium with the gas phase (Bredwell et al., 1999). Different types of bioreactor configurations studied for CO bioconversion to useful products are discussed further in the following sub-sections. Also, the advantages and disadvantages of different bioreactors for CO conversion are summarized in Table 2.7.

2.7.1 Continuous stirred tank reactor

The CSTR is the most common type of bioreactor employed at the laboratory scale. Stirred-tank reactors are often used when high K_La values are desired. The mixing of gaseous substrate is carried out by baffled impellers which enhance the mass transfer between the substrate and microbes inside the reactor (Munasinghe and Khanal, 2010). The hydrodynamic shear force generated by a high level of agitation or mixing creates small sized bubbles from bigger ones, which increases the interfacial area for mass transfer and subsequently the bioavailability of gaseous substrates (Bredwell et al., 1999). In addition, slow rising velocity of finer gas bubbles leads to a prolonged retention time in the liquid media, which leads to high mass transfer rates. In this type of reactor, gaseous substrate is supplied continuously and liquid media containing the nutrients is fed into the bioreactor to support microbial

growth and metabolism (Klasson et al., 1992; Vega et al., 1990). The product formed in the reactor by microbial conversion is drawn out from the system at the same flow rate as the feed to maintain a steadystate in a continuous mode of operation. Younesi et al. (2008) studied the bioconversion of CO rich syngas to hydrogen using a continuous stirred tank bioreactor with an anaerobic photosynthetic bacterium, *Rhodospirillum rubrum*, capable of performing biological water-gas shift reaction. The effect of different agitation speed and gas flow rate was evaluated over a period of two months. The best performance was achieved at 500 rpm agitation speed and 14 ml/min gas flow rate, with a hydrogen production rate and yield of 16 ± 1.1 mmol g^{-1} cell h^{-1} and 87 ± 2.4%, respectively. Ismail et al. (2008) using the same organism reported the optimum conditions for H_2 production from CO in a two-litre bioreactor as 700 rpm agitation speed, 0.44 ± 0.023 atm P_{CO} and a K_La of 86.4 ± 3.5 h^{-1}, which also yielded a maximum CO conversion of 81 ± 5.6% and H_2 production rate of 9.6 mmol/h. These studies clearly demonstrate that a high agitation rate in CSTR is required to achieve high gas liquid mass transfer and for a maximum conversion of CO to H_2. Najafpour et al. (2003) reported H_2 production from syngas using *R. rubrum* in a continuously operated CSTR equipped with a dual-impeller agitation and microsparger system for achieving a high gas liquid mass transfer. The bacterial growth kinetics on CO was described using the Monod model, which gave μ_{max} and K_s values of 0.0225 h^{-1} and 0.0135 g/L, respectively. The H_2 production rate and yield were observed to be 16 mmol H_2 /g cell. h and 80%, respectively.

Aghbashlo et al. (2016) used *Clostridium ljungdahlii* in a continuous stirred tank bioreactor for syngas fermentation to produce ethanol and acetate. The authors mainly focused on studying the effect of different operational parameters, such as agitation speed, media flow rate, syngas flow rate and its composition on the sustainability and renewability of the process using a thermodynamic model. Younesi et al. (2006) found that CO conversion increased with an increase in the gas flow rate and agitation speed during continuous syngas

bioconversion to ethanol and acetate using *Clostridium ljungdahlii* in a continuous tank bioreactor. For a gas flow rate of 14 ml/min and an agitation rate of 550 rpm, the cell concentration and conversion of pure CO were 1.92 g/l and 80%, respectively. The total amount of ethanol and acetate produced during the fermentation is around 11 g/L. Kundiyana et al. (2010) achieved six fold increase in ethanol concentration by *Clostridium ragsdalei* in a pilot scale study using 100 L stirred tank reactor compared to that in batch serum bottle. The ethanol concentration reached highest 25.26 g/L along with the co-products 2-propanol, 1-butanol and acetic acid. Fernández-Naveira et al. (2016) studied CO fermentation by *Clostridium carboxidivorans* in a 2 L bioreactor. Maximum ethanol and butanol concentrations in the study were 5.55 and 2.66 g/L, respectively. In addition to the conversion of CO to alcohols, the acetic and butyric acids were also utilized for alcohol production which resulted in low residual concentrations of these acids at the end of the bioreactor operation. The average CO utilization was around 50 % and reached its highest value (80 %) during the continuous bioreactor study.

Two-stage CSTR has also been studied for ethanol production from CO. Abubackar et al. (2018) studied syngas fermentation to produce ethanol using *Clostridium carboxidivorans* in a two-stage continuous system with two stirred tank reactors arranged in series. The pH of the two reactors was maintained different: the first one was maintained at pH 6 for acidogenesis and the second one at pH 5 for solventogenesis. The second reactor had a provision of cell recycling in order to maintain an optical density (at 600 nm) of 1 in the second bioreactor. The bacterial growth rate in the second reactor was negligible due to low pH condition. Thus, maximum ethanol concentration of 1.51 g/L with an alcohol to acetic acid ratio of 0.32 was achieved in this two-stage continious system.

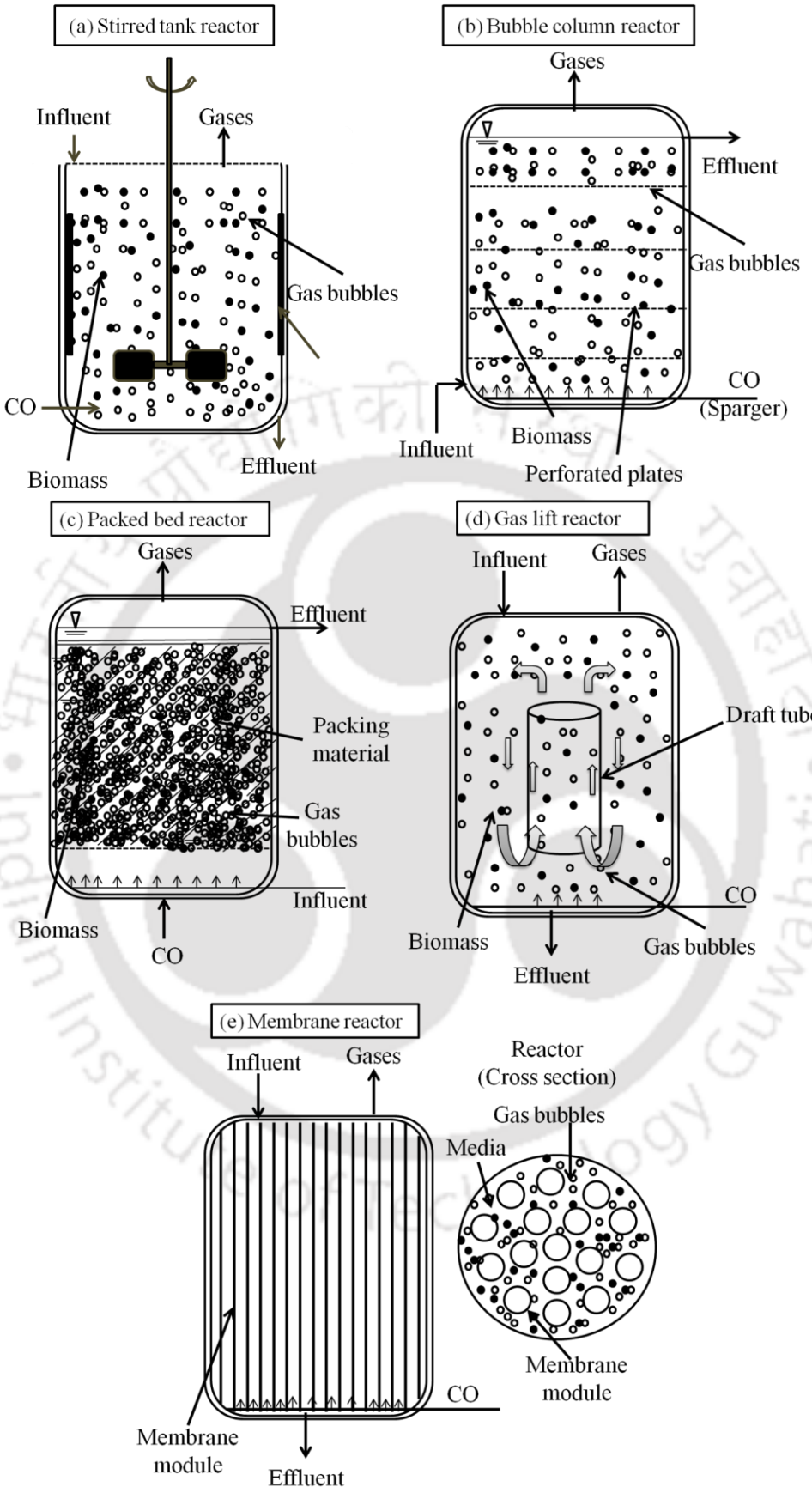

Fig. 2.5 Various bioreactor systems used for CO bioconversion.

Table 2.6 Commonly used bioreactor systems for biological CO conversion and their volumetric mass transfer coefficients

Reactor type	Agitation speed (rpm)	Volumetric mass transfer coefficient $K_L a$ (h^{-1})	Substrate	Reference
CSTR	700	35.5	CO	Klasson et al., (1993)
CSTR	200	14.2	CO	Bredwell et al., (1999)
CSTR	300	35	Syngas	Bredwell et al., (1999)
CSTR	450	101	Syngas	Bredwell et al., (1999)
CSTR	700	86.4	CO	Ismail et al., (2008)
STR	600	154.8	CO	Riggs and Heindel, (2006)
STR	700	192.8	Syngas	Kapic et al., (2006)
STR	300	14.9	CO	Klasson et al., (1993)
STR	400	21.5	CO	Klasson et al., (1993)
TBR	NA	137	Syngas	Cowger et al., (1992)
TBR	NA	121	Syngas	Bredwell et al., (1999)
BCR	NA	72	CO	Chang et al., (2001)
BCR	NA	94.3	CO	Park et al., (2013)
BCR	NA	400	CO	Shen et al., (2014)
PBR	NA	21	Syngas	Bredwell et al., (1999)
GLR	NA	129.6	CO	Munasinghe and Khanal, (2014)
GLR	NA	1.5-2.0	CO	Haddad et al., (2014)
GLR	NA	91.08	CO	Munasinghe and Khanal, (2001)
STR with microbubble sparger	200	90.6	CO	Bredwell et al., (1999)
STR with microbubble sparger	300	104.0	Syngas	Bredwell et al., (1999)

CSTR: Continuous stirred tank reactor, STR: Stirred tank reactor, PBR: Packed bed reactor, TBR: Trickle bed reactor, BCR: Bubble column reactor, GLR: Gas lift reactor NA: Not applicable

2.7.2 Bubble column reactors

Bubble column reactors offer a high gas-liquid mass transfer by providing high surface area for mass transfer and increased turbulence as the bubbles rise through the column of liquid. Small-sized finer bubbles produced in this type of reactor have high surface-to-volume ratios

and low rise-velocities through the liquid, resulting in long residence times in the reactor. The short residence time of gas and high pressure drop in the bubble reactor are some drawbacks limiting its scale-up and commercialization. Other drawbacks include back-mixing and coalescence in bubble column (Datar et al., 2004). But the main attraction of this type of reactor is the ease of obtaining desired cell biomass amount in the reactor. Amos (2004) studied the CO conversion to H_2 using a bubble column reactor with or without gas recycle, and found that between the two types, the reactor with gas recycle performed better with an overall conversion efficiency of over 50% at 10:1 recycle-to-feed ratio. The authors attributed the performance of the bubble column reactor to a long residence time, high cell mass, buffering capacity of the liquid and low inlet CO concentration to the reactor. Rajagopalan et al. (2002) studied CO conversion to ethanol using *Clostridium carboxidivorans* in a continuous 4.5 L bubble column bioreactor. Under steadystate condition, ethanol, butanol, and acetic acid yields were 0.15, 0.075 and 0.025 g/mol CO, respectively. The authors further suggest different approaches to improve performance of the bubble column reactor such as cell recycling to increase cell concentration without altering the ethanol yield, adding H_2 in gas stream to improve CO conversion to ethanol, optimizing nutrient supplements in media, etc.

2.7.3 Packed bed bioreactor/ trickle-bed bioreactor

The trickle-bed bioreactor or trickling filter consists of a tubular reactor with solid support for biomass to grow and attach to. The cells can either be immobilized on the solid packing or suspended in the liquid medium (Bredwell et al., 1999). Though, in general, this type of reactor is operated under counter current flow of liquid to gas, where gaseous substrate rises upwards and the water flows down through the packed bed, it can also be operated in a co-current mode. Special care need to be taken to maintain a low water flow rate to prevent flooding in the column. The liquid flow is mainly provided to keep the cells moist along with

nutrients supplementation for cell growth. Various packing materials have been tested, including wood, activated carbon, lava rock, plastic and porous ceramic supports for effective conversion of CO to H_2 (Amos, 2004). The main advantage of this reactor is increased gas-transfer area with a minimal pressure drop. Also, it is easy to improve the mass transfer by controlling the liquid flow rates. Wolfrum and Watt (2001) studied the effect of reactor packing material on CO conversion by the photosynthetic bacterium *Rubrivivax gelatinosus* using two reactors with different volumes (1 and 5 litre) of same geometry. Devarapalli et al. (2016) used trickle bed bioreactor with 6 mm size soda lime glass beads as packing material for ethanol fermentation from syngas. The study found that increased amount of biomass in the packing and biofilm formed over the beads reduced CO inhibition and enhanced the H_2 conversion and uptake by 1.9 times. It is also found that co-current mode of gas and liquid flows in the reactor reduced the gas channelling effect and reactor flooding problems that were encountered in counter-current operation mode.

2.7.4 Gas lift reactor

Gas lift reactor is simply air-lift bioreactor with gas flowing into it rather than air (Sipma et al., 2007), and is similar to the bubble column reactor, but it differs by the fact that it contains a draft tube. The draft tube is always an inner tube (called gas lift bioreactor with an internal loop) or an external tube (called gas lift bioreactor with an external loop) which improves circulation and gas liquid mass transfer and equalizes shear forces in the reactor. The major advantages of gas lift bioreactor are simple design with no moving parts or agitators, zero energy requirement, homogeneous distribution of nutrient and shear force. Gas stream facilitates the exchange of material between gas phase and media, thus enhancing the effective mass transfer (Table 2.6). Munasinghe and Khanal (2001) reported a very high mass transfer coefficient of 91.08 h^{-1} for CO in a gas lift reactor combined with a 20 mm bubble diffuser compared to other reactor configurations. Haddad et al. (2014) studied CO

conversion to H_2 by *Carboxydothermus hydrogenoformans* in a 35 L gas lift reactor. The effect of different operational conditions, namely gas recirculation rate, CO feeding rate and addition of bacto-peptone to the media, was also evaluated. The ratio of gas recirculation over CO feeding rate was observed to be the most important parameter affected the reactor performance that kinetically limit both the CO conversion and H_2 production rates. Overall, a high H_2 yield of 95% and CO conversion rate of 3.79 L of CO/L.day were reported in this study. Hydrogenogenic CO conversion for biological sulfate reduction was studied by Sipma et al. (2007) using a gas lift reactor and the effect of different HRT was investigated under thermophilic (55^{o}C) condition. The authors reported that at a high retention time (>5.5 h) the CO conversion resulted in hydrogenotrophic methane production, whereas at a short HRT the H_2 production was higher. Overall a CO conversion of 85 % was achieved in this study.

2.7.5 Membrane bioreactor

Membrane bioreactors (MBR) basically consist of membrane module that is partially or completely submerged in liquid media. The CO gas is diffused through the walls of membranes without forming bubbles. The bacteria/biomass grows on the outer wall of the membranes as a biofilm, converting CO to useful product. Several recent studies on hollow fiber membrane (HFM) bioreactor have suggested that the membrane bioreactors (MBR) have the potential to replace the commonly used bioreactors for gas liquid mass transfer applications (Yasin et al., 2015). A number of choice for membrane materials is available, among which hydrophobic membrane materials such as polypropylene (PP), polyethylene (PE) and polyvinylidene fluoride (PVDF) are used most commonly. The advantage of MBR over traditional reactor systems are effective gas liquid mass transfer and low energy requirement; moreover, it provides a high product yield, high reaction rate and increased tolerance to toxic compounds (tar, acetylene, NOx, O_2, etc). Besides, these types of reactors can be operated under high pressure (P_{CO}) conditions (Munasinghe and Khanal, 2010). Main

disadvantages are clogging and biofouling of the membrane due to excessive biomass growth (Yasin et al., 2014). Membrane bioreactor system has not been specifically used for H_2 production form CO, but it has been evaluated for other products, for example, continuous fermentation of ethanol, butanol and acetic acid from syngas. It has also been studied for enhancing hydrogen and oxygen mass transfer in water treatment applications (Lee and Rittmann, 2001; Nerenberg and Rittmann, 2004). Shen et al. (2014a) studied ethanol fermentation from syngas in hollow fiber membrane biofilm reactor using *Clostridium carboxidivorans* P7. The K_La value was found to be higher than most of the commonly used bioreactors. A very high ethanol concentration of 23.93 g/L was achieved with ethanol to acetic acid ratio of 4.79.

2.7.6 Novel bioreactors

Shen et al., (2017) studied ethanol production by *Clostridium carboxidivorans* P7 in a horizontal rotating packed bed (h-RPB) reactor using syngas as the substrate. In this reactor, the reactor is the biosupport packing material is half submerged and half exposed in the headspace, and due to continuous rotation, the biofilm is in alternate contact with liquid media and headspace gas. Using this reactor, a high ethanol titer of 7.0 g/L and a productivity of 6.7 g/L/d was achieved. The K_La of the h-RPB reactor was lower than that in a conventional CSTR, indicating poor mass transfer in the liquid phase of h-PRB, and the mass transfer in the headspace phase played an important role in syngas fermentation.

In another study, ethanol production from syngas was carried out using a monolithic biofilm reactor (MBFR) with *C. carboxidivorans* P7 (Shen et al., 2014a). This study revealed that at optimum process conditions, i.e. 300 mL/min of syngas flow rate, 500 mL/min of liquid flow rate and 0.48/d of dilution rate, etanol concentration and productivity were 4.89 g/L and 2.35

g/L/d, respectively. The syngas utilization and product formation were much higher than that obtained using a conventional bubble column reactor.

Table 2.7 Comparison of different bioreactors used for CO bioconversion

Reactor type	Advantages	Disadvantages
Continuous stirred tank reactor	• Simple to operate • Mixing improve gas-liquid mass transfer • Gaseous substrates are more accessible to microbes due to breaking down of large bubbles into finer ones by increasing rotational speed of impellers	• High agitation causes shear stress on microbes • Large power requirement • High operating cost
Bubble column reactor	• High gas-liquid mass transfer rates • Low operating and maintaining cost • Low shear stress	• Back mixing and coalescence
Trickle bed/ packed bed reactor	• Gas and liquid flow could be either in co-current or counter-current direction • No need of mechanical agitation • Power requirement is less	• Clogging of bed
Membrane bioreactor	• Gases easily diffuses through wall of the membranes • Membrane wall provides excellent support for	• Not yet commercially used for CO conversion or syngas fermentation • High installation cost • Clogging problems

	microbial growth and improves biomass retention • High product yield, high reaction rate, high tolerance to toxic elements	
Gas lift reactor	• Mechanical simplicity • Low energy requirement • No focal points for energy dissipation • Low shear stress • Suitable for process with variable gas feeding requirements	• Not suitable for viscous broths • Minimum process volume • Dead zones inside the reactor • Insufficient mixing at high biomass densities

From the detailed literature review it is clear that only a few previous studies have reported about organisms capable of growing on 100% (*v/v*) CO as most of them could only tolerate < 20% (*v/v*) CO. Also, most of the carboxydotrophic organisms are thermophilic in nature and therefore would require large amount of energy to maintain high temperature during bioreactor operation. The poor solubility of CO in aqueous media is another hurdle for its utilization by microorganisms. Further, any attempt to successfully scale up or commercialize this technology requires continuous operation using bioreactors. Furthermore, suitable applications of CO conversion technology such as biohydrogen production, biological sulfate reduction, heavy metal removal and selenite reduction, etc. could improve its commercial viability.

Chapter 3

Carbon monoxide conversion by anaerobic biomass: screening, pathway elucidation, metagenomic analysis and batch process parameter optimization

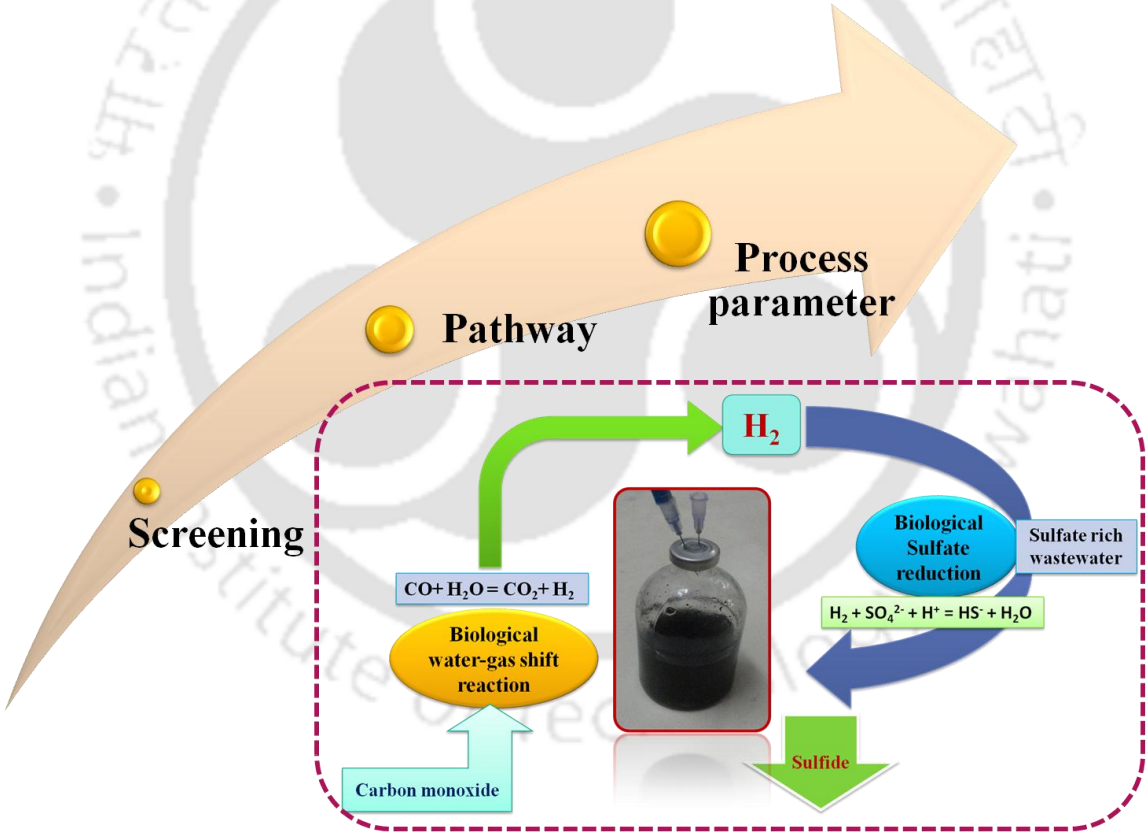

ABSTRACT

Anaerobic mixed microbial consortia from five different sources were initially examined for their biological CO conversion potential. Among the different biomass, the biomass from a large scale upflow anaerobic sludge blanket reactor treating wastewater, located in Kavoor, Karnataka, India, showed a maximum CO conversion efficiency. The CO conversion pathway by the anaerobic biomass was elucidated using methanogenic inhibitor 2-bromoethanosulfonete. The predominantly present microorganisms in the anaerobic biomass were identified to be *Methanomicrobia, Anaerolineae, Proteobacteria, Clostridia, Caldisericia, Desulfovibrio sp*. etc. The effect of three main culture parameters, i.e. inoculum size, initial CO concentration and temperature on simultaneous CO conversion and sulphate reduction was assessed employing the Taguchi experimental design technique. A maximum CO conversion of 85.62% and a maximum sulphate reduction of 56.6% were achieved under the optimum condition of 10 % (v/v) inoculums size, 1.8 mmol/L initial CO concentration and 45 ^{o}C with raw anaerobic biomass.

3.1 Introduction

Carbon monoxide (CO) rich synthesis gas is used for producing wide range of valuable products including H_2 gas. Due to the limitations of conventional CO conversion processes cost-effective and novel technologies for CO conversion, such as biological methods using microorganisms that are beneficial from environmental and economical point of view, are the need of the hour. Since 1980's a number of carboxydotrophic bacteria/archia capable of effective biological CO conversion have been reported. These bacteria are not only able to grow chemolithotrophically on CO but can also convert CO into commercially important compounds such as hydrogen, ethanol, butanol, acetic acid, etc. under ambient temperature and pressure conditions (Bender, 2011; Sipma et al., 2007). Furthermore, some pure strains and microbial consortium are reported to be able to perform biological sulfate reduction using CO as the sole carbon and energy source (Parshina et al., 2010).

Such eco-friendly and sustainable solutions for CO conversion are feasible on small as well as commercial scales owing to the economics of the process (Parshina et al., 2010). Very little amount of literature is available on suitable applications of this technology to improve its commercial viability. Moreover, integrating biological CO conversion with environmental or biofuel applications have not been sufficiently addressed, particularly with respect to continuous CO conversion employing suitable bioreactor system.

Microorganisms that are robust and sturdy are essential for industrial scaleup and commercial success of this technology. From the reported literature, it is evident that only a few numbers of microorganisms have been studied for biological CO conversion to useful products. Most of these available strains have low tolerability to CO, and majority of them cannot survive on more than 20% (*v/v*) CO. There are two ways to solve this problem: firstly, genetic engineering approach for strain improvement and secondly isolation of new organism. Genetic engineering approaches can be utilized to either construct a recombinant strain

capable of high product yield and more tolerance to CO concentration, or using metabolic engineering to reduce multiple product formation and avoid low yield of the desired product. However, a pre-requisite for such an approach is the identification and molecular characterization of catabolic genes involved in the process. From the available literature it is clear that very little is known about the mechanism(s) of CO tolerance in such carboxydotrophs, which will require more detailed research to understand the molecular mechanisms involved and to achieve strains with desired traits, such as growth on CO, high rate of microbial reaction, high product yield and, most importantly, suitability for industrial scaleup (Dragosits and Mattanovich, 2013, Maness et al., 2002). Further, stability of such genetically engineered strains are questionable as there is every possibility of turing back to wild type during large scale operating condition.

On the other hand, a number of recent studies indicate the potential of new organisms from extreme environmental conditions, e.g. hot springs, which may be better suited for CO conversion (Parshina et al., 2010). However, operating large volume reactors at an elevated temperature is both energy consuming and cost intensive. Hence, the research focus needs to be shifted towards exploring mesophilic organisms capable of CO conversion. Recently, a few scientific reports suggests that compared to pure organisms mixed microbial consortium are better suited to handle CO toxicity and are more effective in utilizing CO for their growth and product formation (Liu et al., 2016).

Therefore, the aim of this study was to screen different anaerobic biomass capable of CO conversion to biohydrogen and subsequent sulphate reduction using the *in situ* produced H_2. In addition, identification of the microbes present in the biomass that yielded a maximum CO conversion efficiency and elucidation of the CO bioconversion pathway was examined. Furthermore, the effect of biomass pretreatment and other process conditions viz.

temperature, initial CO concentration and inoculum size on CO conversion and sulfate reduction was studied in detail.

3.2 Materials and methods

3.2.1 Screening of anaerobic biomass for carbon monoxide conversion

3.2.1.1 Collection of anaerobic sludge biomass from different sources

Anaerobic sludge biomass samples were collected from five different sources (Table 3.1). Among these five biomass samples, three were collected from different large scale upflow anaerobic sludge blanket reactors treating domestic wastewater, whereas the other two biomass types were collected from sewage treatment plant (STP) located at IIT Guwahati (IITG) and a lab scale packed bed anaerobic reactor treating sulfate rich wastewater, respectively. While collecting the biomass samples, contact with air was avoided to ensure anaerobic condition, and after collection, the biomass samples were stored in a refrigerator at 4 ºC until further use.

Table 3.1 Source and type of anaerobic biomass collected to examine CO conversion in this study

	Source	Biomass
1.	Kavoor sewage treatment plant, Mangalore (43.5 MLD)	Anaerobic granular sludge
2.	Jakkur sewage treatment plant, Bangalore (10 MLD)	Anaerobic granular sludge
3.	K.R Puram sewage treatment plant, Bangalore (20 MLD)	Anaerobic granular sludge
4.	IITG sewage treatment plant, Guwahati	anaerobic sludge
5.	Lab scale packed bed reactor treating sulfate rich waste water	anaerobic sludge

MLD = million litre per day

3.2.1.2 CO conversion experiments

Tests for assessing CO conversion by biomass samples collected from different sources were performed under anaerobic condition using 120 ml serum bottles (Sigma Aldrich, India) sealed with polytetrafluoroethylene (PTFE) septum. The serum bottles were filled with 50 ml mineral salt medium (MSM) of pH 7.0 along with 0.2% w/v of the respective biomass as the inoculum. The bottles were purged with N_2 gas to remove O_2 prior to supplying CO. The initial CO concentration in the bottles was 1.8 mmol/L. The bottles were incubated at 30°C and 150 rpm on a rotating orbital incubator shaker. All these experiments to test CO conversion were carried out in triplicate.

The composition of the MSM (g/l) is as follows: NaCl (0.3), NH_4Cl (0.2), $CaCl_2.2H_2O$ (0.11), $MgCl_2.6H_20$ (0.1), KH_2PO_4 (0.1), $FeCl_2$ (0.945), $CuCl_2$ (0.013), $ZnCl_2$ (0.07), $CoCl_2$ (0.065), Na_2MoO_4 (0.021), $MnCl_2$ (0.63), $NiCl_2$ (0.13) and yeast extract (0.5). The MSM was buffered using K_2HPO_4 to maintain the pH at 7.0. Bottles without any added biomass or with autoclaved biomass served as the control in these CO conversion experiments.

3.2.2 CO conversion pathway elucidation

In order to understand the CO conversion pathway followed by the microorganisms present, methanogenic inhibitor was added in the batch serum bottles. CO conversion experiments similar to that described in the previous section were performed with bromoethanesulfonate (BES) addition in the range 5-20 mmol/L as inhibitor of methanogenic activity in the anaerobic biomass from Kavoor STP, which showed the best results among the different biomass types with maximum CO conversion efficiency.

3.2.3 Microbial community analysis

For microbial community analysis of the biomass that showed the best results for CO conversion was chosen i.e. anaerobic biomass from Kavoor STP was used. The biomass samples were withdrawn from serum bottles and were immediately transferred to sealed container to maintain anaerobic environment and later sent to AgriGenome Labs Private Limited, Cochin, Kerala, India for metagenomics sequencing and analysis.

3.2.4 Effect of process parameters and biomass pretreatment on CO conversion and sulfate reduction

To examine the effect of different process parameters viz. temperature, inoculum size, CO concentration and biomass pretreatment on CO conversion and sulfate reduction by the anaerobic biomass from Kavoor STP, experiments were performed as per the Taguchi experimental design. The design comprised of nine experimental runs with four main variables, viz. initial CO concentration, inoculum volume, temperature and biomass type. Each variable in these experiments was evaluated at three different levels, and all experiments were conducted in triplicate using serum bottles with MSM containing 1000 mg/L sulfate added as Na_2SO_4. Other conditions followed were the same as mentioned earlier. The three types of biomass pretreatment considered were: heat treated, autoclaved and raw biomass. For heat-pretreatment, the biomass was subjected to a temperature of 60 ºC for 15 min in a boiling water bath. In case of autoclaved biomass, it was subjected to 120 ºC at 15 psi for 20 min in an autoclave. Table 3.2 presents the combination level of the parameters in each experimental run, as per the design. Both CO removal and sulfate reduction were considered as response in each experimental run, and the corresponding signal-to-noise (S/N) ratio was calculated using the following equation (Eq. 3.1):

$$\frac{S}{N} = -10\ [\log\left(\frac{1/Y^2}{n}\right)] \quad \text{.....(3.1)}$$

where Y is the response and n is the number of experimental runs. For statistical analysis of the results, the statistical software Minitab (version 16, PA, USA) was used.

Table 3.2 Taguchi experimental design showing the combinations of the variables and their levels in each experimental run

Exp. Run No	Temperature (°C)	Initial CO concentration (mmol/L)	Inoculum size (% v/v)	Biomass pretreatment
1	30	1.8	5	Heat treated
2	30	2.4	10	Autoclaved
3	30	3.1	15	Raw
4	45	1.8	10	Raw
5	45	2.4	15	Heat treated
6	45	3.1	5	Autoclaved
7	60	1.8	15	Autoclaved
8	60	2.4	5	Raw
9	60	3.1	10	Heat treated

3.2.5 Analytical methods

The head space biogas composition in the serum bottles was examined by a gas chromatograph (GC, Varian 450, The Netherlands) fitted with thermal conductivity detector and a molecular sieve column (Mole strainer 5A, work 80/100, 72 in × 1/8 in). Nitrogen gas (99.9%) was utilized as the injector gas at a steady stream rate of 30 mL/h, and the temperature of injector, column and detector were 50 °C, 90 °C and 105 °C, respectively. Biomass was estimated as mixed liquor volatile suspended solids (MLVSS) as per the method described in the American Public Health Association (APHA, 2005).

Sulfate concentration was determined using the standard barium chloride based turbidimetric method (APHA, 2005). Samples prior to the determination of sulfate were pretreated with $ZnCH_3COONa$ (1N) and NaOH (6N) in order to fix the sulfide present (Sabumon, 2008) followed by centrifugation at 8000 × g for 5 minutes. Buffer solution prepared using

deionized water with KNO_3, $MgCl_2 \cdot 6H_2O$, CH_3COONa and 99% glacial acetic acid was added to a suitable portion of the diluted supernatant solution along with 1 ml of 0.5 M $BaCl_2$. The mixture was continuously stirred before measuring its absorbance using a UV-visible spectrophotometer (Cary 100, Varian, Australia).

For sulfide measurement, 0.05 ml sample was taken into 1.95 ml copper reagent with rapid stirring (1000 rpm). Immediately after mixing for 5s, absorption of the mixture was measured at 480 nm. A mixture containing 0.05 ml sample and 1.95 ml HCl (50 mmol/L) served as the blank (Cord-Ruwisch, 1985). Sulfide concentration in the samples was determined from a calibration curve prepared using different concentrations of standard sulfide versus absorbance at 480 nm.

For volatile fatty acids (VFA) analysis 0.5 ml sample was taken into a dry test-tube and added with 1.5 ml ethylene glycol reagent and 0.2 ml of 19.5N sulphuric acid; the mixture was then heated for 3 min in a boiling water bath. After allowing the contents in the test tube to cool down, 0.5 ml of 10% hydroxylamine hydrochloride solution, 2 ml of 4.5 N NaOH solution and 10 ml of 10% ferric chloride solution were added. The absorbance was measured at 495 nm using a spectrophotometer (Cary 100, Varian, Australia). Biomass was estimated as MLVSS as per the American Public Health Association (APHA, 2005).

3.3 Results and discussion

The main motivation behind this study is to find a suitable anaerobic mesophilic microbial consortium capable of performing CO conversion to H_2 and to integrate it with sulfate reduction in wastewater. In this context, some native anaerobic microbial consortia were screened and the effect of important process parameters on their performance was evaluated.

3.3.1 Screening of anaerobic biomass for hydrogenogenic CO conversion

Anaerobic biomass samples from five different sources were screened on the basis of their CO conversion capabilities. Among five sources three were large scale UASB plant treating combination of industrial and domestic wastewater, one was a sewage treatment plant located at IIT Guwahati, Guwahati, Assam, India, and another one was a lab-scale upflow anaerobic packed bed reactor treating sulfate rich wastewater. Fig. 3.1 shows the time profile of CO conversion by anaerobic biomass samples collected from different sources.

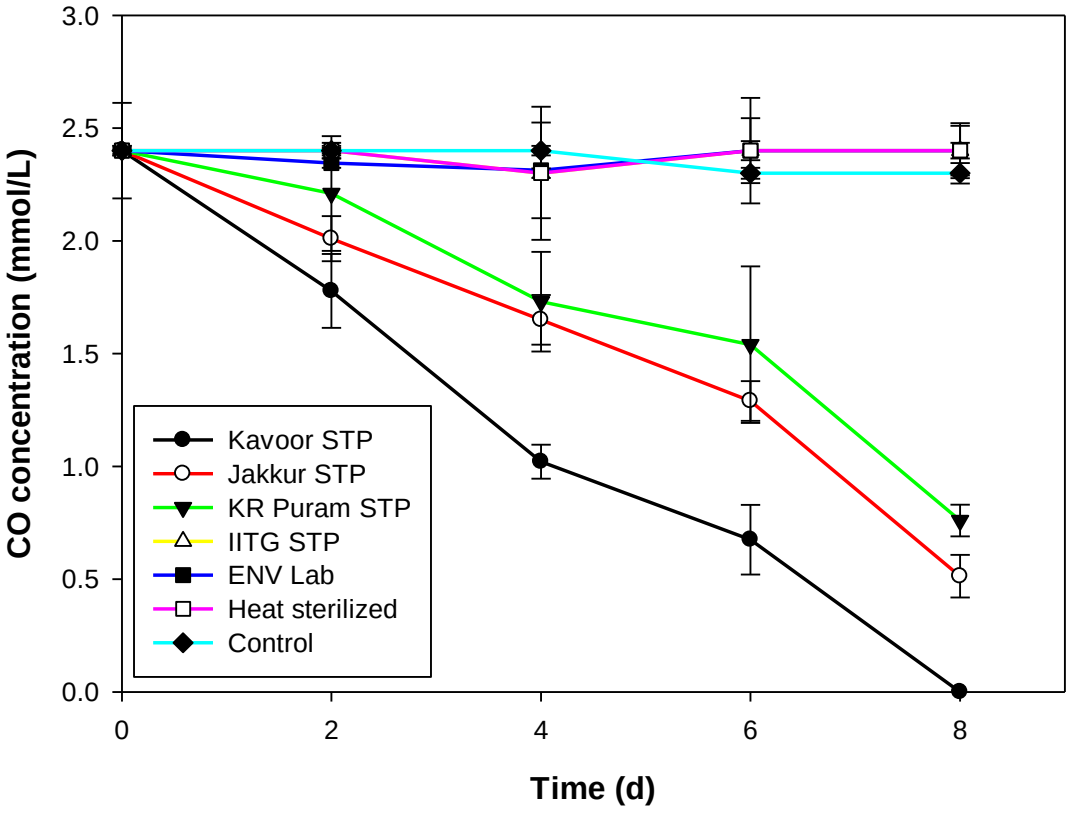

Fig. 3.1 Time profile of CO conversion by anaerobic biomass samples collected from different sources.

These results revealed that although none of the tested biomass samples were previously acclimatized to utilize CO as the sole carbon source, all the three anaerobic biomass collected

from their respective large scale UASB reactors treating wastewater were capable of CO conversion. The other two anaerobic biomass samples, however, did not utilize CO as the sole carbon source (Fig. 3.1). Among the three anaerobic biomass samples, the best CO conversion efficiency was shown by the biomass collected from the Kavoor STP, which showed complete utilization of CO within the eight day incubation period. The other two anaerobic biomass samples from Jakkur and KR Puram STPs, were able to utilize only 77% and 70% of the initial CO content, respectively. The CO conversion is attributed to the metabolic activity of the microorganisms present in the anaerobic biomass as no conversion was observed in the absence of biomass (control) or with heat-sterilized biomass, which served as the control in these experiments (Fig. 3.1). Fig. 3.2 shows the headspace gas composition in the serum bottles added with anaerobic biomass capable of CO conversion.

The granular anaerobic biomass, in general, was more effective in utilizing CO than the simple sludge biomass, which suggests that a certain CO conversion capacity is ubiquitous in such granular biomass from UASB reactor, probably due to the exposure to other toxic gases including CO and CO_2 in such reactors. Granular nature of the anaerobic biomass is another advantage for CO utilization, as reported in an earlier study (Sipma et al, 2003). From the results shown in Fig. 3.2, it is clear that CO was converted to methane and carbon dioxide along with hydrogen at a low initial CO concentration. The production of methane as a major product of CO conversion suggests that the anaerobic biomass contains actively metabolizing methanogenic bacteria. As methanogens are known to utilize the in-situ produced H_2 for methane production, H_2 production was thus small compared to methane and carbon dioxide from CO. The methanogenic bacteria are also well known for utilizing CO by a different pathway which can be either acetotrophic or hydrogenotrophic (Mörsdorf et al., 1992).

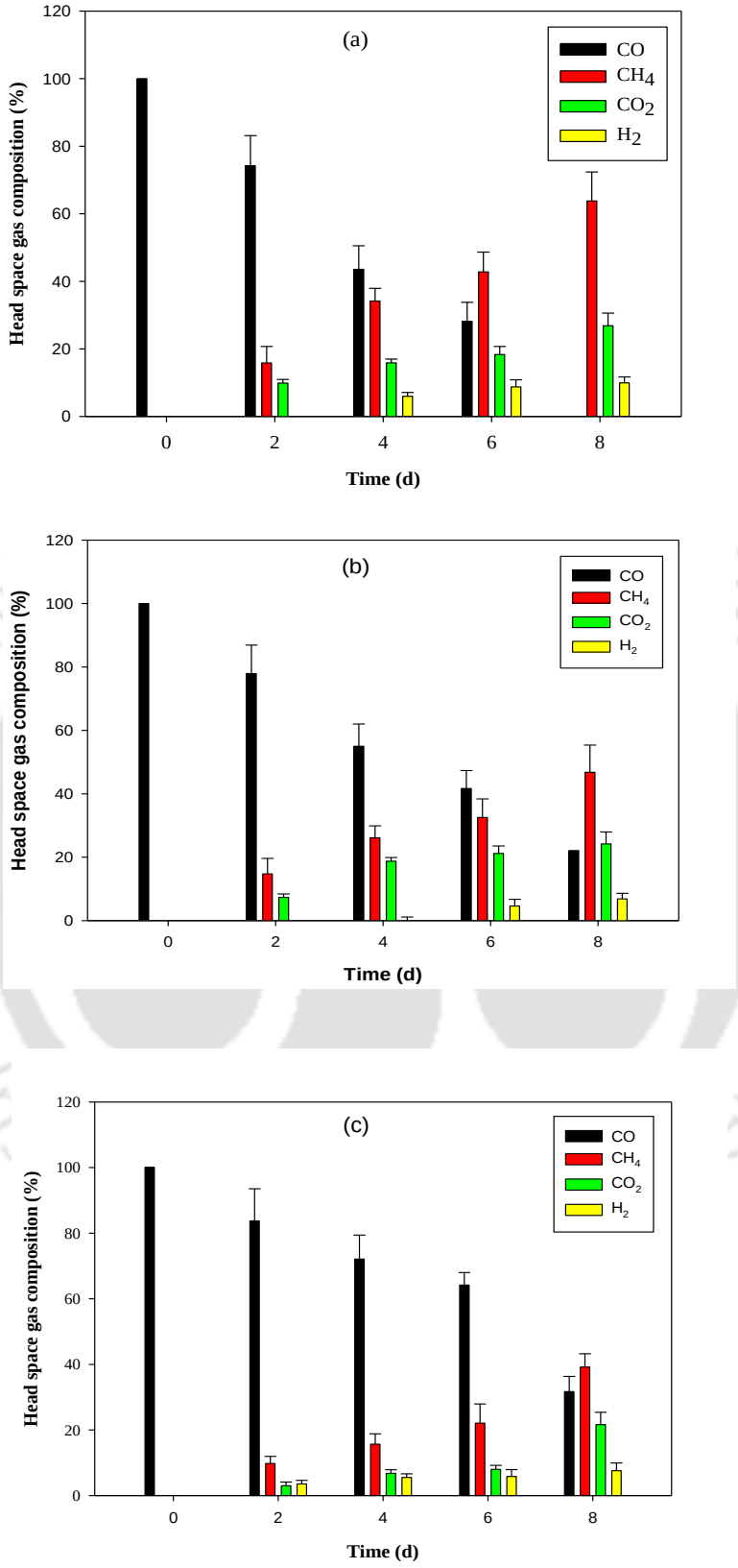

Fig. 3.2 Headspace gas composition in the bottles treating CO with anaerobic biomass from different STPs (a) Kavoor, (b) Jakkur and (c) K.R Puram.

Furthermore, from the results of headspace gas composition obtained at different biomass and at different time periods (Fig. 3.2), it can be well said that the anaerobic biomass converts CO to methane via the hydrogenotrophic pathway. Thus, the following equations (Eq. 3.2 & 3.3) can be used to describe the anaerobic CO conversion by anaerobic biomass in this study (Sipma et al., 2006):

$$CO + H_2O \longrightarrow CO_2 + H_2 \quad \text{……..(3.2)}$$

$$CO + 3\,H_2 \longrightarrow CH_4 + H_2O \quad \text{……..(3.3)}$$

3.3.2 CO conversion pathway

The CO conversion by anaerobic biomass could follow many pathways due to the presence of different classes of bacteria/archea. Some of the microorganisms can even utilize product of CO conversion for their growth and maintenance rather than utilizing CO directly. As the earlier results showed methane to be the main product of CO bioconversion, methanogenic inhibitor BES was added to the batch experiments to illustrate the CO conversion pathway used by anaerobic biomass.

Fig. 3.3 shows the effect of BES addition on headspace biogas composition after five days incubation. The results showed that the final H_2 concentration increased with increase in BES concentration in the media whereas the final CH_4 concentration was reduced. Thus, 10 mmol/L BES concentration was found to be optimum as a higher concentration of 20 mmol/L did not yield any better results. Furthermore, the time profile of CO, H_2 and CH_4 with 10 mmol/L BES revealed that final H_2 concentration increased by 78% due to complete inhibition of methanogenic activity in the biomass with BES addition (Fig. 3.4).

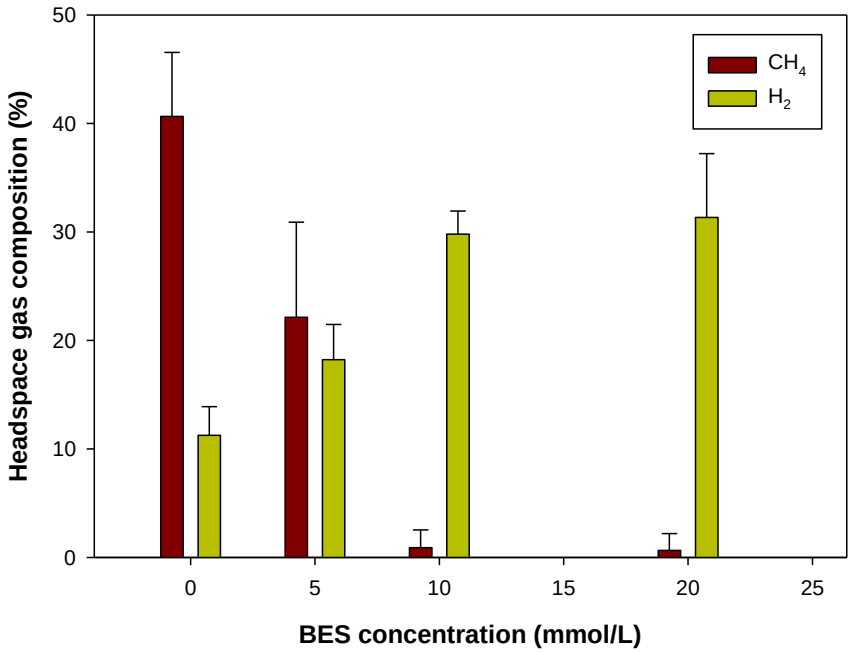

Fig. 3.3 Effect of methanogenic inhibitor on headspace biogas composition.

BES is a widely used methanogen-specific inhibitor and analogous to Coenzyme M (CoM). CoM is a cofactor of methyl - CoM reductase, present in all methanogenic bacteria and archea and performs a key function by carrying methyl group during methane biosynthesis (Liu and Whitman 2008). BES is known to competitively inhibit this methyl group transfer reaction, particularly in hydrogenotrophic methane production system, even at a very low concentration. However, optimum inhibition concentration of BES varies widely depending upon the type of microorganism. Conrad et al. (2000) reported 10 mM as the optimum concentration of BES to inhibit anaerobic methanogens in the rice roots systems. Zinder et al. (1984) found that optimum BES concentration required to inhibit hydrogenotrophic methane production is higher (50 mM) than that required for acetoclastic methane production (1 mM). In this study, a low BES concentration of 10 mM could successfully inhibit hydrogenotrophic methane production, which is in agreement with previous reports (Sipma et al., 2004, Siriwongrungson et al., 2007).

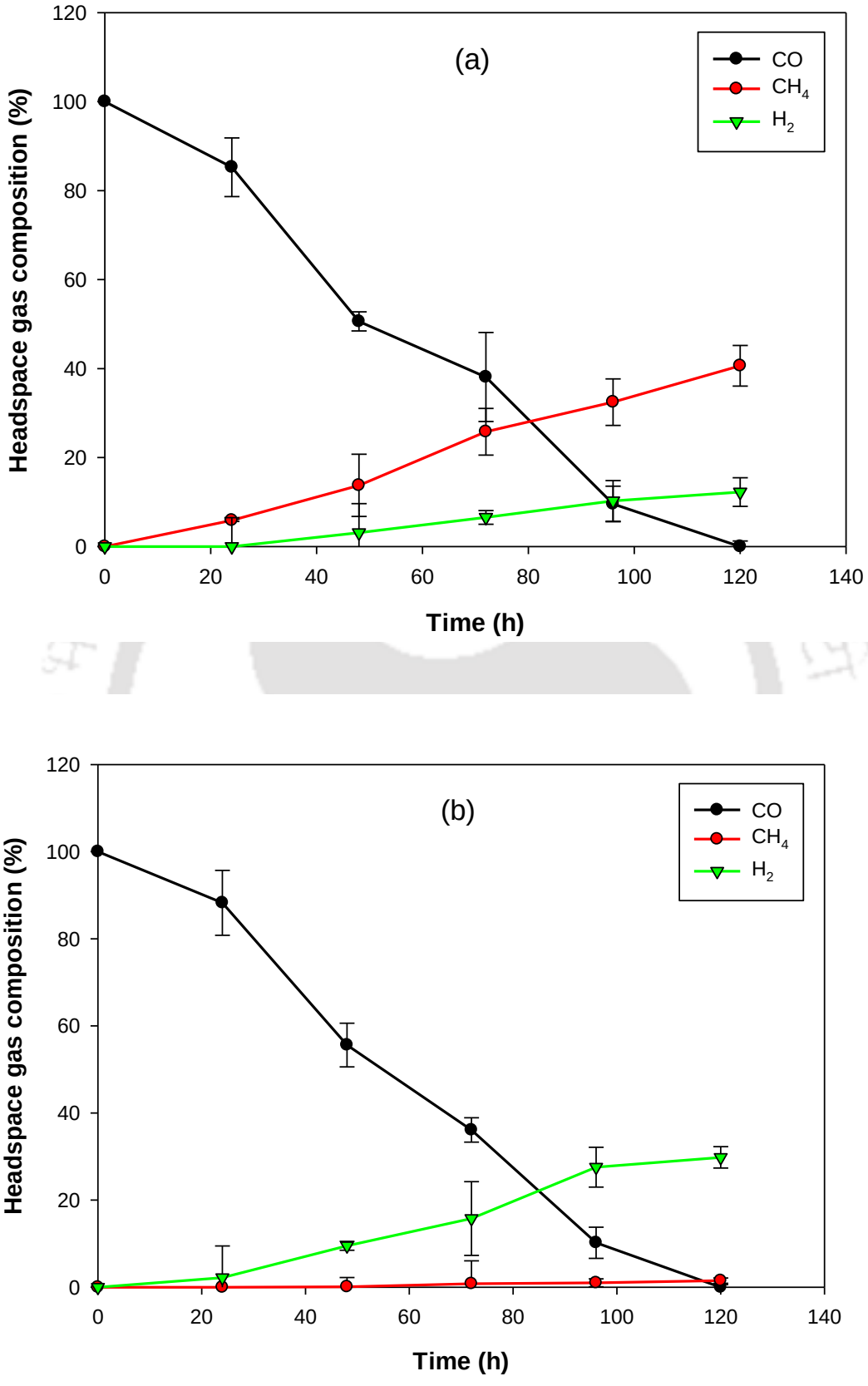

Fig. 3.4 CO, H_2 and CH_4 profile (a) in absence and (b) in presence of BES (10 mmol/L).

Hence, from this investigation and from the literature, the probable CO conversion pathways could be illustrated in Fig. 3.5. There are three possible products from CO conversion by anaerobic biomass, i.e. H_2, acetic acid and CH_4. In this study, it is observed that only the H_2 concentration increased when methanogenic activity was inhibited. The acetic acid concentration did not change significantly and remained at a minimal level in the aqueous media even with BES addition (results not shown). This clearly illustrates that the methane production by the anaerobic biomass was mainly by hydrogenotrophic route. As discussed earlier BES inhibition is not substrate specific, but it rather inhibits the key enzyme methyl - CoM reductase necessary for producing methane; hence, the possible inhibition mechanism due to addition of BES can be confirmed as shown in the schematic.

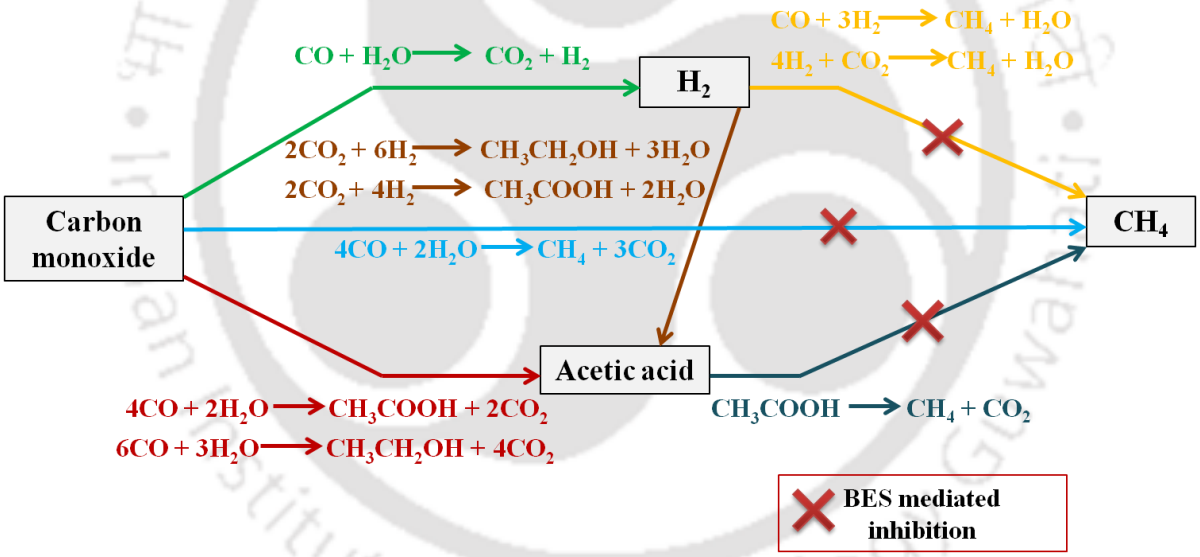

Fig. 3.5 Possible CO conversion pathways and mechanism of BES mediated inhibition.

3.3.3 Microbial community analysis

The 16S small ribosomal subunit gene (16S rRNA), in particular, has been widely used to study and characterize bacterial community compositions in a variety of environmental samples including host associated communities, such as the endogenous human microbiome, and host-free communities, such as soil and ocean environments, etc. Several aspects of the

16S rRNA gene make it optimal as a marker for these types of studies. First, it is ubiquitous among prokaryotic life. Second, its size and high degree of functional conservation result in clock-like mutation rates throughout prokaryotic evolution. Third, and most importantly, the 16S rRNA gene includes both conserved regions, which can be used for designing amplification primers across taxa, as well as nine hyper-variable regions (V1-V9), which can be effectively used to distinguish between taxa.

With the advent of massively parallel sequencing technologies, which generally yield short reads, focus has shifted from sequencing the full 16S rRNA gene to sequencing shorter sub-regions of the gene at great depth. By calculating the geodesic distance between different regions, the phylogenetic relationships based on the V4 sequences were closest to those based on the full-length sequences. This analysis suggests that V4 ranks first in sensitivity as a marker for bacterial and phylogenetic analysis, which is same as taxonomic results obtained using the RDP (Ribosomal Database Project) classifier. In addition, V1-V3 was also highly recommended, and therefore, a combination of V3-V4 region of 16S rRNA gene was selected for this analysis.

Fig. 3.6 shows the relative abundance of different microbes present in the anaerobic biomass samples in Phylum, class, order, family, genus and species level excluding the unknown and unculturable organisms. These sequence reads were assigned to a total of 559201 operational taxonomic units (OTUs). From the results it is found that *Methanomicrobia* (28.61%), *Anaerolineae* (24.18%), *Proteobacteria* (7.17%) are major classes of microorganisms along with small quantities of *Clostridia*, *Caldisericia*, *Acidobacteria*, *Bacteroidia*, etc. are present in the anaerobic biomass. In this analysis, the 'other' indicates organisms that did not make it to in the top 10 category and are estimated to be around 22.63%.

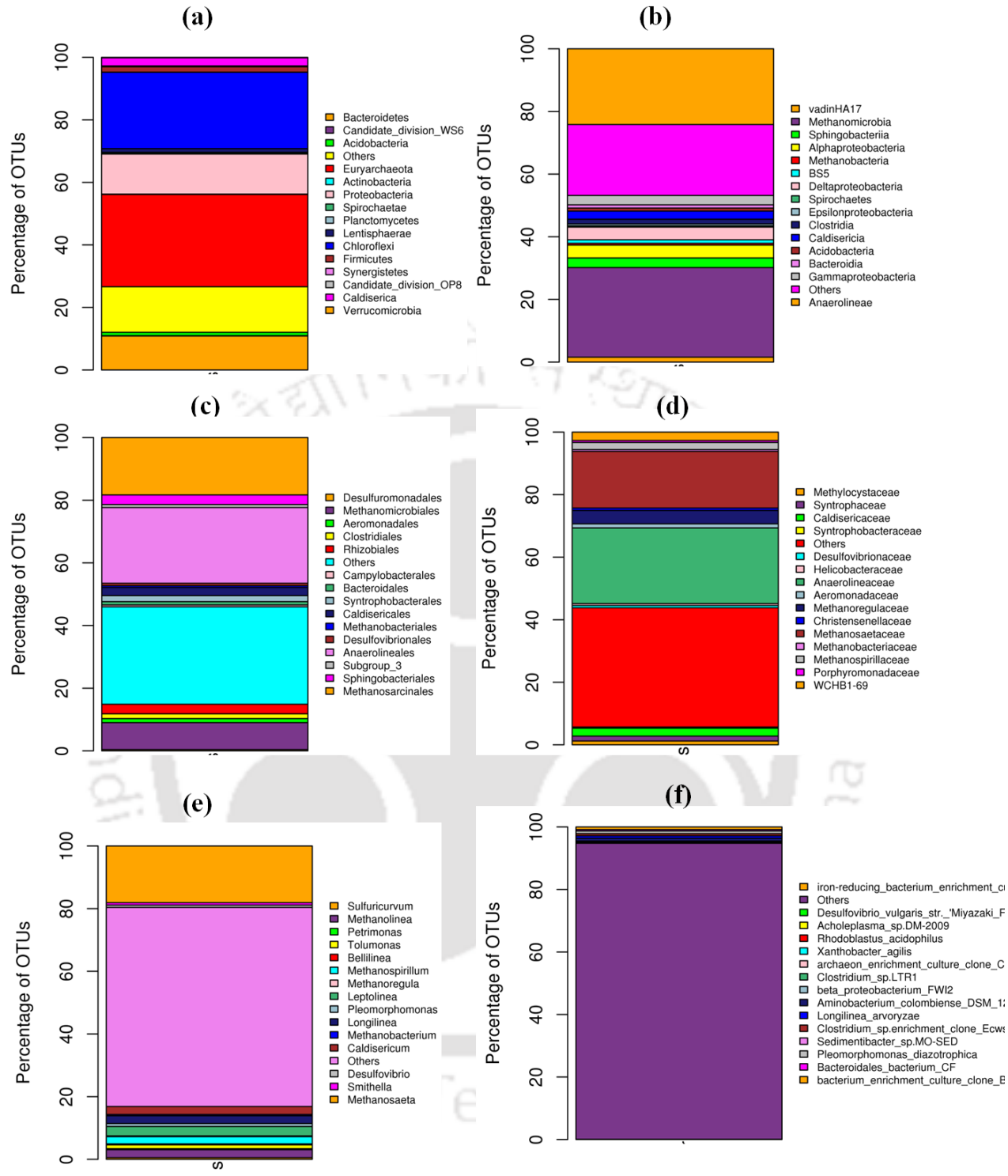

Fig. 3.6 Taxonomic classification of OTUs present in the sludge sample at the level of (a) phylum, (b) class, (c) order, (d) family, (e) genus, (f) species and their relative abundance. For each taxonomic level, only top 10 enriched categories are shown in the figure. Taxa other than top 10 are cumulatively categorized as 'others'.

At the phylum level, *Firmicutes* and *Proteobacteria* sp. were found to be dominant and are well known to be present in anaerobic digestion process treating organic wastes (Sundberg et al., 2013). From the other figures, it can be clearly seen that common anaerobic organisms such as methanogenic, proteobacteria and acidophilic organisms are mainly present in the anaerobic biomass. At the species level more than 90% organisms are within others category at very low numbers in the biomass. Similar finding is also reported earlier by Liu et al. (2016). At the genus level *Desulfovibrio* sp. was detected in samples indicating its potential suitability in biological sulfate reduction using CO as the substrate. None of the identified species present were earlier reported to utilize CO for their growth. The low abundance of CO relating sequences might be due to the possible presence of unknown hydrogenogenic CO-utilizing mesophilic bacteria, as indicated by the higher percentage of unclassified sequences in the anaerobic biomass.

Similar result was reported in a previous study by Luo et al. (2013), in which the absence of known CO-utilizing bacteria and high percentage of unclassified sequences were observed from the bacterial sequences in a continuous reactor converting both CO and sewage sludge to CH_4. The above results strongly indicate the need for more efforts to identify unknown CO-utilizing bacteria, especially from mixed anaerobic culture enriched using CO as the substrate.

3.3.4 Effect of process parameters and biomass pretreatment on CO conversion and sulfate reduction

Fig. 3.7 shows the CO conversion and sulfate reduction efficiencies obtained in the experiments performed as per the Taguchi experimental design (Table 3.2). From the figure, the experimental run 4 gave the best results in terms of sulfate reduction (56.6%) and CO removal (85.62%) compared to other combinations of the variables.

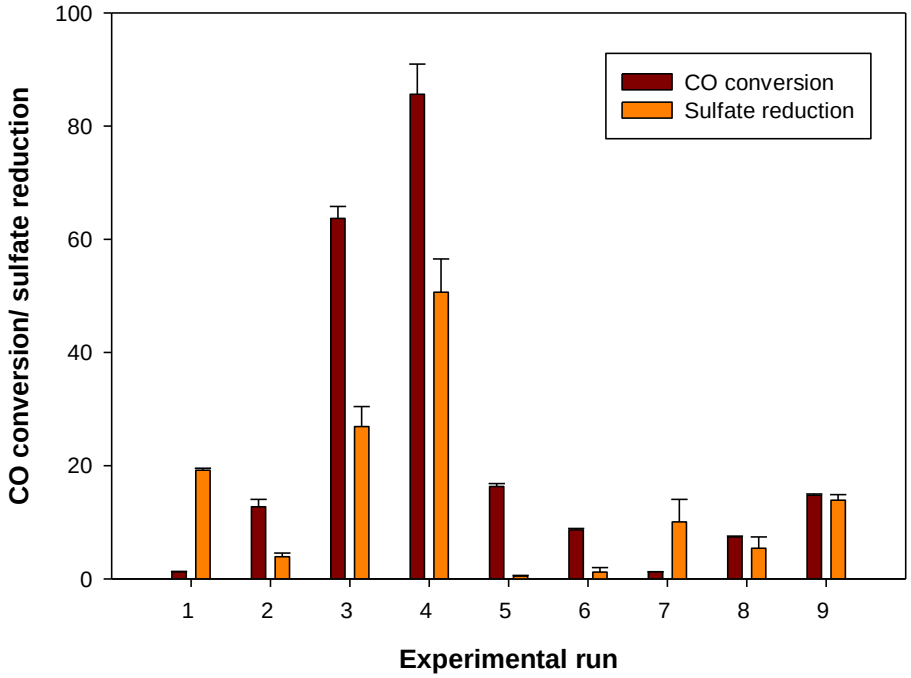

Fig. 3.7 Sulfate reduction and CO conversion efficiencies obtained in the different experimental runs performed as per the Taguchi experimental design.

Based on this observation, optimum levels of the variables were chosen as: 10% (w/v) inoculum size (≈ 0.5 g/L VSS), 1.8 mmol/L initial CO concentration and 45ºC temperature. A verification experiment performed at these optimum values of the parameters further revealed a maximum sulfate reduction (58.17 %) as well as a maximum CO removal (86.24%) by the raw biomass.

Fig. 3.8 illustrates the effect of the four variables on CO conversion and sulfate reduction. It can be seen that for each of the variables tested at three different levels, particular levels of the parameters resulted in a significant increase in the mean response compared to other levels of the variables. For e.g., level 2 of each of the variables (inoculum size, CO partial pressure (P_{CO}) and temperature) was the most significant for both CO conversion and sulfate reduction by the raw anaerobic biomass.

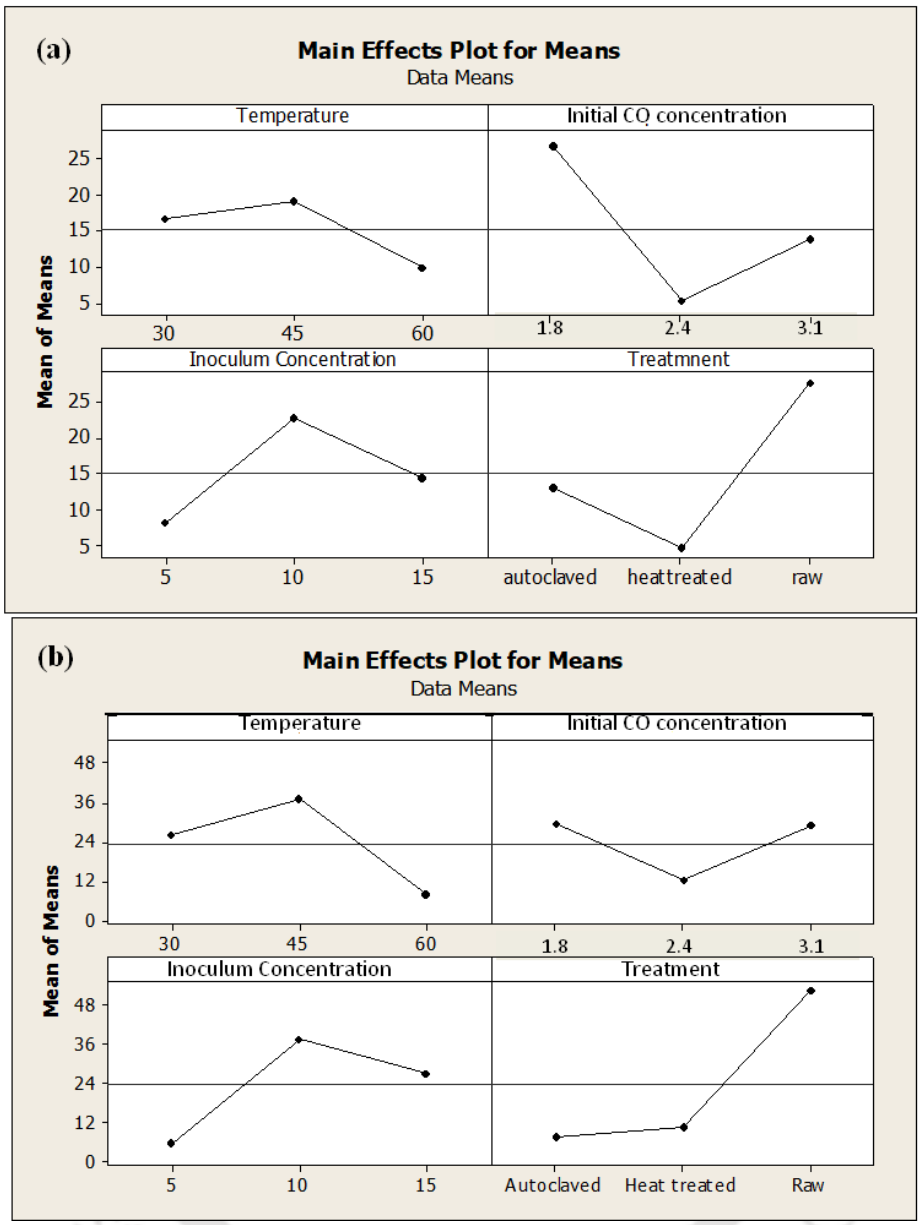

Fig. 3.8 Mean effect plot of the different parameters on (a) sulfate reduction and (b) CO utilization by the anaerobic biomass.

In order to further understand which of these variables affected sulfate reduction in a significant manner, the variables were ranked based on their calculated delta S/N ratio. In general, delta S/N value for a factor, which is calculated by measuring the difference between the maximum and minimum characteristic average S/N ratio of the factor, indicates its relative significance over other factors on a given response; a high delta S/N value of a factor denotes larger significance over the other factors. Whereas S/N ratio of a factor indicates the

effect on a given response, delta S/N ratio can be used as a criterion for ranking factors of their effects on the response (Daverey and Pakshirajan, 2010). In this study, based on the delta S/N ratio obtained for each factor, the four variables were ranked accordingly, and the results are presented in Table 3.3. This ranking suggests that the raw biomass had the maximum effect, whereas initial CO concentration had the least effect on CO conversion and sulfate reduction by the anaerobic biomass from Kavoor STP.

Table 3.3 Values of average signal to noise (S/N) ratio for different variables and their levels, and their ranking based on delta S/N ratio for (a) sulfate reduction and (b) CO conversion

(a)

Level	Temp.	Initial CO concentration	Inoculum size	Biomass pretreatment
1	1.805	2.0347	2.890	12.460
2	6.111	9.1726	12.844	-0.273
3	13.153	9.862	5.334	8.882
Delta[a]	11.348	7.828	9.954	12.733
Rank	2	4	3	1

(b)

Level	Temp.	Initial CO concentration	Inoculum size	Biomass pretreatment
1	25.900	29.377	5.778	7.557
2	36.870	12.168	37.717	10.787
3	7.821	29.047	27.097	52.248
Delta[a]	29.049	17.209	31.939	44.691
Rank	3	4	2	1

[a]Difference between maximum and minimum S/N ratio values

Sipma et al. (2003) suggested heat pretreatment of the granular structure of such methanogenic granular biomass for inhibition of methane formation. However, sulfate reduction efficiencies for different experimental runs revealed that the raw biomass was the most effective among the different parameters as autoclaved or heat treated biomass yielded least CO conversion efficiency. This indicates that though the anaerobic biomass from Kavoor STP is capable of surviving at 45ºC temperature, it is, however, inactivated by heat treatment at 60 ºC for 15 min. The experimental results further reveal that the raw biomass is highly robust and tolerant to CO levels for effective sulfate reduction in wastewater.

3.4 Significant findings

Among the anaerobic biomass collected from different sources, the biomass from Kavoor STP yielded the maximum CO conversion efficiency along with hydrogen production. BES could completely inhibit methanogenic activity by the CO utilizing anaerobic biomass, thus revealing that the CO conversion to CH_4 by the anaerobic biomass was mainly by hydrogenotrophic route. The predominant microorganisms present in the biomass were identified to be *Methanomicrobia, Anaerolineae, Proteobacteria, Clostridia, Caldisericia, Desulfovibrio sp.*, etc. Among the different process parameters, biomass pretreatment and temperature were found to be most significant for both CO conversion and sulfate reduction. The raw anaerobic biomass from Kavoor STP showed a high tolerance towards CO concentration for its conversion.

Chapter 4

Kinetic of biomass growth, substrate utilization and biohydrogen production from carbon monoxide by anaerobic biomass

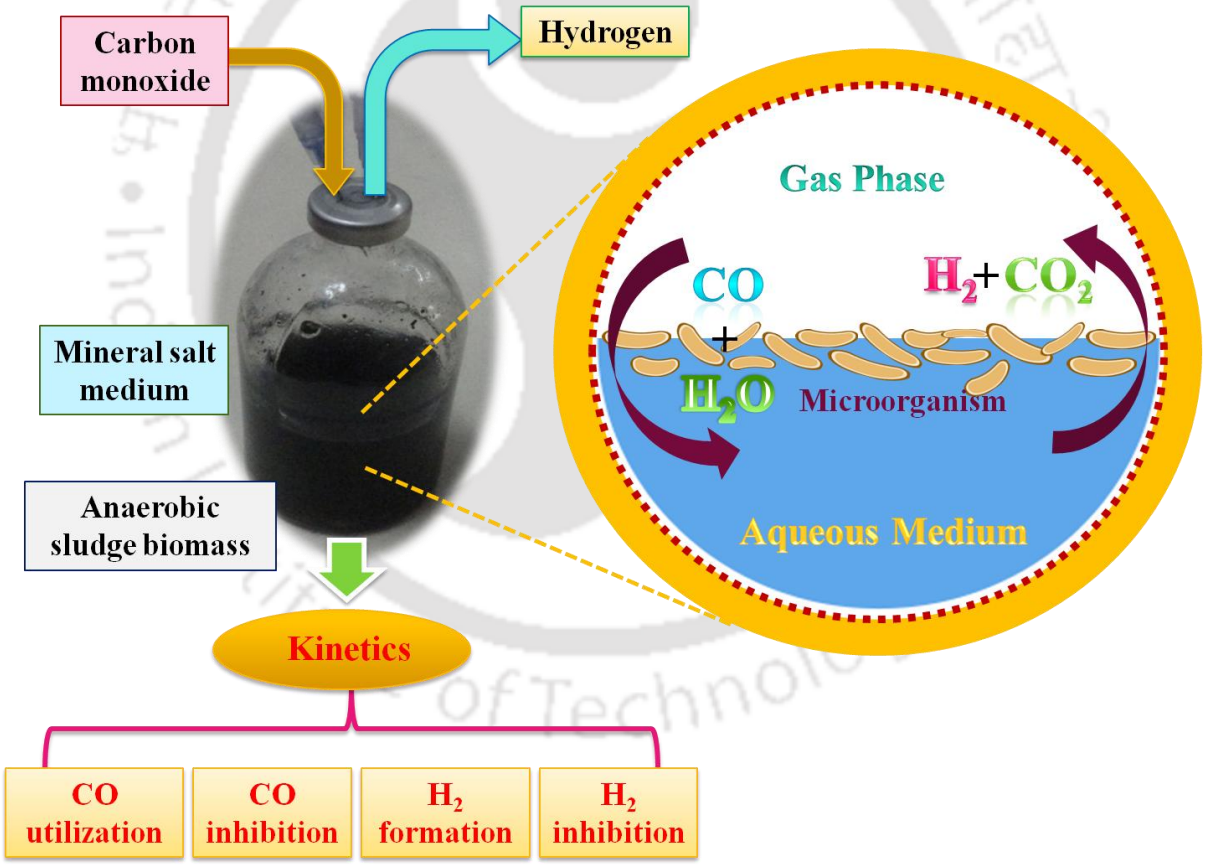

ABSTRACT

In this chapter kinetics of biomass growth, biohydrogen production and CO utilization under batch mode using anaerobic sludge biomass is reported. Experiments were conducted at various initial CO concentrations in the range 1.8-5.12 mmol/L over a period of 144 h in order to assess the effect of CO concentration on biomass growth, substrate utilization and H_2 production. Complete utilization (100 %) of CO was achieved up to an initial concentration of 3.8 mmol/L and it gradually decreased to 84.5% for 4.4 mmol/L and 83.7 % for 5.12 mmol/L. The result of CO utilization were fitted to substrate utilization kinetic models reported in the literature and among the different models the kinetic was best described by growth associated model modified Gompertz model. A maximum yield of H_2 on CO was found to be 70.8% and a maximum H_2 production of 29.9 mmol/L was obtained for an initial CO concentration of 5.12 mmol/L. The experimental results on biohydrogen production matched well with the values predicted using modified Gompertz model. Furthermore, the experimental data on specific growth rate of the ananerobic biomass at different H_2 concentration was fitted to different product inhibition models and the best fit was obtained with Aiba model. This study showed product inhibition on both specific growth rate of biomass and H_2 production due to H_2 accumulation in the gas phase. A very good correlation between the experimental specific growth rate and the Han-Levenspiel model predicted values were obtained with a high determination coefficient (R^2) value of more than 0.96.

4.1 Introduction

Biological hydrogen production technologies are recognized to have more ecological benefits and less energy requirements than the physic-chemical techniques such as thermo-chemical catalytic methods. The available biological routes are dark fermentation, photo fermentation, direct and indirect bio-photolysis and water-gas shift reaction (Levin et al., 2004; Lahijani et al., 2015). Thus, a variety of substrates including glucose, sucrose, starch and waste materials containing these sugars can be used for bio-hydrogen production. However, soluble substrates derived from renewable biomass such as lignocellulosic materials often need processing and pretreatment before it could be utilized by microorganisms. In most cases, it causes loss of valuable biomass and increases the cost of production. In contrast, the carbon monoxide (CO) rich syngas may be a viable alternative to encounter the above problem which is produced from a variety of carbonaceous materials, including waste substartes (Pakshirajan and Mal, 2013; Parshina et al., 2010). The CO content in syngas varies from 10 to 50% (*v/v*) (Grady and Chen, 1998). Despite its toxic effect, CO can be considered as a new and interesting substrate for biological H_2 production through the water-gas shift reaction as shown in equation (4.1) below,

$$CO + H_2O = CO_2 + H_2 \qquad \Delta G^0 = -20.1 \text{ kJ/mol} \qquad \text{.....(4.1)}$$

CO is thermodynamically converted to H_2 and CO_2 under strong equilibrium and the process can be operated at ambient operating conditions which makes it less energy intensive with the use of CO converting microorganisms. The required energy for conversion is supplied by electrochemical reactions involved in the transfer of electrons from CO to H_2O. However, there are key enzymes that are involved in CO conversion to H_2 as follows (Munasinghe and Khanal, 2010): (1) carbon monoxide dehydrogenase (CODH) which oxidizes CO to CO_2 with the production of reducing equivalent in an anaerobic process, (2) CODH-dependent

hydrogenase which causes the reduction of protons to H_2 by using the electrons donated from the previous step mediated by CODH.

Certain bacteria such as purple non-sulfur photosynthetic bacteria and anaerobic carboxydotrophic hydrogenogenic bacteria are shown to catalyze the waste-gas shift reaction. Compared with the photosynthetic bacteria, anaerobic hydrogenogenic bacteria are advantageous for inexpensive production of H_2 as it requires no light and its growth requirements are very simple (Levin et al., 2004). Recently, *Rhodopseudomonas palustris-P4* (Oh et al., 2005; Pakpour et al., 2014), *Caldicellulosirupter saccharolyticus* (Ljunggren et al., 2011) and *Petrobacter succinatimandens* (Pakshirajan and Mal, 2013) have been reported to be involved in bio-hydrogen production from CO as the carbon substrate. However, using a mixed consortium of organisms especially in the form of anaerobic granular sludge biomass seems to be more productive owing to their robust biomass structure and efficient conversion of CO to biohydrogen. Hydrogen produced by microorganisms are known to inhibit biomass growth and reduce the product formation; kinetic models prove useful to investigate such inhibitory effects (Bundhoo and Mohee, 2016). Monod model has been reported to describe the effect of substrate concentration on biomass growth of H_2 generating bacteria, but it does not consider inhibition effect due to substrate/product. The literature is also very limited with regard to information on models that considers inhibitory effect of substrate or product on biohydrogen production, which is highly essential for a better understanding of kinetics of the production process.

Moreover, there are no reports available on biokinetics of inhibition and product formation with CO as a primary substrate. Hence, there is a need to study in detail the kinetics of biohydrogen production from CO and apply suitable models for estimating the biokinetic parameters, which will be helpful in better understanding of the production process. In the previous chapter, anaerobic sludge biomass from five different sources was screened for their

capability to convert CO to H_2. Among the different biomass types, the granular sludge biomass from Kavoor STP proved the best for both CO utilization and H_2 production. However, gaseous substrate concentration can significantly impact the biomass growth and H_2 production. Hence, this study was aimed at investigating the kinetics of biomass growth, CO utilization and H_2 production and its kinetic modeling for a better understanding of biohydrogen production from CO.

4.2 Material and Methods

4.2.1 Kinetics of CO utilization, biomass growth and H_2 formation

The kinetics of CO utilization, biomass growth and H_2 production by anaerobic biomass using CO as the sole carbon and energy source was analyzed for different initial CO concentration in the range 1.8 - 5.12 mmol/L. In these batch experiments, the anaerobic biomass from Kavoor STP was added as the inoculum. All experiments were conducted using 120 ml serum bottles containing MSM as mentioned in the previous chapter (Chapter 3). Following inoculation, the bottles were incubated at 30 ºC temperature in an incubator shaker set at 150 rpm. Biomass dry weight expressed as volatile suspended solids (VSS, g/L), was measured at every 12 h time interval and the biomass specific growth rate (μ) was calculated as per the following Eq. (4.2)

$$\mu = \frac{1}{X}\frac{dX}{dt} \qquad \text{.....(4.2)}$$

where μ is the biomass specific growth rate (h^{-1}), X is the biomass concentration (g/L) corresponding to the time t (h).

The kinetics of CO utilization by anaerobic biomass was analyzed by using four different models: first order, logarithmic, logistic and modified Gompertz model. These model equations are presented in Table 4.1,

Table 4.1 Details of bio-kinetic models tested to study CO utilization at different initial CO concentrations

Sl. No.	Kinetic model	Equation	Estimable parameters	References
1.	First order	$S = S_0 e^{(-Kt)}$	S_0, K	Saravanan et al., 2011
2.	Logarithmic	$S = S_0 + X_0\left[1 - e^{(U_{max}t)}\right]$	S_0, X_0, U_{max}	Saravanan et al., 2011
3.	Logistic	$S = \frac{S_0 + X_0}{1 + \frac{X_0}{S_0}\left[e^{\left(\left(\frac{U_{max}}{K_S}\right)(S_0 + X_0)t\right)}\right]}$	S_0, X_0, U_{max}, K_S	Saravanan et al., 2011
4.	Modified Gompertz	$S_0 - S = S_{max}\mathrm{e}^{\left[-e^{\left[\left(\frac{U_{max}\times 2.71828}{S_{max}}\right)(\lambda - t)+1\right]}\right]}$	S_{max} U_{max}, λ	Mu et al., 2007

In these model equations, S and S_0 are the instantaneous and initial CO concentrations (mmol/L), respectively. X_0 is the initial biomass concentration (g/L), K is the first order rate constant (h^{-1}), U_{max} is the maximum CO utilization rate (mmol/L/h), K_S is the half saturation constant (mmol/L), S_{max} is the maximum concentration of CO utilization (mmol/L) and λ is time of lag phase (h).

Furthermore, in order to study the specific CO utilization rate with different initial CO concentrations, experimental data was fitted to seven biokinetic models reported in the literature (Table 4.2),

Table 4.2 Details of bio-kinetic models tested to study specific CO utilization

Sl. No.	Kinetic model	Equation	Estimable parameters	References
1.	Monod	$U = \frac{q_{max}S}{K_S + S}$	q_{max}, K_S	Mitra et al., 2017
2.	Haldane	$U = \frac{q_{max}S}{K_S + S + \frac{S^2}{K_i}}$	q_{max}, K_S, K_i	Mitra et al., 2017
3.	Han-Levenspiel	$U = \frac{q_{max}S\left[1 - \frac{S}{S_m}\right]^n}{K_S + S\left[1 - \frac{S}{S_m}\right]^m}$	q_{max}, K_S, S_m	Mitra et al., 2017
4.	Edward	$U = \frac{q_{max}S}{K_S + S + \left(\frac{S^2}{K_i}\right)\left(1 + \frac{S}{K_s}\right)}$	q_{max}, K_S, K_i	Mitra et al., 2017
5.	Moser	$U = \frac{q_{max}S^n}{K_S + S^n}$	q_{max}, K_S, n	Mitra et al., 2017
6.	Yano and Koga	$U = \frac{q_{max}S}{K_s + S + \left(\frac{S^2}{K_1}\right)^n}$	q_{max}, K_S, K_1, n	Mitra et al., 2017
7.	Luong	$U = \frac{q_{max}S}{K_s + S}\left[1 - \frac{S}{S_m}\right]^n$	q_{max}, K_S, S_m, n, m	Mitra et al., 2017

In these models, U is the specific CO utilization rate (h^{-1}), q_{max} is the maximum specific CO utilization rate (h^{-1}), S is the CO concentration (mmol/L), S_m is the CO concentration above which net biomass growth ceases (mmol/L), K_s is the half saturation constant (mmol/L), K_i is the inhibition coefficient (mmol/L), K_1 is the positive constant and n and m are empirical constants.

Following the CO utilization kinetics, biomass growth on CO was modeled using modified Gompertz and Logistic kinetic models (Table 4.3),

Table 4.3 Modified Gompertz and Logistic models tested to study biomass growth on CO

Sl. No.	Kinetic model	Equation	Estimable parameters	References
1.	Gompertz	$X - X_0 = X_{max} e^{\left[-e^{\left[\left(\frac{R_{max} \times 2.71828}{X_{max}}\right)(\lambda - t)+1\right]}\right]}$	X_{max} R_{max}, λ	Mu et al., 2007
2.	Logistic	$X - X_0 = \frac{X_{max}}{\left[1 + e^{\left[\left(\frac{4R_{max}}{X_{max}}\right)(\lambda - t)+2\right]}\right]}$	X_{max} R_{max}, λ	Saravanan et al., 2011

Where, X_{max} is the maximum biomass concentration (g/L), R_{max} is the maximum rate of biomass growth (mmol/L/h) and λ is the time of lag phase (h).

In order to study the biohydrogen production from CO by anaerobic biomass experimental data was fitted to modified Gompertz model equation, which is widely used to study hydrogen production or biogas production from a variety of substrates (Lin and Lay, 2004). The equation is as follows:

$$P = P_{max} e^{\left[-e^{\left[\left(\frac{R_{max} \times 2.71828}{P_{max}}\right)(\lambda - t)+1\right]}\right]} \quad \text{……..(4.3)}$$

where, P is cumulative H_2 production (mmol/L), P_{max} is maximum hydrogen production (mmol/L), R_{max} is maximum rate of H_2 production (mmol/L/h) and λ is the time lag phase in H_2 production (h).

All biokinetic parameters from the reported models were estimated by minimizing the sum of squared errors (SSE) between the experimental and predictable data by using the 'Solver' function tool in Excel 2016.

4.2.2 Kinetics of substrate inhibition on biomass growth

The classical Monod model is used to describe the effect of substrate concentrations on specific growth rate of biomass. However, at a high concentration, this model is found to be unsatisfactory because of substrate inhibition on bacteria. Hence, nine different substrate

inhibition models that are widely reported in the literature were used to describe the effect of substrate concentration on specific growth rate of anaerobic biomass in this study and the equation are given in Table 4.4:

Table 4.4 Substrate inhibition models applied to study biomass specific growth rate at different initial CO concentration

Sl. No.	Kinetic model	Equation	Estimable parameters	References
1.	Andrews	$\mu = \frac{\mu_{max} S}{K_S + S + \frac{S^2}{K_i}}$	μ_{max}, K_S, K_i	Saravanan et al., 2011
2.	Aiba	$\mu = \frac{\mu_{max} S}{K_S + S} e^{\left(\frac{-S}{K_i}\right)}$	μ_{max}, K_S, K_i	Agarry et al., 2010
3.	Han and Levenspiel	$\mu = \frac{\mu_{max} S \left[1 - \frac{S}{S_m}\right]^n}{K_S + S \left[1 - \frac{S}{S_m}\right]^m}$	μ_{max}, S_m, K_S, n, m	Saravanan et al., 2011
4.	Luong-inhibition	$\mu = \frac{\mu_{max} S}{K_s + S} \left[1 - \frac{S}{S_m}\right]^m$	μ_{max}, S_m, K_S, m	Mitra et al., 2017
5.	Tiessier	$\mu = \mu_{max} \left[e^{\left(\frac{-S}{K_i}\right)} - e^{\left(\frac{-S}{K_S}\right)}\right]$	μ_{max}, K_S, K_i	Mitra et al., 2017
6.	Edward	$\mu = \frac{\mu_{max} S}{K_S + S + \left(\frac{S^2}{K_i}\right)\left(1 + \frac{S}{K_s}\right)}$	μ_{max}, K_S, K_i	Saravanan et al., 2011
7.	Webb	$\mu = \frac{\mu_{max} S \left(1 + \left(\frac{S}{K_i}\right)\right)}{K_s + S + \left(\frac{S^2}{K_1}\right)^n}$	μ_{max}, K_S, K_i, K_1	Agarry et al., 2010
8.	Tseng and Wayman	$\mu = \left(\mu_{max}\left(\frac{S}{K_s + S}\right)\right) - \left(K_i(S - S_m)\right)$	μ_{max}, K_S, K_i, S_m	Mitra et al., 2017
9.	Yano and Koga	$\mu = \frac{\mu_{max} S}{K_s + S + \left(\frac{S^2}{K_1}\right)^n}$	μ_{max}, K_S, K_1	Mitra et al., 2017

4.2.3 Product inhibition kinetics

In order to investigate the product inhibition due to H_2 on the biomass growth and biohydrogen production by the anaerobic biomass, experiments were carried out at different H_2 concentrations (0.5, 1.2, 1.8, 2.5, 3.2 and 4.5 mmol/L) under a fixed initial CO

concentration of 3.1 mmol/L. The other experimental conditions and the media used were the same as described earlier in section 4.2.1. At respective time intervals CO and H_2 concentration from the headspace and biomass (dry weight basis) were measured using standard procedure as previously described. The experimental data on biomass growth and H_2 production was fitted to four biokinetic models presented in Table 4.5:

Table 4.5 Bio-kinetic models used to study product inhibition on biomass growth and biohydrogen production

Sl. No.	Kinetic model	Equation	Estimable parameters	References
1.	Modified Han-Levenspiel	$\mu = \mu_{max}\left(1 - \frac{C}{C_{Crit}}\right)^n$	μ_{max}, C_{crit}, n	Saravanan et al., 2011
2.	Non-competitive[a]	$\mu = \frac{\mu_{max}}{1+\left(\frac{C}{K_C}\right)^n}$	μ_{max}, K_C, n	Wang et al., 2008
3.	Non-competitive[b]	$\mu = \frac{\mu_{max}K_C}{K_C+C}$	μ_{max}, K_C	Liu et al., 2006
4.	Competitive	$\mu = \frac{\mu_{max}C}{K_S\left(1+\frac{C_{Crit}}{K_C}\right)+C}$	μ_{max}, C_{crit}, K_S, K_C	Saravanan et al., 2008

where, C is the inhibitor concentration (mmol/L), C_{Crit} is the critical inhibitor concentration(mmol/L), K_C is the inhibition constant (mmol/L) and n is the degree of inhibition. For describing the inhibitory effect due to H_2 on its own production by anaerobic biomass, the biomass specific growth rate and maximum specific growth rate were replaced by H_2 production rate (mmol/L/h) and maximum H_2 production rate (mmol/L/h), respectively. The polynomial regression technique was used to estimate the model kinetic parameters of biomass growth rate and H_2 production rate models using Excell 2016.

4.2.4 Analytical methods

Head space biogas composition in the serum bottles was analyzed using a gas chromatograph (GC, Varian 450, The Netherlands) equipped with a thermal conductivity detector (TCD) and

a molecular sieve column (Mole sieve 5A, mesh 80/100, 72 in × 1/8 in). Pure nitrogen was used as the carrier gas at a constant flow rate of 30 ml/min and the temperature of the injector, column and detector were 50 °C, 90 °C and 105 °C, respectively. Anaerobic biomass as volatile suspended solids (VSS) was measured following the standards methods (APHA, 1995). The details of all these methods were provided in Chapter 3.

4.3 Results and discussion

The present study was aimed at elucidating the potential capacity of the anaerobic biomass to uptake CO for H_2 production through the water-gas shift reaction. A separate set of experiments were conducted to analyze the product (H_2) inhibition on H_2 fermentation from CO. Furthermore, different biokinetic models were used to describe the substrate utilization, biomass growth, product formation and inhibition due to the substrate (CO) and accumulation of H_2.

4.3.1 Kinetics of substrate utilization

Fig. 4.1 shows the time course of CO utilization by the anaerobic biomass at different initial CO concentrations; which reveals that the CO was completely utilized (100 %) for an initial concentration up to 3.8 mmol/L; at concentrations 4.4-5.12 mmol/L CO was moderately utilized by the anaerobic biomass (80-85 %). From the CO utilization profile, it is also clear that the time taken by the anaerobic biomass to utilize CO was dependent upon its initial concentration. Furthermore, CO utilization time at a high initial concentration may be divided into two phases: initial lag phase and active degradation phase, no significant lag phase could be observed at low initial CO concentration though. Pakpaur et al. (2014) reported 68 % of initial concentraton of CO was converted into biohydrogen by ananerobic biomass within a short time of 72 h, whereas in this study 100% CO utilization was observed within 84 h. The difference in results could be due to acclimatization of the ananerobic biomass for CO

conversion. Moreover, BES addition to the culture medium ensured the inhibition of methanogenic activity, thereby improving the biohydrogen production level.

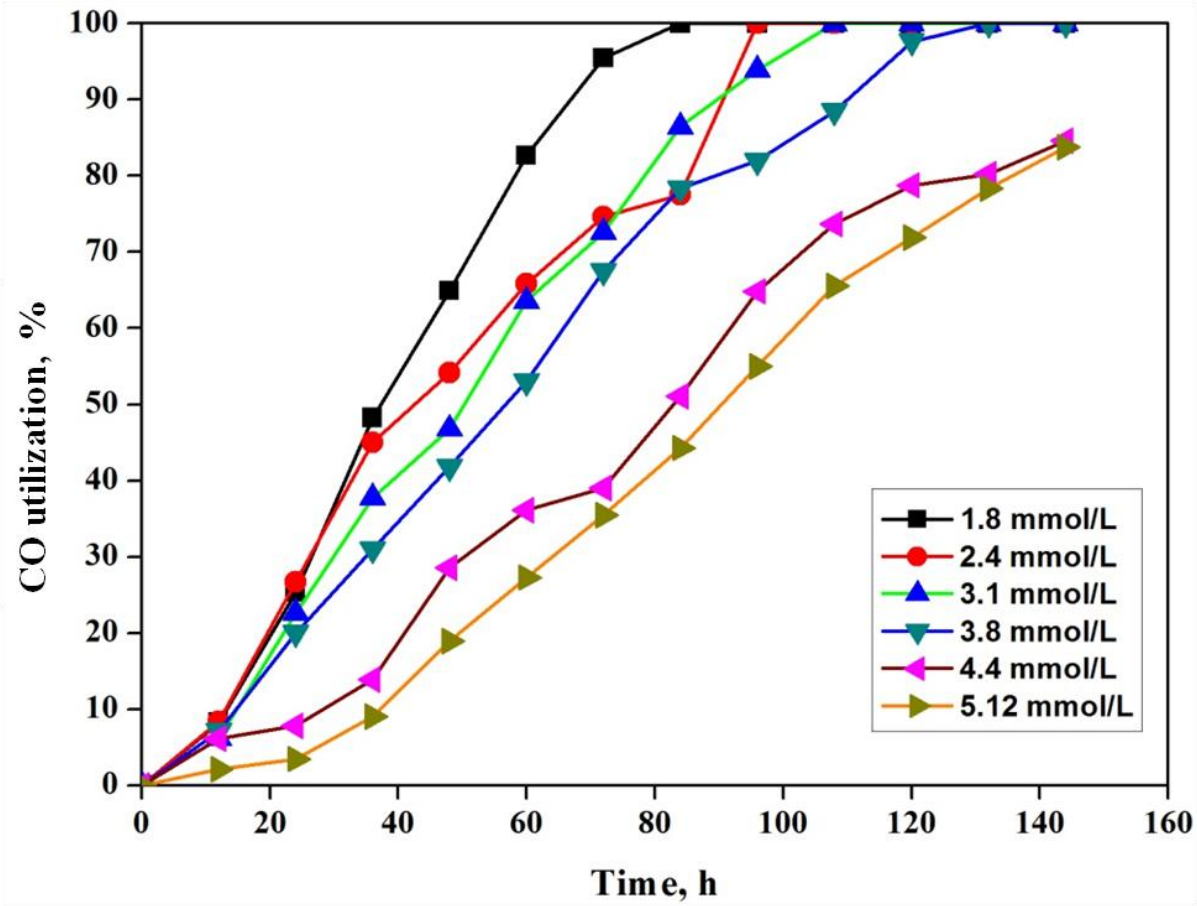

Fig. 4.1 CO utilization profile for different initial CO concentration.

Fig. 4.2 compares the experimental and predicted values of CO utilization by anaerobic biomass using different biokinetic models (Table 4.1). This is the first report on kinetics of CO utilization by anaerobic biomass, where different biokinetic models such as a non-growth associated model based on simple first order kinetic and growth associated models (logarithmic, logistic and modified Gompertz models) were applied for describing the CO utilization by the anaerobic biomass at different initial CO concentrations. The estimated values of biokinetic parameters obtained from these models are presented in Table 4.6.

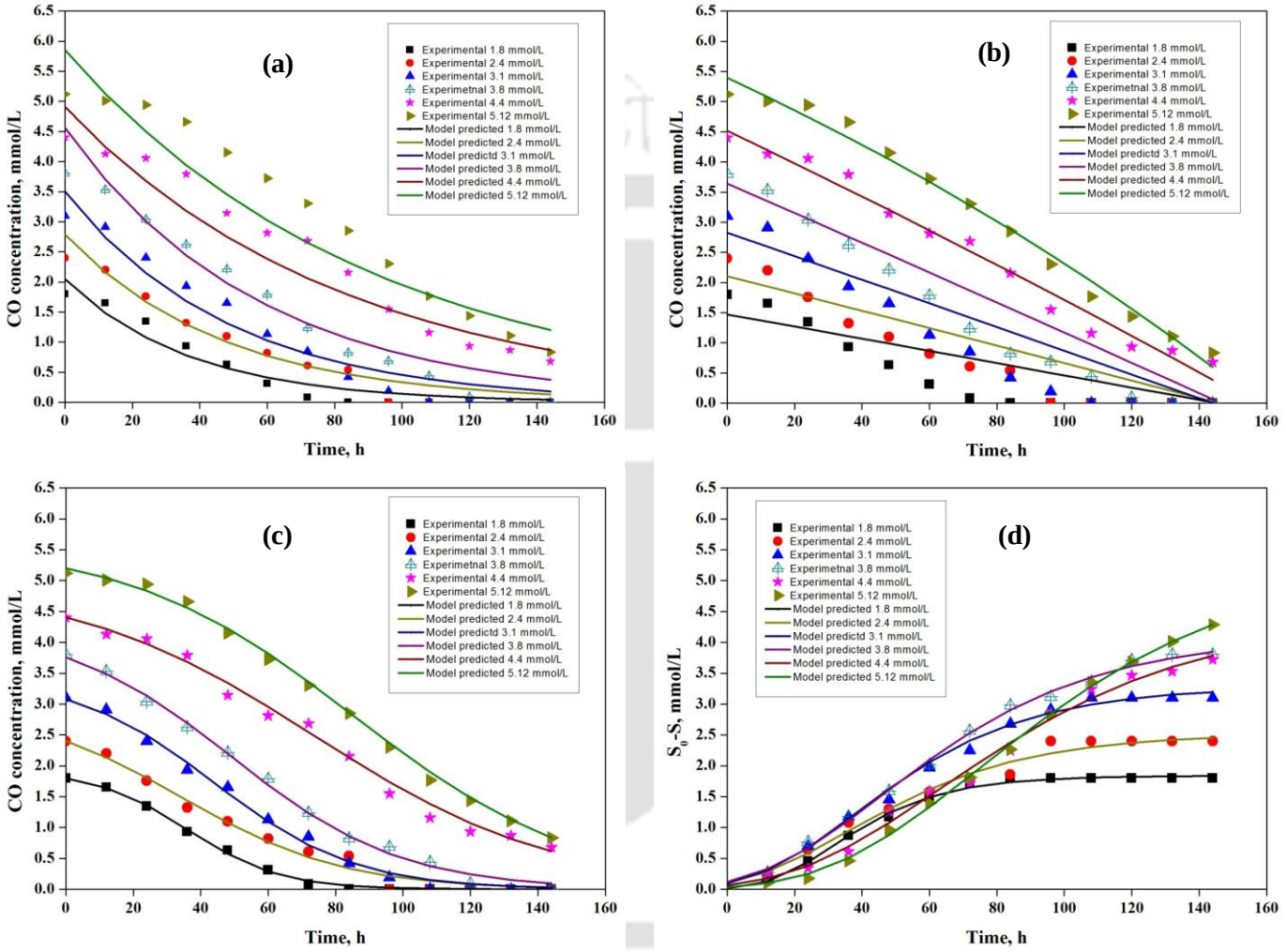

Fig. 4.2 Experimental and predicted values of CO utilization due to (a) First order kinetic (b) Logarithmic (c) Logistic kinetic and (d) modified Gompertz models.

Among the four different models tested, the modified Gompertz model could fit the experimental data (Fig. 4.2d) with a coefficient of determination (R^2) value greater than 0.95 for all initial CO concentrations. It is reported that compared with other kinetic models modified Gompertz model is best suited for explaining biohydrogen production using soluble substrate (Pakpaur et al., 2014; Mu et al., 2007). Compared with non growth associated model based on first order kinetic model both the growth associated models fitted the experimental data well, indicating that the CO utilization was indeed growth associated. From the biokinetics parameters estimated values using the modified Gompertz model, it is observed that the maximum CO utilization increased with increase in the initial CO concentration, which indicated the robust nature of the biomass to utilize CO even at a high concentration. However, the lag phase time (λ) also increased with increase in initial CO concentration indicating need for longer incubation time for complete CO utilization at a high initial CO concentration. The maximum CO utilization rate varied in the range 0.0307 - 0.041 mmol/L/h. The model constant values obtained in this study matched well with the values reported by Mu et al. (2007) for H_2 production using mixed anaerobic culture and organic waste as substrate. These results confirm that the anaerobic biomass is well capabale of utilizing CO as the sole substrate.

Table 4.6 Estimated biokinetic parameters for substrate utilization in the study

Model parameters	Initial CO concentration (mmol/L)					
	1.8	**2.4**	**3.1**	**3.8**	**4.4**	**5.12**
First order						
S_0 (mmol/L)	2.0448	2.7852	3.5036	4.5642	4.9072	5.8532
K (h^{-1})	0.0268	0.0213	0.0204	0.0173	0.0120	0.0109
R^2	0.8355	0.9410	0.8249	0.9749	0.9221	0.9308
Logarithmic						
S_0 (mmol/L)	1.4716	2.1041	2.8246	3.6374	4.5152	5.3920
X_0 (g/L)	86.0110	69.0034	102.4321	76.6743	27.5509	7.7442
U_{max} (mmol/L/h)	0.0001	0.0002	0.0001	0.0003	0.0009	0.0003
R^2	0.5931	0.6845	0.6957	0.7751	0.9719	0.9873
Logistics						
S_0 (mmol/L)	1.7962	2.4034	3.0786	3.7556	4.4080	5.2047
X_0 (g/L)	0.1311	0.5898	0.3750	0.5282	0.5625	0.4120
U_{max} (mmol/L/h)	0.1219	0.1911	0.1971	0.0520	0.0647	0.0736
K_S (mmol/L)	3.2394	6.6086	5.5621	5.5914	11.5321	13.9323
R^2	0.9789	0.9406	0.9560	0.9635	0.9703	0.9797
Modified Gompertz model						
S_{max} (mmol/L)	1.8379	2.5226	3.2822	4.1111	4.4373	5.3499
U_{max} (mmol/L/h)	0.0361	0.0307	0.0410	0.0417	0.0372	0.0331
λ (h)	11.9491	5.2905	8.1212	9.3935	19.429	29.4569
R^2	0.9991	0.9544	0.9942	0.9794	0.9909	0.9913

Furthermore, the effect of initial CO concentration on its specific utilization rate is shown in, Fig. 4.3. It is clear from the figure that the specific substrate utilization rate decreased at higher concentration of the CO, which indicates substrate inhibition on the specific utilization rate similar to biomass growth rate inhibition at a high substrate concentration. The variation specific substrate utilization rate at different initial CO concentrations was modeled in order to describe the inhibition pattern due to CO as its own utilization. There are various different kinetic models used to predict the utilization rate which are originally developed for substrate inhibition on the specific growth rate of biomass. The experimental data obtained in this study was fitted to some well-known models such as Monod, Haldane, Han-Levenspiel, Edward, Moser, Yano-Koga and Luong models. From Fig. 4.3, it is clear that most of these models could accurately fit the experimental data, except the Han-Levenspiel and Monod models.

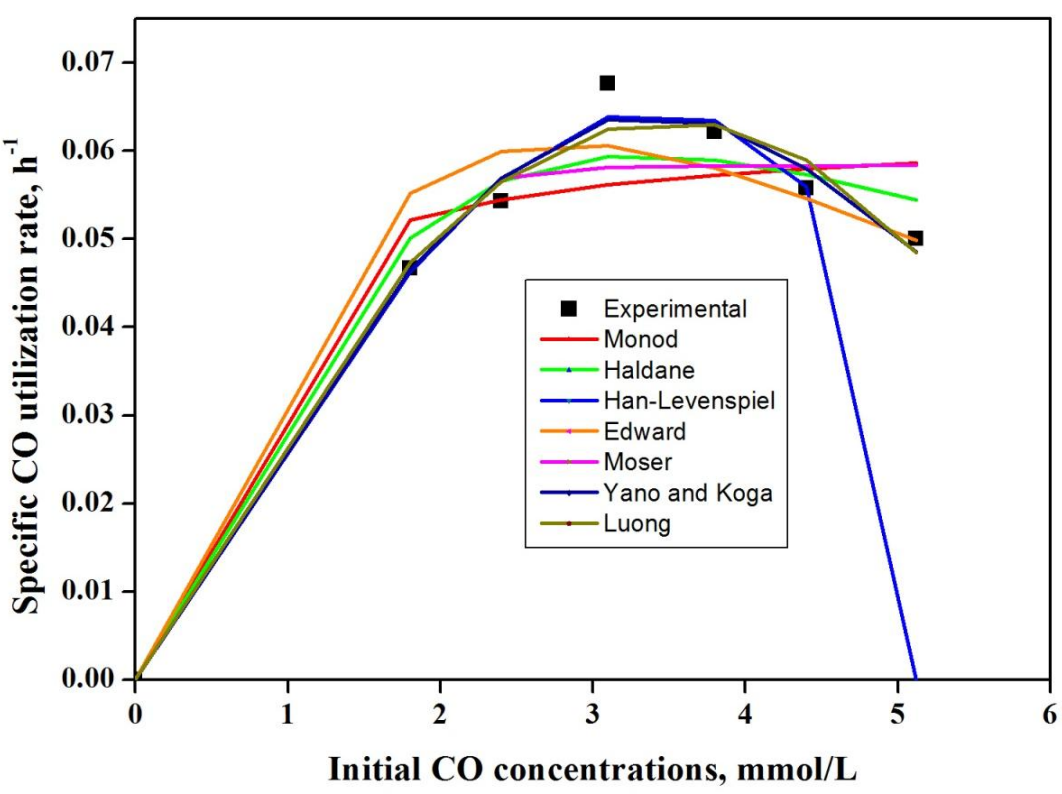

Fig. 4.3 Experimental and predicted values of specific CO utilization rate at different initial CO concentration.

Table 4.7 presents the values of the biokinetic constants obtained from the different specific substrate utilization rate models. From Edward model, which yielded a maximum R_2 value of 0.9987, the values of half saturation constant and inhibition constant 3.5 mmol/L and 6.1 mmol/L, respectively. However, the predicted specific CO utilization rate (0.1871 h^{-1}) was very high compared to the experimental data. Overall, the estimated values of the model kinetic parameters clearly indicate the effectiveness of this anaerobic biomass in utilizing CO even at a high initial concentration.

Table 4.7 Estimated values of biokinetic parameters obtained from the different specific substrate utilization rate models

Model parameters	**q_{max} (h^{-1})**	**K_S (mmol/L)**	**K_i (mmol/L)**	**S_m (mmol/L)**	**n**	**m**	**K_1 (mmol/L)**	**R^2**
Monod	0.0628	0.36	-	-	-	-	-	0.9877
Haldane	2.0143	54.5	0.2	-	-	-	-	0.9905
Han and Levenspiel	0.4086	13.61	-	5.72	3.01	14.55	-	0.8801
Edward	0.1871	3.5	6.1	-	-	-	-	0.9987
Moser	0.0583	26.97	-	-	7.93	-	-	0.9912
Yano and Koga	0.3124	10.1	-	-	2.15	-	6.9	0.9985
Luong	1.9318	59.43	-	6.79	1.34	-	-	0.9978

4.3.2 Kinetics of biomass growth on CO

Fig. 4.4 shows the influence of different CO concentration on the anaerobic biomass growth, which clearly reveals that the cells quickly entered stationary phase following a very brief

period of growth phase. However, the maximum biomass growth value was low compared to the values obtained using soluble substrate (acetate, lactate, etc.) (Oh et al., 2005; Mu et al., 2007). A maximum biomass growth is obtained within 120 h for all initial CO concentrations before it reached a steady state value. Maximum biomass concentration was found to be 0.423 g/L at 84 h for a CO concentration of 3.1 mmol/L. Oh et al. (2005) reported a biomass concentration of 1 g/L due to *Rhodopsedomonas palustris P4* within 50 h of culture from 1 mmol/L of CO. However, compared with soluble substrates, such as acetate, lactate, etc., CO as a substrate yielded a low biomass growth which is in agreement with this study. For estimating the biokinetic parameters involved in biomass growth from CO the experimental data was fitted to the modified Gompertz and Logistic model reported in the literature (Wang et al., 2009).

Fig. 4.4 shows the experimental and predicated values using the two different models. The kinetic parameters estimated by fitting the data to the two models for different initial CO concentrations are presented in Table 4.8. The modified Gompertz model fitted the experimental data more accurately than the Logistic model with a R^2 value greater than 0.99. The biomass growth rate increased with an increase in the initial CO concentration from 1.8 to 2.4 mmol/L; however, after 2.4 mmol/L initial CO concentration the biomass growth rate was reduced. The estimated biokinetic parameters of X_{max} and R_{max} values are lower than those reported by Mu et al. (2006) who used simple acetate as the carbon source in their study; these values reported by Mu et al. (2006) were 9.46 g vss/L and 0.07 g vss/L/h, respectively. The differences in the values of these parameters could be attributed to the fact that CO as a substrate did not strongly promote the growth of the anaerobic biomass, but leads to formation of intermediate products, such as H_2. Hence, further investigations were carried out to ascertain the kinetics of H_2 production from CO as the substrate using the anaerobic biomass.

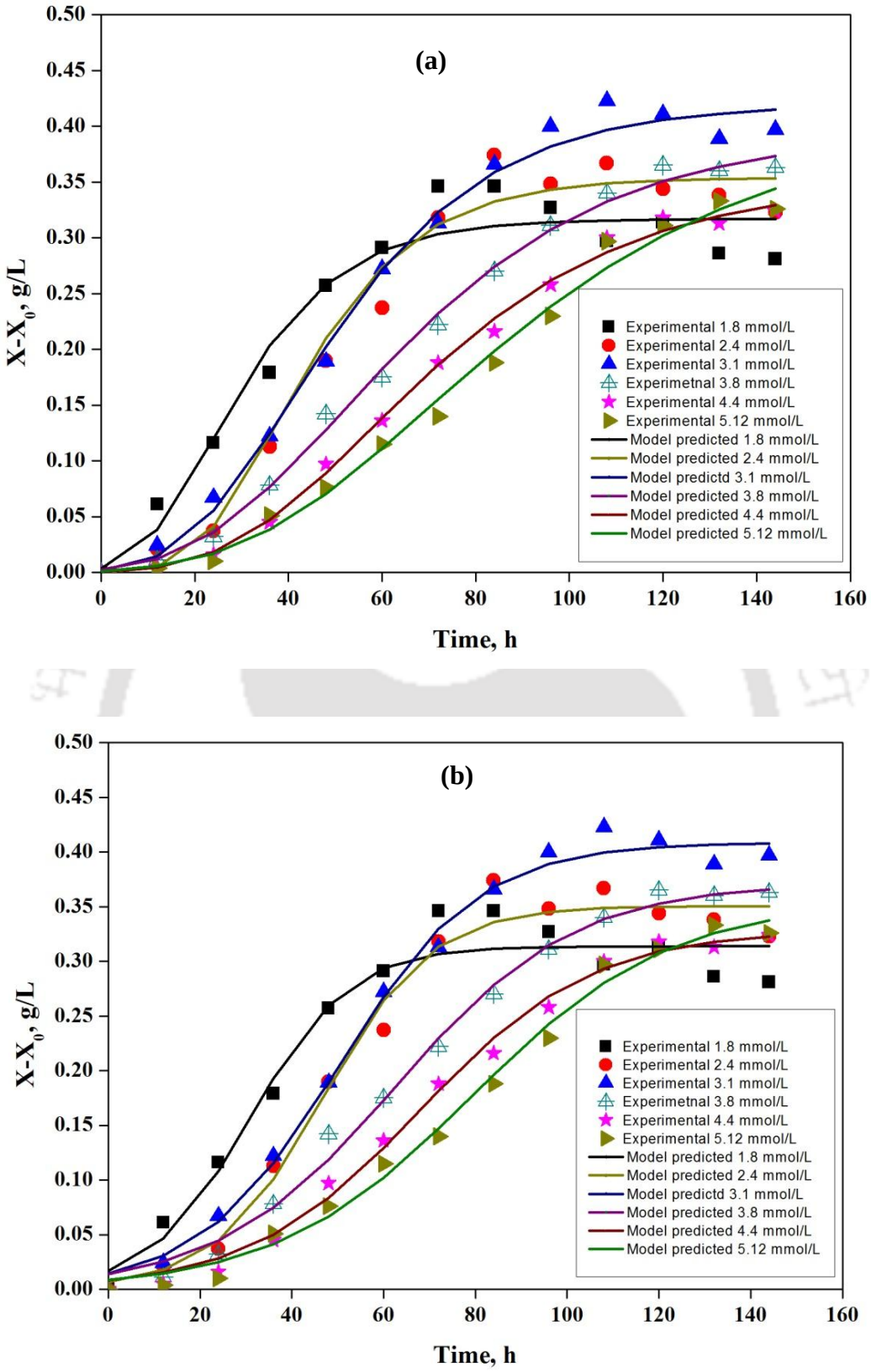

Fig. 4.4 Experimental and predicted biomass growth profile at different initial CO concentration using (a) modified Gompertz (b) Logistic models.

Table 4.8 Estimated biomass growth kinetic parameters obtained using modified Gompertz Logistic models

Model parameters	Initial CO concentration (mmol/L)					
	1.8	**2.4**	**3.1**	**3.8**	**4.4**	**5.12**
Modified Gompertz						
X_{max}(g/L)	0.3169	0.3541	0.4198	0.3944	0.3509	0.4031
R_{max} (mmol/L/h)	0.0075	0.0076	0.0065	0.0045	0.0041	0.0037
λ (h)	8.1074	20.0211	17.0749	19.951	26.6369	30.1902
R^2	0.9924	0.9946	0.9998	0.9912	0.9952	0.9913
Logistic						
X_{max} (g/L)	0.3138	0.3506	0.4085	0.3711	0.3281	0.3535
R_{max} (mmol/L/h)	0.0072	0.0074	0.0067	0.0047	0.0043	0.0041
λ (h)	9.3141	23.0704	19.7450	23.9438	30.6903	36.5139
R^2	0.9519	0.9779	0.9726	0.9542	0.9565	0.9686

4.3.3 Kinetics of biohydrogen production

Fig. 4.5 clearly establishes that the anaerobic biomass was capable of metabolizing the gaseous substrate CO to form H_2. The hydrogen produced, however, varied depending upon the initial CO levels. Moreover, no methane or any other volatile compounds were detected in the biogas. A maximum biohydrogen values of 3.63 mmol/L was produced for an initial CO concentration of 5.12 mmol/L and without any substrate inhibition. However, the biomass took a prolonged time period to convert CO to H_2 at high initial CO concentrations. The CO bioconversion to H_2 involves two main enzymes: CO dehydrogenase (CODH) which oxidizes CO to CO_2 along with the production of reducing equivalents. The secondary CODH enzyme is CODH-dependent hydrogenase which reduces protons to H_2 by using the electrons donated from the CODH mediated reaction (Kim et al., 2003).

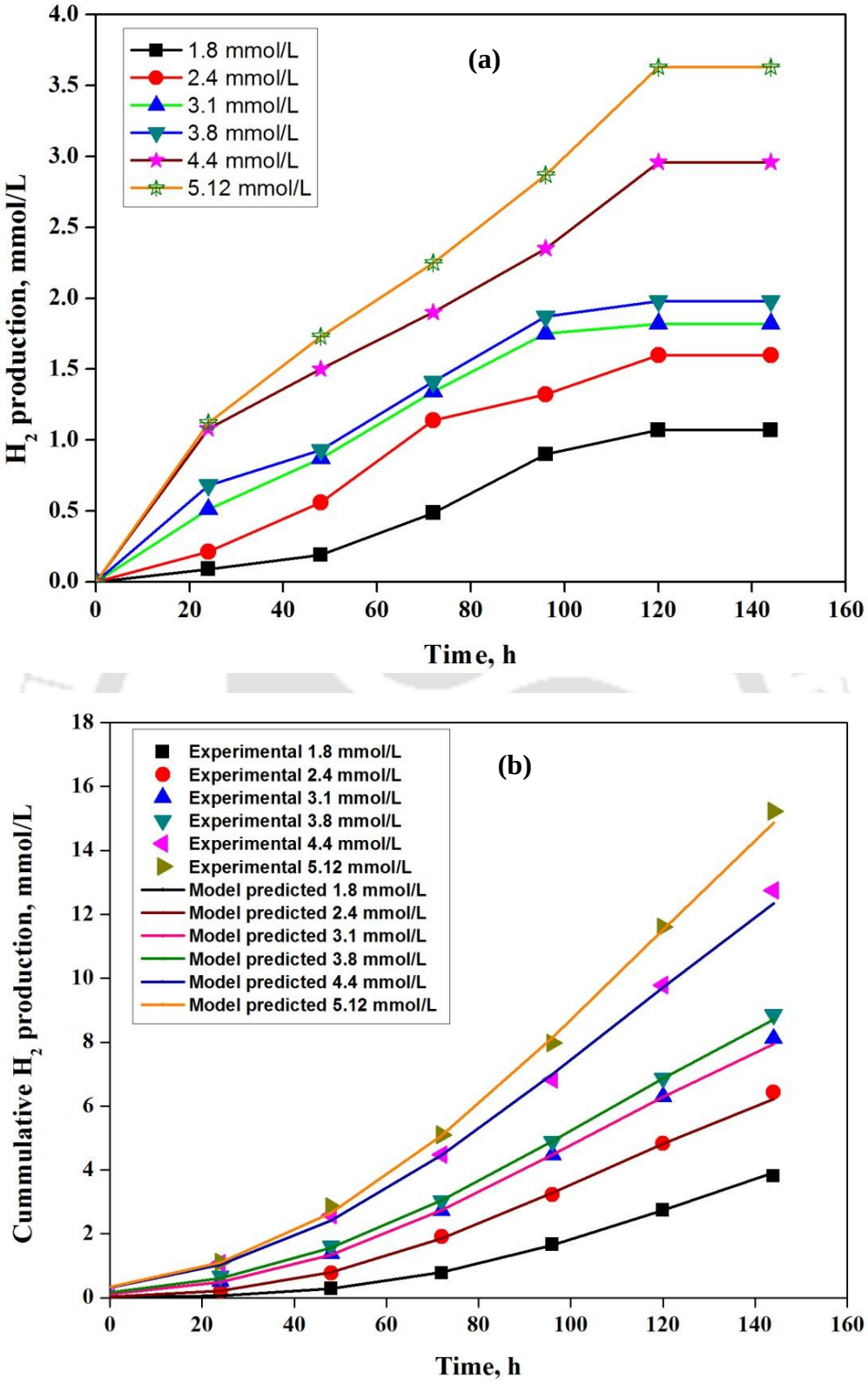

Fig. 4.5 Biohydrogen production and cumulative bio-hydrogen production at different initial CO concentration.

The values of H_2 yield from CO are presented in Table 4.9, which shows that a maximum yield of 70.8 % is achieved for an initial CO concentration of 5.12 mmol/L. In the literature, Najapour et al. (2006) reported 88% of yield of H_2 using CO rich syngas with *R. rubrum* which is higher than the yield obtained in this study. Pakpour et al (2014) reported a maximum yield of 86% but using 1.5 g/L of sodium acetate as a primary carbon source with *R. palustris*. However, in all these studies, pure culture and sometimes additional carbon sbstarte supplemented media were used, whereas in this study anaerobic biomass that contains a mixed consortium of organisms was used. The difference in the H_2 yield may also be due to the different culture conditions followed, which need to be optimized for achieving a maximum H_2 yield from CO, particularly when using such mixed consortium of microorganisms. Analysis of the kinetics of cumulative H_2 production at different initial CO concentration shown in Fig 4.5b revealed that the H_2 concentration increased gradually with an increase in the cultivation time followed by a rapid increase until it reached a saturation value. Thus, the modified Gompertz model could successfully predict the cumulative hydrogen production behavior by the anaerobic biomass at the different initial CO concentrations.

The determination coefficient (R^2) values between the experimental and the model predicted hydrogen values were found to be high ($R^2 > 0.94$) (Table 4.9). The estimated values of H_2 production (P_{max}) and H_2 production rate from the model were found to be 29.9 mmol/L and 0.14 mmol/L/h, respectively, for an initial CO concentration of 5.12 mmol/L. Moreover, the specific H_2 production rate values correlated well with the corresponding initial CO concentration used. In the literature, Chen et al. (2006) reported a P_{max} value of 178 ml/L for an initial substrate concentration of 32.3 g COD/L with food waste as the substrate. These results suggests that H_2 production rate using simple sugar is higher than that obtained using a gaseous substrate, such as CO. Hence, based on the low yield of H_2 from CO using the

anaerobic biomass containing mixed consortium of bacteria it could be suggested that the H_2 produced could be diverted to the formation of other intermediates products such as acetate, formic acid, etc. which need to be further confirmed by analyzing the VFA contents in the liquid media.

Table 4.9 Estimated values of kinetic parameters for hydrogen production using modified Gompertz Model

Model parameters	**Initial CO concentration (mmol/L)**					
	1.8	**2.4**	**3.1**	**3.8**	**4.4**	**5.12**
Hydrogen yield (%)	59.4	66.6	58.7	59.1	67.2	70.8
P_{max} (mmol/L)	8.8350	10.4778	13.3832	15.6271	23.4913	29.9888
R_{max} (mmol/L/h)	0.0489	0.0643	0.0759	0.0820	0.1137	0.1423
λ (h)	64.080	45.036	37.075	36.279	34.557	39.053
Specific hydrogen production rate (mmol/g/h)	8.6524	13.6187	15.1496	18.3743	29.4752	33.4831
R^2	0.9991	0.9552	0.9665	0.9708	0.9446	0.9559

4.3.4 Kinetics of substrate inhibition on biomass growth

It is well known that substrates provide necessary energy for hydrogen producing bacteria, thereby influencing the biomass growth and fermentative hydrogen production. Monod model is the most commonly used kinetic model for describing the effect of substrate on specific growth rate of microorganisms. But, this model is unsatisfactory as substrate at high concentration inhibits the biomass growth. The effect of maintenance energy on biomass growth and metabolism is also ignored throughout the process. Goswami et al. (2012) suggested that a decrease in the value of specific growth rate with respect to time during exponential phase is an indication of inhibition due to intracellular product accumulation. In

such cases, kinetic models that provide correction for substrate inhibition can be used to study the growth kinetics of microorganisms during fermentation process. In this study, different unstructured models, viz. Andrews and Noack, Aiba and Edwards, Han and Levenspiel, Luong inhibition, Tiessier-type substrate inhibition, Edward and Jackson, Webb, Tseng and Wayman and Yano and Wayman models were examined to study the substrate inhibition due to CO on the anaerobic biomass growth. All these models were fitted to the experimental data for varying initial CO concentrations. Fig. 4.6 compares the experimental vs model predicted biomass specific growth rate at different initial CO concentrations and Table 4.10 presents the estimated biokinetic parameters from these models.

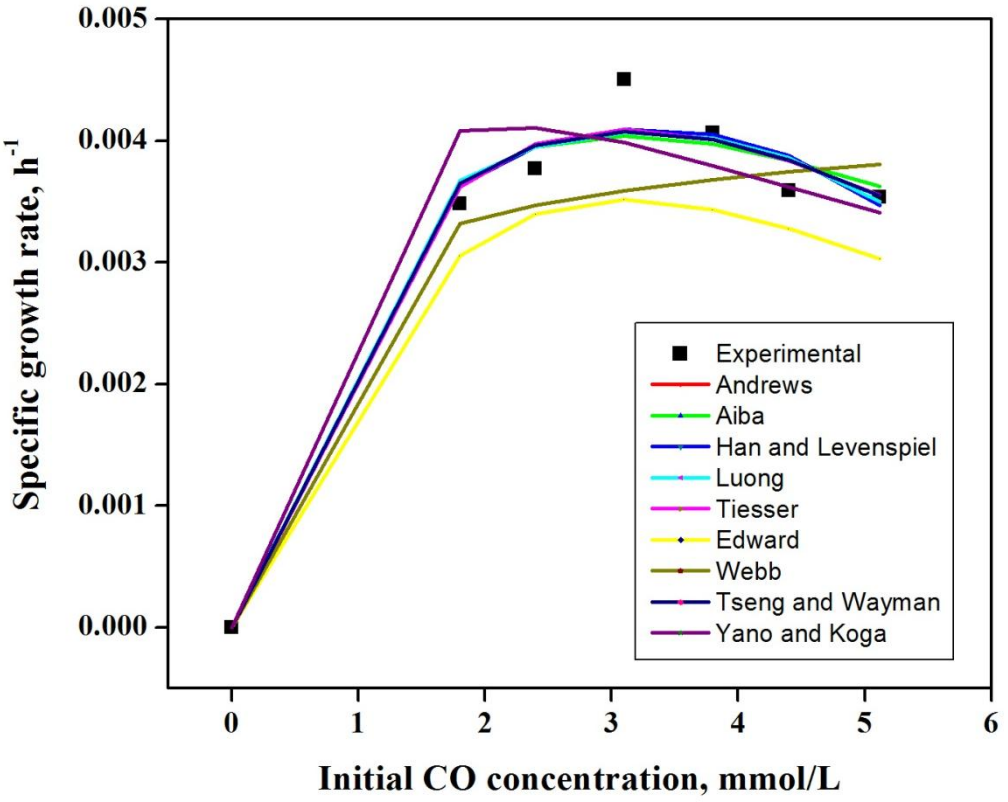

Fig. 4.6 Experimental and model predicted biomass specific growth rate at different initial CO concentrations.

Among the various substrate inhibition models tested in this study, the Aiba model was found to be the best (R^2 = 0.976) to describe inhibitory effect of CO on specific biomass growth

rate. This model has been widely used to describe the inhibitory effect of substrate concentration on specific growth rate of biomass particularly hydrogen producing bacteria. This model is based on a non-linear relationship between specific growth rate of biomass and substrate concentration. The specific growth rate increased with increase in initial CO concentration for low concentration values up to 3.1 mmol/L and above which the value decreased. From Aiba model, values of the biokinetic parameters (μ_{max}, K_S and K_i) were to be 0.0135 h^{-1}, 3.1488 mmol/L and 6.1247 mmol/L, respectively (Table 4.10).

Table 4.10 Estimated biokinetic parameters from different substrate inhibition models examined in this study

Model parameter	μ_{max} (h^{-1})	K_S (mmol/L)	K_i (mmol/L)	S_m (mmol/L)	n	m	K_1 (mmol/L)	R^2
Andrews	0.0088	1.2399	3.8000	-	-	-	-	0.9742
Aiba	0.0135	3.1488	6.1217	-	-	-	-	0.9760
Han and Levenspiel	0.0062	1.3655	-	6.3187	0.32	-	-	0.9750
Luong-inhibition	0.007	1.3394	6.3404	-	-	0.28	-	0.9702
Tiessier	0.0199	2.3781	4.1831	-	-	-	-	0.9713
Edward	0.0128	4.8056	4.5899	-	-	-	-	0.4879
Webb	0.0033	0.2321	-	-	5.66	-	4.30	0.4850
Tseng and Wayman	0.0002	2.4837	3.7987	10.2543	-	-	-	0.5098
Yano and Koga	0.0088	1.2399	-	-	-	-	3.80	0.5096

The maximum specific growth rate was found to be 0.0135 h^{-1} for an initial 3.1 mmol/L CO concentration. This value is significantly low compared with that reported by van Niel et al. (2003) which reported a maximum specific growth rate of 0.27 h^{-1} but using sucrose as the

substrate. The low value of μ_{max} obtained in this study due to the conversion of CO to H_2 and other intermediates/products than for biomass formation, as noted previously. Inhibition of biomass growth by substrate at a high initial substrate concentration is quite common in fermentation, but the level of tolerance varies among microbial species and it also depends on the nature of the substrate (Lasko et al., 2000). The estimated value of the inhibition constant K_i (6.1247 mmol/L) due to CO in this study indicates very good tolerance of the anaerobic biomass towards the gaseous substrate.

4.3.5 Kinetics of product inhibition on biomass growth and biohydrogen production

The effect of different H_2 concentration on biomass growth, biohydrogen production and CO utilization can be seen from Fig. 4.7. From Fig. 4.7a, the biomass concentration decreased when the H_2 concentration increased from 0.5 to 4.5 mmol/L, and a maximum biomass concentration was found to be 0.81 g/L for an initial H_2 concentration of 0.5 mmol/L. Fig. 4.7b reveals that the CO utilization by the anaerobic biomass is also affected due to an increase in the H_2 concentration, and H_2 concentration after 3.2 mmol/L is found to inhibit CO utilization by the anaerobic biomass. For initial H_2 concentrations lower than 3.2 mmol/L bacterial growth was strongly inhibited, and it is more severe at a high H_2 concentration in the range 3.2 - 4.5 mmol/L. These results indicate a significant H_2 induced inhibition on the growth of the anaerobic biomass. It is known that accumulation of H_2 can lead to changes in intracellular pH of bacteria, increase the energy for maintenance and it can also inhibit enzymes such as hydrogenase and CODH (Mu et al., 2007). All these factors are therefore attributed to H_2 inhibition on biomass growth and CO utilization by the anaerobic biomass.

Furthermore, the experimental data on specific biomass growth and H_2 production rates were fitted to biokinetic models (Table 4.5) reported in the literature to study product (H_2) inhibition on specific growth rate of biomass and product formation.

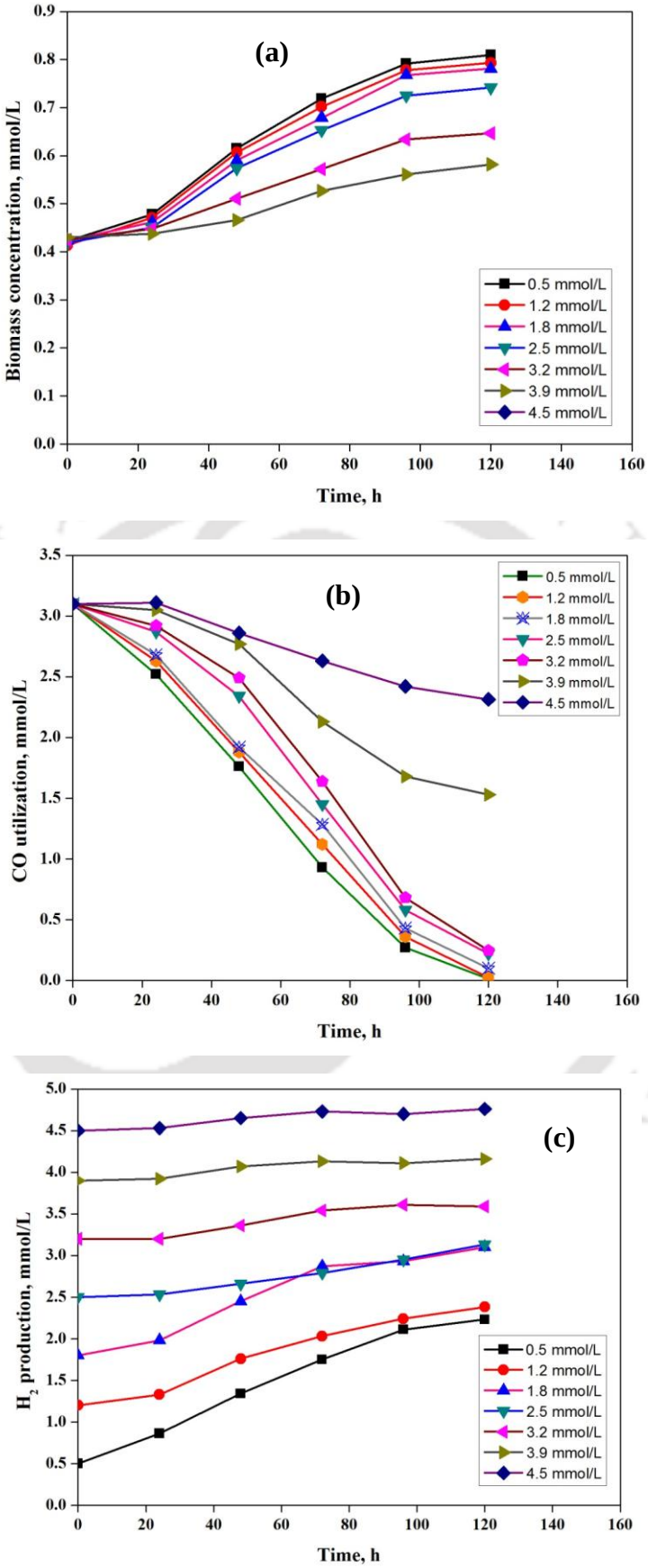

Fig. 4.7 (a) Biomass growth, (b) CO utilization and (c) H_2 production at different initial H_2 concentrations.

Fig. 4.8 shows the experimental and predicted values of specific biomass growth rate and H_2 production due to the different models. Table 4.11 shows the estimated model parameters for H_2 inhibition on biomass growth and product formation. From Fig. 4.8a, it is found that the experimental data on inhibitory effect of H_2 on biomass specific growth rate could be well described by the modified Han-Levenspiel model; the estimated values of the model parameters μ_{max}, C_{Crit} and n were found to be 0.0056 h^{-1}, 5.62 mmol/L and 1.92, respectively. The experimentally determined critical concentration of H_2 above which the biomass was inhibited matched well with the model predicted value of 5.62 mmol/L. The specific growth rate of biomass is also in good agreement with the value reported by Goncalves et al. (1991). The inhibitory effect of H_2 on the biohydrogen production rate was also investigated by replacing the specific biomass growth rate in the model equations with H_2 production rate. A plot of H_2 production rate at different initial H_2 concentrations (Fig. 4.8b) clearly revealed that the H_2 production rate decreased with increase in the initial H_2 concentration. The kinetic parameters μ_{max}, C_{Crit} and n for H_2 production were determined to be 0.0218 mmol/L h, 5.11 mmol/L and 0.46, respectively.

A number of literature reports are available on inhibition of product formation and biomass growth due to H_2 accumulation in the system. For example, van Niel et al. (2003) reported that the H_2 inhibition on biohydrogen production rate with the critical inhibition H_2 concentration of 5.11mmol/L, which matching the results obtained in the present study. Adams, (1990) reported H_2 to restrict the growth of microorganisms and inhibit its own production at a high concentration of 3.2 mmol/L by inhibiting the hydrogenase enzyme activity of the microorganisms. Based on Henry's law constant for H_2, the critical dissolved H_2 concentration is found to be 26.9 µM for the 0.021 mmol/L h of gas phase maximum H_2 production in this study.

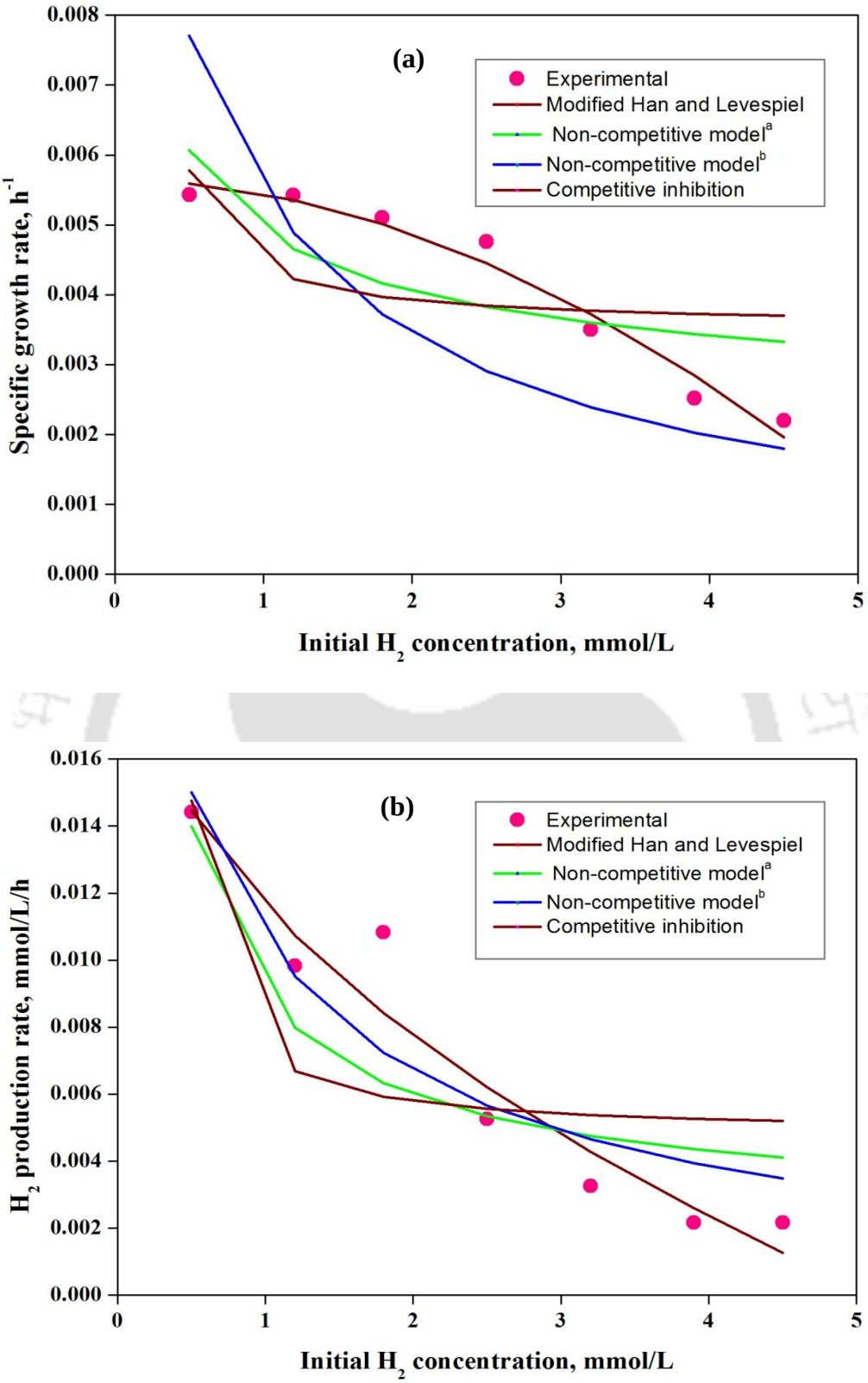

Fig. 4.8 Experimental and predicted values of (a) specific growth rate of biomass and (b) H_2 production rate at different product (H_2) concentration.

Table 4.11 Estimated values of different model parameters on H_2 inhibition on biomass growth and hydrogen production by anaerobic biomass

Model parameters	μ_{max} (h^{-1})	C_{Crit} (mmol/L)	K_S (mmol/L)	K_C (mmol/L)	n	R^2
Specific growth rate of biomass						
Modified Han-Levenspiel	0.0056	5.6192	-	-	1.9153	0.9694
Non-competitive[a]	0.0016	-	-	4.90288	-0.438	0.4846
Non-competitive[b]	0.0020	-	-	4.5	-	0.1566
Competitive	0.0035	5.1534	-0.1041	6.0158		0.2892
H_2 production rate[‡]						
Modified Han-Levenspiel	0.0218	5.1119	-	-	0.4649	0.9680
Non-competitive[a]	0.0020	-	-	4.5706	-0.8	0.6730
Non-competitive[b]	0.0255	-	-	0.7117	-	0.7048
Competitive	0.0048	3.6353	-0.2294	7.7291	-	0.5136

[‡] Unit of μ_{max} is mmol/L/h for H_2 production rate in estimation of model parameters

Ljunggren et al. (2011) reported product inhibition due to H_2 for fermentative biohydrogen production using glucose as the substrate and values of the kinetic parameters μ_{max}, C_{Crit} and n were determined to be 8.4 mmol/L/h, 4.78 mol/mol and 0.46, respectively, which are comparable with the current study. However, the unique aspect of this study is kinetic analysis of biohydrogen production using the gaseous substrate CO. The results obtained in this study further confirm that a high H_2 concentration value is inhibitory to H_2 production and biomass growth. Hence, it is suggested that H_2 production in CO fed bioreactor should be carefully monitored so as to recover the product as soon as it is produced in the system.

4.4 Significant findings

Detailed kinetics of CO conversion by the anaerobic biomass revealed that it is well-capable of utilizing CO as the substrate for H2 and other products/intermediates formation. The CO utilization by anaerobic biomass was affected at a high initial concentration and was best described by growth associated modified Gompertz model. A high initial CO concentration was found to be inhibitory to both specific CO utilization rate and specific biomass growth rate, and the kinetics of these two rates were best described by Edward and Aiba models, respectively. Similarly, the effect of CO concentration on biohydrogen production was well described by modified Gompertz kinetic model. H_2 as a product was found to be inhibitory for both biohydrogen production and specific growth rate at a high concentration, and the inhibition kinetics could be described using modified Han-Levenspiel model. Thus, the study revealed that to achieve high CO conversion efficiency, H_2 need to be recovered quickly without allowing it to accumulate in the system, or, there need to be some H_2 utilization mechanism such as H_2 production coupled to sulfate reduction using CO as the sole carbon source.

Chapter 5

Simultaneous removal of heavy metal and sulfate using CO as the sole carbon and energy source

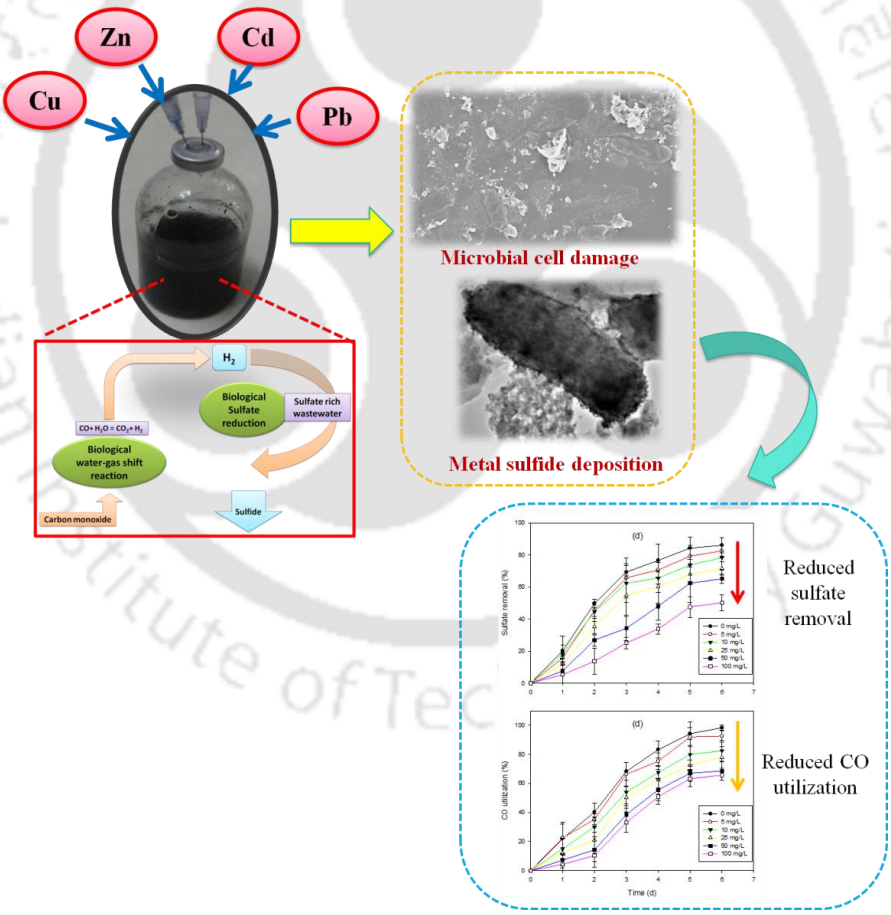

ABSTRACT

This chapter investigated the effect of heavy metals as a co-pollutant on biological sulfate reduction using CO as the sole carbon and energy source. The effect of difficult heavy metals, viz. Cu, Zn, Cd and Pb at initial concentrations in the range 5-100 mg/L was investigated. Among these metals, Pb showed a maximum inhibitory effect on sulfate reduction and CO utilization by the anaerobic biomass. The biological sulfate reduction was unaffected in the presence of Cu and Zn with more than 60 % sulfate reduction even at a high initial metal concentration of 100 mg/L. In the presence lead, CO utilization efficiency reduced from 92.54 to 67.32 % with an increase in the initial metal concentration from 5 to 100 mg/L. Due to sulfate reduction by anaerobic biomass, heavy metals were removed by sulfide precipitation, but the metal removal efficiency largely depended upon the type of heavy metal and its initial concentration. Fourier-transform infrared spectroscopy (FTIR), TEM-EDS, and Field-emission transmission electron microscope (FETEM) and field-emission scanning electron microscopy (FESEM) with energy dispersive X-ray spectroscopy (EDX). Field-emission scanning electron microscopy microscopy (FESEM) with energy dispersive X-ray spectroscopy (EDX) and fourier transform infrared spectroscopy (FTIR) spectra of the metal loaded biomass confirmed that the precipitates formed during the process consisted of mainly the metal sulfides. Field-emission transmission electron microscope (FETEM) image of the metal loaded biomass revealed that the metal sulfide precipitates were formed outside the cell surface. The results have significant implications in the biological treatment of sulfate rich wastewaters using CO the carbon and energy source.

5.1 Introduction

Sulfate rich wastewater released from industrial sources contains other inorganic pollutants such as heavy metals. For example, Mining and metallurgical industries produces a large volume of wastewater containing both sulfate and heavy metals at very high concentrations (Roy et. al., 2015; Hazarika et. al., 2015). However, the type of heavy metals present and its concentrations largely depend upon the industrial source, geographical location and process involved. Durand (2012) reported the presence of Al, Ca, Co, Fe, Mg, Mn, Ni and Zn along with a high amount of sulfate in wastewater released from gold mines in Gauteng and North West Province in South Africa. Santa Cruz et al. (2013) found SO_4^{2-}, Mn, Zn, Al, Cu, Ni, Co, U in acid mine drainage in Western Spain. Equeenuddin et al. (2010) reported discharges from coal mines in Makum coal field, Assam, India, are highly enriched with SO_4^{2-}, Fe, Al, Mn, Ni, Pb and Cd, whereas Cr, Cu, Zn and Co are also present in small amounts. Tutu et al. (2008) studied the composition of acid mine drainage in Witwatersrand Basin, South Africa and found high amount SO_4^{2-}, Al, Fe, Cu, Mn, whereas Co, Ni and Zn were present below the permissible limit for these heavy metals.

From these above mentioned studies it is clear that irrespective of its varied sources and geographical location different heavy metals are present in sulfate containing wastewater, and any serious effort to treat it biologically need to consider their effect on process efficiency. On the other hand simultaneous removal of these heavy metals along with sulfate is also necessary to achieve the effluent standards set by regulatory bodies. Biological sulfate reduction process can be useful in this context as metal removal by converting it to their insoluble metal sulfide form by SRBs is well reported in the literature (Kiran et. al., 2017; Simate and Ndlovu, 2014). Also, use of this technology makes it possible for recovery of heavy metals from wastewater, which could improve economic viability of the process.

However, heavy metals exert toxic effect on almost all of the living organisms including SRBs. Due to absence of organics in such wastewaters biological treatment requires external addition of suitable carbon source and electron donor. An ideal carbon source should be renewable and cheaply available, such as those derived from waste resources. In this present study, CO is explored as an alternative carbon source for biological treatment of sulfate rich wastewater containing heavy metals as co-pollutants. The individual effect of Cu, Zn, Cd and Pb, which are commonly found in sulfate rich wastewater on biological sulfate reduction using CO as the sole carbon and energy source using anaerobic biomass was examined. Removal of these heavy metals by sulfide precipitation and its detailed characterization using various instrumental techniques were also studied.

5.2 Materials and methods

5.2.1 Experimental methodology

In order to study the effect of heavy metals on biological sulfate reduction and CO utilization by anaerobic biomass experiments were performed using 120 ml serum bottles (Sigma Aldrich, India) sealed with polytetrafluoroethylene (PTFE) septum and filled with 50 ml mineral salt media (MSM) medium of pH 7.0 along with 0.2% w/v biomass as the inoculum. The composition of the MSM media was the same as given in Chapter 2. The bottles were purged with N_2 gas to remove O_2 prior to introducing CO. The initial CO and sulfate concentration in the bottles were kept at 3.1 mmol/L and 1000 mg/L, respectively, for all the experiments. To inhibit any methanogenic activity 10 mM concentration of 2-bromoethanosulfonate (BES) was added in all the serum bottles. The heavy metals Cu, Zn, Cd and Pb were added individually as $CuCl_2 \cdot 2H_2O$, $ZnSO_4 \cdot 7H2O$, $CdSO_4 \cdot 3H_2O$ and $Pb(NO_3)_2$ to the serum bottles from their respective stock solutions (1000 mg/L) so as to give a desired concentration in the range 5-100 mg/L. Bottles without any added heavy metals

served as the control in the experiments. The bottles were incubated at 30°C and 150 rpm on a rotating orbital incubator shaker for 6 days. Both gas phase and liquid samples were withdrawn at regular time interval from the serum bottles for analysis of the heavy metals, sulfate and CO, etc. All the experiments were carried out in triplicates and results were represented in the mean ± standard deviation format. The removal efficiency of sulfate, CO and the metals were calculated using the following equation

$$\%\, removal = \frac{C_i - C_f}{C_i} \times 100 \quad \text{.....(5.1)}$$

where, C_i and C_f are the initial and final concentrations of the individual parameters (sulfate (mg/L), CO (mmol/L), metal (mg/L), etc.)

5.2.2 Morphological analysis and characterization of metal bioprecipitates

For characterizing the metal precipitates formed due to biological sulfate reduction by anaerobic biomass using CO as the sole carbon and energy source, the precipitates were analyzed using Fourier-transform infrared spectroscopy (FTIR), field-emission transmission electron microscopy (FETEM) and field-emission scanning electron microscopy (FESEM) with energy dispersive X-ray spectroscopy (EDX). FTIR analysis was carried out to understand the changes in functional groups of the anaerobic biomass due to sulfate reduction for heavy metal removal. For the FTIR analysis, biomass samples taken during the experiments were obtained by centrifuging the samples at 37,000×*g* for 15 min, followed by washing with distilled water, and the pellets obtained were vacuum dried and analyzed using a FTIR spectroscope (IR Affinity-1, SHIMADZU, Japan). For FETEM analysis, samples of metal laden biomass was loaded on a copper grid coated with carbon and observed under FETEM (JEOL, 2100F, Japan). For FESEM analysis, the metal bioprecipitates were oven-dried at 30°C for overnight, gold coated in a sputter coater and then analyzed for its morphology and elemental composition using FESEM-EDX (Zeiss, Sigma, Germany).

5.2.3 Analytical methods

The head space biogas composition in the serum bottles was analyzed using a gas chromatograph (GC, Varian 450, The Netherlands) equipped with a thermal conductivity detector (TCD) and a molecular sieve column (Mole sieve 5A, mesh 80/100, 72 in × 1/8 in) using methods as described earlier in Chapter 3. Volatile suspended solids (VSS) were measured following the standards methods (APHA, 1995). Sulfate concentration was determined using the standard barium chloride based turbidimetric method (APHA, 2005). Metal concentration in the samples was determined using an atomic absorption spectrometer (Varian, AA240, Netherlands) as per the APHA (2005). Sulfide concentration in the samples was measured as per the method described by Cord-Ruwisch (1985). All these methods were described in detail in Chapter 3.

5.3 Results and discussion

Sulfate rich wastewater, particularly from the mining industry, contains other inorganic pollutants, and among which heavy metals are predominant. In this investigation, effect of four most commonly found heavy metals viz. Cu, Cd, Zn and Pb as co-pollutant on biological sulfate reduction using CO as the sole carbon and energy source was evaluated. Also, simultaneous removal of heavy metals along with sulfate and the metal removal mechanism were examined in detail.

5.3.1 Effect of heavy metals on sulfate reduction and CO utilization

The effect of heavy metals as co-pollutants on biological sulfate reduction and CO utilization was studied using the anaerobic sludge biomass from Kavoor STP, which showed efficient CO bioconversion and sulfate reduction (Chapter 3). Fig. 5.1 shows the sulfate removal profile in the presence of different individual heavy metals i.e Cu, Zn, Cd and Pb at various

initial metal concentrations. It is evident that a low initial concentration (5-10 mg/L) of Cu and Zn did not affect the sulfate reduction efficiency, which varied between 84 and 88 %. However, an increase in the intial metal concentration after 10 mg/L decreased the sulfate reduction efficiency (66.4 and 60.25 % at 100 mg/L in case of Cu and Zn, respectively). In the case of Cd, the inhibitory effect on sulfate reduction was moderate and it ranged between 59.3 and 82.56% for an initial concentration in the range 5-100 mg/L. Pb showed the most significant inhibition on sulfate reduction with only 50.38% sulfate removal at a high initial concentration of 100 mg/L.

Fig. 5.2 shows the CO utilization profile by anaerobic biomass in the presence of different heavy metals at different initial concentrations used in this study. The CO utilization was more than 98% in case of control without any heavy metal addition in the media. However, CO was less utilized in the presence of heavy metal and the performance deteriorated with an increase in the metal concentration in the media. Similar to sulfate reduction results, Cu and Zn showed the least inhibition on CO utilization. Even at 100 mg/L concentration the CO utilization efficiency was more than 80%. Whereas, in the case of Cd and Pb the CO utilization efficiency ranged from 71.5 to 92.58% and 67.32 to 92.54%, respectively.

Fig. 5.3 presents the effect of heavy metal presence as a co-pollutant on sulfate reduction and CO utilization rates. From the results it is clear that heavy metals significantly affected both the rate of sulfate reduction and CO utilization. The differential effect due to different heavy metals is similar to the findings of sulfate reduction and CO utilization efficiencies, wherein, Pb showed the maximum inhibition followed by Cd, Cu and Zn.

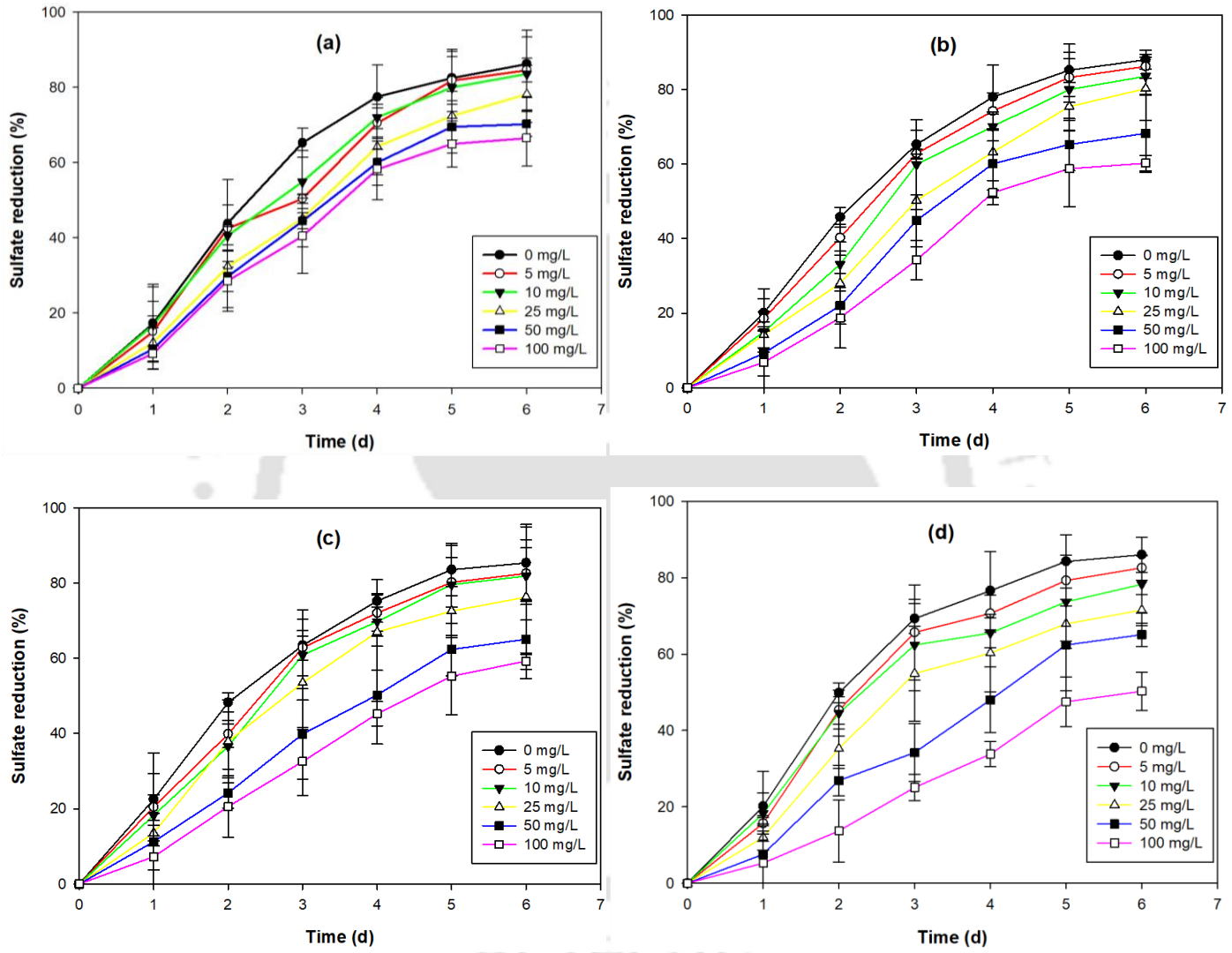

Fig. 5.1 Sulfate reduction by the anaerobic biomass in the presence of heavy metals; (a) Cu, (b) Zn, (c) Cd and (d) Pb.

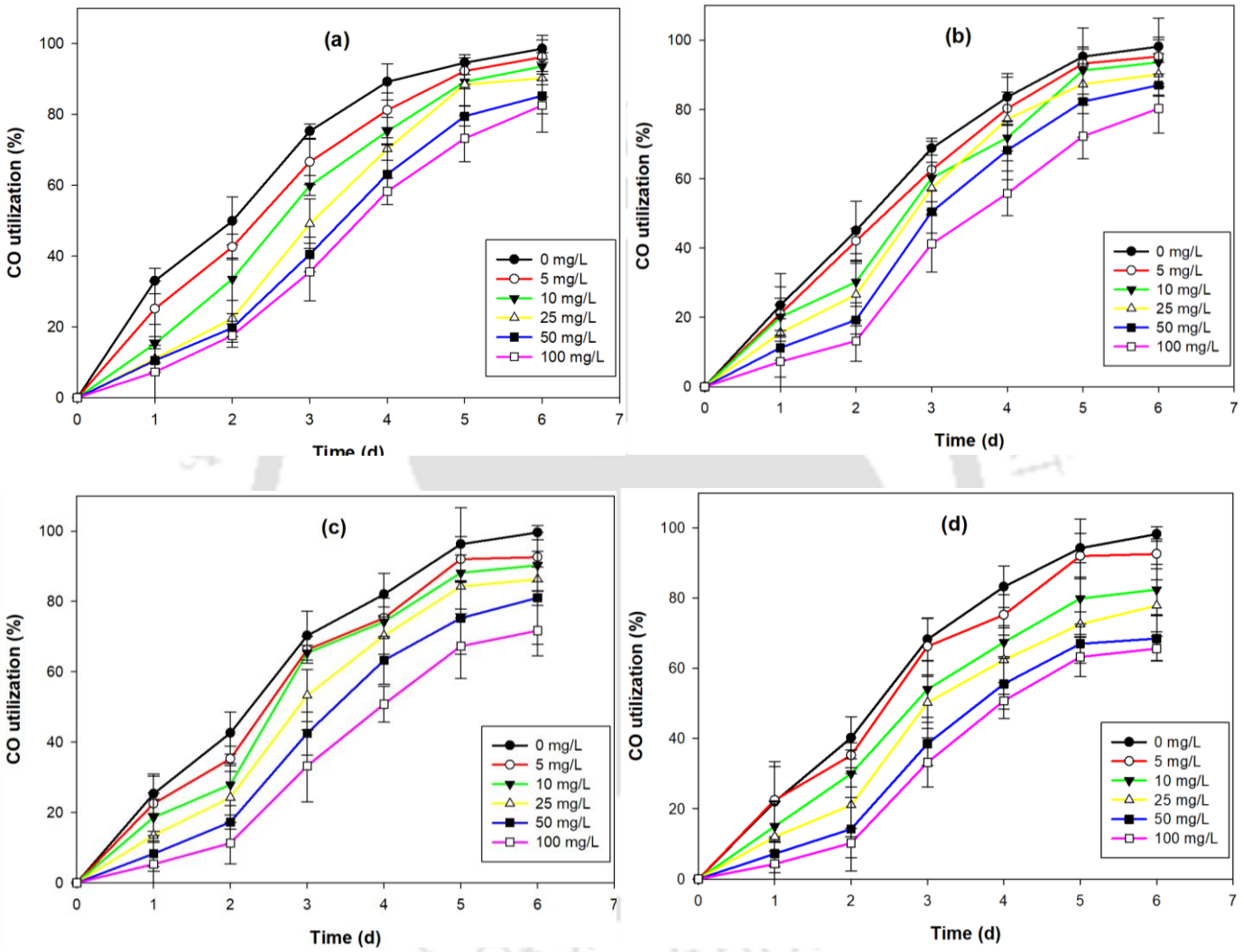

Fig. 5.2 CO utilization by anaerobic biomass in the presence of heavy metal: (a) Cu, (b) Zn, (c) Cd and (d) Pb.

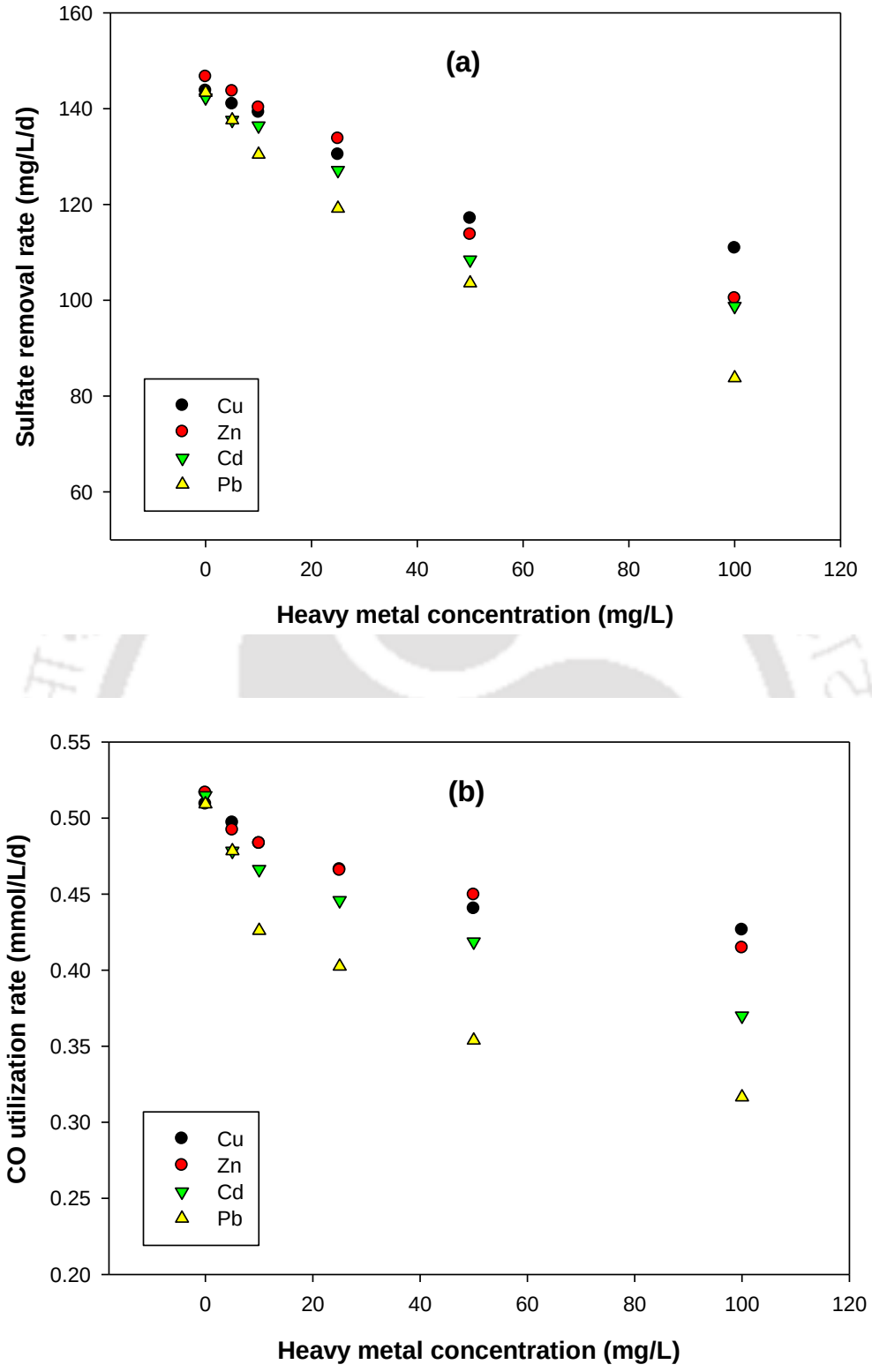

Fig. 5.3 Effect of heavy metals on (a) sulfate removal rate and (b) CO utilization rate.

The toxic effect of heavy metals on different macro and microorganisms is well reported in the literature (Kiran et. al., 2017). In general, heavy metals are capable of deactivating key enzymes, denature essential proteins, and compete with micronutrients and other necessary cations in the growth media, thereby decreasing the cellular activity and prolonging the lag phase (Teclua et al., 2009). It is also reported that formation of metal sulfide precipitates around cell surface could hinder transport of sulfate and essential ions inside the cell (Barbosa et al. 2014). In the present study the formation of metal sulfide bioprecipitates were confirmed by FETEM analysis of the biomass samples taken during the experiments. Similar findings have been reported in many other previous studies (Kiran et al., 2016; Utgikar et al. 2002; Jong and Parry 2003).

Both the sulfate reduction and CO utilization efficiencies decreased with an increase of heavy metal concentration in the media, suggesting that inhibition of SRB activity due to the heavy metals at an dissolved heavy metal concentration (Velasco et al., 2008). Moreover, a strong inhibitory effect due to a high concentration of Cd or Pb compared with Cu and Zn confirm the highly toxic toxic nature of Cd and Pb on the metabolism of SRB (Guo et al., 2010). It is reported that toxicity of heavy metals depends upon the metal type and speciation, type of microorganisms, their defence mechanisms, presence or absence of other co-pollutants and culture conditions (Mal et al., 2016; Ayano et al., 2013; Kieu et al., 2011). For example, Kiran et al (2016) studied simultaneous sulfate reduction and heavy metal removal using anaerobic biomass from three different sources, and found Cd and Zn to be more toxic at 50 mg/L concentration on biomass growth, sulfate reduction and substrate (COD) utilization compared to Fe, Pb, Ni, Cu for all the three biomass types. Costa et al. (2017) reported a significant decrease in sulfate reduction efficiency due to presence of heavy metals (Cu and Zn) in a sequential batch reactor treating sulfate rich wastewater using ethanol as the carbon source. Guo et al. (2017) found that the sulfate reduction was significantly inhibited even

when the concentration of Cr^{6+} exceeded 20 mg/L. In order to avoid heavy metal toxicity, different techniques such as immobilization of anaerobic biomass are suggested to improve sulfate reduction and CO utilization efficiency even at high initial metal concentration (Mothe et al., 2018).

However, there are no studies reported thus far on the effect of heavy metals on sulfate reduction using CO as the carbon and energy source. Moreover, from the results obtained in this study, it is observed that although heavy metal as a co-pollutant decreased the sulfate reduction and CO utilization by the anaerobic biomass, the values are relatively better than those reported in the literature. In fact, for certain metals and concentrations, the values are much higher than the results found in the literature on SRB activity (sulfate reduction and COD removal).

5.3.2 Heavy metal removal

Due to their high water solubility and bioaccumulation potential, heavy metals discharged from industries can adversely affect the ecosystem by entering into the food chain. Once it enters the food chain high concentrations of heavy metals could accumulate in the human or other animal body, damaging their internal organ and can cause serious danger to their life (Babel and Kurniawan, 2004). Therefore, it is necessary to treat metal containing wastewater prior to its discharge to the environment. In this context, biological sulfate reduction by SRB used in this study is advantageous as it could simultaneously remove heavy metal by sulfide precipitation. Other advantages of biological heavy metal removal by sulfide precipitation includes efficient removal even at a low pH, low sludge production (Gallegos-Garcia et al., 2009), low cost over physico-chemical treatment methods, and possible recovery of metals from wastewater (Bijmans et al., 2011).

Fig. 5.4 shows the results of heavy metal removal by anaerobic biomass at the end of the six day experimental period. For all the heavy metals, removal efficiency decreased with an increase in initial metal concentration. From the figure it can be seen that Cu removal was the best among all the heavy metals studied, which ranged between 76.2 and 95.35%. The Pb and Cd removal efficiencies were moderate (more than 70 %) except at 100 mg/L initial Cd concentration, and in which case it was 62.78%. Zn showed the least removal efficiencies, which was 86.5 and 58.63% at 5 to 100 mg/L initial concentration, respectively. There was no considerable difference in removal rates of the different heavy metals at a low initial metal concentration in the range 5-25 mg/L (Fig. 5.5). The removal rate values were about 0.75, 1.5 and 3.5 mg/L/d for 5, 10 and 25 mg/L of initial metal concentrations, respectively. However, for the high initial metal concentrations of 50 and 100 mg/L, the removal rate values significantly varied and ranged from 5.5 to 6.9 mg/L/d and 9.7 to 12.53 mg/L/d, respectively. Both removal efficiency and removal rate of the metals were in the order Cu>Pb>Cd>Zn.

The mechanism of heavy metal removal by biological sulfate reduction process is well known, in which sulfide produced by SRB react with metal ions to form insoluble metal sulfide precipitates. The variations in the removal efficiency of the different heavy metals are attributed to their different solubility product values with sulfide. The metal removal efficiency values found in this study closely followed the solubility product values of the respective individual metals. For example, the reason for best removal efficiency in case of Cu compared to other heavy metals used in this study could be explained by its low solubility product value of 6×10^{-37} (Johnson and Hallberg, 2005). The heavy metal removal efficiency values were comparable with the values reported in the literature (Kiran et al., 2016; Mal et al., 2016; Sahinkaya et al., 2013).

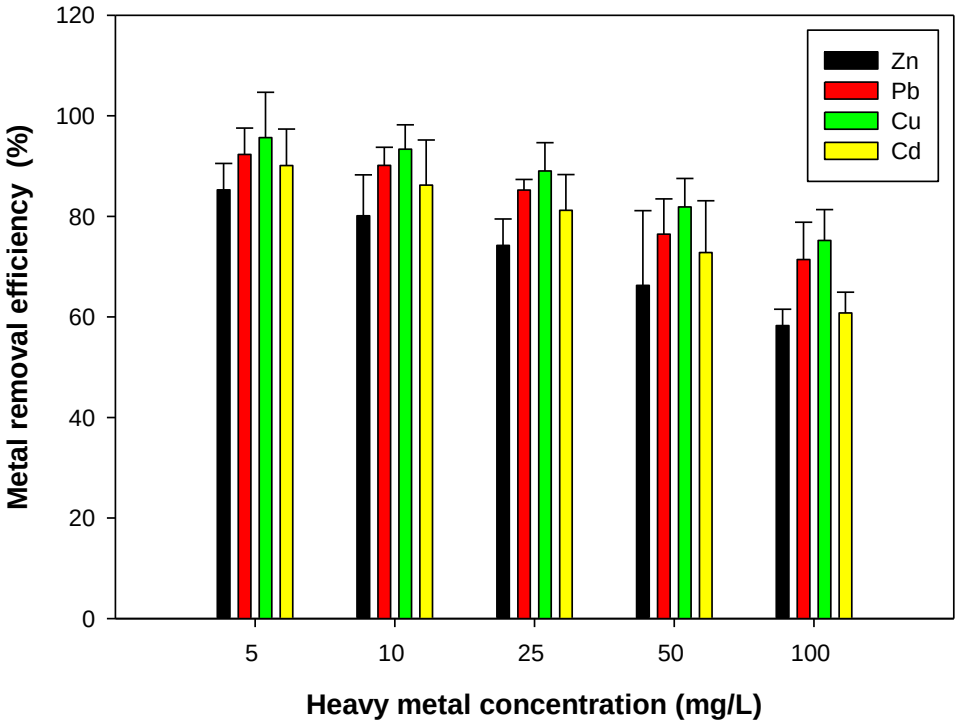

Fig. 5.4 Heavy metal removal by anaerobic sludge biomass.

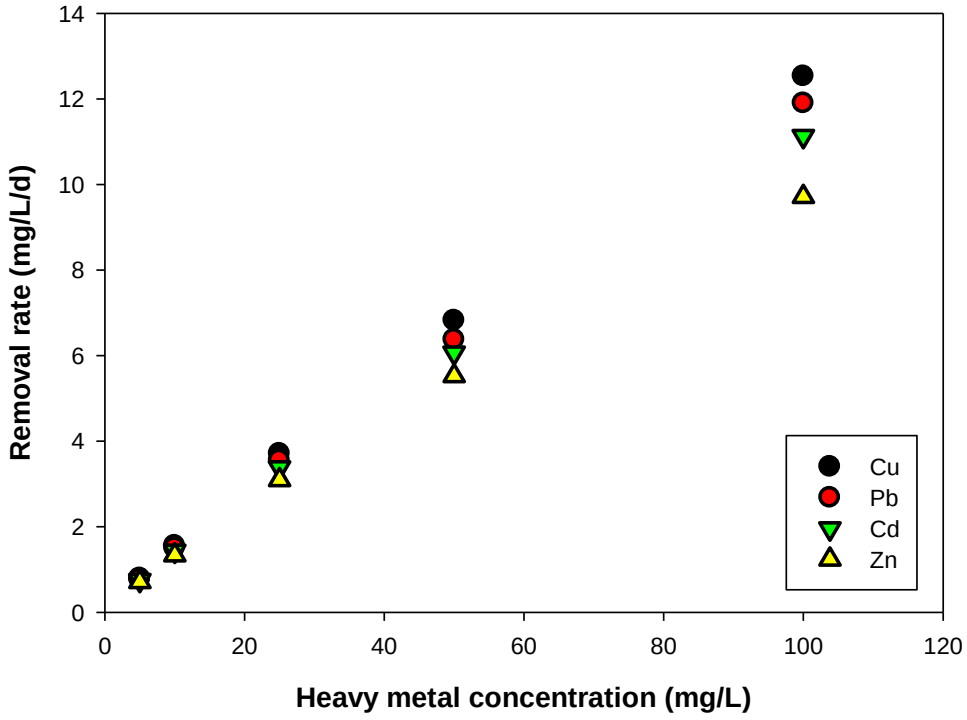

Fig. 5.5 Heavy metal removal rate for different initial metal concentration.

Kiran et al. (2016) reported more than 95% removal of Cu at a low metal concentration of 10 mg/L, whereas the removal efficiency dropped to 85% for 50 mg/L of initial concentration of the metal. Guo et al. (2017) found ~99% removal of Zn and Mn, and 80% Cr removal at 10 mg/L of initial heavy metal concentration by sulfate reduction process. Similar to these literature reports this current study also found a very high (<90%) metal removal efficiency at a low initial concentration. Even at a high initial metal concentration though the sulfate reduction efficiency was low, enough sulfide was produced to successfully precipitate metals from solution.

5.3.3 Morphological analysis and characterization of the metal bioprecipitates

Techniques such as FTIR, FESEM-EDX, FETEM provides an insight into the mechanism of heavy metal stress on biomass and the metal removal process. The FTIR analysis was carried out to observe changes in the functional groups present on the anaerobic biomass due to metal bioprecipitation by sulfate reduction. Fig. 5.6 shows the FTIR spectra of the different heavy metal loaded anaerobic biomass along with that of the control biomass, which was treated in the absence of any added heavy metal in the media. Sharp peaks at 565, 913, 1028, 1109, 1250 and 1450 cm^{-1} are mainly due to the presence of sulfate or sulfide functional groups indicating the formation of metal sulfide bioprecipitates (Kiran et al., 2015; Collman et al., 2009). Presence of peak at 1536 cm^{-1} is due to N-H stretching of amine group (Vaitheeswari et al., 2015; Feio Maria et al., 2004). Bands corresponding to the neutral C=O complex stretching is observed at 1643 cm^{-1}. From the figure a large stretch at 2854, 2925 and 3436 cm^{-1} is observed due to symmetric and asymmetric O-H stretching of hydroxyl groups (Kiran et al., 2015; Singh et al. 2011).

To study and compare the morphology of the metal loaded biomass with that of the control biomass, FESEM and FETEM analyses were carried out. From FESEM images (Fig. 5.7)

morphological difference in the microbial cell due to the presence of heavy metal is apparent. Some of the bacterial cell even shows clear sign of cell wall disintegration, probably due to the metal toxicity. FETEM image shows the presence of cell associated metal sulfides, which are formed due to the reaction of hydrogen sulfide formed with heavy metals present in the media (Fig. 5.8b). In the control biomass no such precipitate is observed (Fig. 5.8a).

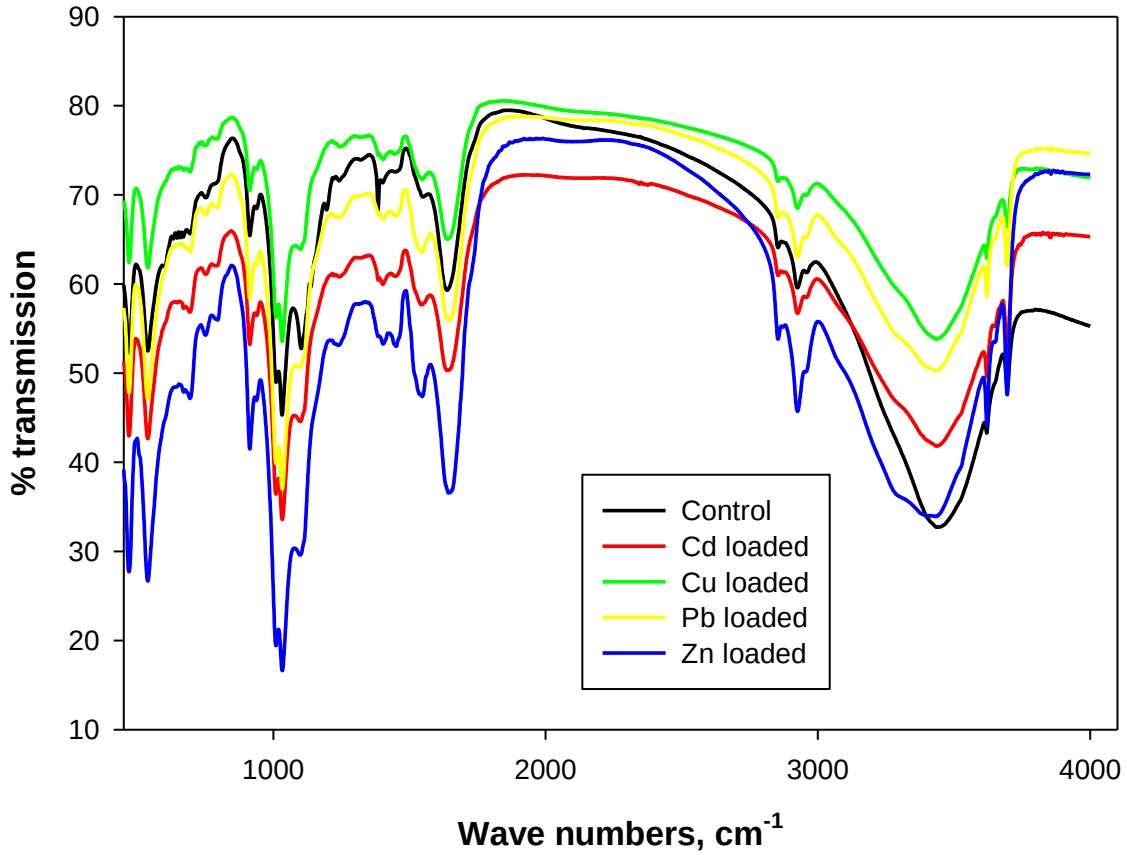

Fig. 5.6 FTIR spectra of the metal loaded biomass and control biomass.

Elemental composition of the metal loaded biomass is analysed using EDX spectrum combined with FESEM. Fig. 5.9 presents the EDX spectrum of the individual metal loaded biomass along with the corresponding FESEM image; Fig. 5.9e shows the EDX spectrum of the control biomass. The presence of different metals in the EDX spectrum confirmed the

metal sulfide precipitation. Along with heavy metals other elements such as carbon, oxygen, nitrogen, sulfur, sodium, phosphorous, chlorine, calcium, magnesium, potassium and iron in the bioprecipitates were mainly contributed by MSM.

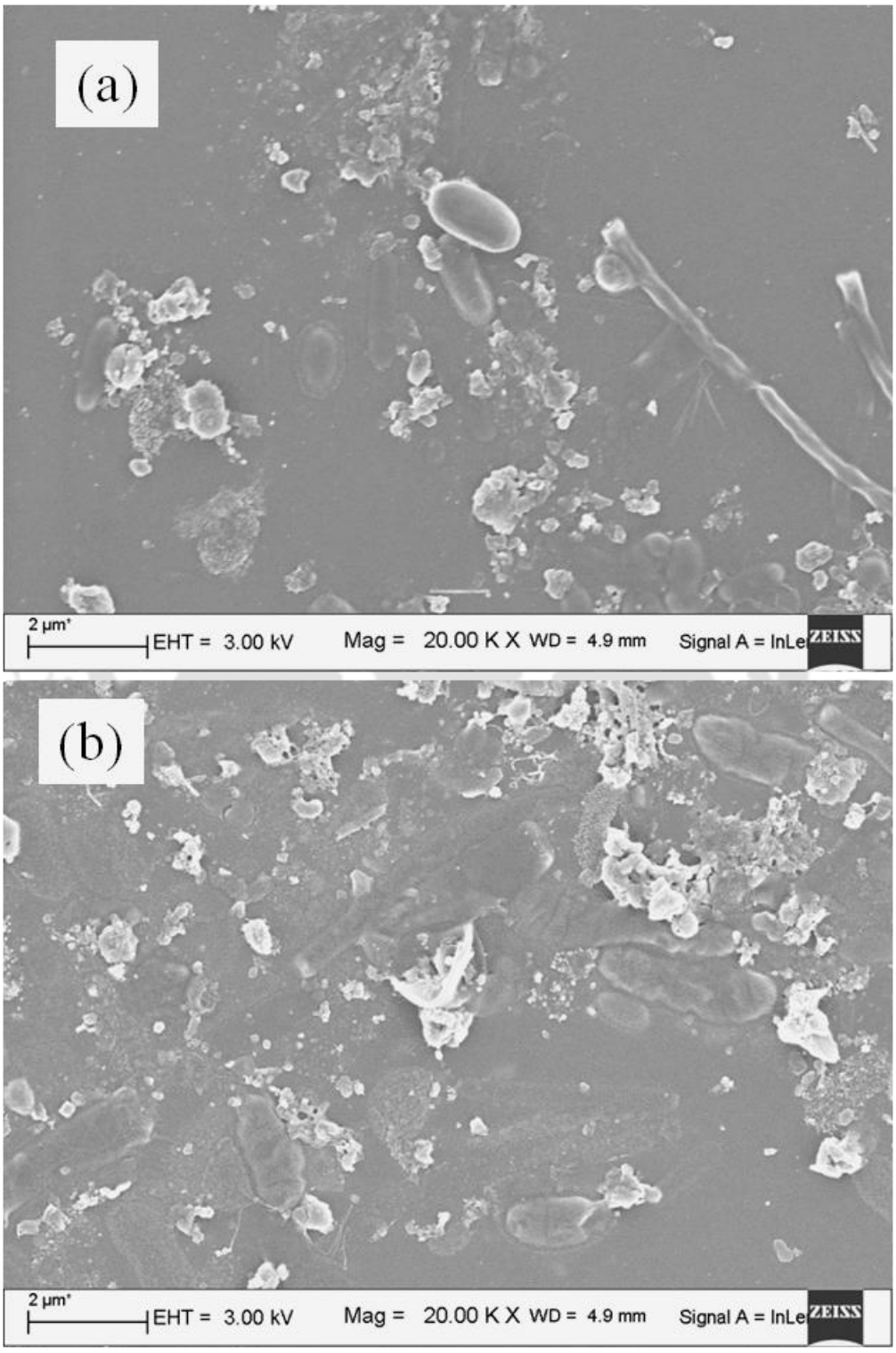

Fig. 5.7 FESEM image of (a) control biomass and (b) Pb loaded biomass.

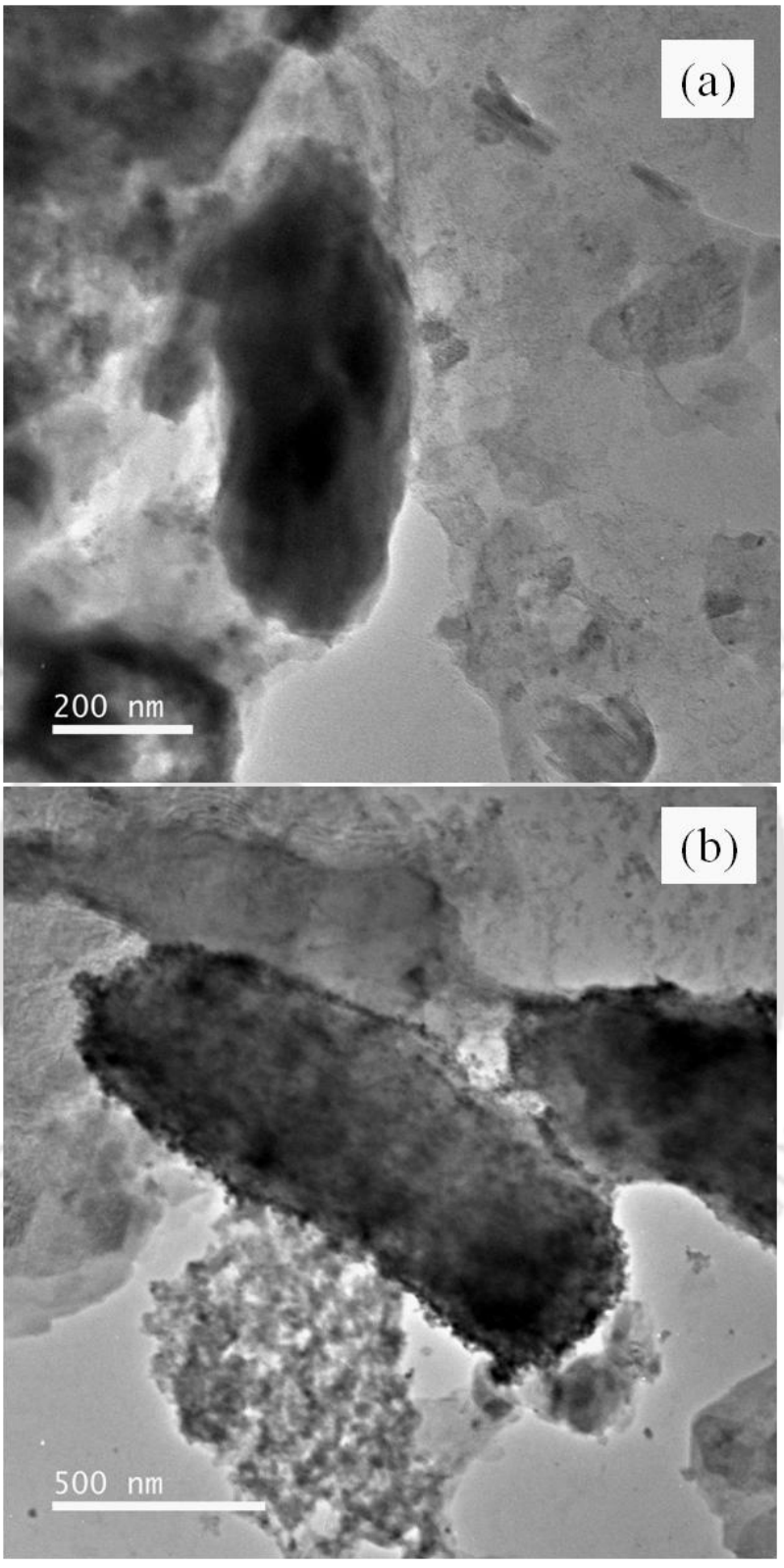

Fig. 5.8 FETEM image of (a) control biomass and (b) Pb loaded biomass.

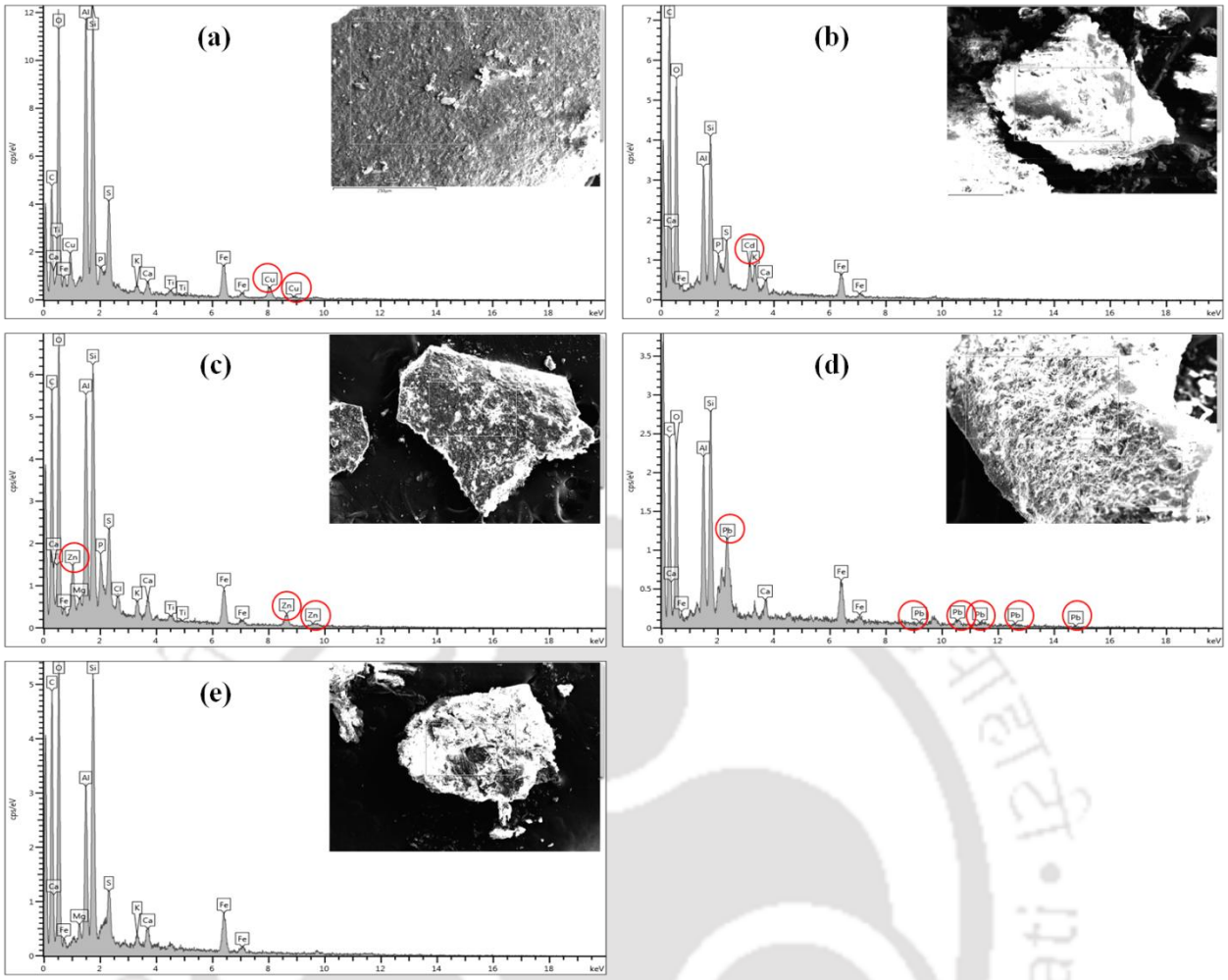

Fig. 5.9 EDX of bioprecipitate along with FESEM images for (a) Cu loaded biomass, (b) Cd loaded biomass, (c) Zn loaded biomass, (d) Pb loaded biomass and (e) control biomass.

5.4 Significant findings

Simultaneous metal removal and sulfate reduction using CO as the sole carbon and energy source was achieved by the anaerobic biomass. The metal removal efficiency followed the order Cu > Pb > Cd > Zn. This study showed significant inhibitory effect of Cu, Cd, Zn and Pb on sulfate reduction and CO utilization by the anaerobic biomass particularly at high initial concentration. Among the heavy metals, Pb showed the maximum inhibitory effect. The heavy metal removal mechanism is due to biological reduction of sulfate to sulfide,

followed by formation of metal sulfide precipitates. Formation of metal sulfide precipitates was confirmed by instrumental techniques such as FTIR, FESEM-EDX.

Chapter 6

Evaluation of biologically synthesized nanoparticles for enhanced CO bioavailability for improving CO bioconversion and sulfate reduction

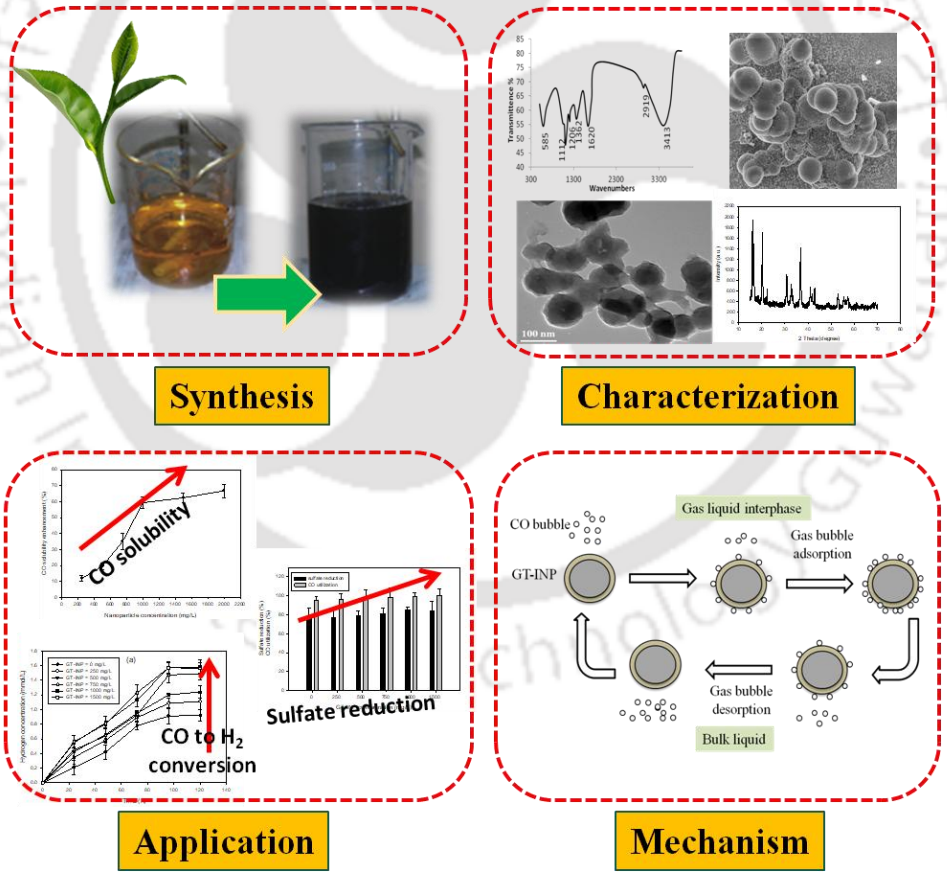

ABSTRACT

This chapter details the synthesis and characterization of green tea synthesized iron nanoparticle (GT-INP) and its effect on biohydrogen production from CO and on biological sulfate reduction by anaerobic biomass. Analysis of the GT-INP by UV-visible spectroscopy revealed spherical or quasi-spherical shape of the iron oxide nanoparticles. The XRD analysis confirmed the presence of iron oxide (Fe_3O_4) and iron(III) oxide-hydroxide (FeO(OH)) in the GT-INP. The appearance of strong vibrational bands in the FTIR spectra indicated the presence of amide, C-N and hydroxyl groups due to flavonoids, alkaloids and polyphenols as capping agent in the GT-INP. The FESEM and FETEM analyses revealed that the GT-INP were within 50-90 nm range with a spherical shaped aggregated structure. In the presence of GT-INP at 1000 mg/L, a maximum enhancement (56%) in aqueous solubility of CO was achieved along with a maximum H_2 production of 1.58 mmol/L by anaerobic biomass, which is nearly 44 % more than that obtained without any GT-INP addition. For all initial sulfate concentrations (250-1000 mg/L) used in this study, very high CO utilization and sulphate reduction efficiencies were obtained due to GT-INP addition, and in some cases the reaction rates improved.

6.1 Introduction

Rampant industrial development combined with ever growing population not only caused stress on the available resources, but also contributed to a high level of environmental pollution. Available water resources are often polluted by release of industrial effluent which contains both organic and inorganic contaminants. Contamination of drinking water supplies from industrial waste is a result of various types of industrial processes and disposal practices. Industries that use large amounts of water for processing have the potential to pollute waterways through the discharge of their waste into streams and rivers, or by run-off and seepage of stored wastes into nearby water sources. Sulfur containing compounds are one such pollutants in wastewater which when discharged untreated pose a serious threat to the environment. Many industries such as food processing (molasses, seafood, edible oil, etc.), pharmaceutical, and pulp and paper, generate wastewater with a high initial sulfate concentration. Despite a there are number of physico-chemical methods available for sulfate rich wastewater treatment, biological methods are more sustainable and less energy-cost incentive. In order to keep the process cost even further low, waste resources such as high chemical oxygen demand (COD) containing wastewater or waste gases (CO/CO_2/flue gas etc.) can be used as an alternative source for carbon and energy.

CO is emitted in large amount by incomplete combustion of fossil fuels during domestic and industrial processes. For example blast furnace gas contains 25% (v/v) CO, whereas automobile exhaust gas contains CO in the range 0.5 to 12%. CO is also a known toxic pollutant, which adversely affects human, animals and environment alike. However, CO can also serve as an alternative substrate for carboxydotrophic sulphate reducers for treatment of sulphate rich wastewater. In Chapter 3 an anaerobic biomass obtained from large scale upflow anaerobic sludge blanket reactor was shown to reduce sulfate with CO as the sole carbon and energy source. But the process is limited by low solubility of CO in water i.e

0.025 g per kg of water at 30 °C. This low solubility and gas-liquid mass transfer ($k_L a$) of CO reduces the process efficiency by lowering the bioavailibilty of CO to microorganisms. Modification in reactor agitation system or increase in agitation speed can be a possible solution to this CO bioavailability problem, but it requires additional power input which invariably increases the process cost. Different researchers have taken a number of other approaches including addition of surfactant, alcohol, metal salts, small particles, etc. to enhance the CO solubility. Among these different additives, nanoparticles seems to be more attractive as not only it is effective in small amount but also different surface modification can further increase the CO solubility. Zhu et al. (2008) studied mesoporous silica nano particles coated with hydroxyl groups, mercaptopropyl groups and organic groups to enhance gas liquid mass transfer. It was observed that surface activated nano particles enhanced the CO-water mass transfer, and the mercaptopropyl groups grafted nano particles yielded a maximum CO-water mass transfer (upto 1.9 times increase). The presence of functional groups on nano particles and their hydrophobicity is reported to significantly enhance the CO water mass transfer (Kim and Lee, 2016; Zhu et al., 2008). Similarly, in aerobic systems, increase in dissolved oxygen concentration in water due to addition of magnetite (Fe_3O_4) nanoparticles coated with oleic acid is reported (Olle et al., 2006).

In this present study in order to improve the aqueous solubility of CO by enhancing the gas-liquid mass transfer coefficient, biologically reduced iron nano particles were used. Green tea extract was chosen for synthesizing iron nanoparticle as it is reported to contain a number of phytochemicals namely flavins, catechin, flavonoids, tannins, caffeine, polyphenols, gallic acid, boheic acid, etc. which impart hydrophobic functional groups on nanoparticles for binding with the solution, thereby increasing the CO-water mass transfer. Besides characterization, effect of green tea based nanoparticle on H_2 production from CO and subsequent sulphate reduction by anaerobic biomass was examined.

6.2 Materials and methods

6.2.1 Synthesis of iron nanoparticles

For synthesis of green tea iron nanoparticle (GT-INP), procedure as described by Wang et al. (2014) was followed. Green tea was obtained from a local market in Guwahati, Assam, India. Green tea extract was first prepared by boiling 24 g of green tea in 400 ml of distilled water at 80 °C for 1 hour, followed by filtration. The extract was then added to 0.1 M $FeSO_4$ at 2:1 ratio to form GT-INP, which was indicated by an immediate appearance of black colour precipitate. The GT-INP was finally separated by vacuum filtration, washed with ethanol and dried overnight before use in the experiments. Fig 6.1 is a the schematic of the nanoparticle synthesis procedure followed in this study.

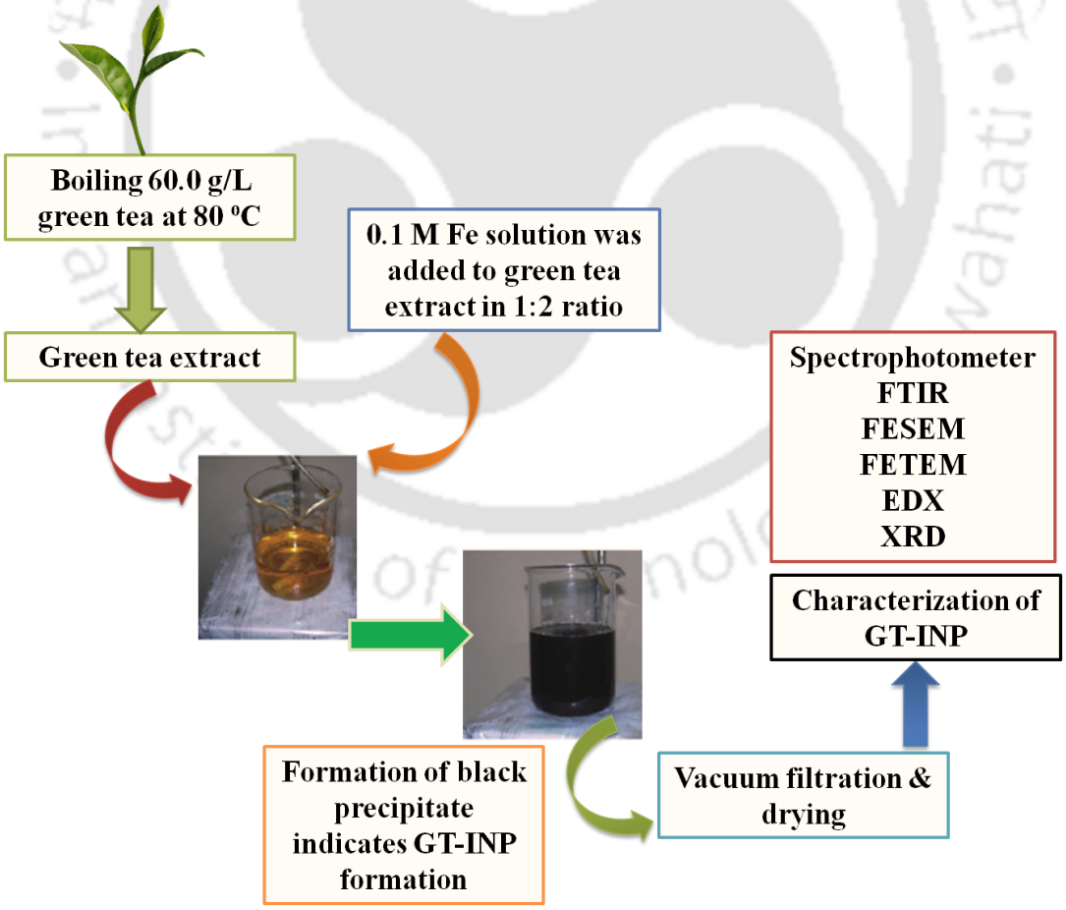

Fig. 6.1 Schematic of GT-INP synthesis procedure.

6.2.2 Characterization of GT-INP

The GT-INPs were characterized by UV-Vis spectroscopy, field emission scanning electron microscopy (FESEM), field-emission scanning electron microscopy - energy dispersive X-ray spectroscopy (FESEM-EDX), field-emission transmission electron microscopy (FETEM) (XRD) and fourier transform infrared spectroscopy (FTIR) analysis. For morphology and elemental composition analysis of the GT-INP, a sample of the GT-INP was affixed onto adhesive tapes supported on metallic disks and gold coated using a sputter coater, followed by observation under FESEM-EDX (Zeiss, Sigma, Germany). For FETEM analysis, GT-INP was loaded on a copper grid coated with carbon and observed under FETEM (JEOL, 2100F, Japan). For FTIR analysis, samples were prepared by mixing 1 % (w/w) GT-INP with 100 mg of KBr powder and the pellet obtained was analyzed using a FTIR spectroscope (PerkinElmer, Spectrum Two, Singapore).

6.2.3 Effect of GT-INP on CO solubility in water

Aqueous solubility of CO was measured using a 100 ml sealed serum bottles filled with deionized water. To measure enhancement in CO solubility by GT-INP addition, required amount of nanoparticles were added in the bottle, the bottles were then purged with nitrogen to create oxygen-free environment. CO was then injected into the bottle until the internal pressure reached to 120 kPa. The solution was agitated at 200 rpm for 20 min and 5 ml of liquid sample was withdrawn for measuring the dissolved CO concentration by using a spectrophotometer based myoglobin assay (Zhu et al., 2009). In this assay, shift in absorption spectra of deoxy-myoglobin (MbFe(II)) due to its reaction with CO to form carbonmonoxy-myoblobin (MbCO) is indicative of CO concentration in liquid samples.

6.2.4 Effect of GT-INP on CO bioconversion to H_2 and sulfate reduction

The effect of GT-INP addition on biohydrogen production from CO and sulfate reduction was studied in batch system consisting of 120 ml serum bottles (Sigma Aldrich, India) sealed with polytetrafluoroethylene (PTFE) septum with 50 ml MSM media. Composition of the MSM and other experimental conditions followed were given earlier in Chapter 3. The concentration of GT-INP was taken in the range from 0 to 1500 mg/L for evaluating its effect of biohydrogen production by anaerobic biomass. The pH was maintained at 7.0 and an inocculum of 0.2% w/v of the anaerobic sludge biomass was added to every bottle. The bottles were purged with N_2 gas to remove O_2 prior to supplying CO. The initial CO concentration in the bottles was 3.1 mmol/L. 2-Bromoethanosulfonate (BES) in the concentration of 10 mmol/L was added to serum bottles to inhibit any methanogenic activity. The bottles were incubated at 30°C and 150 rpm on a rotating orbital incubator shaker. All these experiments were carried out in triplicate.

Further to check the effect of GT-INP on sulfate reduction different concentration of GT-INP ranged from 0-1500 mg/L were added to the serum bottles. As the 1000 mg/L of GT-INP concentration showed maximum biohydrogen production and sulfate reduction, the effect of different initial sulfate concentrations (250-1000 mg/L) on sulfate reduction at the same GT-INP concentration was examined.

6.2.5 Analytical methods

The head space gas composition in the serum bottles was analyzed using a gas chromatograph (GC, Varian 450, The Netherlands) equipped with a thermal conductivity detector (TCD) and a molecular sieve column (Mole sieve 5A, mesh 80/100, 72 in × 1/8 in) using methods as described earlier in Chapter 3. Sulfate concentration was determined using

the standard barium chloride based turbidimetric method (APHA, 2005). All these methods were described in detail in Chapter 3.

5.3 Results and discussion

This study explored iron nanoparticle synthesized using green tea extract for enhancing CO utilization and sulfate reduction by anaerobic biomass by improving the CO-water mass transfer and its bioavailability.

5.3.1 Characterization of GT-INP

The formation of GT-INP in solution was confirmed by change in colour of the solution to black colour, which was subsequently characterized using different technique. Fig. 6.2a shows UV - visible spectra of the GT-INP, which reveals an absorption peak at 280 nm due to spherical or quasi-spherical shaped iron oxide nanoparticles (Mohanraj et al., 2014). According to Mie's theory, spherical or quasi-spherical nanocrystals exhibit a single surface plasmon resonance (SPR) band, whereas anisotropic particles show two or three bands, depending on their shape (Mohanraj et al., 2014).

X-ray diffraction (XRD) pattern of dried GT-INP is shown in Fig. 6.2b. Relatively sharp peaks in the figure are due to small size of the particles, and the peaks were assigned to iron oxide (Fe_3O_4) and Iron(III) oxide-hydroxide (FeO(OH)). According to Shahwan et al. (2011), sharp peaks at 17, 20, 22, 32, 41, 42, 48, 49, 61 are due to FeO(OH) and at 30, 37, 43, 52, 57, 58, 59, 64, 69 are due to Fe_3O_4. Previous studies report that Fe^0 and α-Fe crystalline type structures are found when zero valent iron is synthesized following the borohydride reduction method (Uzum et al., 2009); it is also reported that Fe^0 produced by reduction with extracts obtained green tea or sorghum bran (Hoag et al., 2009; Njagi et al., 2011) are amorphous in nature with no diffraction lines for Fe^0 in XRD pattern.

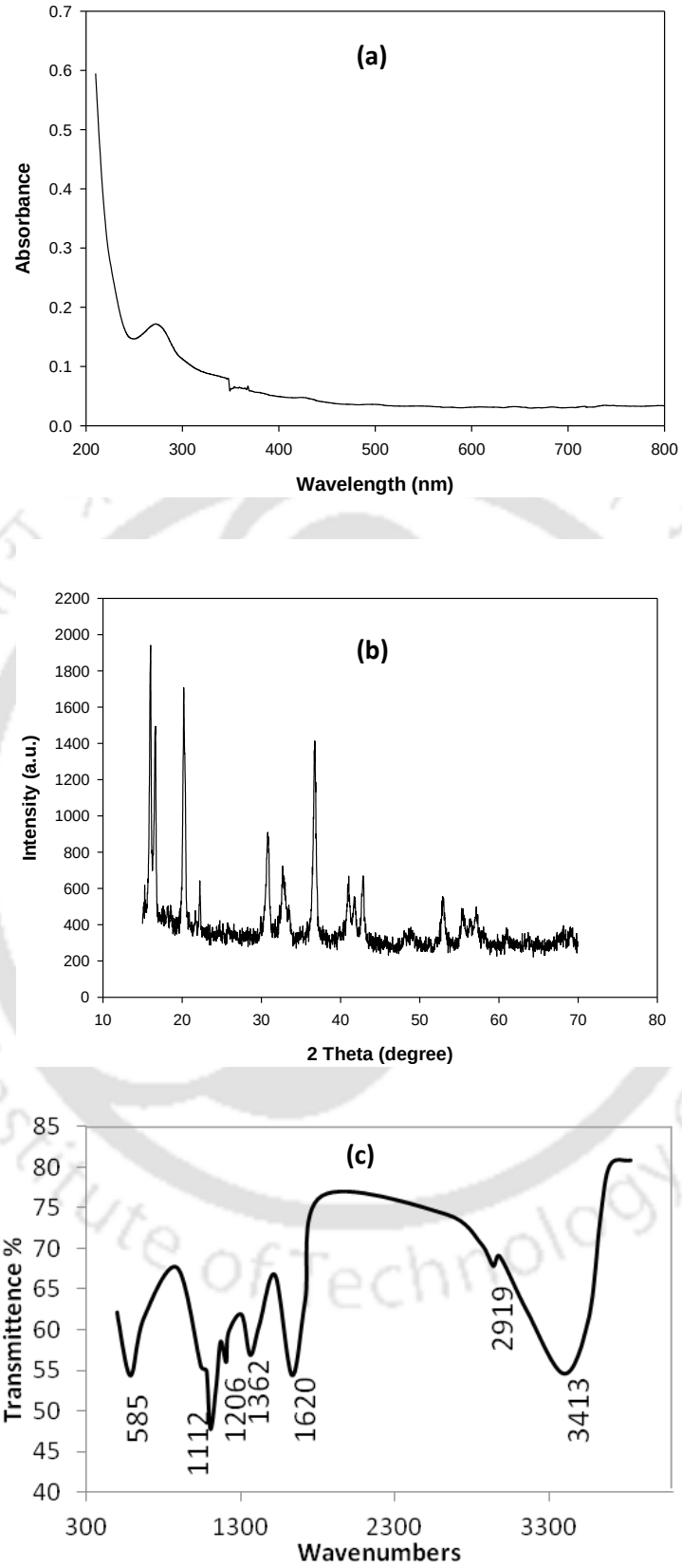

Fig. 6.2 Characterization of GT-INP (a) UV-vis spectra, (b) XRD pattern and (c) FTIR spectra.

Table 6.1 Different functional groups on GT-INP

Frequency (cm^{-1})	Functional group	Band observed due to GT-INP
3300-3450	-OH, -NH stretching	3413
2910-2920	-CH stretching	2919
1600-1640	-COO, C=O stretching	1620
1300-1450	Amide or sulfamide bond	1362
1270	-C-O stretching	1206
1030-1070	S=O stretching	1112
580	Fe-O	585

FTIR spectra (Fig. 6.2c) of the GT-INP shows bands at 586, 1112, 1206, 1362, 1620, 2919 and 3423 cm^{-1} which correspond to different functional groups present on the surface of GT-INP; and these functional groups serves as the reducing and capping agent for GT-INP synthesis (Table 6.1). The bands at 3423 and 1620 cm^{-1} are assigned to the hydroxyl group and proteins, respectively. The absorption peak at 2919 cm^{-1} is designated to C−H stretching vibration modes in the hydrocarbon chains. The band at 1362 cm^{-1} is due to C−N stretching or the O−H bending. The band at 1112 cm^{-1} is attributed to the C−N stretching vibration of aliphatic amines. The presence of iron oxide nanoparticles is further confirmed by the strong absorption band seen at 586 cm^{-1}, which is assigned to the Fe−O bond of Fe_2O_3 (Togashi et al., 2011). These findings indicate that the GT-INP are coated with polyphenols, proteins and amines available in the green tea extract used during the synthesis of GT-INP. The same groups also served as reducing and capping agents for the GT-INP.

The other properties, such as size, structure and surface morphology of the GT-INP were studied using FESEM analysis. The FESEM images (Fig. 6.3a) reveal that the GT-INP were spherical in shape with size ranging from 50 to 90 nm. The surface was found to be rough and often formed aggregated irregular structures. Li et al. (2006) reported that the iron

nanoparticles are colloidal in nature and exhibit a strong tendency to aggregate as well as adhere to the surfaces of natural materials, e.g. soil and sediment. The morphology and structure of the GT-INP were similar to those reported in the literature (Klačanová et al., 2012; Huang et al., 2014).

From FESEM-EDX analysis of GT-INP, shown in Fig. 6.3b, it is found to be composed of C, O, N, Fe, S, Na and K atoms. The atoms other than Fe in the GT-INP were contributed by the green tea extract, which indicates successful capping due to biomolecules present in the extract.

Fig. 6.3c shows FETEM micrograph of the GT-INP. It can be seen from the figure that the nanoparticles are mostly spherical in shape and exist as chain-like aggregated structure. According to a study by Li et al. (2006), size distribution of over 400 iron nanoparticles revealed that the size of more than 80 % of the particles are less than 100 nm size whereas 50 % of the particles are less than 60 nm. The size of the GT-INP in this study is below 100 nm confirming the findings of the literatures.

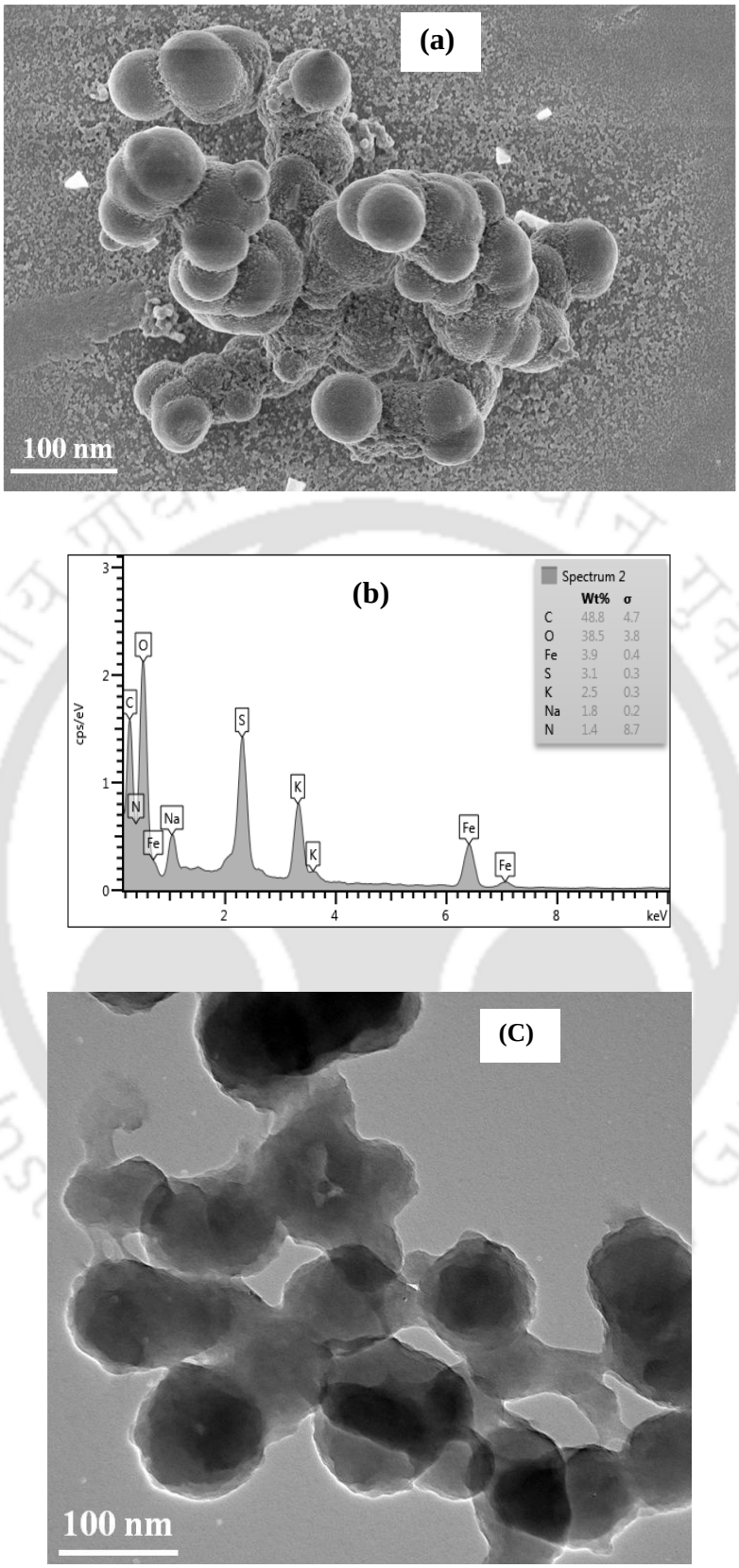

Fig. 6.3 Micrograph analysis of GT-INP (a) FESEM, (b) FESEM-EDX and (c) FETEM analysis.

6.3.2 Effect of GT-INP on CO aqueous solubility of CO

From the literature it can be found that few studies have reported about the ability of surface modified nanoparticles in enhancing CO-water solubility; but this current study for the first time have used biologically synthesized nanoparticle for enhancing the aqueous solubility of CO. Hence, this study was focused on evaluating the GT-INP for CO bioconversion to H_2 and sulfate reduction by improving CO-water mass transfer.

Fig. 6.4 shows the effect of GT-INP addition on CO solubility in water. It is evident that the dissolved CO concentration significantly increased with an increase in the GT-INP concentration. A maximum enhancement in CO solubility, i.e 51.6 %, is observed with the addition of 1000 mg/L of GT-INP compared to that without any added nanoparticles. Increase in gas solubility due to addition of chemically synthesized nanoparticles is widely reported in the literature. For instance, Kim and Lee (2016) found 224 % increase in CO solubility by the addition of functionalized cobalt ferrite-silica nanoparticles.

The authors concluded that the mesoporous structure of silica increased the specific surface area of the nanoparticles. In another study by the same authors, methyl functionalized silica nanoparticles were evaluated for enhancing the CO solubility (Kim et al., 2014), and 273 % and 156 % increase in soluble CO and H_2 concentrations, respectively, were reported due to the addition of methyl-functionalized silica nanoparticles.

The increase in CO solubility due to nanoparticles involves three main mechanisms. First is the shuttling or grazing effect where excess amount of gas from gas phase is supplied to bulk liquid by adsorption-desorption; second is reduction in the gas-liquid boundary, and third is increase in the specific gas-liquid interfacial area. Ruthiya et al. (2005) attributed all these three mechanisms for enhancing mass transfer coefficient by gas phase reactant adhesion of gas bubbles on nanoparticles at the gas - liquid interface (Fig. 6.5).

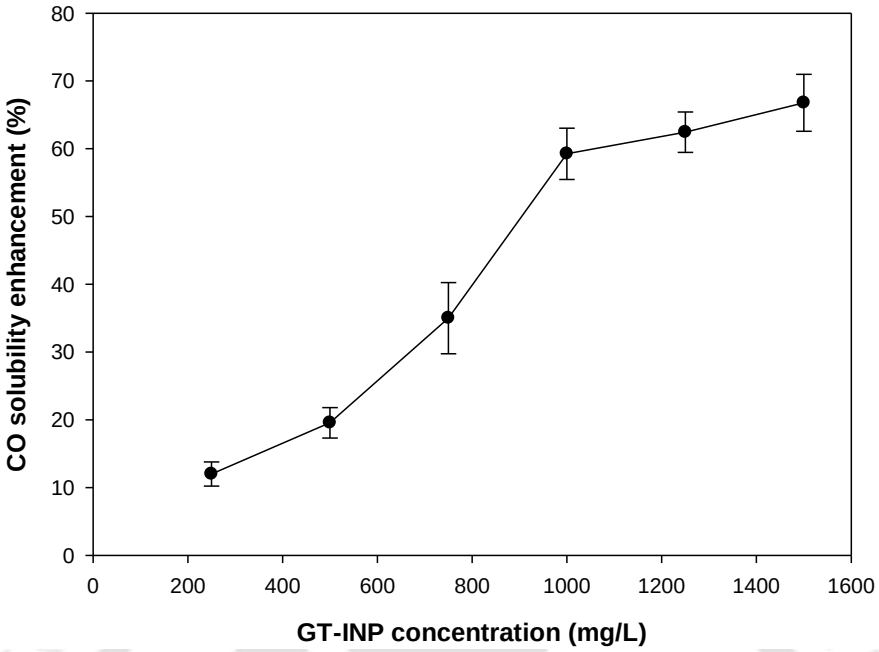

Fig. 6.4 Effect of GT-INP addition on CO solubility in water.

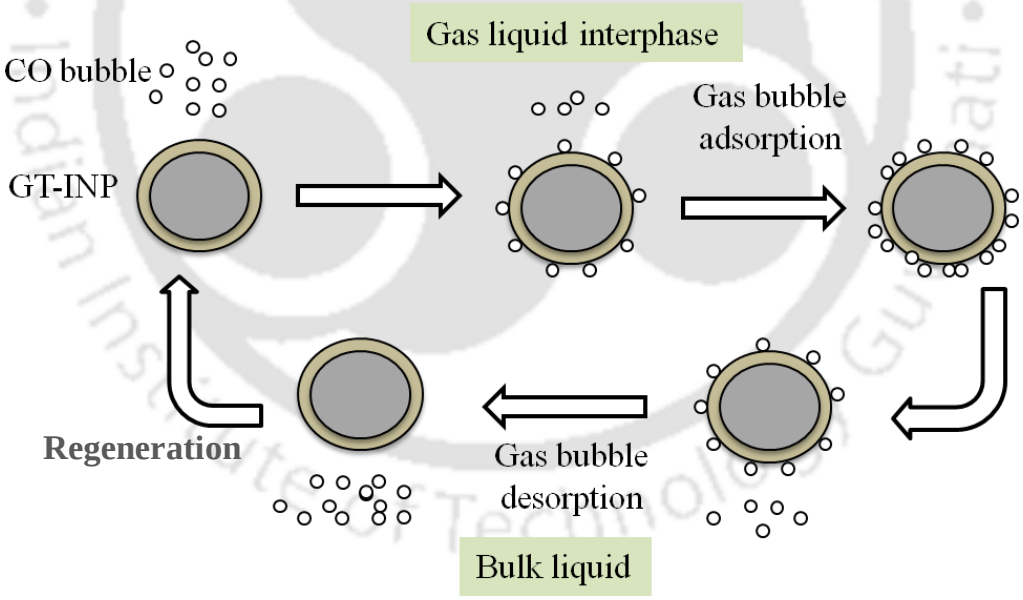

Fig. 6.5 Mechanism involved in GT-INP mediated CO solubility enhancement.

The enhancement in CO solubility obtained in this study using GT-INP are lower as compared with those reported in the literature. This difference in the CO solubility enhancement due to nanoparticles is attributed to different functional groups present on the

nanoparticles. In this study, hydrophobic functional groups, such as amides, polyphenols, proteins, etc. obtained from green tea extract were present on the nanoparticle surface, are less effective than the functional groups, such as oleic acid, methyl etc. used by other authors for surface modification of chemically synthesized nanoparticles reported in the literature for enhancing the aqueous solubility of CO. These findings highlight the importance of surface modification of nanoparticles with hydrophobic functional groups, e.g. methyl and isopropyl, for further enhancing in CO solubility water.

6.3.3 Effect of GT-INP on CO bioconversion to H_2

In the previous chapter it was seen that the product formation, i.e. H_2 production, is directly proportional to the CO utilized. Hence, the effect of GT-INP on H_2 production by improving the CO utilization was examined in detail.

Fig. 6.6a shows H_2 production profile by the anaerobic biomass in the presence of GT-INP. In the experiments without any added nanoparticles, a lag phase in H_2 production was seen for initial 24 h time, followed by a gradual increase in H_2 concentration upto 0.92 mmol/L. Whereas, in the experiments with GT-INP added to the media the H_2 production was rapid without any lag phase and continued upto 96 h and after which it remained constant. A maximum H_2 production of 1.58 mmol/L in the experiments was obtained at 1000 mg/L concentration of GT-INP, which is nearly 44 % more than that obtained without any GT-INP addition. Similarly, in the previous experiments a maximum CO solubility was achieved due to addition of 1000 mg/L of GT-INP in the media. These results clearly demonstrate the potential of GT-INP for enhancing biohydrogen production from CO by improving CO solubility in aqueous media, and, therefore, its bioavailability.

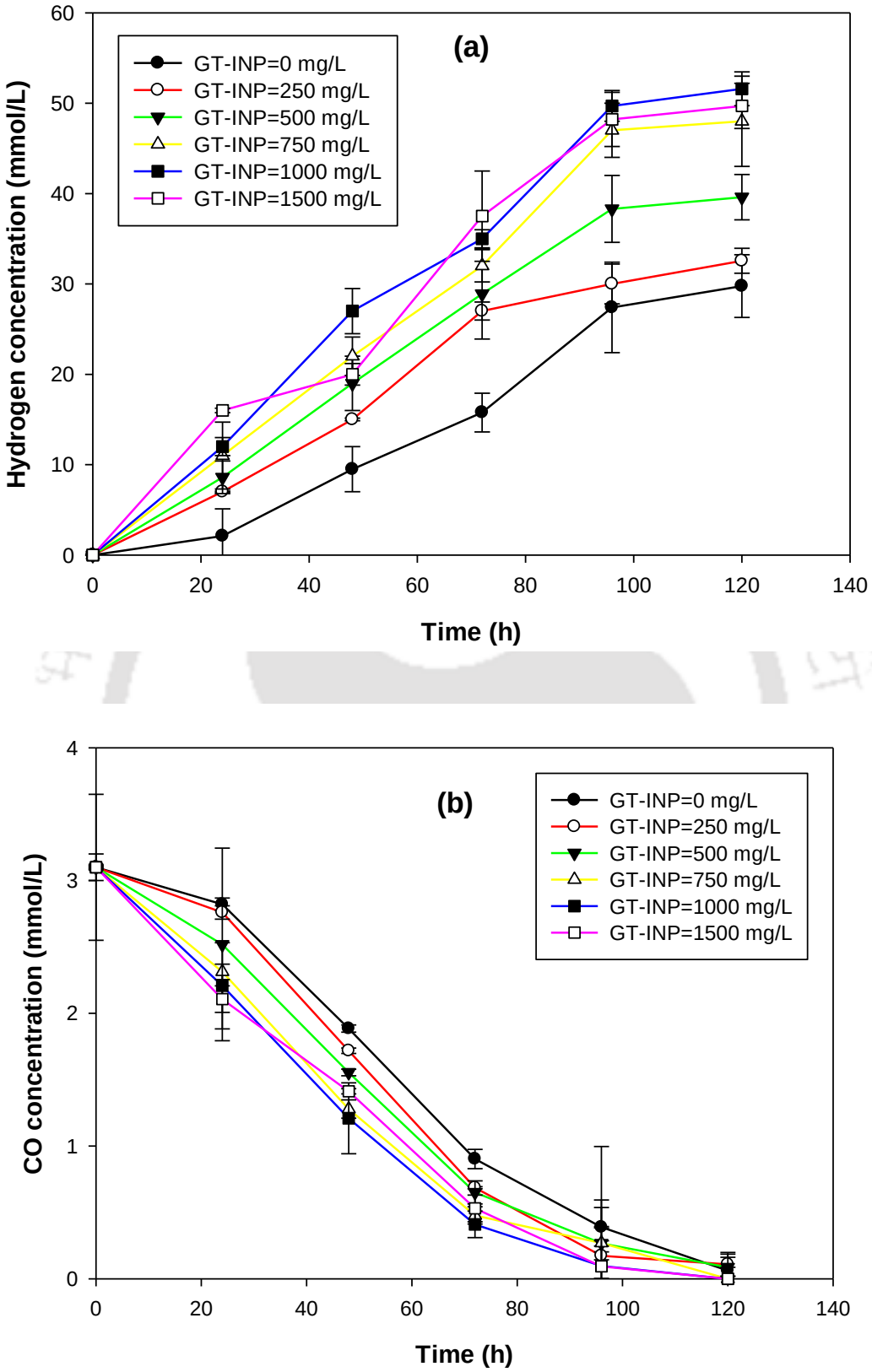

Fig. 6.6 Effect of GT-INP addition at different concentrations in the media on: (a) H_2 production and (b) CO conversion.

The CO utilization profile matched well with that of the H_2 production (Fig. 6.6b), and the CO utilization was in the range 97.2 to 100 % due to GT-INP addition in the media. Thus, a high concentration of GT-INP in the media resulted in very high and quick utilization of CO, which is similar to the results of H_2 production.

In addition to improving the CO gas-liquid mass transfer, iron naoparticles are known to influence the metabolic pathway involved in H_2 fermentation. Yang and Wang (2018) reported change in microbial community from *Enterobacter* sp. to *Clostridium* sp. due to addition of iron nanoparticle which improved fermentative H_2 production from grass. Also, the authors observed enhanced electron transfer between ferredoxin and hydrogenase due to iron nanoparticle, which improved the enzyme activity by the necessary Fe^{2+}.

Mohanraj et al. (2014) reported changes in metabolic products from acetate/butyrate type to hydrogen from glucose by *Clostridium acetobutylicum* due to iron nanoparticle addition, which resulted in enhanced biohydrogen production. However, contrary to this literature report, VFA production in this study (Fig. 6.7) increased four-fold due to the addition of GT-INP at a high concentration (1000-1500 mg/L) when compared to that of control (Fig. 6.7). The VFA production did not vary significantly at a low GT-INP concentration (250-750 mg/L). A probable reason for this increase in the VFA production could be due to the high amount of H_2 produced that was channelized towards VFA production rather than towards methane production as BES was added as an inhibitor of methanogenic activity. The VFA concentrations ranged between 2-10 mg/L, which is very low as compared with H_2 produced by the anaerobic biomass in the presence of GT-INP.

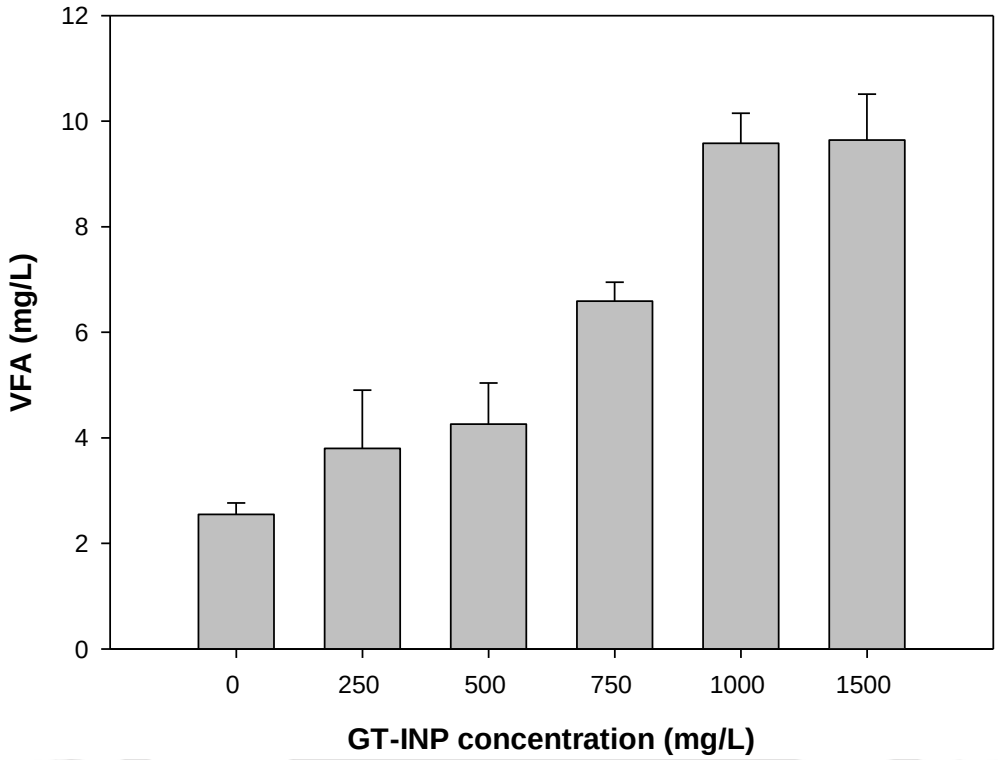

Fig. 6.7 Effect of GT-INP addition on VFA production.

6.3.4 Effect of GT-INP on biological sulfate reduction

The need for alternative carbon source and electron donor for biological sulfate reduction had lead to use of waste substrates such as CO. However, due to poor solubility of CO there is a need to improve the process efficiency, and, therefore, GT-INP was used to improve CO solubility in aqueous media and its bioconversion to H_2 for sulfate reduction.

Fig. 6.8 depicts the effect of different concentrations of GT-INP on sulfate reduction and CO utilization by the anaerobic biomass. Sulfate reduction as well as CO utilization were better in presence of GT-INP than those without any nanoparticle addition in the media, 1000 mg/L of GT-INP addition resulted in a maximum sulfate reduction efficiency. Further experiments with different initial sulfate concentrations with GT-INP added to the media showed improved results of both sulfate reduction and CO utilization (Fig. 6.9). Complete sulfate

reduction and CO utilization were observed for low initial sulfate concentrations of 250 and 500 mg/L. Although the sulfate reduction efficiency values for these two initial concentrations were similar in both presence or absence of GT-INP in the media, a clear difference in the time taken for sulfate reduction confirmed the strong positive effect due to GT-INP on biohydrogen production from CO.

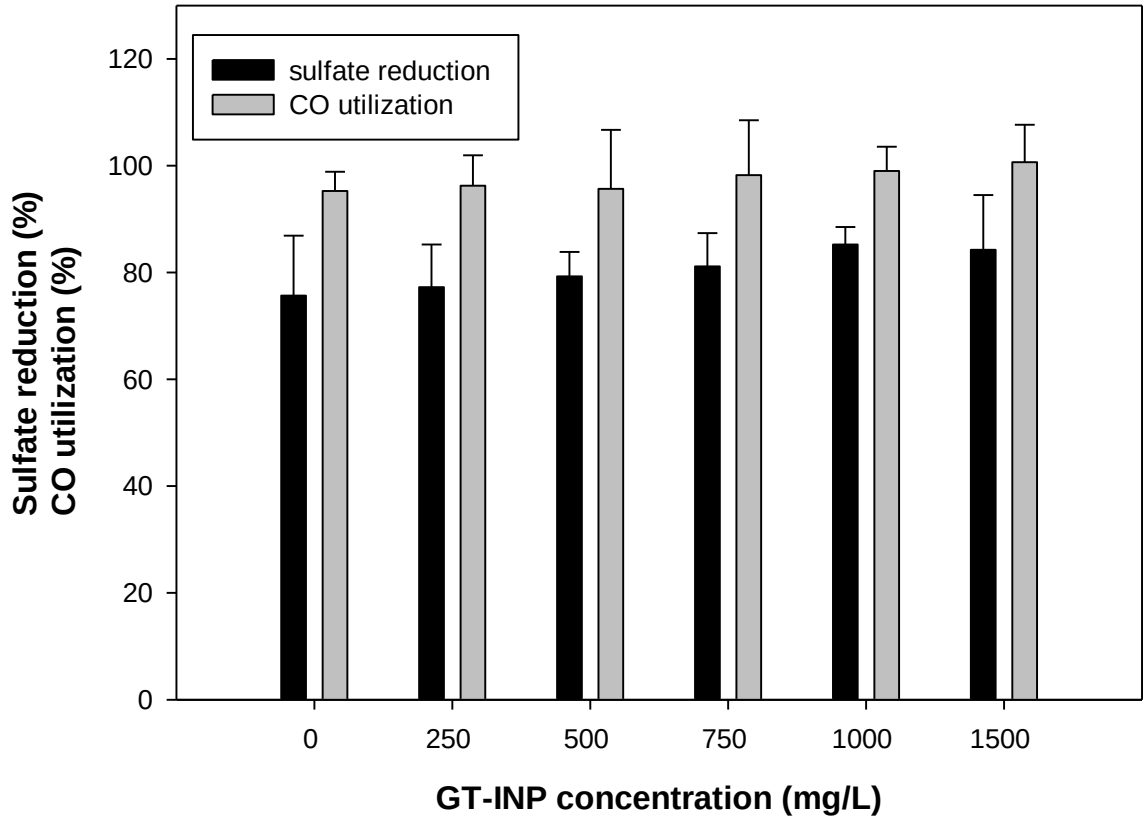

Fig. 6.8 Effect of GT-INP addition on sulfate reduction and CO utilization.

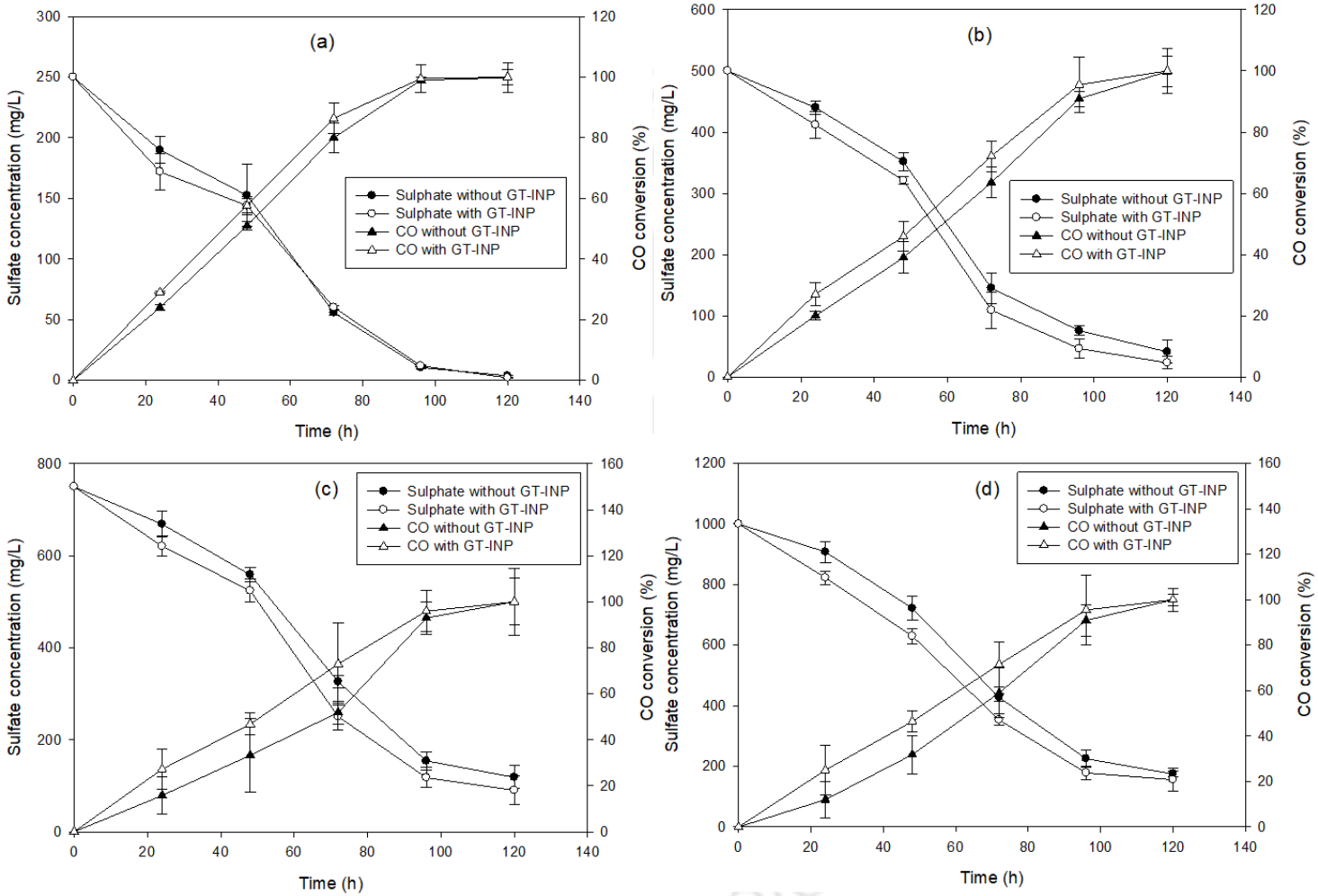

Fig. 6.9 Effect of GT-INP addition on sulfate reduction for different initial sulfate concentrations (a) 250 mg/L, (b) 500 mg/L, (c) 750 mg/L and (d) 1000 mg/L.

In case of 750 mg/L of initial sulfate concentration and in the absence of GT-INP the sulfate reduction was 84 %, whereas the value was slightly high (89 %) in the presence of GT-INP. At 1000 mg/L of initial sulfate concentration, the sulfate reduction values were low (78 % and 84.5 %) in absence and in presence of GT-INP, respectively. However, the CO utilization was maximum in all these cases (Fig. 6.9). These results indicate that although the CO was efficiently converted it was insufficient for reducing the sulfate at a high initial concentrations i.e due to low COD to sulfate ratio. From the literature, it is known that an optimum COD to sulfate ratio of 0.67 is essential for achieving a maximum sulfate reduction efficiency with soluble carbon source such as lactate, acetate, glucose, etc. However, in case of gaseous substrates, e.g. CO, CO_2, H_2 etc. the ratio needs to be optimized.

6.4 Significant findings

Characterization of the biologically synthesized GT-INP revealed spherical or semi spherical shaped aggregated nanoparticle with a size range of 50-90 nm. From FTIR and FESEM-EDX analyses presence of amide, hydroxyl groups on the nanoparticle surface was detected, moreover, it was confirmed that the nanoparticle is coated with flavonoids, alkaloids and polyphenols, etc. from green tea extract. Addition of GT-INP in the liquid media increased the CO solubility, with a maximum enhancement of 56 % at 1000 mg/L of GT-INP. The effect of GT-INP synthesized using green tea extract on hydrogenogenic CO conversion and sulfate reduction was studied. Hydrogen production and sulphate reduction profile showed improved results with GT-INP addition when compared with that of experiments without adding nanoparticle. Moreover, from the experimental results it is clear that GT-INP is effective in not only enhancing hydrogenogic CO conversion and biological sulfate reduction but also reducing the reaction time.

Chapter 7

Performance evaluation of gas lift and moving bed biofilm bioreactor systems for hydrogenogenic CO conversion and sulfate reduction under continuous operation mode

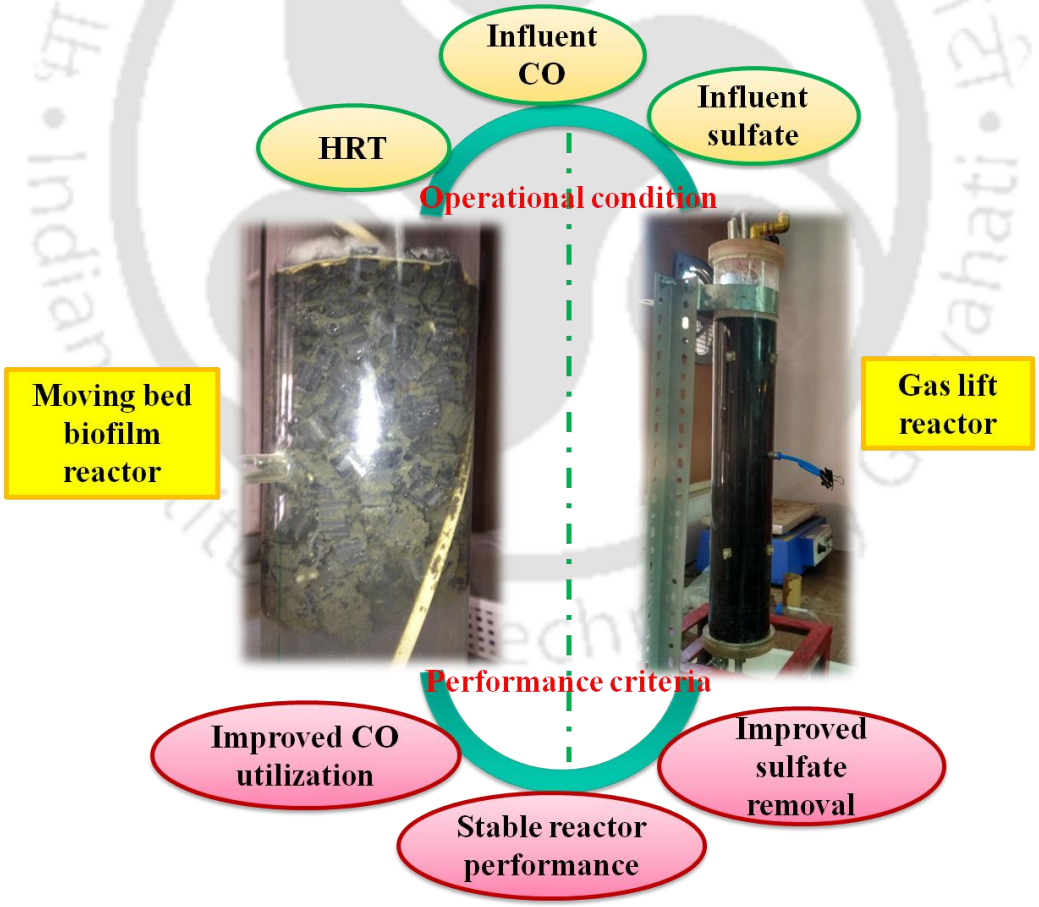

ABSTRACT

This chapter reports hydrogenogenic CO conversion and sulfate reduction under continuous operation mode using an internal loop gas lift bioreactor (GLR) and a moving bed biofilm reactor (MBBR). The results showed that with increase in the CO flow rate the H_2 production increased; however, the CO conversion efficiency reduced. A maximum H_2 concentration of 8.5 mmol/L was obtained for 36 mmol/L of inlet CO concentration. Biodesulfuruization using CO as the sole carbon and energy source was further studied using the anaerobic biomass in the two bioreactor systems. The effect of hydraulic retention time (HRT), sulfate loading rate and CO loading rate on sulfate reduction and CO conversion was examined. The results revealed that among three different HRT (72, 48 and 24 h), 48 h HRT gives best results with 97.2 % and 95.6 % sulfate reduction for GLR and MBBR, respectively. Best results in terms of sulphate reduction were obtained for low inlet sulphate and high CO loading conditions. The CO utilization was very high at 80 % during the first two phase of the study; however, further increase in inlet CO concentration reduced its utilization. The sulfate removal rates correlated well with the different sulfate loading rates used in the study, thus revealing a stable performance of both the reactor systems. Compared with GLR, MBBR system proved better in terms of stable performance for a prolonged operation period.

7.1 Introduction

Sulfate rich wastewater, generated and discharged from many industrial processes, including mining activity, thermal power plants, coal burning, pulp and paper processing, agricultural activity, edible oil production, molasses fermentation, tannery operations and food processing wastewater, is a major source of environmental pollution (Cao et al., 2012; Moosa et al., 2002; Shin et al., 1997). Sulfate presence in the environment can affect public water supplies and pose health threat to life forms (Speece, 1996). In the absence of dissolved oxygen and nitrate, sulfate acts as a source of oxygen or electron acceptor and is converted to sulphide (H_2S). This phenomenon creates odor and corrosion problems (Sawyer et al., 2003). The recommended upper concentration limit of sulfate in water intended for human consumption is 250 mg/L (Sawyer et al., 2003). Therefore, it is essential to treat sulfate rich wastewater prior to its discharge into the environment.

Conventional physicochemical methods for treating sulfate rich wastewater have certain limitations such as need for solid-liquid separation, disposal of the solid phase and relatively high cost and energy consumption (Sarti and Zaiat, 2011). To overcome such limitations, focus has been shifted to biological sulfate removal using sulfate reducing bacteria (SRB). Under anaerobic conditions, sulfate can be used as a terminal electron acceptor by SRB that couple oxidation of a substrate (organic or inorganic) to the reduction of sulfate and use the energy produced for its growth and maintenance (Liamleam and Annachhatre, 2007). However, the process requires an external carbon and energy source, which is based on its suitability for the process and its availability at a reasonable cost (Dries et al., 1998). From the literature, it is understood that compared to simple alcohols (e.g. ethanol) and short chain volatile fatty acids (e.g. lactate, butyrate, propionate and acetate) H_2 is more attractive because of its free energy of sulfate reduction is highly favorable over that of methanogenesis (Weijma et al., 2002). However, the use of pure H_2 is neither feasible nor economical for

sulphate reduction, thus necessitating the use of much cheaper and easily available source of H_2. In this context, use of CO derived H_2 can be considered a very good alternative to pure H_2 (Parshina et al., 2010).

Proper design of bioreactor and its mode of operation is one of the main challenges for successful scale up of sulfate reduction process using CO as the sole carbon and energy source (Yasin et al., 2015; Parshina et al., 2010). The key parameters necessary while considering a suitable bioreactor are mainly related to CO gas-liquid mass transfer, which includes agitation speed, impeller design, power consumption, temperature, pressure conditions, bioreaction kinetics, etc. Both batch and continuously operated bioreactors have been employed for CO conversion to useful products, but very less literature reports are available on sulfate reduction using CO or any other gaseous substrate.

In this study, two bioreactor systems: suspended and attached growth reactor systems, namely gas lift reactor (GLR) and moving bed biofilm reactor (MBBR), were evaluated for their performance to remove sulfate by using CO as the sole carbon and energy source. The GLR is one of the most commonly used bioreactor for CO conversion owing to its proven advantages such as high gas liquid mass transfer without causing shear stress on the microorganism, mechanical simplicity and low energy requirement, etc. On the other hand biofilm based systems provides high biomass retention, high tolerance towards toxic substrates by having a layered biomass structure, etc. Moreover, the bed clogging problem faced by conventional biofilm reactors, viz. trickling bed reactor and/or packed bed reactor, can be overcome in a MBBR. The GLR and MBBR systems were chosen for this study as they are highly suited for processes with variable gas feeding requirements.

Hence, this study mainly focused on sulfate reduction and CO conversion using MBBR and GLR under different operating conditions and optimization of key process parameters,

namely hydraulic retention time (HRT), influent sulfate concentration and inlet CO concentration.

7.2 Materials and methods

7.2.1 Rector setup

7.2.1.1 Gas lift reactor

An indigenous internal loop gas lift reactor made of perspex material was evaluated for CO conversion to biohydrogen and sulfate reduction under continuous mode of operation. The effective volume of the reactor was 2.7 L with a removable draft tube located concentrically inside the reactor. For introducing CO into the reactor a single nozzle was placed at the bottom of the draft tube. The nozzle and the other parts used in fabricating the reactor were made of acrylic material. The gas flow into the reactor was measured and controlled by a rotameter with a needle valve. The schematic of the experimental set-up is shown in Fig. 7.1 and photographs of the reactor are shown in Fig. 7.2. The dimensions of the different reactor parts are presented in Table 7.1.

Table 7.1 Dimensions of the gas lift reactor used in this study

Reactor part	Dimension
External tube diameter	Outer dia: 90 mm Inner dia: 80 mm
Internal tube diameter	Outer dia: 60 mm Inner dia: 50 mm
External tube height	600 mm
Internal tube height	350 mm
Top clearance	15 mm
Bottom clearance	15 mm

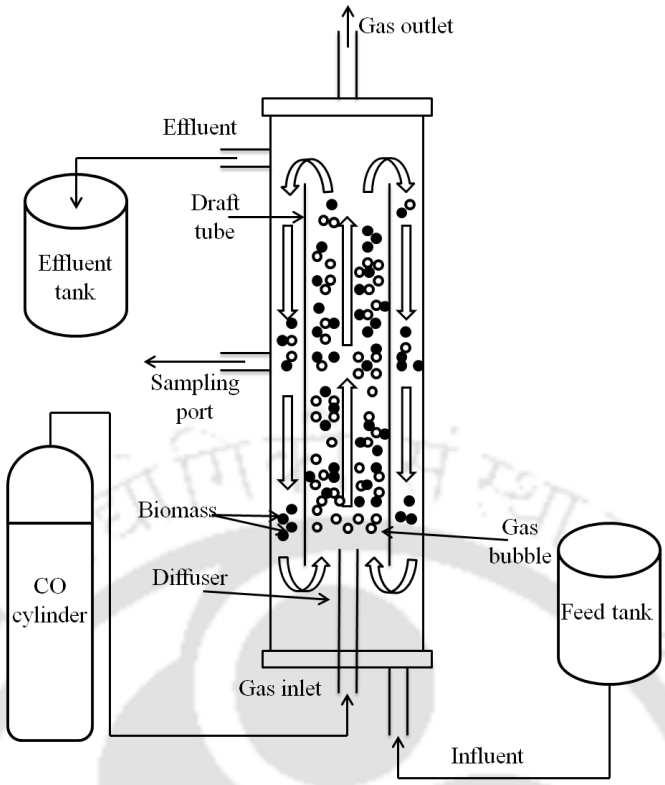

Fig. 7.1 Schematic of the gas lift reactor experimental setup.

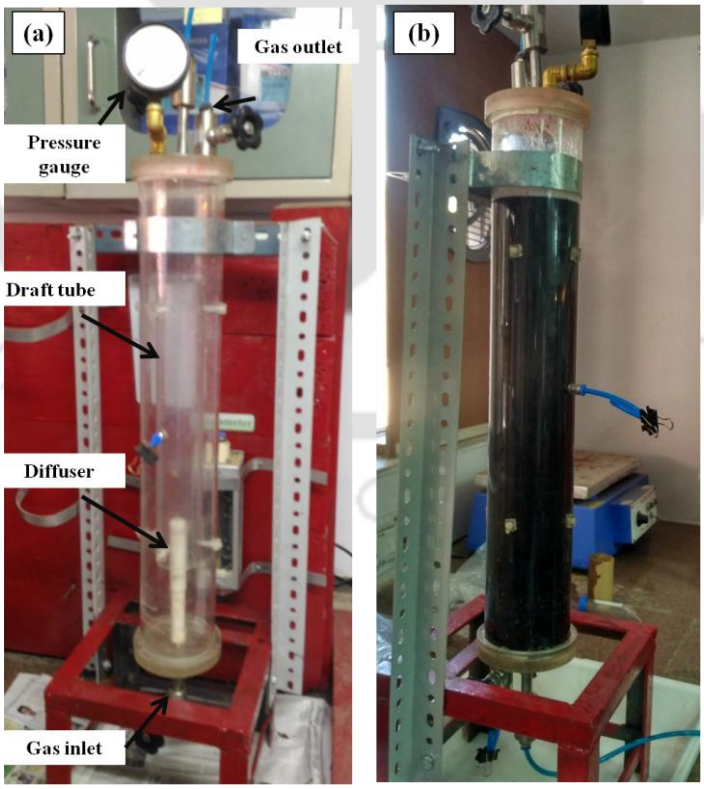

Fig. 7.2 Photograph of experimental setup showing (a) empty gas lift reactor and (b) reactor during continuous experiments.

7.2.1.2 Moving bed biofilm reactor

The MBBR was fabricated indigenously using perspex made column of 600 mm height and 10 mm thickness to evaluate the CO conversion and sulfate reduction under continuous mode of operation. The bioreactor had an effective volume of 2.7 L and a reaction volume of 2.5 L, with a nozzle type gas diffuser at the bottom for introducing CO into the reactor. The gas flow into the reactor was measured and controlled by a rotameter with a needle valve. The MBBR was filled with 20 mm × 20 mm × 10 mm size Kaldness K1 media as biosupport material at 30 % by volume. Provisions for introducing and withdrawing liquid media from the bottom and top, respectively, were made using peristaltic pump. The schematic of the experimental set-up and photographs of the reactor are shown in Fig 7.3 and 7.4, respectively.

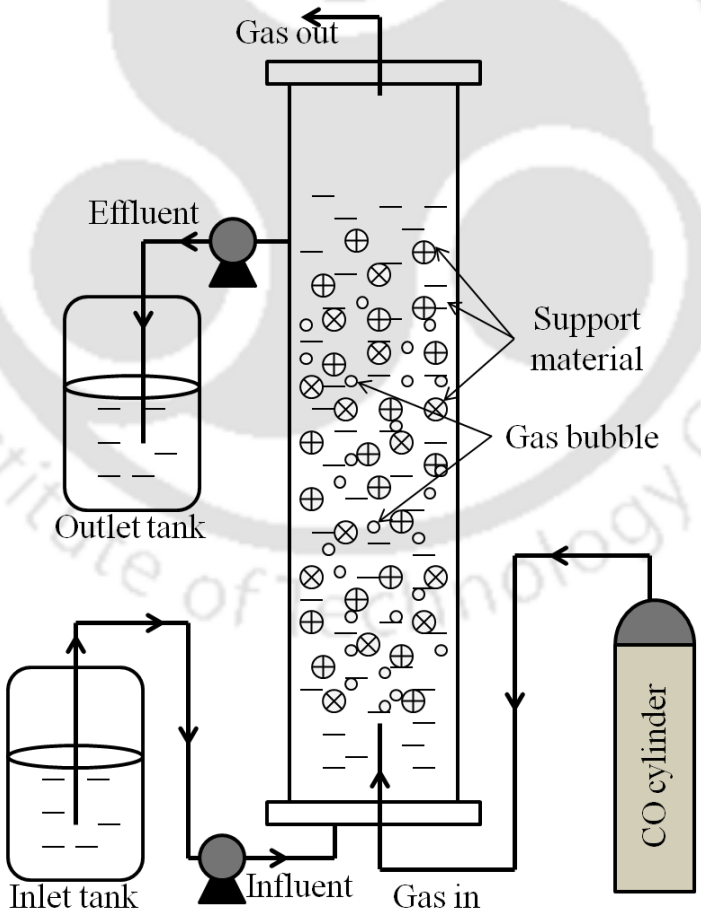

Fig. 7.3 Schematic of moving bed biofilm reactor experimental setup.

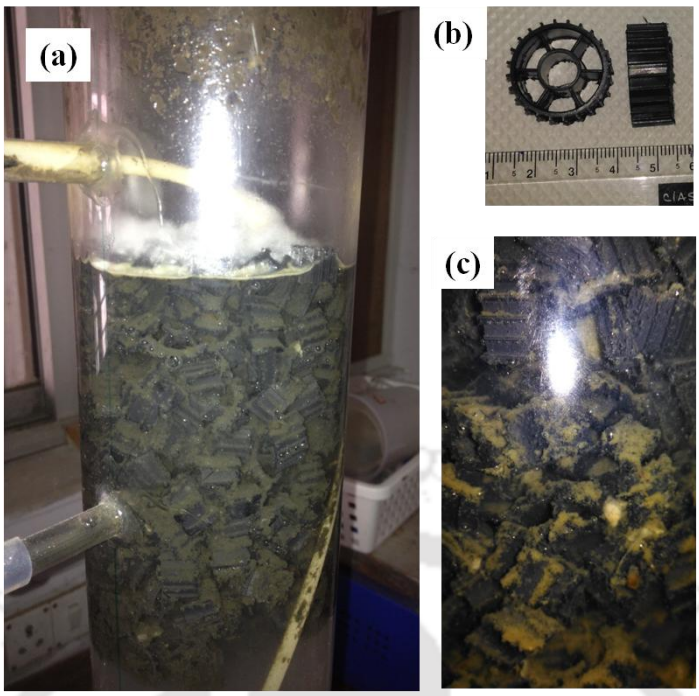

Fig. 7.4 Photograph of experimental setup showing (a) MBBR with the biosupport material, (b) empty biosupport material and (c) MBBR with biofilm formed on the biosupport material.

7.2.2 Startup operation and hydrogenogenic CO conversion

For initial biofilm development over the biosupport material, MBBR was operated with MSM supplemented with 1 g/L of lactate. In addition, CO was provided into the reactor at a low flowrate of 0.01 L/h to acclimatize the anaerobic sludge to grow and metabolize using CO as a substrate. For inoculum 250 ml of anaerobic biomass was directly added to the reactor prior to the startup operation. This startup operation was carried out for 30 days, following which the CO was used as the sole carbon source. The biofilm formed over the biosupport material was characterized using field-emission scanning electron microscopy (FESEM). The results were reported using CO as the sole carbon and energy source in the experiments. In case of GLR, there were no such startup operation required and experiments were immediately carried out with the anaerobic biomass for hydrogenogenic CO conversion.

The effect of inlet CO concentration on hydrogen production and CO utilization was studied at a fixed hydraulic retention time of 48 h using both the reactors. The inlet CO concentration

in the experiments was initially 9.06 mmol/L and it was gradually increased to 15, 21.5, 29 and 36 mmol/L. Composition of the MSM was the same as described in earlier chapter (Chapter 3). Samples were collected at regular time intervals to analyze gas composition and VFA concentration in the reactor outlet. The percentage CO conversion was calculated using the following equation (eq. 7.1)

$$\% \text{ CO conversion} = \frac{C_i - C_o}{C_i} \times 100 \quad \ldots\ldots\ldots\ldots (7.1)$$

where, C_i and C_o are the inlet and outlet CO concentrations (mmol/L), respectively.

7.2.3 Biological sulfate reduction using CO as the sole carbon source

For studying biological sulfate reduction using CO fed reactor under continuous operation mode, experiments were carried out in three phases (I, II and III) by varying hydraulic retention time (HRT), inlet sulfate concentration and CO flow rate, respectively. In the first phase, the HRT was varied from 72 h to 48 h and finally to 24 h, whereas the inlet sulfate concentration and CO concentration were kept constant at 250 mg/L and 15.0 mmol/L, respectively. In Phase II, the influent sulfate concentration was increased to 500, 750 and finally to 1000 mg/L, whereas the CO concentration and HRT were maintained at 15.0 mmol/L and 48 h HRT, respectively. For evaluating the effect of high inlet CO concentration at a high inlet sulfate concentration of 1000 mg/L in Phase III, the inlet CO concentration was first fixed at 21.5 mmol/L and later increased to 29 mmol/L. All these experimental conditions were same for both the reactors, but during Phase I (24 h HRT) of MBBR operation biofilm formed on the biosupport material got damaged and disintegrated, and due to which extra time was provided for the biofilm to recover and before the reactor could be further operated. Table 7.2 provides the experimental details followed during the continuous bioreactor operation. Each sample was analyzed in triplicate and the results presented are in mean± standard deviation format.

Table 7.2 Operating conditions followed for studying sulfate reduction and CO utilization using GLR and MBBR system

Operation period (d)		Phase	HRT (h)	Influent sulfate concentration (mg/L)	Inlet CO concentration (mmol/L)
GLR	MBBR				
1-17	1-12	I	72	250	15
18-33	13-22		48	250	15
34-48	23-30		24	250	15
-	31-41		48	250	15
49-63	42-51	II	48	500	15
64-76	52-65		48	750	15
77-89	66-77		48	1000	15
90-101	78-90	III	48	1000	21.5
102-114	91-106		48	1000	29.0

The following equations were used to calculate loading rate, removal rate and percentage removal of sulfate, respectively, in the study:

$$\text{Inlet loading rate (ILR)} = \frac{QC_i}{V} \quad \text{.....(7.2)}$$

$$\text{Removal rate (RR)} = \frac{Q(C_i - C_o)}{V} \quad \text{.....(7.3)}$$

$$\%\ \text{removal} = \frac{(C_i - C_o)}{C_i} \times 100 \quad \text{.....(7.4)}$$

where, Q is the inlet flow rate (L/h), C_i and C_o are the inlet and outlet sulfate concentrations (mg/L), respectively, and V is the working volume of the reactor.

7.2.4 Analytical methods

The gas composition at the inlet and outlet of the bioreactor was analyzed using a gas chromatograph (GC, Varian 450, The Netherlands) equipped with a thermal conductivity detector (TCD) and a molecular sieve column (Mole sieve 5A, mesh 80/100, 72 in × 1/8 in) using methods as described earlier in Chapter 3. Sulfate concentration was determined using

the standard barium chloride based turbidimetric method (APHA, 2005). Sulfide concentration in the samples was measured as per the method described by Cord-Ruwisch (1985). For volatile fatty acids (VFA) analysis hydroxylamine hydrochloride based spectrophotometric method was used (APHA, 2005). Detailed methodology of all these procedures was provided previously in Chapter 3.

7.3 Results and discussion

For a successful large scale application of biological sulfate reduction using CO, the choice of a suitable reactor system is essential. In the previous chapters CO conversion and sulfate reduction using anaerobic biomass from Kavoor STP under batch condition showed very promising results. In order to evaluate the performance of a bioreactor with the anaerobic biomass, a gas lift reactor and a moving bed biofilm reactor were chosen. The results obtained during continuous operation using both the reactors are presented herein.

7.3.1 Biofilm characterization

FESEM analysis was used to characterize biofilm formed over support materials in MBBR (Fig. 7.5) which clearly revealed profuse growth of the anaerobic bacteria onto the biosupport material. No efforts were made to measure the thickness or composition of the biofilm formed on support materials, which itself could be an independent study and could help in better understanding of the biofilm formation.

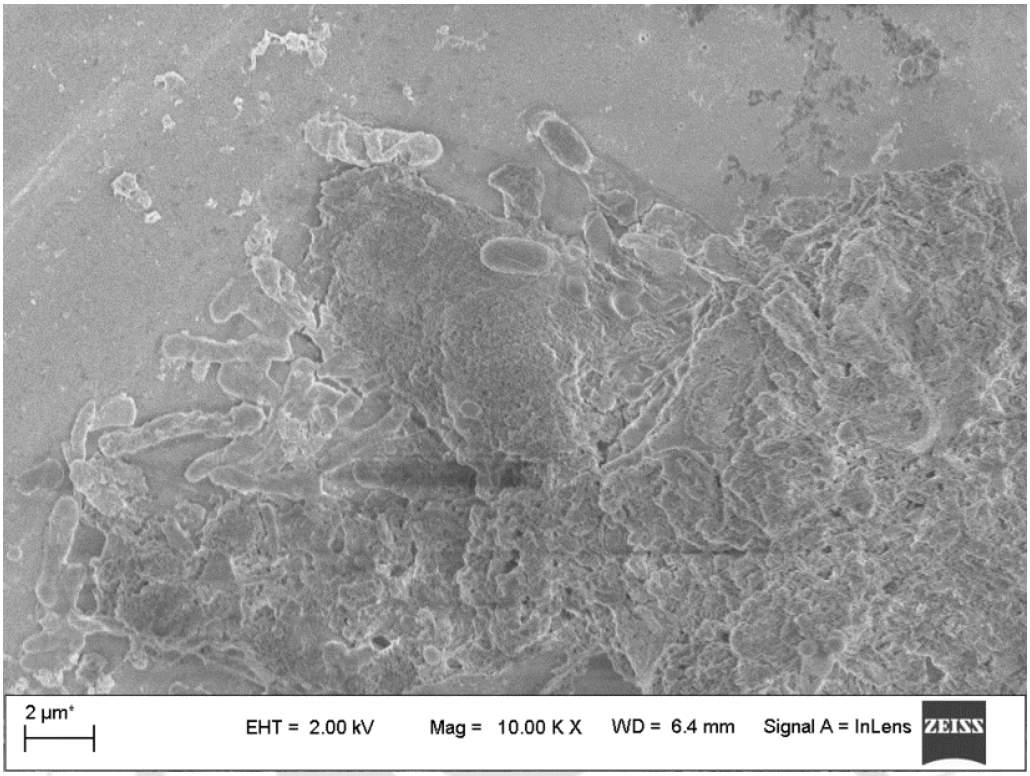

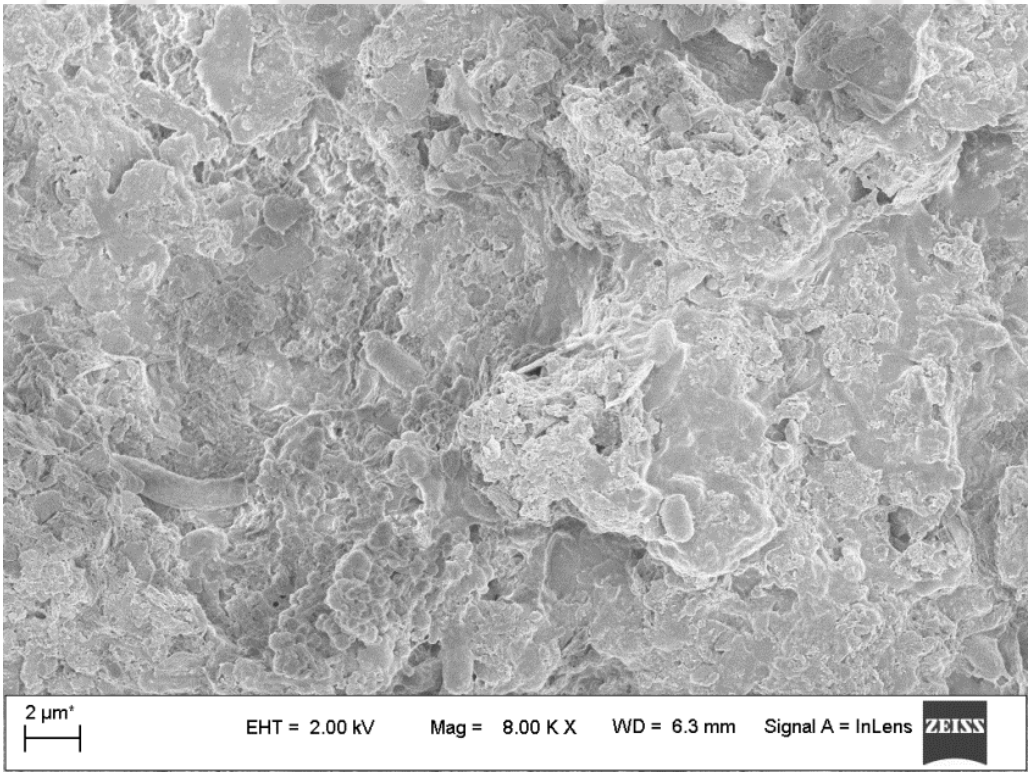

Fig. 7.5 FESEM images of the biofilm formed over biosupport material at its different positions.

7.3.2 Hydrogenogenic CO conversion

Initial experiments to study CO conversion to H_2 using GLR and MBBR were performed at different inlet CO concentrations and without any sulfate addition in the influent in order to avoid competition of H_2 by SBRs for sulfate reduction. In addition, methanogenic inhibitor BES was added in the media to prevent any methanogenic activity in the bioreactor systems.

Fig. 7.6 depicts the H_2 and VFA produced at different inlet CO concentrations for both the reactor systems. The H_2 concentration was initially low at 5.4 and 5.7 mmol/L for MBBR and GLR, respectively, for inlet CO concentration of 9.6 mmol/L. In case of GLR, the value gradually increased upto 7.6, 12.1, 15.6 and 20.5 mmol/L for 15, 21.5, 29 and 36 mmol/L of inlet CO concentrations, respectively (Fig. 6.6a). Similar observation was also made in the case of MBBR, which yielded H_2 concentration values of 5.6, 9.1, 13.25, 17.4 and 19.5 for the different inlet CO concentrations (Fig. 7.6b).

The VFA concentration was below 2 mg/L for the first 20 days of operating the GLR under hydrogenogenic phase and after which it ranged between 5 and10 mg/L; later it reached a maximum concentration of 20 mg/L towards the end of this phase. In case of MBBR, the VFA concentration gradually increased with an increase in inlet CO concentration until it reached 20 mg/L. However, the VFA concentration in both the reactor systems was significantly low than that reported in the literature for fermentative H_2 production using different soluble substrates. Moreover, due to BES addition in this study, no methane production was observed during the continuous operation at different inlet CO concentrations. These results clearly showed that the maximum carbon flux is directed towards H_2 production, without forming undesired products, such as VFA or CH_4, in this study.

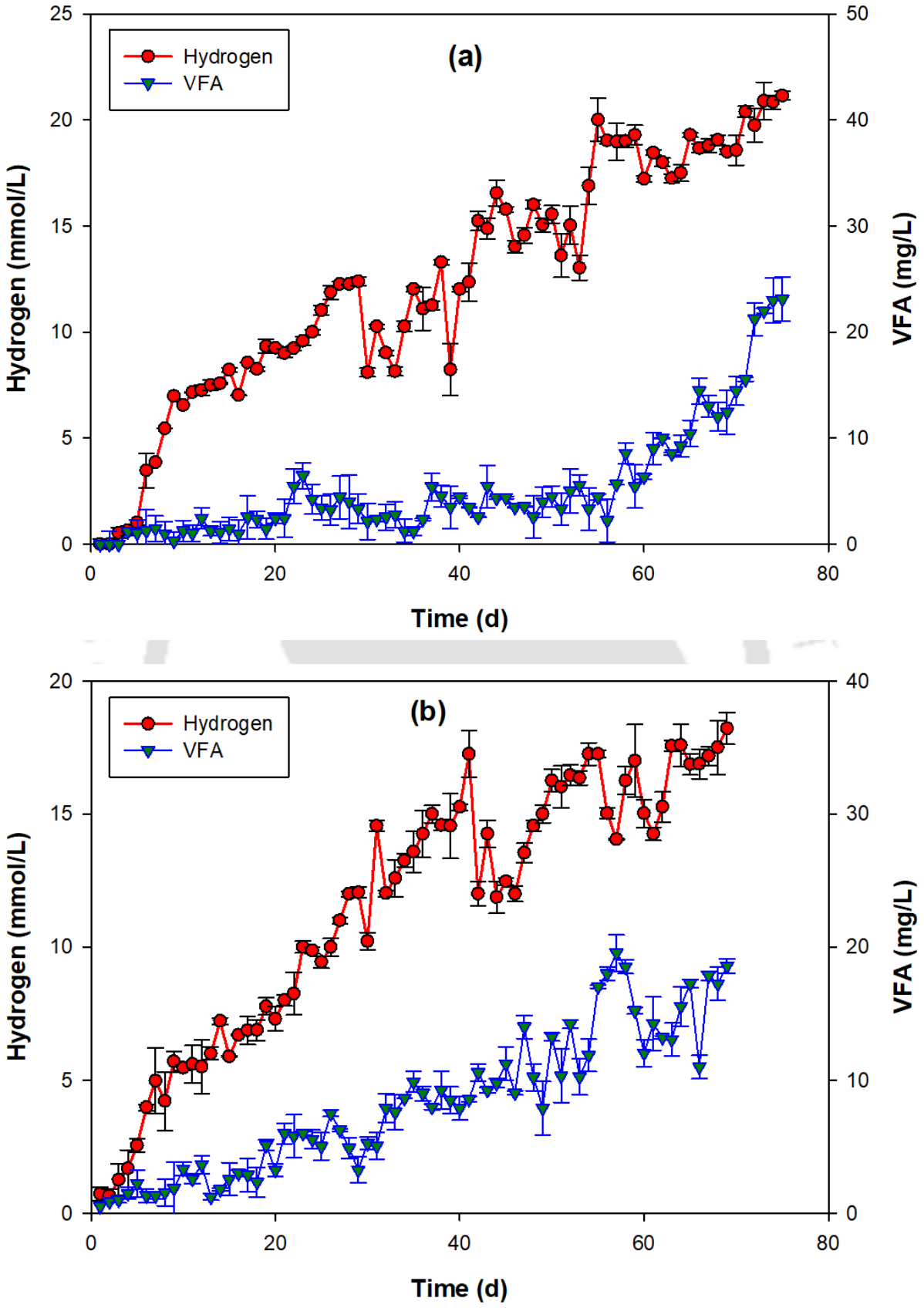

Fig. 7.6 Time profile of H_2 and VFA production from CO using the continuously operated (a) GLR and (b) MBBR.

Overall, the performance of both the reactor systems was satisfactory at all different inlet CO concentrations; however, GLR proved to be better in terms of H_2 production values compared to that of MBBR particularly at high inlet CO concentrations. On the contrary, MBBR performance was more stable than that of the GLR at low inlet CO concentrations, as high inlet flowrate resulted in turbulent mixing in the MBBR system leading to loss of attached biomass and biomass washout, which however could not be causing some of the attached biomass to be disintegrated.

Fig. 7.7 shows the CO concentration in inlet and outlet gas stream along with % CO conversion obtained using the continuously operated GLR and MBBR. The reactor operation was started with 9.05 mmol/L of influent CO concentration, in which the CO conversion rate was initially low at 52 and 65 % for GLR and MBBR, respectively, and the values gradually reached up to 92 and 95 %, respectively. The CO feed was then step wise increased to 15, 21.5, 29, and 36 mmol/L concentration. The % CO conversion decreased with each increase in the inlet CO concentrations and the values were 80, 73, 66 and 48 % for GLR, and for MBBR the values were 82, 72, 52 and 43% at different inlet CO concentrations. However, from the figure it is clear that the CO utilization profile was more stable in MBBR compared to GLR for most of the concentrations. The main reason behind this is high biomass retention capacity in MBBR, which contained both suspended and immobilized anaerobic biomass in the form of biofilm.

The reactor performance in terms of both CO conversion and H_2 production in this study is found to be better when compared with those reported in the literature. For example, Liu et al. (2016) investigated H_2 production using a UASB reactor with anaerobic granular sludge biomass, and reported only 38.8 % CO conversion even at a low CO loading of 45 mmol/d. With gas recirculation in the reactor, the CO conversion efficiency reached a maximum of

85.9 %. The H_2 concentration obtained in the outlet gas stream was also low compared to that obtained in the present study.

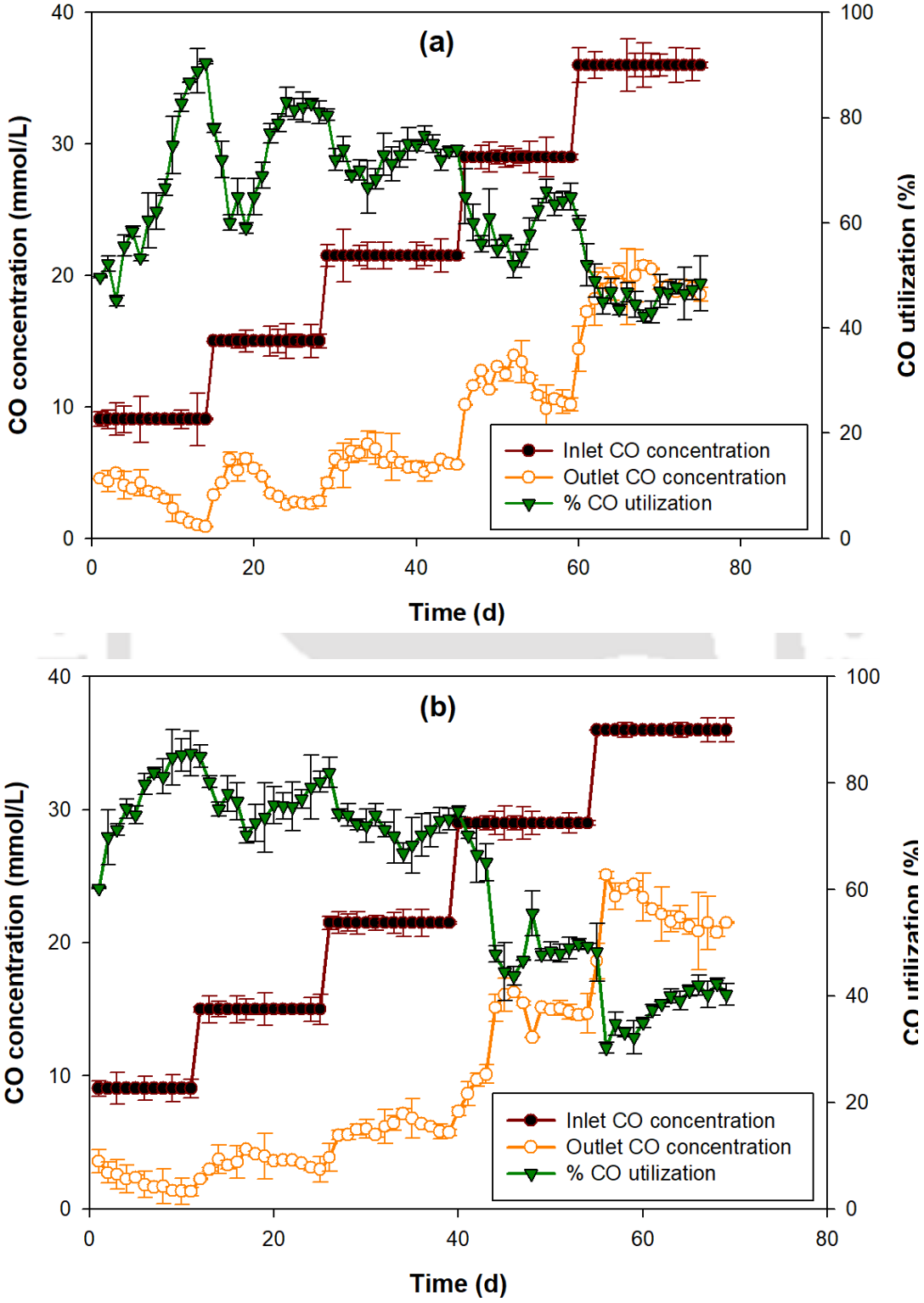

Fig. 7.7 Time profile of CO conversion at different inlet CO concentrations in the continuously operated (a) GLR and (b) MBBR.

7.3.3 Sulfate reduction

In order to study sulfate reduction in wastewater using CO as the sole carbon and energy source continuous experiments were carried out using the two reactor systems in three different phases, as detailed earlier. The effect of process parameters such as HRT (24-72 h), influent sulfate concentration (250-1000 mg/L) and inlet CO concentration (15-29) on sulfate reduction and CO bioconversion was examined.

Fig. 7.8 shows the time profile of influent/effluent sulfate concentration and % sulfate removal obtained in this study. During phase I of the reactor operation to study the effect of HRT, the influent sulfate concentration and inlet CO concentration were kept constant at 250 mg/L and 15 mmol/L, respectively. During this phase of the reactor operation at 72 h HRT a maximum sulfate removal efficiency of ~ 97.2 % and 95.6 % for GLR and MBBR, respectively, was achieved. When the HRT was reduced to 48 h, a sudden drop in the sulfate removal efficiency was observed; however the removal efficiency improved to more than 94 % in case of GLR within a time period of 16 days. When the HRT was further reduced to 24 h, the reactor performance deteriorated and the sulfate removal efficiency was only 62 %. In case of MBBR, the sulfate reduction efficiencies were 92.3 % and 78.5% for 48 and 24 h HRT, respectively. These results clearly reveal a significant effect due to HRT on the reactor performance for sulfate removal, which is mainly because of insufficient time available for the SRB to utilize the *in situ* produced H_2 at a low HRT value.

During phase II of the reactor operation to study the effect of influent sulfate concentration, the inlet CO concentration and HRT were kept constant at 15 mmol/L and 48 h, respectively. With an increase in the influent sulfate concentration, the sulfate reduction efficiency initially reduced but it gradually improved to reach 89.2 % and 85.66 % for GLR and MBBR, respectively (Fig. 7.8).

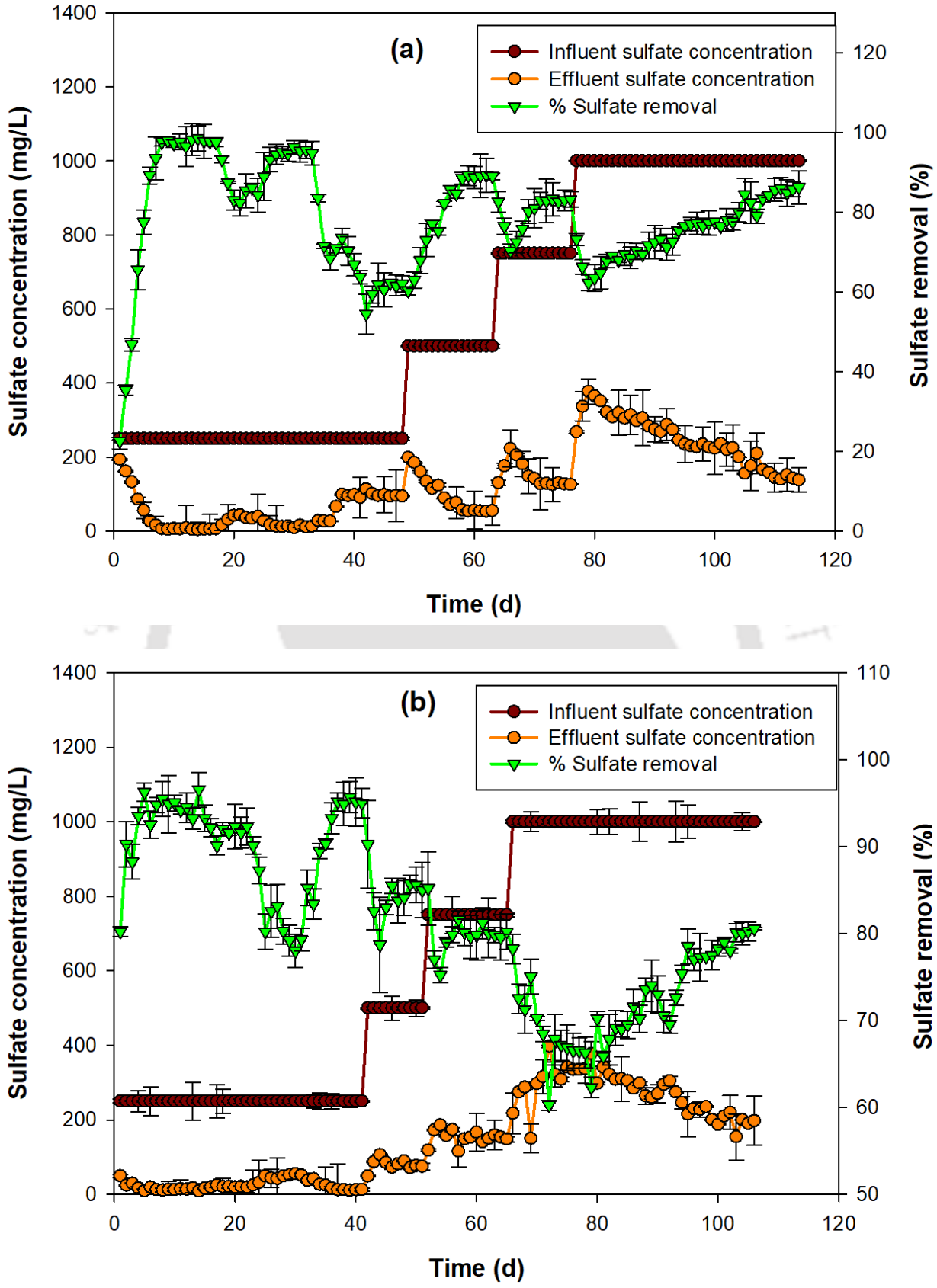

Fig. 7.8 Time profile of sulfate reduction in the continuously operated (a) GLR and (b) MBBR.

The sulfate concentration was further increased to 750 mg/L and reactor performance stabilized after 13 days with 83% sulfate reduction efficiency for GLR. Similarly, the sulfate reduction efficiency with the MBBR reached a stable value of 81.21 % but only after a prolonged period of operation, i.e. after 60 days. When the influent sulfate concentration was increased to 1000 mg/L, a very low sulfate removal efficiency was obtained in case of both the reactor systems, the values were 71.3 % and 66.5% for GLR and MBBR, respectively. During phase III, the reactor performance improved with an increase in the inlet CO concentration. Thus, the low sulfate removal obtained at very high influent sulfate concentrations during Phase II of the reactor operation is attributed to the excess amount of sulfate in relation to CO amount in the reactor, i.e., a low CO to sulfate ratio resulted in the poor performance of the bioreactor system. At 1000 mg/L influent sulfate concentration and 48 h HRT, the sulfate reduction efficiency gradually increased with an increase in the CO flow rate and the value was ~ 77 % for GLR, whereas for MBBR it was 74.5%. The sulfate removal efficiency further increased to 86.2 % and 81.7 % for GLR and MBBR, respectively, with an increase in inlet CO concentration to 29 mmol/L.

Fig. 7.9 shows the value of inlet and outlet CO concentration along with CO conversion efficiency during the continuous experiments using MBBR and GLR. The inlet CO concentrations was the same during the first two phases of the study but some variation in the CO utilization and outlet CO concentration could be seen from the figure. However, variations in the CO utilization were minimum and ranged between 80 and 95 % with both the bioreactors, which indicates a superior capability of the anaerobic biomass to utilize CO at a low inlet concentration. During the later phase (Phase III) of the reactor operation, an increase in the inlet CO concentration upto 29 mmol/L slightly lowered the CO utilization from 75 % and 71 % for GLR and MBBR, respectively. This could be attributed to the reduced CO gas residence time in the reactor with increase in the inlet CO flow rate.

However, H_2 produced from CO, even at a high inlet CO concentration was sufficient for sulfate removal from the inlet stream (Fig. 7.8). Thus, it could be concluded that among the different process parameters - HRT, inlet sulfate and CO concentrations, the effect due to inlet CO concentrations in the bioreactor system was highly significant on continuous CO utilization by the anaerobic biomass.

The results of CO conversion and sulfate reduction obtained in this study are in agreement with those reported in the literature (Sipma et al., 2007; van Houten et al., 2009; van Houten et al, 1996). For example, Sipma et al. (2007) reported a stable sulfate reduction of 17 mmol/L/d using a CO fed gas lift bioreactor operated at an elevated temperature of 50-55 °C. The authors found that lowering the HRT reduced the chance of H_2 utilization for methane production. Contrary to this literature report, a low HRT of 24 h is found to be detrimental to sulfate reduction in this study, which could be due to a low rate of H_2 formation under mesophillic condition. Hence, a slightly high HRT required for sulfate reduction with CO as the substrate when using mesophillic microorganisms in continuously operated bioreactor.

Hao et al. (2014) reviewed the utility of pure H_2, CO derived H_2, mixture of CO/H_2 for continuous sulfate reduction with the main advantage that no organic residual is present in the reactor effluent. On the other hand, major disadvantages with these substrates are CO toxicity and poor mass transfer of both CO and H_2. However, these drawbacks were not seen in the present study, as the bioreactor was mostly operated at a low CO flow rate that is well below its inhibitory limits. Also, it is reported in the literature that granular biomass and layered biofilm structures are highly resistant towards toxic substrates as different classes of bacteria could proliferate at different layers inside the biomass structure. Hence, it could be well said that the bioreactor systems with anaerobic biomass used in the study were highly efficient in

treating sulfate rich wastewater via *in situ* produced H_2 from CO under continuous loading condition.

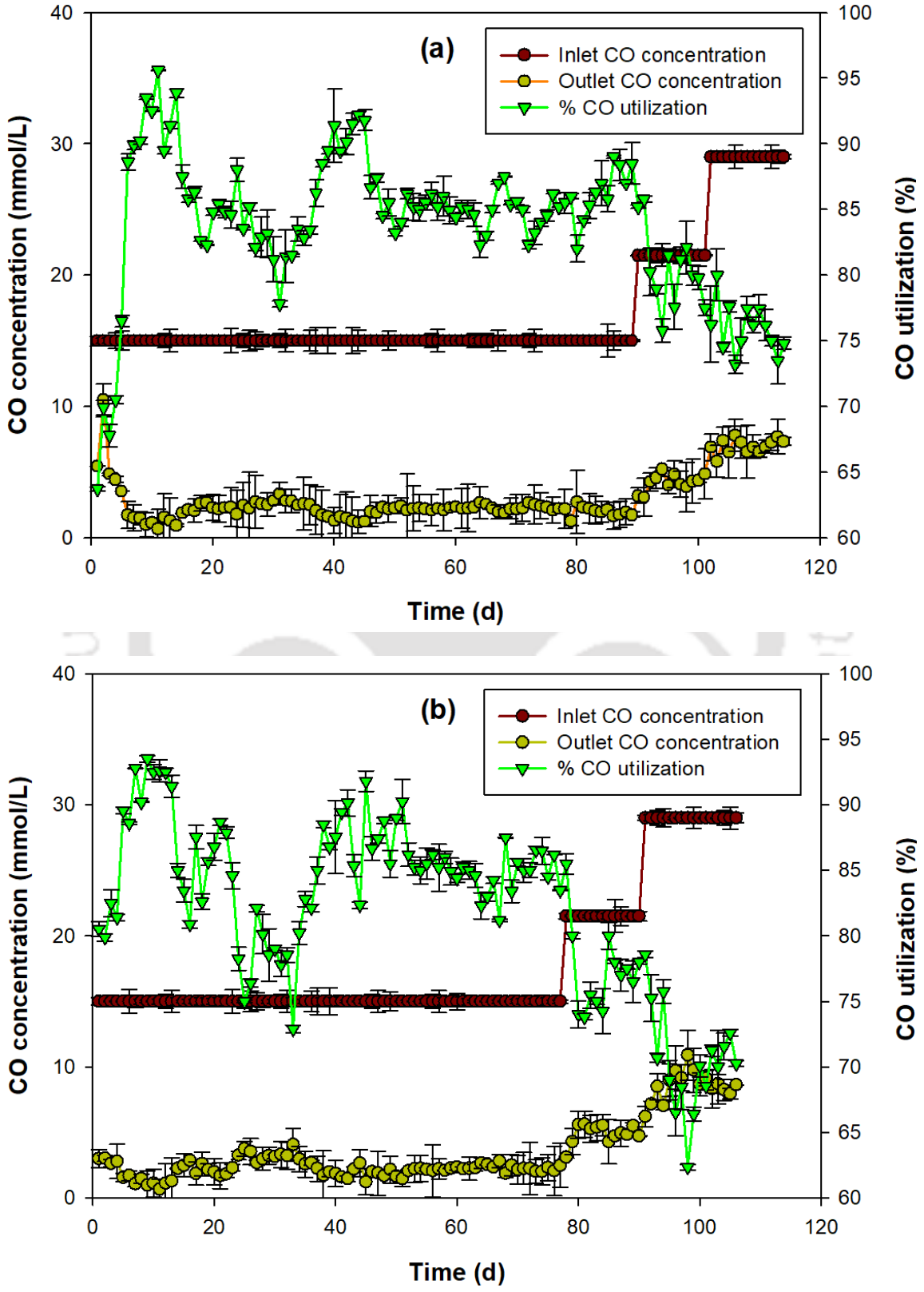

Fig. 7.9 Time profile of CO conversion in the continuously operated (a) GLR and (b) MBBR.

Fig. 7.10 depicts the soluble sulfide and VFA concentrations during the different phases of the bioreactor operation. The VFA concentration was initially around 2.5-5.0 mg/L probably due to incomplete conversion of CO. However, in case of GLR, VFA production increased to ~10 mg/L at a the later time period of the Phase I of reactor operation. Further increase in the influent sulfate concentration during Phase II operation lowered the VFA production to around 5.0-6.0 mg/L. In case of MBBR, the VFA concentration was low (< 5 mg/L) during the initial two phases probably due to a high biomass activity; only during the last phase when substrate (CO) concentration was in excess the amount reached nearly 20 mg/L. Similarly, in case of GLR, when the CO flow rate was increased during Phase III, VFA concentration increased to almost 19.3 mg/L. This is mainly due to the high amount of H_2 and CO_2 produced in this phase; high VFA production often occurs due to homoacetogenic bacteria present in the anaerobic biomass. However, compared with other literature reports the overall VFA concentration was quite low in this study.

A low VFA concentration profile during the continuous bioreactor operation is also attributed to the high inlet sulfate concentration in the reactor to the available CO as it is known that sulfate reduction at a high sulfate concentration requires additional carbon source such as VFA other than the *in situ* produced H_2 from CO (Ozuolmez et al., 2015; Sánchez-Andrea et al., 2014).

Soluble sulfide concentration profile shown in Fig. 7.10 correlated well with the inlet sulfate concentration and sulfate reduction efficiency. Low effluent soluble sulfide concentrations of 28, 42.5, 51.3 mg/L were observed during Phases I, II and III, respectively in case of GLR. The soluble sulfide values were 22, 33.5 and 42 mg/L for MBBR during three different phases for reactor operation. These results strongly suggest that the sulfate was mostly converted to gaseous sulfide (e.g H_2S) that escaped along with the exit gas stream from the bioreactor systems.

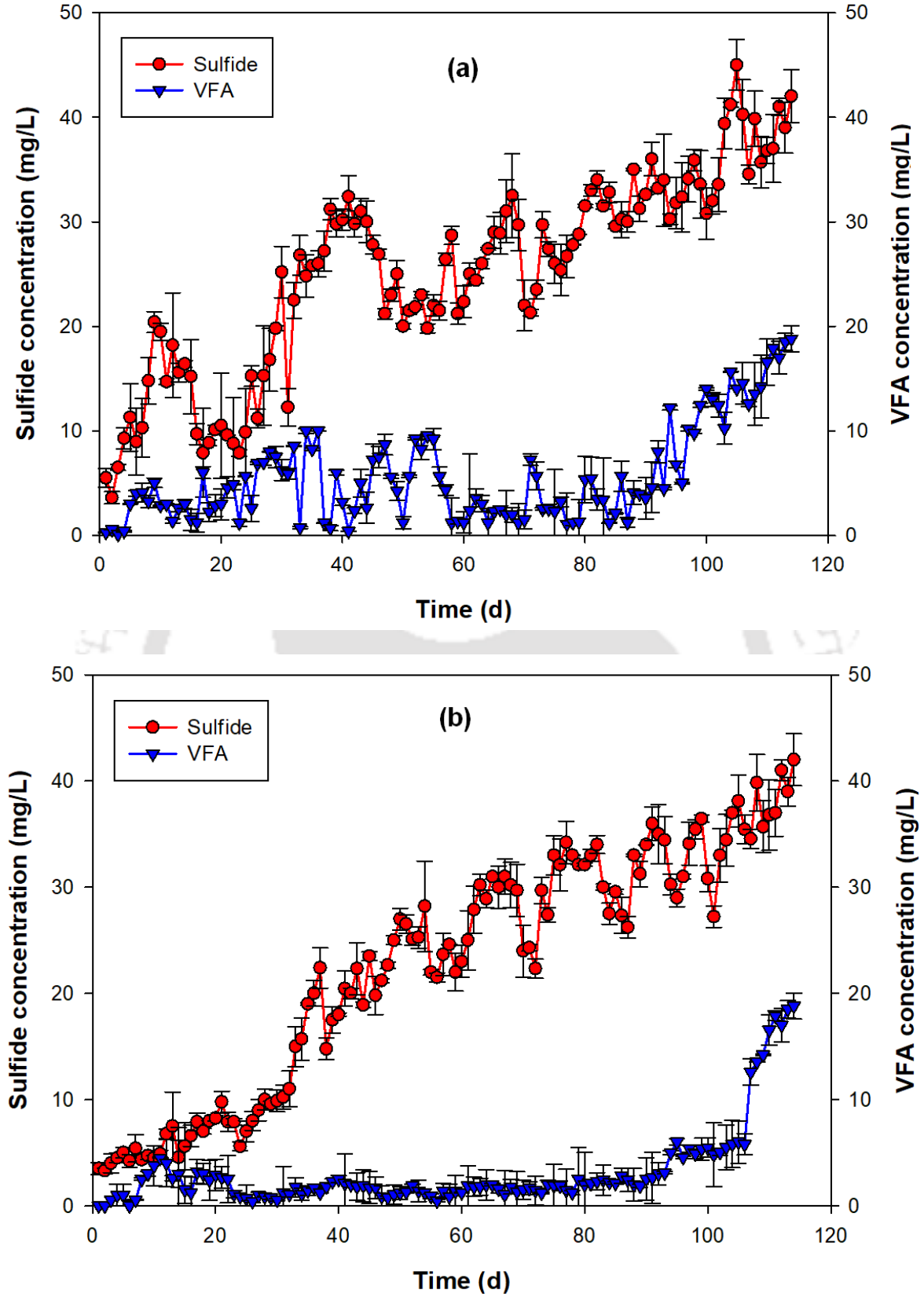

Fig. 7.10 Continuous profile of dissolved sulfide and VFA production during the different phases of reactor operation using (a) GLR and (b) MBBR.

Fig. 7.11 shows the performance of the continuously operated bioreactor systems in terms of sulfate removal rate with respect to different sulfate loading rates. The line passing through the origin of the figure indicates a stable performance of the system at different input conditions. It can be seen from the figure that at low sulfate loading rates of 3.42, 5.21 and 10.42 mg/L/h, sulfate removal rates were stable for both the reactors. However, at a loading rate above 10.42 mg/L/h, sulfate removal rate values were offset from the line passing through the origin indicating that sulfate loading rates beyond this point are inhibitory to the reactor performance. Therefore, in order to achieve satisfactory performance, it is desirable to operate the bioreactor at less than 10.42 mg/L/h sulfate loading rate. Sipma et al. (2007) achieved sulfate reduction rate as high as 17 mmol/L/d in a CO fed gas lift rector with thermophilic biomass and at a 3 h HRT. These results indicate that very high sulfate removal rate could be achieved with CO using the GLR system with the anaerobic biomass.

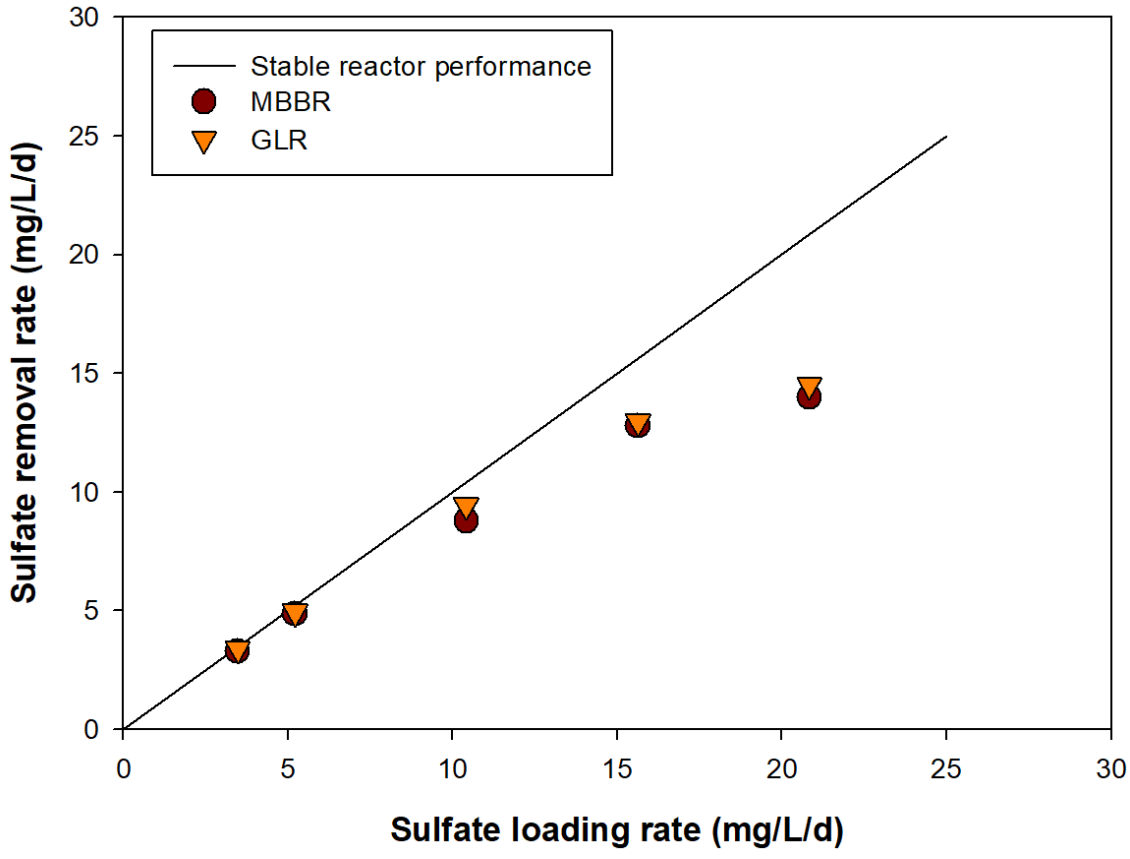

Fig. 7.11 Sulfate reduction rate as function of inlet sulfate loading rate in the bioreactors.

7.4 Significant findings

Continuous CO bioconversion was studied using two different bioreactor systems: a GLR with suspended anaerobic biomass and a MBBR with both attached and suspended anaerobic biomass. Both the reactors showed stable performance in terms of hydrogenogenic CO conversion for different inlet CO concentration. However, GLR was slightly better in terms of H_2 production and CO utilization, particularly at high inlet CO concentrations. With increase in the inlet CO concentration the H_2 production increased for both the reactors, however, the CO conversion efficiency reduced.

Similar to the hydrogenogenic CO conversion 48 h HRT yielded the maximum sulfate removal efficiency with both GLR and MBBR. Best results in term of sulphate reduction were however obtained at low inlet sulfate concentration and high CO loading conditions with both the bioreactor systems. The GLR performance was from the MBBR for both sulfate reduction and CO utilization; however, due to high biomass retention, MBBR performance was more stable than that of GLR, which contained only the suspended biomass. Overall, this study demonstrated scale up potential of the MBBR system for continuous CO bioconversion, which has not been reported so far in the literature.

Chapter 8

Summary and conclusions

Syngas, contains a rich amount of CO and it is an excellent feed stock for producing a wide range of useful chemicals such as ethanol, methanol, hydrogen, acetate, acetone, diesel, etc. The conventional methods for CO conversion to useful products rely on thermochemical-catalytic processes. But, disadvantages such as very high operating cost, limited choice of metallic catalyst, perishable nature of the catalyst, high energy requirement, etc. have led to the search for alternative, sustainable and green methods such as biological conversion. Carboxydotrophic bacteria and archia are not only able to grow on CO but can also convert CO into biohydrogen and other commercially important compounds such as ethanol, butanol, acetic acid methane, etc. However, application of CO bioconversion to hydrogen and its application in reductive processes, e.g. biological sulfate reduction, is less known. Sulfate rich wastewater generated by various industries needs to be treated prior to its discharge into environment owing to its serious environmental health effects. Biological sulfate reduction by sulfate reducing bacteria requires an efficient and cheap carbon source and electron donor. In this context, CO or CO rich syngas could be very useful from the perspective of wastewater treatment and recovery of resources. Hence, this study is focused on biological CO conversion to H_2 and environmental applications.

Initially, the inherent capability of anaerobic biomass from five different sources to utilize CO as the sole carbon source was examined. These different anaerobic biomass were screened for their ability to utilize CO at pH 7 and temperature 30^{o}C. The results revealed that among the five different sources three anaerobic granular sludge biomass form large scale UASB plant treating sewage were capable of converting CO to methane and carbon dioxide as the main products along with small amount of hydrogen. Addition of 2-bromoethanosulfonate in the media completely inhibited hydrogenotrophic methanogenesis activity of the biomass and resulted in considerable increase in the final H_2 concentration. The effect of initial CO concentration, temperature, inoculum size and biomass pretreatment

on CO conversion and sulfate reduction using anaerobic biomass revealed maximum CO utilization and sulfate reduction with the raw anaerobic biomass. Metagenomic analysis of the anaerobic biomass showed that bacteria were present in the anaerobic biomass that belonged to *Methanomicrobia, Clostridia, Acidobacteria, Gammaproteobacter, Bacteroidia* classes; moreover bacteria belonging to *Desulfovibrio* sp. were present which were responsible for sulfate reduction using CO. Lack of any known CO relating sequences was attributed to the presence of large unknown hydrogenogenic CO-utilizing mesophilic bacteria, as specified by the high percentage of unclassified sequences in the anaerobic biomass.

Detailed kinetics of CO conversion by anaerobic biomass at different initial CO concentrations revealed an efficient utilization of CO as the sole substrate for biohydrogen production. However, the CO utilization reduced, whereas, H_2 production increased with increase in initial CO concentration. Both the CO utilization and H_2 production were best described by using the modified Gompertz kinetic model. The specific CO utilization rate and specific biomass growth rate profiles were well fitted to different substrate inhibition kinetic models and the best fit was obtained using Edward and Aiba model, respectively, these two parameters. The results revealed that increase in initial CO concentration above 3.1 mmol/L of CO is inhibitory to both specific CO utilization and specific biomass growth. The biokinetic parameters from these models showed that CO as a substrate did not strongly promote the growth of the anaerobic biomass, but it leads to formation of intermediate products, such as H_2. From, the results obtained in this study it was further confirmed that a high H_2 concentration value is inhibitory to H_2 production and biomass growth, and the inhibition kinetics due to H_2 was best described using the modified Han-Levenspiel model. Based on these kinetic studies, it was suggested that H_2 production in a CO fed bioreactor should be carefully monitored so as to recover the product as soon as it is produced in the

system. Moreover, the H_2 production could be coupled with an immediate H_2 utilization step, such as sulfate reduction using CO as the sole carbon source, in order to avoid H_2 accumulation in the system.

Simultaneous heavy metal removal and sulfate reduction with CO as the sole carbon and energy source was achieved using the anaerobic biomass. The heavy metal removal efficiency values closely followed the solubility product values of the individual metal sulfides. The metal removal mechanism was confirmed to be due to formation of insoluble metal sulfide precipitates using different instrumental techniques such as FTIR, FESEM-EDX and FETEM. However, the presence of heavy metal was found to both CO utilization and sulfate reduction by anaerobic biomass. Among the different metals tested Pb showed a maximum negative impact due to its well known toxicity towards microorganisms including SRBs present in anaerobic biomass.

The effect of iron nanoparticle (GT-INP) synthesized using green tea extract on CO solubility and hydrogenogenic CO conversion was further studied. Characterization of the GT-INP revealed spherical or semi spherical shaped aggregated nanoparticle with a size in the range between 50-90 nm. By FTIR analysis, presence of active compounds such as amide, hydroxyl, flavonoids, alkaloids and polyphenols, etc. from green tea extract over GT-INP was confirmed. The enhancement in CO aqueous solubility due to addition of GT-INP was mainly due to 'grazing effect' by which small-sized particle enhanced gas-liquid mass transfer by repetitive adsorption and desorption of gas bubbles on the particles. Compared with previous studies reported in the literature on using nanoparticles for CO-water mass transfer enhancement, this study demonstrated for the first time the utility of biologically synthesized nanoparticle for enhancing aqueous solubility of CO. Biohydrogen production and sulphate reduction profile with nanoparticle addition were found to be higher when compared with the

results obtained without nanoparticle addition in the media. The mechanism of action was attributed to an improved bioavailability of CO to the anaerobic biomass.

Finally, in order to examine the scale up potential of the CO bioconversion process two bioreactor systems, namely an internal loop GLR and a MBBR, were used. The results showed that the H_2 production gradually increased with an increase in the inlet CO concentration for both the bioreactor systems. However, The CO utilization profile reduced due to low CO residence time at a high inlet CO concentration. Production of volatile fatty acids, mainly acetate, was also observed in the bioreactor systems; however, the VFA concentration in the effluent was low and it did not affect the biohydrogen production from CO.

Using the two bioreactor systems, best results in terms of sulfate reduction using CO as the sole carbon source were obtained for low inlet sulfate, high CO loading conditions and a minimum HRT of 48 h. The CO utilization was mostly unaffected during the continuous bioreactor operation, but at a high inlet CO concentration the CO utilization was slightly low. It was observed that the sulfide produced due to sulfate reduction in the bioreactor systems was in gaseous form, which, therefore, needs to be removed from the exit gas stream before releasing it into the environment. Compared to MBBR the GLR performance was better at high loading conditions; however, the MBBR showed more stable performance over the different operating conditions, indicating its application for large scale CO bioconversion. Overall, this study demonstrated the excellent potential of the indigenous mesophilic anaerobic biomass for not only CO conversion to H_2 but also for environmental applications such as sulfate reduction and heavy metal removal from wastewater.

The industrial scale application of such CO utilizing organisms for biological sulfate reduction has not been demonstrated yet, and therefore, it could be adopted by industries such as coal, thermal power stations and oil-natural gas reforming industries for treating sulfate

containing waste streams by utilizing CO-rich synthesis gas or other waste gases as wastewater from these industries are generally low in chemical oxygen demand and require the addition of organic matter or carbon source for effective sulfate removal, synthesis gas produced by these industries can, therefore, serve as an inexpensive substitute to other carbon source for biological sulfate reduction. Moreover, the operational costs involved could be greatly reduced in case of on-site production of synthesis gas from coal, thus minimizing the transportation costs involved. Fig. 8.1 shows a proposed scheme of process outline for biological sulfate reduction using CO in such industries.

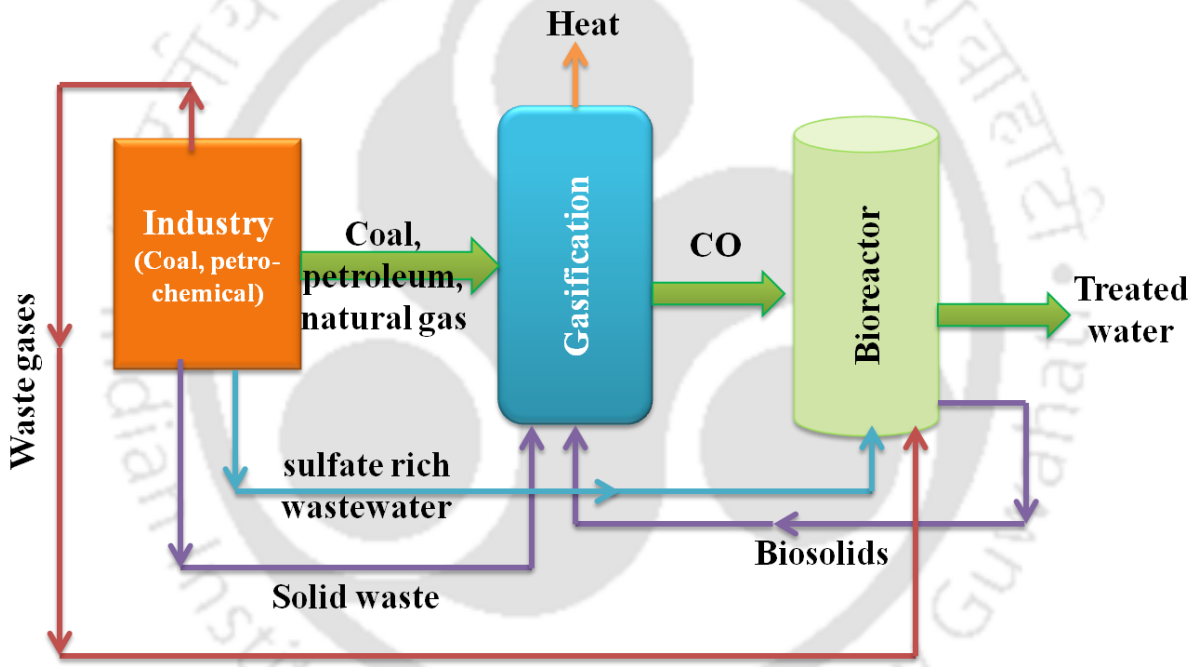

Fig. 8.1 Schematic showing a proposed process outline for biological sulfate reduction using CO.

In addition to the above, following are some more suggestions for future work based on this thesis:

1) Genetic engineering or metabolic engineering of the CO utilizing anaerobic biomass for enhancing the biohydrogen production

2) Scaled up of the MBBR system to treat sulfate rich wastewater using CO rich syngas as the substrate
3) Long-term reactor performance prediction using machine learning techniques such as artificial neural networks
4) Techno-economic feasibility of the CO bioconversion to H_2 and its environmental applications

Bibliography

- Abubackar, H. N., Fernández-Naveira, Á., Veiga, M. C. and Kennes, C. (2016) Impact of cyclic pH shifts on carbon monoxide fermentation to ethanol by *Clostridium autoethanogenum*. *Fuel*, *178*, 56-62.
- Abubackar, H. N., Veiga, M. C. and Kennes, C. (2011) Biological conversion of carbon monoxide: rich syngas or waste gases to bioethanol. *Biofuels, Bioproducts and Biorefining*, 5(1), 93-114.
- Abubackar, H. N., Veiga, M. C. and Kennes, C. (2012) Biological conversion of carbon monoxide to ethanol: effect of pH, gas pressure, reducing agent and yeast extract. *Bioresource Technology*, 114, 518-522.
- Abubackar, H. N., Veiga, M. C. and Kennes, C. (2015) Carbon monoxide fermentation to ethanol by *Clostridium autoethanogenum* in a bioreactor with no accumulation of acetic acid. *Bioresource technology*, *186*, 122-127.
- Adams, M. W. (1990) The structure and mechanism of iron-hydrogenases. *Biochimica et Biophysica Acta (BBA)-Bioenergetics*, *1020*(2), 115-145.
- Aghbashlo, M., Tabatabaei, M., Dadak, A., Younesi, H. and Najafpour, G. (2016) Exergy-based performance analysis of a continuous stirred bioreactor for ethanol and acetate fermentation from syngas via Wood–Ljungdahl pathway. *Chemical Engineering Science*, *143*, 36-46.
- Ahmed, A., Cateni, B. G., Huhnke, R. L. and Lewis, R. S. (2006) Effects of biomass-generated producer gas constituents on cell growth, product distribution and hydrogenase activity of *Clostridium carboxidivorans* P7T. *Biomass and Bioenergy*, *30*(7), 665-672.
- Ahmed, A. and Lewis, R. S. (2007) Fermentation of biomass-generated synthesis gas: Effects of nitric oxide. *Biotechnology and Bioengineering*, *97*(5), 1080-1086.
- Alauddin, Z. A. B. Z., Lahijani, P., Mohammadi, M. and Mohamed, A. R. (2010) Gasification of lignocellulosic biomass in fluidized beds for renewable energy development: A review. *Renewable and Sustainable Energy Reviews*, 14(9), 2852-2862.
- Ail, S. S. and Dasappa, S. (2016) Biomass to liquid transportation fuel via Fischer Tropsch synthesis–technology review and current scenario. *Renewable and sustainable energy reviews*, *58*, 267-286.
- Alves, J. I. van Gelder, A. H. Alves, M. M. Sousa, D. Z. and Plugge, C. M. (2013) *Moorella stamsii* sp. nov., a new anaerobic thermophilic hydrogenogenic carboxydotroph isolated from digester sludge. *International journal of systematic and evolutionary microbiology*, 63(11), 4072-4076.
- Alonso, D. M., Bond, J. Q. and Dumesic, J. A. (2010) Catalytic conversion of biomass to biofuels. *Green Chemistry*, *12*(9), 1493-1513.
- APHA, (1995) Standard Methods for the Examination of Water and Wastewater, 19th edn. American Public Health Association, Washington, DC. Ayres, R.U.,
- Ayres, E. H. (2009) Crossing the energy divide: moving from fossil fuel dependence to a clean-energy future. Pearson Prentice Hall. New Jersey.
- Bahmanyar, A., Khoobi, N., Mozdianfard, M. R. and Bahmanyar, H. (2011) The influence of nanoparticles on hydrodynamic characteristics and mass transfer

performance in a pulsed liquid–liquid extraction column. *Chemical Engineering and Processing: Process Intensification*, *50*(11-12), 1198-1206.

- Bai, H., Han, Y., Kang, Y. and Sun, J. (2013) Removal of Cu (II) and Fe (III) from aqueous solutions by dead sulfate reducing bacteria. *Frontiers of Chemical Science and Engineering*, *7*(2), 177-184.
- Balasubramanian, C., Joseph, B., Gupta, P., Saini, N. L., Mukherjee, S., Di Gioacchino, D. and Marcelli, A. (2014) X-ray absorption spectroscopy characterization of iron-oxide nanoparticles synthesized by high temperature plasma processing. *Journal of Electron Spectroscopy and Related Phenomena*, *196*, 125-129.
- Ballesteros, M., Oliva, J. M., Negro, M. J., Manzanares, P. and Ballesteros, I. (2004) Ethanol from lignocellulosic materials by a simultaneous saccharification and fermentation process (SFS) with *Kluyveromyces marxianus* CECT 10875. *Process Biochemistry*, *39*(12), 1843-1848.
- Beckers, L., Hiligsmann, S., Lambert, S. D., Heinrichs, B. and Thonart, P. (2013) Improving effect of metal and oxide nanoparticles encapsulated in porous silica on fermentative biohydrogen production by Clostridium butyricum. *Bioresource Technology*, *133*, 109-117.
- Bender, G., Pierce, E., Hill, J. A., Darty, J. E. and Ragsdale, S. W. (2011) Metal centers in the anaerobic microbial metabolism of CO and CO_2. *Metallomics*, 3(8), 797-815.
- Berzin, V., Kiriukhin, M. and Tyurin, M. (2012) Selective production of acetone during continuous synthesis gas fermentation by engineered biocatalyst *Clostridium* sp. MAceT113. *Letters in applied microbiology*, 55(2), 149-154.
- Blanco-Andujar, C., Ortega, D., Pankhurst, Q. A. and Thanh, N. T. K. (2012) Elucidating the morphological and structural evolution of iron oxide nanoparticles formed by sodium carbonate in aqueous medium. *Journal of Materials Chemistry*, *22*(25), 12498-12506.
- Bredwell, M. D. and Worden, R. M. (1998) Mass Transport Characteristics of Microbubbles: Experimental Studies. *Biotechnol. Prog.* 14 (1), 31-28.
- Bredwell, M. D., Srivastava, P. and Worden, R. M. (1999) Reactor design issues for synthesis-gas fermentations. *Biotechnology progress*, *15*(5), 834-844.
- Bredwell, M. D., Telgenhoff, M. D., Barnard, S. and Worden, R. M. (1997). Effect of surfactants on carbon monoxide fermentations by *Butyribacterium methylotrophicum*. *Applied Biochemistry and Biotechnology*, *63*(1), 637-647.
- Breen, J., Meunier, F. and Ross, J. H. (1999) Mechanistic aspects of the steam reforming of methanol over a $CuO/ZnO/ZrO_2/Al_2O_3$ catalyst. *Chemical communications*, (22), 2247-2248.
- Bonura, G., Cordaro, M., Cannilla, C., Arena, F. and Frusteri, F. (2014) The changing nature of the active site of Cu-Zn-Zr catalysts for the CO_2 hydrogenation reaction to methanol. *Applied Catalysis B: Environmental*, *152*, 152-161.
- Bundhoo, M. Z. and Mohee, R. (2016) Inhibition of dark fermentative bio-hydrogen production: a review. *International Journal of Hydrogen Energy*, *41*(16), 6713-6733.

- Cao, W., Zhang, H., Wang, Y. and Pan, J. (2012) Bioremediation of polluted surface water by using biofilms on filamentous bamboo. *Ecological Engineering*, 42, 146-149.
- Chang, S., Li, J. Z. and Liu, F. (2011) Evaluation of different pretreatment methods for preparing hydrogen-producing seed inocula from waste activated sludge. *Renewable Energy*, 36(5), 1517-1522.
- Chang, I. S., Kim, B. H., Lovitt, R. W. and Bang, J. S. (2001) Effect of CO partial pressure on cell-recycled continuous CO fermentation by *Eubacterium limosum* KIST612. *Process Biochemistry*, *37*(4), 411-421.
- Clark, J. H. (2007) Green chemistry for the second generation biorefinery—sustainable chemical manufacturing based on biomass. *Journal of Chemical Technology & Biotechnology: International Research in Process, Environmental & Clean Technology*, *82*(7), 603-609.
- Collman, J. P., Ghosh, S., Dey, A. and Decréau, R. A. (2009) Using a functional enzyme model to understand the chemistry behind hydrogen sulfide induced hibernation. *Proceedings of the National Academy of Sciences*, *106*(52), 22090-22095.
- Costa, J. M., Rodriguez, R. P. and Sancinetti, G. P. (2017) Removal sulfate and metals Fe^{+2}, Cu^{+2}, and Zn^{+2} from acid mine drainage in an anaerobic sequential batch reactor. *Journal of Environmental Chemical Engineering*, *5*(2), 1985-1989.
- Cowger, J. P., Klasson, K. T., Ackerson, M. D., Clausen, E. and Caddy, J. L. (1992) Mass-transfer and kinetic aspects in continuous bioreactors using *Rhodospirillum rubrum*. *Applied Biochemistry and Biotechnology*, *34*(1), 613-624.
- Damartzis, T. and Zabaniotou, A. (2011) Thermochemical conversion of biomass to second generation biofuels through integrated process design—A review. *Renewable Sustainable Energy Reviews*, *15*(1), 366-378.
- Datar, R. P., Shenkman, R. M., Cateni, B. G., Huhnke, R. L. and Lewis, R. S., (2004) Fermentation of biomass-generated producer gas to ethanol. *Biotechnology and Bioengineering*, 86, 587–594.
- Dashekvicz, M. P. and Uffen, R. L. (1979) Identification of a carbon monoxide metabolizing bacterium as a strain of *Rhodopseudomonas gelatinosa* (Molisch) Vanniel. *International Journal of Systematic Bacteriology.* 29(2): 145–148.
- Das, D. (2009) Advances in biohydrogen production processes: an approach towards commercialization. *International Journal of Hydrogen Energy*, 34(17), 7349-7357.
- Daverey, A. and Pakshirajan, K. (2010) Kinetics of growth and enhanced sophorolipids production by *Candida bombicola* using a low-cost fermentative medium. *Applied Biochemistry and Biotechnology*, 160(7), 2090-2101.
- Davidova, M. N., Tarasova, N. B., Mukhitova, F. K., & Karpilova, I. U. (1994). Carbon monoxide in metabolism of anaerobic bacteria. *Canadian journal of microbiology*, *40*(6), 417-425.
- Devarapalli, M., Atiyeh, H. K., Phillips, J. R., Lewis, R. S. and Huhnke, R. L. (2016) Ethanol production during semi-continuous syngas fermentation in a trickle bed reactor using *Clostridium ragsdalei*. *Bioresource Technology*, *209*, 56-65.

- Do, Y. S., Smeenk, J., Broer, K. M., Kisting, C. J., Brown, R., Heindel, T. J. and DiSpirito, A. A. (2007) Growth of *Rhodospirillum rubrum* on synthesis gas: Conversion of CO to H_2 and poly-β-hydroxyalkanoate. *Biotechnology and Bioengineering*, *97*(2), 279-286.
- Dries, J., De Smul, A., Goethals, L., Grootaerd, H. and Verstraete, W. (1998) High rate biological treatment of sulfate-rich wastewater in an acetate-fed EGSB reactor. *Biodegradation*. 9(2), 103-111.
- Durand, J. F. (2012) The impact of gold mining on the Witwatersrand on the rivers and karst system of Gauteng and North West Province, South Africa. *Journal of African Earth Sciences*, *68*, 24-43.
- Equeenuddin, S. M., Tripathy, S., Sahoo, P. K. and Panigrahi, M. K. (2010) Hydrogeochemical characteristics of acid mine drainage and water pollution at Makum Coalfield, India. *Journal of Geochemical Exploration*, *105*(3), 75-82.
- Fan, Y., Li, C., Lay, J. J., Hou, H. and Zhang, G. (2004) Optimization of initial substrate and pH levels for germination of sporing hydrogen-producing anaerobes in cow dung compost. *Bioresource Technology*, *91*(2), 189-193.
- Feio, M. J., Zinkevich, V., Beech, I. B., Llobet-Brossa, E., Eaton, P., Schmitt, J. and Guezennec, J. (2004) Desulfovibrio alaskensis sp. nov., a sulphate-reducing bacterium from a soured oil reservoir. *International Journal of Systematic and Evolutionary Microbiology*, *54*(5), 1747-1752.
- Fernando, S., Adhikari, S., Chandrapal, C. and Murali, N. (2006) Biorefineries: current status, challenges, and future direction. *Energy & Fuels*, *20*(4), 1727-1737.
- Frascari, D., Zanaroli, G., Bucchi, G., Rosato, A., Tavanaie, N., Fraraccio, S., Pinelli, D. and Fava, F. (2013) Trichloroethylene aerobic cometabolism by suspended and immobilized butane-growing microbial consortia: A kinetic study. *Bioresource Technology*, 144, 529-538.
- Fujikawa, H., Kai, A. and Morozumi, S. (2004) A new logistic model for Escherichia coli growth at constant and dynamic temperatures. *Food Microbiology*, *21*(5), 501-509.
- Ganigué, R., Sánchez-Paredes, P., Bañeras, L. and Colprim, J. (2016) Low fermentation pH is a trigger to alcohol production, but a killer to chain elongation. *Frontiers in Microbiology*, *7*, 702.
- Gao, J., Atiyeh, H. K., Phillips, J. R., Wilkins, M. R. and Huhnke, R. L. (2013) Development of low cost medium for ethanol production from syngas by *Clostridium ragsdalei*. *Bioresource Technology*, *147*, 508-515.
- Ghasemi, E., Mirhabibi, A., Edrissi, M., Aghababazadeh, R. and Brydson, R. M. (2009) Study on the magnetorheological properties of Maghemite-Kerosene ferrofluid. *Journal of Nanoscience and Nanotechnology*, *9*(7), 4273-4278.
- Grady, J. L. and Chen, G. J. (1998) *U.S. Patent No. 5,821,111*. Washington, DC: U.S. Patent and Trademark Office.
- Gonçalves, L. M. D., Ramos, A., Almeida, J. S., Xavier, A. M. R. B. and Carrondo, M. J. T. (1997) Elucidation of the mechanism of lactic acid growth inhibition and

production in batch cultures of *Lactobacillus rhamnosus*. *Applied Microbiology and Biotechnology*, *48*(3), 346-350.

- Gong, J., Yue, H., Zhao, Y., Zhao, S., Zhao, L., Lv, J. and Ma, X. (2012) Synthesis of ethanol via syngas on Cu/SiO_2 catalysts with balanced Cu^0–Cu^+ sites. *Journal of the American Chemical Society*, *134*(34), 13922-13925.
- Gopi Kiran, M., Pakshirajan, K. and Das, G. (2015) Heavy metal removal using sulfate-reducing biomass obtained from a lab-scale upflow anaerobic-packed bed reactor. *Journal of Environmental Engineering*, *142*(9), C4015010.
- Goswami, G., Chakraborty, S., Chaudhuri, S. and Dutta, D. (2012) Optimization of process parameters by response surface methodology and kinetic modeling for batch production of canthaxanthin by *Dietzia maris* NIT-D (accession number: HM151403). *Bioprocess and biosystems engineering*, *35*(8), 1375-1388.
- Guiot, S. R., Cimpoia, R. and Carayon, G. (2011) Potential of wastewater-treating anaerobic granules for biomethanation of synthesis gas. *Environmental Science & Technology*, *45*(5), 2006-2012.
- Haddad, M., Cimpoia, R. and Guiot, S. R. (2014) Performance of *Carboxydothermus hydrogenoformans* in a gas-lift reactor for syngas upgrading into hydrogen. *International Journal of Hydrogen Energy*, 39(6), 2543-2548.
- Hahn-Hägerdal, B., Galbe, M., Gorwa-Grauslund, M. F., Lidén, G. and Zacchi, G. (2006) Bio-ethanol–the fuel of tomorrow from the residues of today. *Trends in Biotechnology*, *24*(12), 549-556.
- Henstra, A. M. and Stams, A. J. (2011) Deep conversion of carbon monoxide to hydrogen and formation of acetate by the anaerobic thermophile *Carboxydothermus hydrogenoformans*. *International Journal of Microbiology*, *2011*. doi:10.1155/2011/641582.
- Hao, T. W., Xiang, P. Y., Mackey, H. R., Chi, K., Lu, H., Chui, H. K., van Loosdrecht, M. C. and Chen, G. H. (2014) A review of biological sulfate conversions in wastewater treatment. *Water Research*, 65, 1-21.
- Haynes, W. M. (Ed.). (2012) CRC handbook of chemistry and physics. CRC press.
- Hallenbeck, P. C. and Benemann, J. R. (2002) Biological hydrogen production; fundamentals and limiting processes. *International Journal of Hydrogen Energy*, *27*(11-12), 1185-1193.
- Hazarika, J., Pakshirajan, K., Sinharoy, A. and Syiem, M. B. (2015) Bioremoval of Cu (II), Zn (II), Pb (II) and Cd (II) by *Nostoc muscorum* isolated from a coal mining site. *Journal ofAapplied Phycology*, *27*(4), 1525-1534.
- Henstra, A. M., Sipma, J., Rinzema, A. and Stams, A. J. (2007) Microbiology of synthesis gas fermentation for biofuel production. *Current Opinion in Biotechnology*, 18(3), 200-206.
- Hoag, G. E., Collins, J. B., Holcomb, J. L., Hoag, J. R., Nadagouda, M. N. and Varma, R. S. (2009). Degradation of bromothymol blue by 'greener' nano-scale zero-valent iron synthesized using tea polyphenols. *Journal of Materials Chemistry*, 19(45), 8671-8677.

- Hocking, W. P., Roalkvam, I., Magnussen, C., Stokke, R. and Steen, I. H. (2015) Assessment of the carbon monoxide metabolism of the hyperthermophilic sulfate-reducing Archaeon *Archaeoglobus fulgidus* VC-16 by comparative transcriptome analyses. *Archaea*, http://dx.doi.org/10.1155/2015/235384.
- Huang, H. J., Ramaswamy, S., Tschirner, U. W. and Ramarao, B. V. (2008) A review of separation technologies in current and future biorefineries. *Separation and purification technology*, *62*(1), 1-21.
- Huang, L., Weng, X., Chen, Z., Megharaj, M. and Naidu, R. (2014) Green synthesis of iron nanoparticles by various tea extracts: comparative study of the reactivity. *Spectrochimica Acta Part A: Molecular and Biomolecular Spectroscopy*, *130*, 295-301.
- Hurst, K. M. and Lewis, R. S. (2010) Carbon monoxide partial pressure effects on the metabolic process of syngas fermentation. *Biochemical Engineering Journal*, 48(2), 159-165.
- IAPA. (2008) Carbon monoxide in the workplace, technical report. Industrial Accident Prevention Association.
- Iwasa, N., Mayanagi, T., Ogawa, N., Sakata, K. and Takezawa, N. (1998) New catalytic functions of Pd–Zn, Pd–Ga, Pd–In, Pt–Zn, Pt–Ga and Pt–In alloys in the conversions of methanol. *Catalysis Letters*, *54*(3), 119-123.
- Ismail, K. S. K., Najafpour, G., Younesi, H., Mohamed, A. R. and Kamaruddin, A. H. (2008) Biological hydrogen production from CO: bioreactor performance. *Biochemical Engineering Journal*, 39(3), 468-477.
- Jahangiri, H., Bennett, J., Mahjoubi, P., Wilson, K. and Gu, S. (2014) A review of advanced catalyst development for Fischer–Tropsch synthesis of hydrocarbons from biomass derived syn-gas. *Catalysis Science & Technology*, *4*(8), 2210-2229.
- Jung, G. Y., Jung, H. O., Kim, J. R., Ahn, Y. and Park, S. (1999a) Isolation and characterization of *Rhodopseudomonas palustris* P4 which utilizes CO with the production of H_2. *Biotechnology Letter*, 21(6): 525–529.
- Jung, G. Y., Kim, J. R., Jung, H. O., Park, J. Y. and Park, S. (1999b) A new chemoheterotrophic bacterium catalyzing water-gas shift reaction. *Biotechnology Letter*, 21(10): 869–873.
- Jung, G. Y., Kim, J. R., Park, J. Y. and Park, S. (2002) Hydrogen production by a new chemoheterotrophic bacterium *Citrobacter* sp. Y19. *International Journal of Hydrogen Energy*, 601–610.
- Kalamaras, C. M. and Efstathiou, A. M. (2013) Hydrogen production technologies: current state and future developments. In *Conference papers in science* (Vol. 2013). Hindawi. http://dx.doi.org/10.1155/2013/690627
- Kapic, A. and Heindel, T. J. (2006) Correlating gas-liquid mass transfer in a stirred-tank reactor. *Chemical Engineering Research and Design*, *84*(3), 239-245.
- Kaster, J. A. Michelsen, D. L. and Velander, W. H. (1990) Increased Oxygen Transfer in a Yeast Fermentation Using a Microbubble Dispersion. Applied Biochemistry and Biotechnology, 24/25, 469-484.

- Kerby, R. L., Ludden, P. W. and Roberts, G. P. (1995) Carbon monoxide-dependent growth of *Rhodospirillum rubrum*. *Journal of Bacteriology*, 177(8): 2241–2244.
- Kharas, K. and Durand, J. P. (2011) *U.S. Patent No. 7,923,405*. Washington, DC: U.S. Patent and Trademark Office.
- Kim, J., Park, C., Kim, T. H., Lee, M., Kim, S., Kim, S. W. and Lee, J. (2003) Effects of various pretreatments for enhanced anaerobic digestion with waste activated sludge. *Journal of bioscience and bioengineering*, *95*(3), 271-275.
- Kim, M. S., Bae, S. S., Kim, Y. J., Kim, T. W., Lim, J. K., Lee, S. H., Choi, A. R., Jeon, J. H., Lee, J. H., Lee, H. S. and Kang, S. G. (2013) CO-dependent H_2 production by genetically engineered *Thermococcus onnurineus* NA1. *Applied and Environmental Microbiology*, 79, 2048–2053.
- Kim, J. R., Oh, Y. K., Yoon, Y. J., Lee, E. Y. and Park, S. U. N. G. H. O. O. N. (2003) Oxygen sensitivity of carbon monoxide-dependent hydrogen production activity in *Citrobacter* sp. *Journal of Microbiology and Biotechnology*, *13*(5), 717-724.
- Kim, Y. K. and Lee, H. (2016) Use of magnetic nanoparticles to enhance bioethanol production in syngas fermentation. *Bioresource Technology*, 204, 139-144.
- Kim, Y. K., Park, S. E., Lee, H. and Yun, J. Y. (2014) Enhancement of bioethanol production in syngas fermentation with *Clostridium ljungdahlii* using nanoparticles. *Bioresource Technology*, 159, 446-450.
- Kiran, M. G., Pakshirajan, K. and Das, G. (2017) An overview of sulfidogenic biological reactors for the simultaneous treatment of sulfate and heavy metal rich wastewater. *Chemical Engineering Science*, *158*, 606-620.
- Klasson, K. T., Gupta, A., Clausen, E. C. and Gaddy, J. L. (1993) Evaluation of mass-transfer and kinetic parameters for *Rhodospirillum rubrum* in a continuous stirred tank reactor. *Applied Biochemistry and Biotechnology*, 39–40, 549–557.
- Kochetkova, T. V. Rusanov, I. I. Pimenov, N. V. Kolganova, T. V. Lebedinsky, A. V. Bonch-Osmolovskaya, E. A. and Sokolova, T. G. (2011) Anaerobic transformation of carbon monoxide by microbial communities of Kamchatka hot springs. *Extremophiles*, 15(3), 319-325.
- Kundiyana, D. K., Wilkins, M. R., Maddipati, P. and Huhnke, R. L. (2011a) Effect of temperature, pH and buffer presence on ethanol production from synthesis gas by "*Clostridium ragsdalei*". *Bioresource Technology*, *102*(10), 5794-5799.
- Kundiyana, D. K., Huhnke, R. L. and Wilkins, M. R. (2011b) Effect of nutrient limitation and two-stage continuous fermentor design on productivities during "*Clostridium ragsdalei*" syngas fermentation. *Bioresource Technology*, *102*(10), 6058-6064.
- Kundiyana, D. K., Huhnke, R. L. and Wilkins, M. R. (2010) Syngas fermentation in a 100-L pilot scale fermentor: design and process considerations. *Journal of Bioscience and Bioengineering*, *109*(5), 492-498.
- Kumar, M., Sinharoy, A. and Pakshirajan, K. (2018) Process integration for biological sulfate reduction in a carbon monoxide fed packed bed reactor. *Journal of Environmental Management*, 219, 294-303.

- Kumar, G., Park, J. H., Sivagurunathan, P., Lee, S. H., Park, H. D. and Kim, S. H. (2017) Microbial responses to various process disturbances in a continuous hydrogen reactor fed with galactose. *Journal of bioscience and bioengineering*, *123*(2), 216-222.
- Kumar, K. M., Mandal, B. K., Kumar, K. S., Reddy, P. S. and Sreedhar, B. (2013) Biobased green method to synthesise palladium and iron nanoparticles using *Terminalia chebula* aqueous extract. *Spectrochimica Acta Part A*, 102, 128-133.
- Lagoa-Costa, B., Abubackar, H. N., Fernández-Romasanta, M., Kennes, C. and Veiga, M. C. (2017) Integrated bioconversion of syngas into bioethanol and biopolymers. *Bioresource Technology*, *239*, 244-249.
- Lahijani, P., Zainal, Z. A., Mohammadi, M. and Mohamed, A. R. (2015) Conversion of the greenhouse gas CO_2 to the fuel gas CO via the Boudouard reaction: A review. *Renewable and Sustainable Energy Reviews*, *41*, 615-632.
- Lasko, D. R., Zamboni, N. and Sauer, U. (2000) Bacterial response to acetate challenge: a comparison of tolerance among species. *Applied Microbiology and Biotechnology*, *54*(2), 243-247.
- Lens, P. N. L., Visser, A., Janssen, A. J. H., Pol, L. H. and Lettinga, G. (1998) Biotechnological treatment of sulfate-rich wastewaters. *Critical Reviews in Environmental Science and Technology*, *28*(1), 41-88.
- LeValley, T. L., Richard, A. R. and Fan, M. (2014) The progress in water gas shift and steam reforming hydrogen production technologies–a review. *International Journal of Hydrogen Energy*, *39*(30), 16983-17000.
- Levin, D. B., Pitt, L. and Love, M. (2004) Biohydrogen production: prospects and limitations to practical application. *International Journal of Hydrogen Energy*, *29*(2), 173-185.
- Liamleam, W. and Annachhatre, A.P. (2007) Electron donors for biological sulfate reduction. *Biotechnology Advances*, 25(5), 452-463.
- Liew, F., Henstra, A. M., Köpke, M., Winzer, K., Simpson, S. D. and Minton, N. P. (2017) Metabolic engineering of *Clostridium autoethanogenum* for selective alcohol production. *Metabolic Engineering*, 40, 104-114.
- Liew, F., Martin, M. E., Tappel, R. C., Heijstra, B. D., Mihalcea, C. and Köpke, M. (2016) Gas fermentation—a flexible platform for commercial scale production of low-carbon-fuels and chemicals from waste and renewable feedstocks. *Frontiers in Microbiology*, 7, 694.
- Lin, C. Y. and Lay, C. H. (2004) Effects of carbonate and phosphate concentrations on hydrogen production using anaerobic sewage sludge microflora. *International Journal of Hydrogen Energy*, *29*(3), 275-281.
- Lin, J., Wang, A., Qiao, B., Liu, X., Yang, X., Wang, X. and Zhang, T. (2013) Remarkable performance of Ir1/FeOx single-atom catalyst in water gas shift reaction. *Journal of the American Chemical Society*, *135*(41), 15314-15317.
- Liu, K., Atiyeh, H. K., Tanner, R. S., Wilkins, M. R. and Huhnke, R. L. (2012) Fermentative production of ethanol from syngas using novel moderately alkaliphilic strains of *Alkalibaculum bacchi*. *Bioresource Technology*, *104*, 336-341.

- Liu, K., Atiyeh, H. K., Stevenson, B. S., Tanner, R. S., Wilkins, M. R. and Huhnke, R. L. (2014a) Mixed culture syngas fermentation and conversion of carboxylic acids into alcohols. *Bioresource Technology*, *152*, 337-346.
- Liu, K., Atiyeh, H. K., Stevenson, B. S., Tanner, R. S., Wilkins, M. R. and Huhnke, R. L. (2014b) Continuous syngas fermentation for the production of ethanol, n-propanol and n-butanol. *Bioresource Technology*, *151*, 69-77.
- Liu, X., Zhu, Y. and Yang, S. T. (2006) Construction and characterization of ack deleted mutant of *Clostridium tyrobutyricum* for enhanced butyric acid and hydrogen production. *Biotechnology Progress*, *22*(5), 1265-1275.
- Liu, Z. H., Maszenan, A. M., Liu, Y. and Ng, W. J. (2015) A brief review on possible approaches towards controlling sulfate-reducing bacteria (SRB) in wastewater treatment systems. *Desalination and Water Treatment*, *53*(10), 2799-2807.
- Liu, Y., Wan, J., Han, S., Zhang, S. and Luo, G. (2016) Selective conversion of carbon monoxide to hydrogen by anaerobic mixed culture. *Bioresource Technology*, 202, 1-7.
- Ljunggren, M., Willquist, K., Zacchi, G. and van Niel, E. W. (2011) A kinetic model for quantitative evaluation of the effect of hydrogen and osmolarity on hydrogen production by *Caldicellulosiruptor saccharolyticus*. *Biotechnology for biofuels*, *4*(1), 31.
- Lupton, F. S., Conrad, R. and Zeikus J. G. (1984) CO metabolism of *Desulfovibrio vulgaris* strain Madison: physiological function in the absence or presence of exogenous substrates. *FEMS Microbiology Letter*, 23, 263–268.
- Luo, G., Wang, W. and Angelidaki, I. (2013) Anaerobic digestion for simultaneous sewage sludge treatment and CO biomethanation: process performance and microbial ecology. *Environmental science & technology*, 47(18), 10685-10693.
- Maddipati, P., Atiyeh, H. K., Bellmer, D. D. and Huhnke, R. L. (2011) Ethanol production from syngas by *Clostridium* strain P11 using corn steep liquor as a nutrient replacement to yeast extract. *Bioresource Technology*, *102*(11), 6494-6501.
- Mahmoudi, H., Mahmoudi, M., Doustdar, O., Jahangiri, H., Tsolakis, A., Gu, S. and LechWyszynski, M. (2017) A review of Fischer Tropsch synthesis process, mechanism, surface chemistry and catalyst formulation. *Biofuels Engineering*, *2*(1), 11-31.
- Maness, P. C., Smolinski, S., Dillon, A. C., Heben, M. J. and Weaver, P. F. (2002) Characterization of the oxygen tolerance of a hydrogenase linked to a carbon monoxide oxidation pathway in *Rubrivivax gelatinosus*. *Applied and environmental microbiology*, 68(6), 2633-2636.
- Maness, P. C., Huang, J., Smolinski, S., Tek, V. and Vanzin, G. (2005) Energy generation from the CO oxidation-hydrogen production pathway in Rubrivivax gelatinosus. *Applied and Environmental Microbiology*, *71*(6), 2870-2874.
- Mendes, D., Mendes, A., Madeira, L. M., Iulianelli, A., Sousa, J. M. and Basile, A. (2010) The water-gas shift reaction: from conventional catalytic systems to Pd-based membrane reactors—a review. *Asia-Pacific Journal of Chemical Engineering*, *5*(1), 111-137.

- Mohammadi, M., Najafpour, G. D., Younesi, H., Lahijani, P., Uzir, M. H. and Mohamed, A. R. (2011) Bioconversion of synthesis gas to second generation biofuels: a review. *Renewable and Sustainable Energy Reviews*, 15(9), 4255-4273.
- Mohanraj, S., Kodhaiyolii, S., Rengasamy, M. and Pugalenthi, V. (2014a) Green synthesized iron oxide nanoparticles effect on fermentative hydrogen production by *Clostridium acetobutylicum*. *Applied biochemistry and biotechnology*, 173(1), 318-331.
- Mohanraj, S., Kodhaiyolii, S., Rengasamy, M. and Pugalenthi, V. (2014b) Phytosynthesized iron oxide nanoparticles and ferrous iron on fermentative hydrogen production using Enterobacter cloacae: evaluation and comparison of the effects. I*nternational Journal of Hydrogen Energy*, *39*(23), 11920-11929.
- Monteiro, A. A. M. G., Boaventre, R. A. R. and Rodrigues, A. E. (2000) Phenol biodegradation by *Pseudomonas putida* DSM 548 in a batch reactor. *Biochemical Engineering Journal*, 6(1), 45–49.
- Mörsdorf, G., Frunzke, K., Gadkari, D. and Meyer, O. (1992) Microbial growth on carbon monoxide. *Biodegradation*, 3(1), 61-82.
- Moosa, S., Nemati, M. and Harrison S. T. L. (2000) A kinetic study on anaerobic reduction of sulfate; Part I: Effect of sulfate concentration, *Chemical Engineering Science*, 57, 2773-2780.
- Mu, Y., Yu, H. Q. and Wang, G. (2007) A kinetic approach to anaerobic hydrogen-producing process. *Water research*, *41*(5), 1152-1160.
- Mu, Y., Wang, G. and Yu, H. Q. (2006) Kinetic modeling of batch hydrogen production process by mixed anaerobic cultures. *Bioresource Technology*, *97*(11), 1302-1307.
- Munasinghe, P. C. and Khanal, S. K. (2010a) Biomass-derived syngas fermentation into biofuels: opportunities and challenges. *Bioresource Technology*, 101(13), 5013-5022.
- Munasinghe, P. C. and Khanal, S. K., (2010b) Syngas fermentation to biofuel: evaluation of carbon monoxide mass transfer coefficient (kLa) in different reactor configurations. *Biotechnology Progress*, 26, 1616–1621.
- Munasinghe, P. C. and Khanal, S. K., (2014) Evaluation of hydrogen and carbon monoxide mass transfer and a correlation between the myoglobin-protein bioassay and gas chromatography method for carbon monoxide determination. *RSC Advances*, 4, 37575–37581.
- Nagy, E., Feczkó, T. and Koroknai, B. (2007) Enhancement of oxygen mass transfer rate in the presence of nanosized particles. *Chemical Engineering Science*, *62*(24), 7391-7398.
- Naik, S. N., Goud, V. V., Rout, P. K. and Dalai, A. K. (2010) Production of first and second generation biofuels: a comprehensive review. *Renewable and Sustainable Energy Reviews*, *14*(2), 578-597.
- Najafpour, G., Younesi, H. and Mohamed, A. R. (2003) Continuous hydrogen production via fermentation of synthesis gas. *Petroleum and Coal*, *45*(3/4), 154-158.

- Najafpour, G., Younesi, H. and Mohamed, A. R. (2006) A survey on various carbon sources for biological hydrogen production via the water-gas reaction using a photosynthetic bacterium (*Rhodospirillum rubrum*). *Energy Sources, Part A*, *28*(11), 1013-1026.
- Najafpour, G., Ismail, K. S. K., Younesi, H., Mohamed, A. R. and Kamaruddin, A. H. (2004) Hydrogen as clean fuel via continuous fermentation by anaerobic photosynthetic bacteria, *Rhodospirillum rubrum*. *African Journal of Biotechnology*, *3*(10), 503-507.
- Ndisang, J. F., Tabien, H. E. N. and Wang, R. (2004) Carbon monoxide and hypertension. *Journal of Hypertension*, 22(6), 1057-1074.
- Njagi, E. C., Huang, H., Stafford, L., Genuino, H., Galindo, H. M., Collins, J. B. and Suib, S. L. (2010) Biosynthesis of iron and silver nanoparticles at room temperature using aqueous sorghum bran extracts. *Langmuir*, 27(1), 264-271.
- Ntaikou, I., Antonopoulou, G. and Lyberatos, G. (2010) Biohydrogen production from biomass and wastes via dark fermentation: a review. *Waste and Biomass Valorization*, *1*(1), 21-39.
- Ogawa, T., Inoue, N., Shikada, T., Inokoshi, O. and Ohno, Y. (2004) Direct dimethyl ether (DME) synthesis from natural gas. *Studies in Surface Science and Catalysis*, *147*, 379-384.
- Oh, Y. K., Seol, E. H., Kim, M. S. and Park, S. (2004) Photoproduction of hydrogen from acetate by a chemoheterotrophic bacterium *Rhodopseudomonas palustris P4*. *International journal of hydrogen energy*, *29*(11), 1115-1121.
- Oh, S. and Logan, B. E. (2005) Hydrogen and electricity production from a food processing wastewater using fermentation and microbial fuel cell technologies. *Water Research*, *39*(19), 4673-4682.
- Oh, Y. K., Seol, E. H., Kim, J. R. and Park, S. (2003) Fermentative biohydrogen production by a new chemoheterotrophic bacterium *Citrobacter* sp. Y19. *International Journal of Hydrogen Energy*, *28*(12), 1353-1359.
- Oh, Y. K., Kim, Y. J., Park, J. Y., Lee, T. H., Kim, M. S. and Park, S. (2005) Biohydrogen production from carbon monoxide and water by *Rhodopseudomonas palustris* P4. *Biotechnology and Bioprocess Engineering*, *10*(3), 270.
- Olle, B. Bucak, S. Holmes, T. C. Bromberg, L. Hatton, T. A. and Wang, D. I. C. (2006) Enhancement of oxygen mass transfer using functionalized magnetic nanoparticles. *Industrial & Engineering Chemistry Research*, 45(12), 4355–4363.
- OSHA. (2002) Carbon monoxide poisoning, OSHA fact sheet https://www.osha.gov/OshDoc/data_General_Facts/carbonmonoxide-factsheet.pdf. accessed 17th Dec, 2014.
- Pakhare, D. and Spivey, J. (2014) A review of dry (CO_2) reforming of methane over noble metal catalysts. *Chemical Society Reviews*, *43*(22), 7813-7837.
- Pakpour, F., Najafpour, G., Tabatabaei, M., Tohidfar, M. and Younesi, H. (2014) Biohydrogen production from CO-rich syngas via a locally isolated *Rhodopseudomonas palustris* PT. *Bioprocess and Biosystems Engineering*, *37*(5), 923-930.

- Pakshirajan, K. and Mal, J. (2013) Biohydrogen production using native carbon monoxide converting anaerobic microbial consortium predominantly *Petrobacter* sp. *International Journal of Hydrogen Energy*, 38(36), 16020-16028.
- Park, S., Yasin, M., Kim, D., Park, H. D., Kang, C. M., Kim, D. J. and Chang, I. S. (2013) Rapid enrichment of (homo) acetogenic consortia from animal feces using a high mass-transfer gas-lift reactor fed with syngas. *Journal of Industrial Microbiology & Biotechnology*, *40*(9), 995-1003.
- Parshina, S. N., Sipma, J., Henstra, A. M. and Stams, A. J. (2010) Carbon monoxide as an electron donor for the biological reduction of sulphate. *International journal of microbiology*, doi:10.1155/2010/319527
- Petrus, L. and Noordermeer, M. A. (2006) Biomass to biofuels, a chemical perspective. *Green Chemistry*, *8*(10), 861-867.
- Phillips, J. R., Atiyeh, H. K., Tanner, R. S., Torres, J. R., Saxena, J., Wilkins, M. R. and Huhnke, R. L. (2015) Butanol and hexanol production in Clostridium carboxidivorans syngas fermentation: medium development and culture techniques. *Bioresource Technology*, *190*, 114-121.
- RJ, B. S., Loganathan, M. and Shantha, M. S. (2010) A review of the water gas shift reaction kinetics. *International Journal of Chemical Reactor Engineering*, *8*(1). https://doi.org/10.2202/1542-6580.2238
- Richter, H., Martin, M. E. and Angenent, L. T. (2013) A two-stage continuous fermentation system for conversion of syngas into ethanol. *Energies*, *6*(8), 3987-4000.
- Richter, H., Molitor, B., Wei, H., Chen, W., Aristilde, L. and Angenent, L. T. (2016) Ethanol production in syngas-fermenting Clostridium ljungdahlii is controlled by thermodynamics rather than by enzyme expression. *Energy & Environmental Science*, *9*(7), 2392-2399.
- Riggs, S. S. and Heindel, T. J. (2006) Measuring carbon monoxide gas—liquid mass transfer in a stirred tank reactor for syngas fermentation. *Biotechnology Progress*, *22*(3), 903-906.
- Roy, A. S., Hazarika, J., Manikandan, N. A., Pakshirajan, K. and Syiem, M. B. (2015) Heavy metal removal from multicomponent system by the cyanobacterium *Nostoc muscorum*: kinetics and interaction study. *Applied Biochemistry and Biotechnology*, *175*(8), 3863-3874.
- Ruthiya, K.C. (2005) Mass Transfer and Hydrodynamics in Catalytic Slurry Reactors. Technische Universiteit Eindhoven, Netherlands, pp. 67–98.
- Sant'Anna, F. H., Lebedinsky, A. V., Sokolova, T. G., Robb, F. T. and Gonzalez, J. M. (2015) Analysis of three genomes within the thermophilic bacterial species *Caldanaerobacter subterraneus* with a focus on carbon monoxide dehydrogenase evolution and hydrolase diversity. *BMC genomics*, 16(1), 757.
- Santa Cruz, L., Garralón, A., Escribano, A., Gómez, P., Turrero, M. J., Peña, J. and Sánchez, L. (2013) Chemical characteristics of acid mine drainage from an As-W mineralized zone in western Spain. *Procedia Earth and Planetary Science*, *7*, 284-287.

- Saravanan, P., Pakshirajan, K. and Saha, P. (2008). Growth kinetics of an indigenous mixed microbial consortium during phenol degradation in a batch reactor. *Bioresource Technology*, 99(1), 205-209.
- Saravanan, P., Pakshirajan, K. and Saha, P. (2009). Hydrodynamics and batch biodegradation of phenol in an Internal Loop Airlift Reactor. *International Journal of Environmental Engineering*, *2*(1-3), 303-315.
- Saravanan, P., Pakshirajan, K. and Saha, P. (2011) Biodegradation kinetics of phenol by predominantly *Pseudomonas* sp. in a batch shake flask. *Desalination and Water Treatment*, *36*(1-3), 99-104.
- Sarkar, N., Ghosh, S. K., Bannerjee, S. and Aikat, K. (2012). Bioethanol production from agricultural wastes: an overview. *Renewable energy*, 37(1), 19-27.
- Sarti, A. and Zaiat, M., (2011) Anaerobic treatment of sulfate-rich wastewater in an anaerobic sequential batch reactor (AnSBR) using butanol as the carbon source. *Journal of Environmental Management*, 92(6), 1537-1541.
- Scott, T. C. DePaoli, D. W. and Sisson, W. G. (1994) Further Development of the Electrically Driven Emulsion-Phase Contactor. *Industrial & Engineering Chemistry Research*, 33, 1237-1244.
- Shahwan, T., Sirriah, S. A., Nairat, M., Boyacı, E., Eroğlu, A. E., Scott, T. B. and Hallam, K. R. (2011) Green synthesis of iron nanoparticles and their application as a Fenton-like catalyst for the degradation of aqueous cationic and anionic dyes. *Chemical Engineering Journal*, 172(1), 258-266.
- Shen, Y., Brown, R. C. and Wen, Z. (2017) Syngas fermentation by Clostridium carboxidivorans P7 in a horizontal rotating packed bed biofilm reactor with enhanced ethanol production. *Applied Energy*, *187*, 585-594.
- Shen, Y., Brown, R. and Wen, Z. (2014) Syngas fermentation of Clostridium carboxidivoran P7 in a hollow fiber membrane biofilm reactor: Evaluating the mass transfer coefficient and ethanol production performance. *Biochemical Engineering Journal*, *85*, 21-29.
- Shi, S. F., Jia, J. F., Guo, X. K., Zhao, Y. P., Chen, D. S., Guo, Y. Y. and Zhang, X. L. (2012) Biocompatibility of chitosan-coated iron oxide nanoparticles with osteoblast cells. *International Journal of Nanomedicine*, *7*, 5593.
- Shirtum R. P., Trent, D. L., Tirtowidjojo, C. A. and Gillis, P. A. Shear Mixing Apparatus and Use Thereof, U.S. Patent Number 5845993, Dec. 8, 1998.
- Simate, G. S. and Ndlovu, S. (2014) Acid mine drainage: Challenges and opportunities. *Journal of Environmental Chemical Engineering*, *2*(3), 1785-1803.
- Singla, A., Verma, D., Lal, B. and Sarma, P. M. (2014) Enrichment and optimization of anaerobic bacterial mixed culture for conversion of syngas to ethanol. *Bioresource technology*, *172*, 41-49.
- Sipma, J., Henstra, A. M., Parshina, S. N., Lens, P. N., Lettinga, G. and Stams, A. J. (2006). Microbial CO conversions with applications in synthesis gas purification and bio-desulfurization. *Critical Reviews in Biotechnology*, 26(1), 41-65.

- Sipma, J., Osuna, M. B., Lettinga, G., Stams, A. J. and Lens, P. N. (2007). Effect of hydraulic retention time on sulfate reduction in a carbon monoxide fed thermophilic gas lift reactor. *Water Research*, 41(9), 1995-2003.
- Sipma, J., Lens, P. N. L., Stams, A. J. M. and Lettinga, G. (2003) Carbon monoxide conversion by anaerobic bioreactor sludges. FEMS Microbiol. Ecol. 44(2), 271-277.
- Sinharoy, A., Manikandan, N. A. and Pakshirajan, K. (2015) A novel biological sulfate reduction method using hydrogenogenic carboxydotrophic mesophilic bacteria. *Bioresource Technology*, 192, 494-500.
- Sivagurunathan, P., Kumar, G., Bakonyi, P., Kim, S.H., Kobayashi, T., Xu, K.Q., Lakner, G., Tóth, G., Nemestóthy, N. and Bélafi-Bakó, K. (2016). A critical review on issues and overcoming strategies for the enhancement of dark fermentative hydrogen production in continuous systems. *International Journal of Hydrogen Energy*, *41*(6), 3820-3836.
- Slepova, T. V., Sokolova, T. G., Lysenko, A. M., Tourova, T. P., Kolganova, T. V., Kamzolkina, O. V., Karpov, G. A. and Bonch-Osmolovskaya, E. A. (2006) *Carboxydocella sporoproducens* sp. nov., a novel anaerobic CO-utilizing/H_2-producing thermophilic bacterium from a Kamchatka hot spring. *International Journal of Systematic and Evolutionary Microbiology*, 56: 797–800.
- Slepova, T. V., Rusanov, I. I., Sokolova, T. G., Bonch-Osmolovskaya, E. A. and Pimenov, N. V. (2007) Radioisotopic tracing of carbon monoxide conversion by anaerobic thermophilic prokaryotes. *Microbiology*. 76: 523–529.
- Slepova, T. V., Sokolova, T. G., Kolganova, T. V., Tourova, T. P. and Bonch-Osmolovskaya, E. A., (2009) Carboxydothermus siderophilus sp. nov., a novel thermophilic hydrogenogenic carboxydotrophic dissimilatory Fe(III)-reducing bacterium from Kamchatka hot spring. *International Journal of Systematic and Evolutionary Microbiology*, 59: 213–217.
- Sokolova, T. G., Henstra, A. M., Sipma, J., Parshina, S. N., Stams, A. J. and Lebedinsky, A. V. (2009) Diversity and ecophysiological features of thermophilic carboxydotrophic anaerobes. *FEMS Microbiology Ecology*, 68(2), 131-141.
- Sokolova, T. G., Kostrikina, N. A., Chernyh, N. A., Tourova, T. P., Kolganova, T. V. and Bonch-Osmolovskaya, E. A. (2002) *Carboxydocella thermautotrophica* gen. nov., sp. nov., a novel anaerobic, CO-utilizing thermophile from a Kamchatkan hot spring. *International Journal of Systematic and Evolutionary Microbiology*, *52*(6), 1961-1967.
- Sosna, M. K., Sokolinskii, Y. A., Shovkoplyas, N. Y. and Korolev, E. V. (2007) Application of the thermodynamic method to developing the process of producing methanol and dimethyl ether from synthesis gas. *Theoretical Foundations of Chemical Engineering*, *41*(6), 809-815.
- Stams, A. J. M., Van Dijk, J. B., Dijkema, C. and Plugge, C. M. (1993) Growth of syntrophic propionate-oxidizing bacteria with fumarate in the absence of methanogenic bacteria. *Applied and Environmental Microbiology*, *59*(4), 1114-1119.

- Subramani, V., and Gangwal, S. K. (2008) A review of recent literature to search for an efficient catalytic process for the conversion of syngas to ethanol. *Energy & Fuels*, 22(2), 814-839.
- Sundberg, C., Al-Soud, W. A., Larsson, M., Alm, E., Yekta, S. S., Svensson, B. H., Sørensen, S. J. and Karlsson, A. (2013). 454 pyrosequencing analyses of bacterial and archaeal richness in 21 full-scale biogas digesters. *FEMS microbiology ecology*, *85*(3), 612-626.
- Sun, Y. P., Li, X. Q., Cao, J., Zhang, W. X. and Wang, H. P. (2006) Characterization of zero-valent iron nanoparticles. *Advances in Colloid and Interface Science*, *120*(1-3), 47-56.
- Sun, R., Zhang, L., Zhang, Z., Chen, G. H. and Jiang, F. (2018) Realizing high-rate sulfur reduction under sulfate-rich conditions in a biological sulfide production system to treat metal-laden wastewater deficient in organic matter. *Water Research*, *131*, 239-245.
- Tsakoumis, N. E., Rønning, M., Borg, Ø., Rytter, E. and Holmen, A. (2010) Deactivation of cobalt based Fischer–Tropsch catalysts: a review. *Catalysis Today*, *154*(3-4), 162-182.
- Tsouris, C. and Tavlarides, L. L. (1994) Breakage and Coalescence Models for Drops in Turbulent Dispersions. *AIChE J. 40* (3), 395-406.
- Tutu, H., McCarthy, T. S. and Cukrowska, E. (2008) The chemical characteristics of acid mine drainage with particular reference to sources, distribution and remediation: The Witwatersrand Basin, South Africa as a case study. *Applied Geochemistry*, *23*(12), 3666-3684.
- Ueki, T., Nevin, K. P., Woodard, T. L. and Lovley, D. R. (2014). Converting carbon dioxide to butyrate with an engineered strain of *Clostridium ljungdahlii*. *MBio*, *5*(5), e01636-14.
- U.S. EPA (United States Environmental Protection Agency). (2015) 2011 National Emissions Inventory, Version 2, technical support document. Draft report. pp 371.
- Üzüm, Ç., Shahwan, T., Eroğlu, A. E., Hallam, K. R., Scott, T. B. and Lieberwirth, I. (2009). Synthesis and characterization of kaolinite-supported zero-valent iron nanoparticles and their application for the removal of aqueous Cu^{2+} and Co^{2+} ions. *Applied Clay Science*, 43(2), 172-181.
- Vaitheeswari, S., Sriram, R., Brindha, P. and Kurian, G. A. (2015) Studying inhibition of calcium oxalate stone formation: an in vitro approach for screening hydrogen sulfide and its metabolites. *International Brazilian Journal of Urology*, *41*(3), 503-510.
- Van Houten, R. T., Pol, L. W. H. and Lettinga, G. (1994) Biological sulfate reduction using gas-lift reactors fed with hydrogen and carbon dioxide as energy and carbon source. *Biotechnology and Bioengineering*, 44, 586-594.
- Van Houten, R. T., Van der Spoel, H., van Aelst, A.C., Pol, H., Look, W. and Lettinga, G. (1996) Biological sulfate reduction using synthesis gas as energy and carbon source. *Biotechnology and Bioengineering*, 50, 136-144.

- van Houten, B. H., van Doesburg, W., Dijkman, H., Copini, C., Smidt, H. and Stams, A. J. (2009) Long-term performance and microbial community analysis of a full-scale synthesis gas fed reactor treating sulfate-and zinc-rich wastewater. *Applied Microbiology and Biotechnology*, 84(3), 555-563.
- Vanzin, G. F., Huang, J., Smolinski, S., Kronoveter, K. and Maness, P. C. (2002) Biological hydrogen from fuel gases. In *Proceedings of the US DOE Hydrogen Program Review.*
- van Niel, E. W., Claassen, P. A. and Stams, A. J. (2003) Substrate and product inhibition of hydrogen production by the extreme thermophile, *Caldicellulosiruptor saccharolyticus*. *Biotechnology and bioengineering*, *81*(3), 255-262.
- Vanzin, G., Yu, J., Smolinski, S., Tek, V., Pennington, G. and Maness, P. C. (2010) Characterization of genes responsible for the CO-linked hydrogen production pathway in *Rubrivivax gelatinosus. Applied and Environmental Microbiology*, 76(11), 3715-3722.
- Vasudevan, P. T. and Briggs, M. (2008) Biodiesel production—current state of the art and challenges. *Journal of Industrial Microbiology & Biotechnology*, 35(5), 421.
- Venvik, H. J. and Yang, J. (2017) Catalysis in microstructured reactors: Short review on small-scale syngas production and further conversion into methanol, DME and Fischer-Tropsch products. *Catalysis Today*, *285*, 135-146.
- Wainaina, S., Horváth, I. S. and Taherzadeh, M. J. (2018) Biochemicals from food waste and recalcitrant biomass via syngas fermentation: A review. *Bioresource Technology*, 248, 113-121.
- Wang, J. and Wan, W. (2009) Kinetic models for fermentative hydrogen production: a review. *International Journal of Hydrogen Energy*, *34*(8), 3313-3323.
- Wang, Y., Zhao, Q. B., Mu, Y., Yu, H. Q., Harada, H. and Li, Y. Y. (2008) Biohydrogen production with mixed anaerobic cultures in the presence of high-concentration acetate. *International Journal of Hydrogen Energy*, *33*(4), 1164-1171.
- Weber, K., Erdem, O. F., Bill, E., Weyhermüller, T. and Lubitz, W. (2014) Modeling the Active Site of [NiFe] Hydrogenases and the [NiFeu] Subsite of the C-Cluster of Carbon Monoxide Dehydrogenases: Low-Spin Iron (II) Versus High-Spin Iron (II). *Inorganic Chemistry*, 53(12), 6329-6337.
- Weghoff, M. C. and Müller, V. (2016) CO metabolism in the thermophilic acetogen Thermoanaerobacter kivui. *Applied and Environmental Microbiology*, AEM-00122.
- Weijma, J., Gubbels, F., Pol, L. H., Stams, A. J. M., Lens, P. and Lettinga, G. (2002) Competition for H_2 between sulfate reducers, methanogens and homoacetogens in a gas-lift reactor. *Water Science and Technology*, 45, 75-80.
- Weng, X., Huang, L., Chen, Z., Megharaj, M. and Naidu, R. (2013) Synthesis of iron-based nanoparticles by green tea extract and their degradation of malachite. *Industrial Crops and Products*, *51*, 342-347.
- Wolfrum, E. J. and Watt, A. S. (2001) "Bioreactor Design Studies for a Novel Hydrogen-Producing Bacterium." *Proceedings of the 2001 U.S. DOE Hydrogen Program Review.* NREL/CP-570-30535. Golden, CO: National Renewable Energy Laboratory.

- Worden, R. M., Bredwell, M. D. and Grethlein, A. J. (1997) Engineering issues in synthesis-gas fermentations. In *ACS Symposium Series*, 666, 320-335. Washington, DC: American Chemical Society.
- Xu, D. and Lewis, R. S. (2012) Syngas fermentation to biofuels: Effects of ammonia impurity in raw syngas on hydrogenase activity. *Biomass and Bioenergy*, *45*, 303-310.
- Yang, G. and Wang, J. (2018) Improving mechanisms of biohydrogen production from grass using zero-valent iron nanoparticles. *Bioresource Technology*, 266, 413-420.
- Yang, J., Ma, W., Chen, D., Holmen, A. and Davis, B. H. (2014) Fischer–Tropsch synthesis: A review of the effect of CO conversion on methane selectivity. *Applied Catalysis A: General*, *470*, 250-260.
- Yasin, M., Jeong, Y., Park, S., Jeong, J., Lee, E. Y., Lovitt, R. W., Byung, H. K., Jinwon, L. and Chang, I. S. (2015) Microbial synthesis gas utilization and ways to resolve kinetic and mass-transfer limitations. *Bioresource Technology*, 177, 361-374.
- Yasin, M., Park, S., Jeong, Y., Lee, E. Y., Lee, J. and Chang, I. S. (2014) Effect of internal pressure and gas/liquid interface area on the CO mass transfer coefficient using hollow fibre membranes as a high mass transfer gas diffusing system for microbial syngas fermentation. *Bioresource Technology*, 169, 637–643.
- Yoneda, Y., Yoshida, T., Kawaichi, S., Daifuku, T., Takabe, K. and Sako, Y. (2012) *Carboxydothermus pertinax* sp. nov., a thermophilic, hydrogenogenic, Fe (III)-reducing, sulfur-reducing carboxydotrophic bacterium from an acidic hot spring. *International Journal of Systematic and Evolutionary Microbiology*, 62(7), 1692-1697.
- Younesi, H., Najafpour, G., Ismail, K. S. K., Mohamed, A. R. and Kamaruddin, A. H. (2008) Biohydrogen production in a continuous stirred tank bioreactor from synthesis gas by anaerobic photosynthetic bacterium: *Rhodopirillum rubrum*. *Bioresource Technology*, 99(7), 2612-2619.
- Younesi, H., Najafpour, G. and Mohamed, A. R. (2005) Ethanol and acetate production from synthesis gas via fermentation processes using anaerobic bacterium, *Clostridium ljungdahlii*. *Biochemical Engineering Journal*, *27*(2), 110-119.
- Zavarzina, D. G., Sokolova, T. G., Tourova, T. P., Chernyh, N. A., Kostrikina, N. A. and Bonch-Osmolovskaya, E. A. (2007) *Thermincola ferriacetica* sp. nov., a new anaerobic, thermophilic, facultatively chemolithoautotrophic bacterium capable of dissimilatory Fe(III) reduction. Extremophiles 11: 1–7.
- Zhang, J., Taylor, S. and Wang, Y. (2016) Effects of end products on fermentation profiles in *Clostridium carboxidivorans* P7 for syngas fermentation. *Bioresource Technology*, *218*, 1055-1063.
- Zhao, Y., Haddad, M., Cimpoia, R., Liu, Z. and Guiot, S. R. (2013) Performance of a Carboxydothermus hydrogenoformans-immobilizing membrane reactor for syngas upgrading into hydrogen. *International Journal of Jydrogen Energy*, *38*(5), 2167-2175.

- Zhao, Y., Cimpoia, R., Liu, Z. and Guiot, S. R. (2011a) Kinetics of CO conversion into H 2 by Carboxydothermus hydrogenoformans. *Applied Microbiology and Biotechnology*, *91*(6), 1677.
- Zhao, Y., Cimpoia, R., Liu, Z. and Guiot, S. R. (2011b) Orthogonal optimization of *Carboxydothermus hydrogenoformans* culture medium for hydrogen production from carbon monoxide by biological water-gas shift reaction. *International Journal of Hydrogen Energy*, *36*(17), 10655-10665.
- Zhu, M. and Wachs, I. E. (2015) Iron-based catalysts for the high-temperature water–gas shift (HT-WGS) reaction: A review. *ACS Catalysis*, *6*(2), 722-732.
- Zhu, H., Shanks, B. H. and Heindel, T. J. (2008) Enhancing CO− water mass transfer by functionalized MCM41 nanoparticles. *Industrial & Engineering Chemistry Research*, *47*(20), 7881-7887.
- Zhu, H., Shanks, B. H., Choi, D. W. and Heindel, T. J. (2010) Effect of functionalized MCM41 nanoparticles on syngas fermentation. *Biomass and bioenergy*, *34*(11), 1624-1627.
- Zhu, H., Shanks, B. H., and Heindel, T. J. (2009) Effect of electrolytes on CO− water mass transfer. *Industrial & Engineering Chemistry Research*, *48*(6), 3206-3210.
- Zuidervaart, E. Reuter, M. A. Heerema, R. H. Van der Lans, R. G. J. M. and Derksen, J. J. (2000) Effect of dissolved metal sulphates on gas liquid oxygen transfer in agitated quartz and pyrite slurries. *Minerals Engineering, 13* (14-15), 1555–1564.

List of publications

❖ **Book chapter**

1. Arindam Sinharoy, Manoj Kumar and Kannan Pakshirajan (2018) An overview of bioreactor configurations and operational strategies for dark fermentative biohydrogen production, In: Bioreactors for Bioenergy and Waste abatement, Singh, Yousuf, Mahapatra, Liu (Ed.), CRC Press, Taylor & Francis Group, USA. (Accepted for publication)

❖ **Publications in international journal**

1. Arindam Sinharoy, N. Arul Manikandan and Kannan Pakshirajan (2015) A novel biological sulfate reduction method using hydrogenogenic carboxydotrophic mesophilic bacteria. Bioresource Technology, 192, 494-500.
2. Manoj Kumar, Arindam Sinharoy and Kannan Pakshirajan (2018). Process integration for biological sulfate reduction in a carbon monoxide fed packed bed reactor. Journal of Environmental Management, 219, 294-303.

❖ **Presentation in international/national conferences**

1. K. Pakshirajan and A. Sinharoy, Biohydrogen production using carboxydtrophic hydrogenogenic biomass in a carbon monoxide fed anaerobic moving bed biofilm reactor, International Conference in Challenges in Environmental Science & Engineering (CESE-2018), November 4 – 8, Bangkok, Thailand.
2. A. Sinharoy and K. Pakshirajan, Bioconversion of carbon monoxide to hydrogen in a moving bed biofilm reactor, International Conference on Waste Management (Recycle-2018), February 22-24, 2018, IIT Guwahati, Assam.
3. A. Sinharoy and K. Pakshirajan, Effect of iron nanoparticle on biohydrogen production form carbon monoxide using a gas lift bioreactor with anaerobic granular sludge biomass, International Conference on Advanced Nanomaterials and Nanotechnology (ICANN-2017), December 18-21, 2017, IIT Guwahati, Assam.
4. A. Sinharoy and K. Pakshirajan, Effect of process conditions on biological sulphate reduction using carbon monoxide in a gas lift reactor, Bioprocessing India (BPI-2017), December 9-11, 2017, IIT Guwahati, Assam.
5. A. Sinharoy and K. Pakshirajan, Iron nanoparticle enhanced biodesulfurization with carbon monoxide utilizing bacteria, 5th International conference on research frontiers in Chalcogen cycle science and Technology, December 19–21, 2016, Goa, India.

6. A. Sinharoy and K. Pakshirajan, Biological sulphate reduction with carbon monoxide utilizing bacteria, 5th International conference on research frontiers in Chalcogen cycle science and Technology, December 19–21, 2016, Goa, India.
7. K. Pakshirajan and A. Sinharoy, Syngas fermentation under mesophilic condition for biohydrogen production, 4th Bioprocessing India Conference (BPI-2016), Center of Innovative and Applied Bioprocessing (CIAB), December 15-17, 2016, Mohali, Punjab, India.
8. A. Sinharoy and K. Pakshirajan, Nanoparticle mediated enhanced biological carbon monoxide conversion using anaerobic microbial consortia, International conference of waste management, Recycle – 2016, April 1-2, 2016, IIT Guwahati, Assam, India.
9. A. Sinharoy and Kannan Pakshirajan, Biological carbon monoxide conversion using granular anaerobic sludge bacteria, International conference on Agriculture, Forestry, Horticulture, Aquaculture, Animal Sciences, Food Technology, Biodiversity and Climate Change: Sustainable Approaches, October 30-31, 2014, Krishi Sanskriti, JNU, New Delhi, India.

❖ **Manuscripts under preparation**

1. Arindam Sinharoy and Kannan Pakshirajan, Biological carbon monoxide conversion for bioenergy and environmental applications.
2. Arindam Sinharoy, V. Divyabaskaran and Kannan Pakshirajan, Kinetics of biomass growth, substrate utilization and biohydrogen production from CO by anaerobic biomass.
3. Arindam Sinharoy and Kannan Pakshirajan, Simultaneous removal of heavy metals and sulfate using CO as the sole carbon and energy source.
4. Arindam Sinharoy and Kannan Pakshirajan, Novel green tea based iron nanoparticle for enhanced CO bioconversion and sulfate reduction.
5. Arindam Sinharoy and Kannan Pakshirajan, Comparative study of a gas lift reactor and moving bed biofilm reactor for hydrogenogenic CO conversion and sulfate reduction under continuous mode of operation.
6. Arindam Sinharoy and Kannan Pakshirajan, Biological selenite reduction using CO as the sole carbon and energy source.